Final REPORT

WY-2404F

State of Wyoming Department
of Transportation

Integrating Human Behavior toward the Development of Safer Cooperative Automated Transportation: Implementation of SHRP2 Naturalistic Driving Study

December 2023

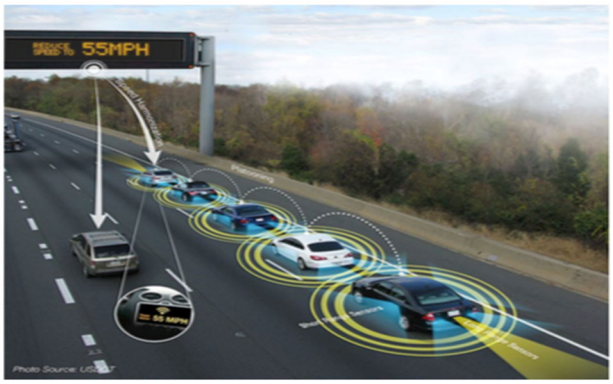

Principal Investigator:

Dr. Mohamed M. Ahmed, P.E., M. ASCE

Professor and Interim Department Head
University of Cincinnati

Authors:

Mohamed M. Ahmed, Ph.D., P.E.
Md Nasim Khan, Ph.D., P.E.
Anik Das, Ph.D., P.E.
Mandip Sigdel, M.Sc.
Vamsi Maddineni, M.Sc.

Sponsored by Wyoming Department of Transportation (Grant No: RS07221)
Department of Civil and Architectural Engineering,
University of Wyoming
1000 E. University Ave, Laramie, WY 82071
mahmed@uwyo.edu
Phone: 307-766-5550 Fax: 307-766-2221

Disclaimer and Notices

This document is disseminated under the sponsorship of the Wyoming Department of Transportation (WYDOT) in the interest of information exchange. WYDOT assumes no liability for the use of the information contained in this document. WYDOT does not endorse products or manufacturers. Trademarks or manufacturers' names appear in this report only because they are considered essential to the objective of the document.

Quality Assurance Statement

WYDOT provides high-quality information to serve Government, industry, and the public in a manner that promotes public understanding. Standards and policies are used to ensure and maximize the quality, objectivity, utility, and integrity of its information. WYDOT periodically reviews quality issues and adjusts its programs and processes to ensure continuous quality improvement.

Working in Partnership

The second Strategic Highway Research Program (SHRP2) is a partnership of the Federal Highway Administration (FHWA), the American Association of State Highway and Transportation Officials (AASHTO), and the Transportation Research Board (TRB).

No additional restrictions — You may not apply legal terms or technological measures that legally restrict others from doing anything the license permits.

You do not have to comply with the license for elements of the material in the public domain or where your use is permitted by an applicable exception or limitation.

No warranties are given. The license may not give you all of the permissions necessary for your intended use. For example, other rights such as publicity, privacy, or moral rights may limit how you use the material.

Non-copyrightable work generated by Artificial Intelligence

For all work in this report that was generated using an artificial intelligence tool and that cannot be copyrighted, and which will be available on any public domain, Author waives all rights to that portion of the work generated by artificial intelligence under copyright laws. Others may copy, modify, and distribute the specified artificial intelligence generated work without permission. Authors make no warranties about the work, and disclaim all liabilities for all use of that work. When using or citing the work, you should not imply endorsement by the author, contractor, or WYDOT.

No Generative Artificial Intelligence Training

Without any way limiting the author or other copyright owner's exclusive right under copyright, the owner of this report, which includes the authors, contractor and WYDOT, does not consent to the content being used or downloaded for the purposes of developing, training, or operating any artificial intelligence (AI) tool or model, or other machine learning systems operated by any generative artificial intelligence (GAI) model, which could include but is not limited to machine learning (ML) tools, large language models (LLM), generative adversarial networks (GAN), open AI programs (OpenAI), generative pre-trained transformers (GPT), or their sublicensees. Any use of this publication to train generative AI technologies or their sublicenses is expressly prohibited. The owner of this report reserve all rights to license uses of this work and any artificial intelligence tool that is capable of generating works must obtain the owner's specific and express permission to generate any works using data and information from this report.

Declaration of Generative Artificial Intelligence and Artificial Intelligence Assisted Technologies

During the preparation of this work, author(s) used ChatGPT in and edited the content as needed, and takes full responsibility for the content of this report. Further, to the best of the author(s) knowledge, the work generated from any artificial intelligence (AI) assisted technologies used in this report does not infringe upon any copyright, or plagiarize anyone else's' work. Neither the author nor WYDOT can guarantee the accuracy or completeness of the information generated in this report by AI.

Technical Report Documentation Page

1. Report No. WY- 2404F	**2. Government Accession No.**	**3. Recipient's Catalog No.**	
4. Title and Subtitle Integrating Human Behavior toward the Development of Safer Cooperative Automated Transportation: Implementation of SHRP2 Naturalistic Driving Study		**5. Report Date** December 2023 **6. Performing Organization Code**	
7. Author(s) Mohamed Ahmed, Ph.D., P.E.- orcid.org/0000-0002-1921-0724 Anik Das, Ph.D. - orcid.org/0000-0003-4674-5334 Md Nasim Khan, Ph.D. - orcid.org/0000-0001-5996-091X Mandip Sigdel - orcid.org/0009-0007-4082-0213 Vamsi Maddineni- orcid.org/0009-0000-7346-5480		**8. Performing Organization Report No.**	
9. Performing Organization Name and Address Department of Civil and Architectural Engineering University of Wyoming 1000 E. University Avenue, Dept. 3295 Laramie, Wyoming 82071		**10. Work Unit No. (TRAIS)** **11. Contract or Grant No.** RS07221	
12. Sponsoring Organization Name and Address Wyoming Department of Transportation 5300 Bishop Blvd, Bldg. 6100 Cheyenne, WY 82009-3340		**13. Type of Report and Period Covered** Final Report January 2020 - December 2023 **14. Sponsoring Agency Code** WYDOT	
15. Supplementary Notes Vince Garcia, P.E., GIS/ITS Program Manager			
16. Abstract Cooperative Automated Transportation (CAT), encompassing Connected Vehicles (CV), Autonomous Vehicles (AV), and Connected and Automated Vehicles (CAV), represents a transformative shift in the transportation landscape. CAT offers benefits such as improved safety, reduced congestion, enhanced traffic operations, increased productivity, and environmental advantages. Nevertheless, integrating CAT seamlessly into existing infrastructure and navigating mixed traffic scenarios presents formidable challenges. An essential facet of this integration is understanding how the traffic would act in a mixed environment involving human-driven vehicles and connected automated vehicles. This study capitalizes on the comprehensive dataset from the Second Strategic Highway Research Program (SHRP2) Naturalistic Driving Study (NDS) to gain profound insights into lane change human behavior, essential for effective microsimulation for the mixed traffic environment. This research delves into the effective utilization of SHRP2 NDS data and addresses the effective ways to ensure safety and operational efficiency across varying Market Penetration Rates (MPRs) and Levels of Autonomy in CAT. The findings aim to pave the way for the seamless and safe adoption of Cooperative Automated Transportation systems in mixed traffic environments.			
17. Key Words Naturalistic Driving Study, SHRP2, Driver Behavior and Performance, Road Weather Management, Speed Selection, Lane Keeping, Lane Change, Gap Acceptance, Car following, Surrogate Measures of Safety, Deep Learning, Feature Selection, Microsimulation, Variable Speed Limit, Wyoming, Connected and Automated Vehicles, Level of Autonomy, Market Penetration Rate, Performance Evaluation, Safety and Operations		**18. Distribution Statement** This document is available through the National Transportation Library and the Wyoming State Library. Copyright @2016. All rights reserved, State of Wyoming, Wyoming Department of Transportation, and University of Wyoming.	
19. Security Classification (of this report) Non-Classified	**20. Security Classification (of this page)** Non-Classified	**21. No. of Pages** **195**	**22. Price**

METRIC CONVERSION FACTORS

SI* (MODERN METRIC) CONVERSION FACTORS

APPROXIMATE CONVERSIONS TO SI UNITS

Symbol	When You Know	Multiply By	To Find	Symbol
		LENGTH		
in	inches	25.4	millimeters	mm
ft	feet	0.305	meters	m
yd	yards	0.914	meters	m
mi	miles	1.61	kilometers	km
		AREA		
in^2	square inches	645.2	square millimeters	mm^2
ft^2	square feet	0.093	square meters	m^2
yd^2	square yard	0.836	square meters	m^2
ac	acres	0.405	hectares	ha
mi^2	square miles	2.59	square kilometers	km^2
		VOLUME		
fl oz	fluid ounces	29.57	milliliters	mL
gal	gallons	3.785	liters	L
ft^3	cubic feet	0.028	cubic meters	m^3
yd^3	cubic yards	0.765	cubic meters	m^3
	NOTE: volumes greater than 1000 L shall be shown in m^3			
		MASS		
oz	ounces	28.35	grams	g
lb	pounds	0.454	kilograms	kg
T	short tons (2000 lb)	0.907	megagrams (or "metric ton")	Mg (or "t")
		TEMPERATURE (exact degrees)		
°F	Fahrenheit	5 (F-32)/9 or (F-32)/1.8	Celsius	°C
		ILLUMINATION		
fc	foot-candles	10.76	lux	lx
fl	foot-Lamberts	3.426	candela/m^2	cd/m^2
		FORCE and PRESSURE or STRESS		
lbf	poundforce	4.45	newtons	N
lbf/in^2	poundforce per square inch	6.89	kilopascals	kPa

APPROXIMATE CONVERSIONS FROM SI UNITS

Symbol	When You Know	Multiply By	To Find	Symbol
		LENGTH		
mm	millimeters	0.039	inches	in
m	meters	3.28	feet	ft
m	meters	1.09	yards	yd
km	kilometers	0.621	miles	mi
		AREA		
mm^2	square millimeters	0.0016	square inches	in^2
m^2	square meters	10.764	square feet	ft^2
m^2	square meters	1.195	square yards	yd^2
ha	hectares	2.47	acres	ac
km^2	square kilometers	0.386	square miles	mi^2
		VOLUME		
mL	milliliters	0.034	fluid ounces	fl oz
L	liters	0.264	gallons	gal
m^3	cubic meters	35.314	cubic feet	ft^3
m^3	cubic meters	1.307	cubic yards	yd^3
		MASS		
g	grams	0.035	ounces	oz
kg	kilograms	2.202	pounds	lb
Mg (or "t")	megagrams (or "metric ton")	1.103	short tons (2000 lb)	T
		TEMPERATURE (exact degrees)		
°C	Celsius	1.8C+32	Fahrenheit	°F
		ILLUMINATION		
lx	lux	0.0929	foot-candles	fc
cd/m^2	candela/m^2	0.2919	foot-Lamberts	fl
		FORCE and PRESSURE or STRESS		
N	newtons	0.225	poundforce	lbf
kPa	kilopascals	0.145	poundforce per square inch	lbf/in^2

*SI is the symbol for the International System of Units. Appropriate rounding should be made to comply with Section 4 of ASTM E380.
(Revised March 2003)

Table of Contents

List of Figures

List of Tables

List of Acronyms

AADT	Average Annual Daily Traffic
AASHTO	American Association of State Highway and Transportation Officials
ABS	Antilock-Braking System
ACC	Adaptive Cruise Control
ADAS	Advanced Driver Assistance Systems
AES	Autonomous Emergency Braking
AIC	Akaike Information Criterion
AMS	Analysis, Modeling, and Simulation
ANN	Artificial Neural Network
ATIS	Advanced Traveler Information System
ATM	Active Traffic Management
AUC	Area Under Curve
AV	Autonomous Vehicles
AVI	Automatic Vehicle Identification
CA	Cluster Analysis
CACC	Cooperative Adaptive Cruise Control
Caltrans	California Department of Transportation
CAN	Controller Area Network
CART	Classification and Regression Tree
CAS	Collision Avoidance Systems
CAT	Cooperative Automated Transportation
CAV	Connected and Autonomous Vehicle
CCTV	Closed-Circuit Television
CMF	Crash Modification Factors
CNDD	Commercially Collected NDD
CNN	Convolutional Neural Network
CORSIM	CORridor SIMulation
CTRE	Iowa State University Center for Transportation Research and Education
CV	Connected Vehicles
CV–VSL	Connected Vehicle-Based Variable Speed Limit
CVO	Commercial Vehicle Operation
CWS	Collison Warning System
DAS	Data Acquisition Systems
DBS	Dynamic Brake Support
DGPS	Differential Global Positioning System
DMS	Dynamic Massage Signs
DNN	Deep Neural Network
DOT	Department of Transportation
DRAC	Deceleration Rate to Avoid Collision
DSRC	Dedicated Short Range Communication
DT	Decision Tree
DTLB	Distance to the Lane Boundary
EFA	Explanatory Factor Analysis

FA	Factor Analysis
FARS	Fatality Analysis Reporting System
FC	Fully Connected
FFS	Free Flow Speed
FHWA	Federal Highway Administration
FOT	Field Operational Test
FRA	Federal Railroad Administration
FV	Following Vehicle
GCV	Generalized-Cross-Validation
GEH	Geoffrey E. Havers
GIS	Geographic Information System
GLCM	Gray Level Co-occurrence Matrix
GPS	Global Positioning System
GPU	Graphics Processing Unit
HAR	Highway Advisory Radio
HCM	Highway Capacity Manual
HMI	Human-Machine Interface
HOG	Histogram of Oriented Gradients
HPMS	Highway Performance Monitoring System
HSIS	Highway Safety Information System
HUD	Head-up Display
IAP	Implementation Assistance Program
ISS	Intelligent Safety Systems
K-NN	K-Nearest Neighbor
LBP	Local Binary Pattern
LCV	Lane-changing Vehicle
LD	Loop Detector
LDW	Lane Departure Warning
LiDAR	Light Detection and Ranging
LOS	Level of Service
LR	Logistic Regression
LSTM	Long Short-Term Memory
LV	Lead Vehicle
MANOVA	Multivariate Analysis of Variance
MARS	Multivariate Adaptive Regression Splines
ML	Machine Learning
MPLA	Market Penetration and Level of Autonomy
MPR	Market Penetration Rate
MSE	Mean Square Error
MUTCD	Manual on Uniform Traffic Control Device
MZSF	Maximum Z Score Among Shadow Features
NB	Naïve Bayes
NCAR	National Center for Atmospheric Research
NCDC	National Climate Data Center
NDD	Naturalistic Driving Data
NDS	Naturalistic Driving Study

NFOT	Naturalistic field operational test
NHTSA	National Highway Traffic Safety Administration
NOAA	National Oceanic and Atmospheric Administration
OBU	On-Board Units
PAM	Partitioning Around Medoids
PCA	Principal Component Analysis
PDO	Property Damage Only
PET	Post Encroachment Time
PII	Personally Identifiable Information
RALPH	Rapidly Adapting Lateral Position Handler
ReLU	Rectified Linear Unit
RF	Random Forest
RID	Roadway Information Database
RMSE	Root Mean Square Error
RNN	Recurrent Neural Network
ROC	Receiver Operating Characteristic Curve
RSLC	Road Surface Luminance Curve
RSS	Residual Sum of Squares
RVD	Radar Vehicle Detection
RWIS	Roadway Weather Information System
SAR	Synthetic Aperture Radar
SCE	Safety-critical Event
SDLP	Standard Deviation of Lane Position
SEM	Structural Equation Modeling
SGB	Stochastic Gradient Boosting,
SHRP2	Second Strategic Highway Research Program
SMoS	Surrogate Measures of Safety
SVM	Support Vector Machine
TIM	Traveler Information Messages
TMC	Traffic Management Center
TTC	Time to Collision
USDOT	United States Department of Transportation
UW	University of Wyoming
V2I	Vehicle-to-Infrastructure
V2V	Vehicle-to-Vehicle
VDOT	Virginia Department of Transportation
VIF	Variance Inflation Factor
VMS	Variable Massage Sign
VMT	Vehicle Miles Travelled
VSL	Variable Speed Limit
VTTI	Virginia Tech Transportation Institute
WRMS	Weather Responsive Management Strategies
WRTM	Weather Responsive Traffic Management
WYDOT	Wyoming Department of Transportation

CHAPTER 1. INTRODUCTION

The emergence of innovative transportation technologies comprises vehicle connectivity, autonomy, and personal mobility are accelerated by the rapid advancement in communication and information technologies along with advanced artificial intelligence on a large scale. Among the most comprehensively researched innovative technologies, Cooperative Automated Transportation (CAT), which includes Connected Vehicles (CV), Autonomous Vehicles (AV), and Connected and Automated Vehicles (CAV) received remarkable interest in recent years and recognized as a "game-changer" in the current transportation system. CV technology refers to a system that includes different advanced wireless communication technologies to allow vehicles to share real-time information with vehicle-to-vehicle (V2V) and vehicle-to-infrastructure (V2I) communications (Intelligent Transportation Systems Joint Program Office (ITSJPO), 2020). AV comprises several technologies including video cameras, radar sensors, light detection, etc. that integrate directly into the vehicle infrastructure to enable vehicles to control themselves partially or fully at different hierarchy levels (Anderson et al., 2016). The CAV incorporates the technologies of CV and AV to operate with any level of connectivity and/or automation ability, as illustrated in Figure 1. The ongoing advancement in automotive technology indicates that vehicles equipped with Automated Driving Systems (ADS) will soon become a widespread reality. This prospect has placed them at the forefront of future research priorities, as emphasized by authoritative bodies like the National Highway Traffic Safety Administration (NHTSA) and the Society of Automotive Engineers (SAE). These organizations recognize the significant potential of ADS in revolutionizing transportation, highlighting their importance in shaping the future of automotive innovation and safety. (NHTSA, 2018; SAE International, 2018). It is anticipated that the introduction of CAT will enhance the people's quality of life in many aspects compared to the traditional human-driven vehicles (HV). Utilizing vehicle automation and connectivity-aided communication, CAT offers unprecedented opportunities to resolve various longstanding transportation problems. The potential benefits of CAT include but are not limited to improving traffic safety by reducing the number of crashes resulted from human errors; alleviating congestion by controlling the behavior of specific vehicles in the platoon when introduced in a mixed traffic stream, thus improve traffic operations; enhancing

human productivity by providing better driver/passenger travel experience; and increasing environmental benefits to the transportation system by reducing vehicle emissions (Martínez-Díaz, Soriguera, and Pérez 2018; Stern et al. 2018; Talebpour and Mahmassani 2016).

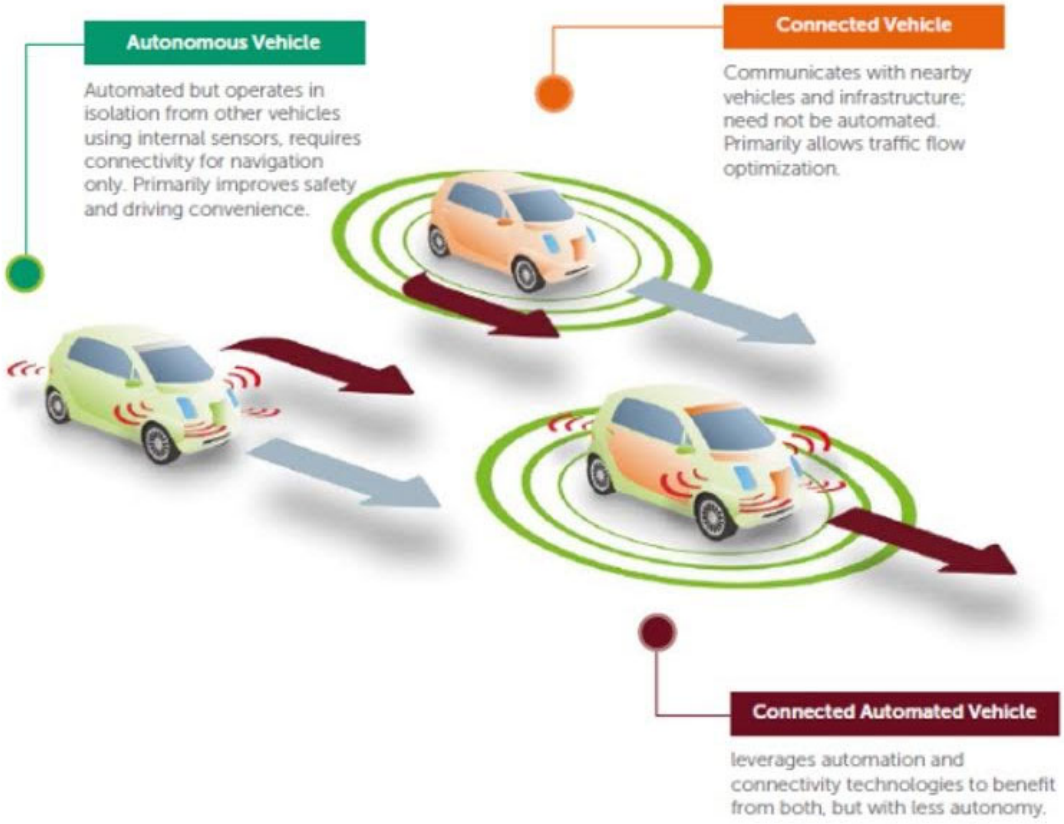

Figure 1 Cooperative Automated Transportation (Source: iCAVE2 Project at University at Buffalo (University at Buffalo 2016))

With the blooming of high-performance mobile processors, affordable and robust sensors/ cameras, and high-speed connectivity, such as 5G technologies, CAT will likely emerge sooner than anticipated on the roadways. However, 100 percent market penetration rates (MPR) of CAT might not be achieved before long because it will be challenging to integrate CAT technologies into all the existing vehicles and roadway facilities. Despite the potential benefits of CAT, there is an increasing concern regarding the transition era of CAT where both CAT and HV will be interacting and sharing the same roadways in a mixed traffic environment. In terms of AV, we are far from level 5 implementation. Many automobile manufacturers are experimenting with automation levels 3 and 4 (e.g., partial/conditional automation), which frequently requires human override, continuous attention of the drivers, and might not work as

intended due to poor visibility, especially in adverse weather when lane markings and the surroundings are not properly visible. In such extreme conditions, many autonomous car manufacturers, including Tesla®, are using the lead vehicle as a guide for automation. Tesla® owner's manual for Model S (2023)-page 96 mentioned that

> "Enhanced Autopilot is a hands-on feature. Keep your hands on the steering wheel at all times and be mindful of road conditions, surrounding traffic, and other road users (such as pedestrians and cyclists). Always be prepared to take immediate action. Failure to follow these instructions could cause damage, serious injury or death."

Alongside this, it is certain that in the near future, there will be a mixed traffic flow comprising HVs alongside the CAT with low autonomy and low market penetration rates. With the advancement in technology, it is understandable that as the market penetration of CAT increases with time so will the advancement in the level of autonomy. This will create a complex mixed traffic environment on different facility types. Therefore, CAT could introduce a variety of traffic problems caused by the complex behavior of human driving. If CAT is not appropriately integrated and tested with human behavior in mind, it might generate unexpected consequences.

In order to overcome these limitations, automated vehicles should mimic human driving to reduce variability and to ensure more harmonious traffic flow. However, mimicking human drivers requires driver behavior cloning, which is a popular approach where human behavior could be integrated into CAT so that it imitates the actions of human drivers. The next challenge is to determine the percentage of behavior cloning required for proper CAT implementation. It is expected that at lower MPRs of CAT, more behavior cloning is required and with the increase of MPR, the requirement for behavior cloning will be reduced. When 100 percent market penetration rate (MPR) and level 5 automation will be achieved, there will be no need for behavior cloning of CAT. However, at low MRP of CAT, it is crucial to determine the appropriate level of behavior cloning of CAT equipped vehicle for ensuring proper safety and operation.

1.1 Exploring Key Data Sources for Capturing Real-World Human Driving Behavior

Although behavior cloning is necessary for proper CAT deployment, it is extremely difficult to achieve due to the unpredictability and peculiar nature of individual human behaviors (Aoude et al. 2012). In order to integrate the heterogeneous nature of human behavior through behavior cloning approach, real-time trajectory-level naturalistic driving data is essential. This led the research team to investigate various data sources, driver simulator studies, and ultimately select data from naturalistic driving studies. In specific, this study utilized data from the Second Strategic Highway Research Program (SHRP2) Naturalistic Driving Study (NDS), which is the most comprehensive naturalistic study in the US. A systematic review under the guidelines of Preferred Reporting Items for Systematic Reviews and Meta-Analyzes (PRISMA) was conducted for 117 studies that were obtained after initial screening of 2304 studies as shown in Figure 2. These 117 studies were reviewed and grouped into seven relevant topics as shown in Figure 3. The topics include driver behavior and performance, crash/near-crash causation, driver distraction, pedestrian/bicycle safety, intersection/traffic signal related studies, detection and prediction using NDSs data, based on their frequency of appearance in the keywords of these studies.

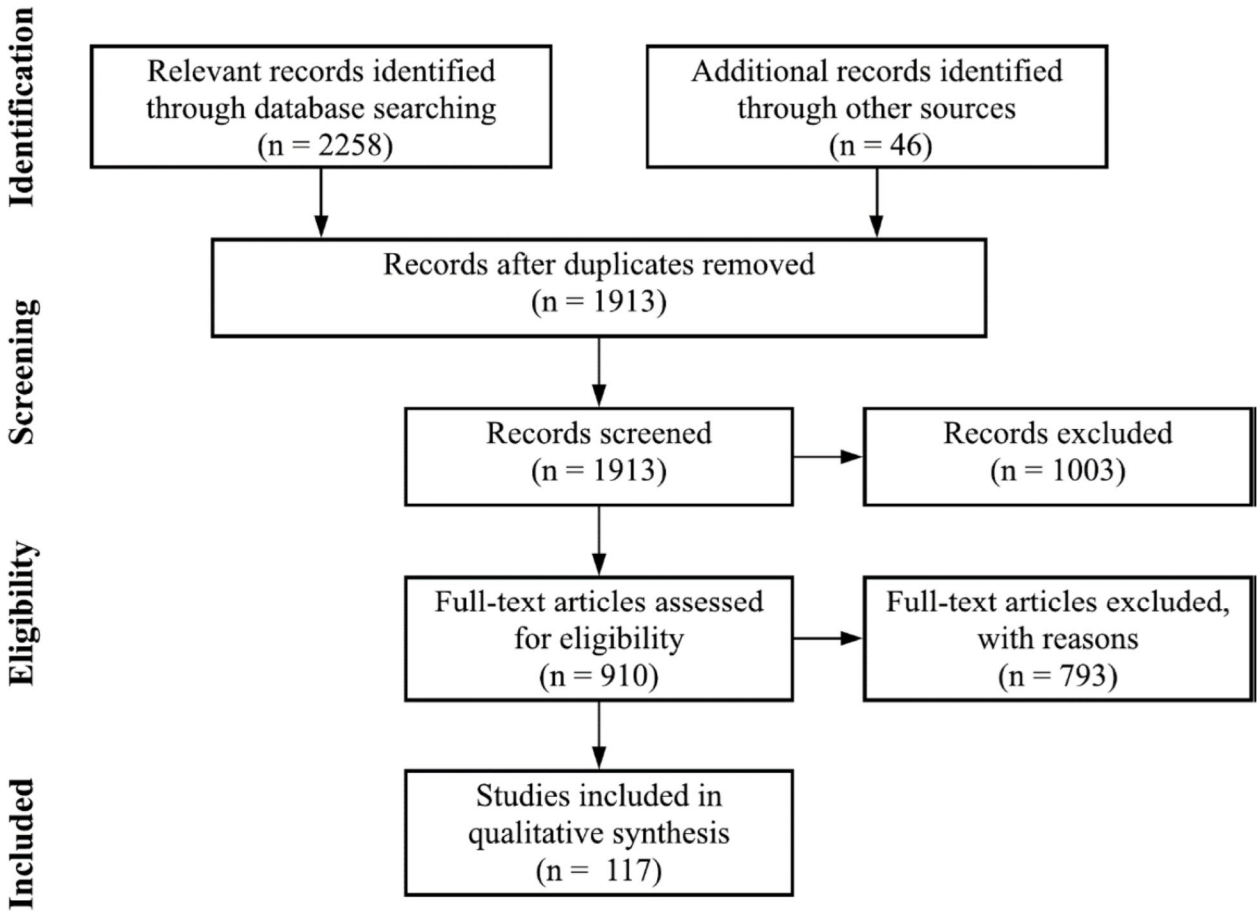

Figure 2 Flowchart for Systematic Review of Naturalistic Studies Using PRISMA Guideline

NDS also collects far more variables than the police report. In addition to the vehicle's position, NDSs collect vehicle kinematics, roadway geometry, traffic conditions, and environmental variables. Unlike in a driving simulator study, which examines driving behavior in a controlled environment, participants drive cars equipped with data collection systems during their normal driving routines (Ahmed et al. 2022). NDS data thus represents actual behavior in normal driving conditions.

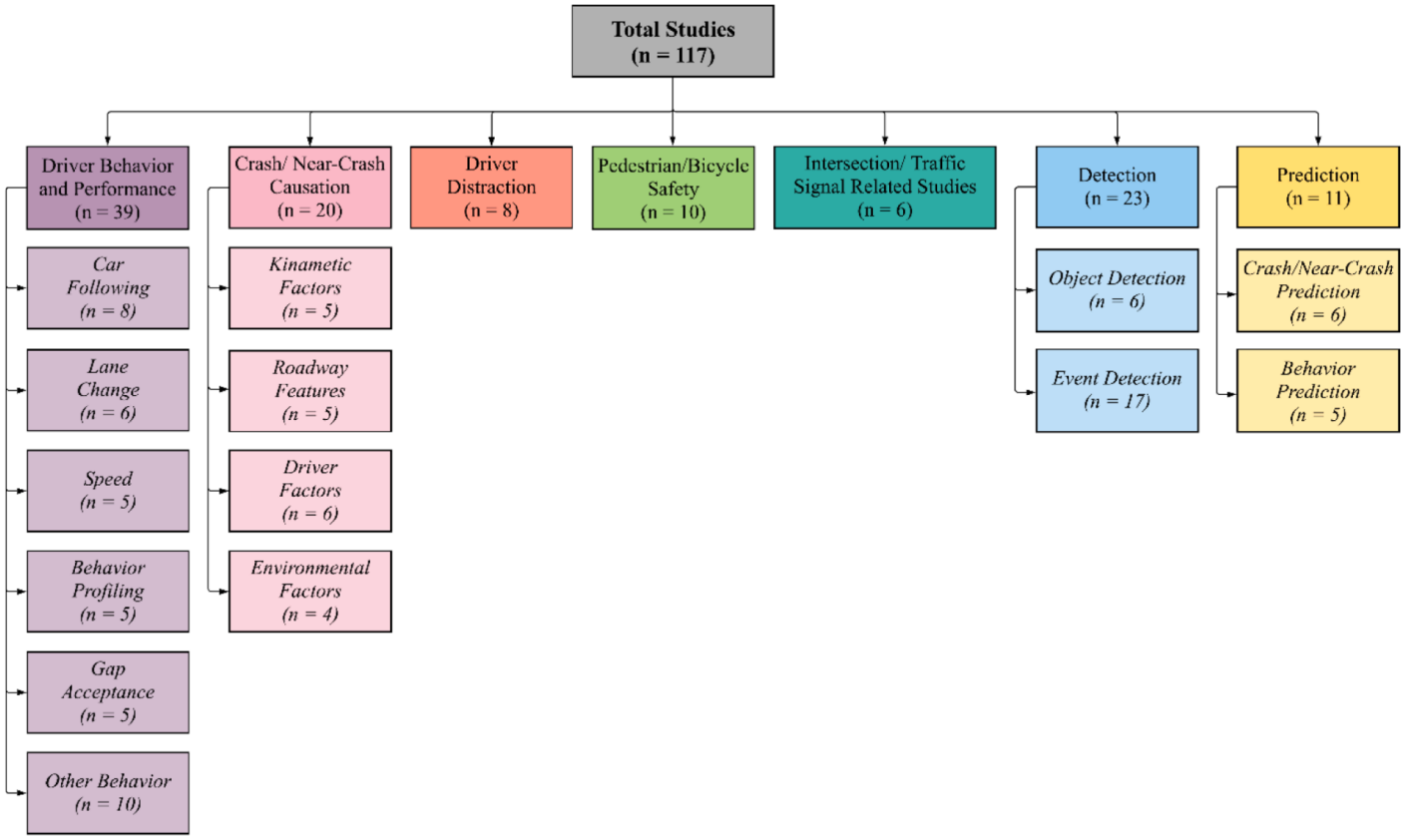

Figure 3 Systematic Classification of Topics Considered in this Study

Moreover, the NDS has opened vistas of opportunities to properly investigate driver behavior in normal as well as safety–critical situations, which are not possible using the traditional aggregated traffic data. NDS data provided researchers with unprecedented opportunities to investigate the safety and operational impacts of driver behavior and other factors related to weather, traffic, and roadway geometry, at a trajectory level. NDSs have provided numerous insightful findings in many areas of traffic safety and operation, including, but not limited to, crash contributing factors; driver distraction; speed, car following, gap acceptance and lane changing behavior; detection and prediction of crashes/near-crashes; detection and prediction of weather; driver behavior profiling; pedestrian safety; intersection and signal control; and work zones. These insightful findings have unprecedented potentials to improve roadway safety and operations via proper integration of human behavior into various countermeasures, such as ADAS, CAV applications, VSL, DMS, and CAS.

The study involving CAVs could be done in various ways, including driving simulator studies, test track studies, and microsimulation studies. Amongst them, microsimulation using software tools like PTV VISSIM, SUMO, VISUM etc., provides a way to understand the complex road behavior environment in a mixed traffic situation in a cost-effective manner, and without wasting huge time and effort required for a real road segment study, and it is the safest and most time efficient method. Despite its benefits, there are several gray areas in the study as microsimulation using software requires the simulation parameters to be up to date and efficiently mimic the human drivers alongside the CAVs. Most of the previous work in the literature has been based on optimizing the longitudinal parameters relating to the driver behaviors like car-following behavior, acceleration, deceleration, stopping sight distance etc. But the lateral parameters in the form of lane changes are studied less and these parameters remain unchanged in many simulation studies. Without every parameter effectively portraying the HDVs and CAVs environment, the simulation results cannot be deemed to be true. The SHRP2 NDS data provides us with the opportunity to effectively utilize it and find the lane change parameters opted by the real time human drivers. This, if combined with the other updated parameters from diverse studies, can help us effectively model an accurate simulation run and thus aid in a realistic microsimulation study. The goal of this study is to utilize the SHRP2 NDS database and find out the lane change parameters associated with the human driven vehicles based on the facility types, and whether conditions that later can be efficiently inputted for the microsimulations involving a mixed traffic environment comprising of HDVs and CAVs.

The following section provides an overview of the project objectives and research questions and outlines the remainder of the report.

1.2 Project Objectives

Considering the research gaps and current limitations of CAT deployment, the primary objectives of this research is to leverage the SHRP2 NDS data to gather an in-depth understanding of human behavior for achieving proper behavior cloning and to integrate the findings toward the development of an effective CAT. The research objectives will be achieved by investigating the following two research questions:

1. Can SHRP2 NDS data be effectively utilized for finding parameters relating to human behavior that can be used to model a CAT environment?
2. To what degree we should integrate behavior cloning into CAT to ensure proper safety and operations at different MPRs?

1.3 Report Organization

The remainder of this report presents the findings from the project. The report is organized as follows:

- Chapter 2 - This chapter explores tasks such as data acquisition, data processing algorithm development using statistical and data mining techniques, and the creation of lane change behavior parameters for a realistic Microsimulation study involving mixed HV - CAT environments. It also investigates the adjustment of lane change parameters to develop microsimulation models for assessing safety and operational impacts of adverse weather. Through in-depth analysis, the goal is to enhance our understanding of these complex relationships and provide valuable insights to transportation research.
- Chapter 3 - Starting from this chapter, different methodologies for development of CAT algorithm, CAT Modeling and simulation, the calibration and validation of model and its impact will be studied. This chapter will utilize the findings from previous chapters to efficiently model CAT at changing market penetration and level of autonomy and its safety and operational impact on the traffic will be evaluated.
- Chapter 4 - This chapter evaluates the impact of present infrastructure on CAT capability on freeway using microsimulation.
- Chapter 5 - This chapter will evaluate the impact of CAT on work zone safety and operations using a weather sensitive microsimulation approach.
- Chapter 6 – This chapter mainly focuses on the CAT advancement through platooning and delves into safety, operations aspects of platooning and required infrastructure modifications needed for better adoption of this technology
- Chapter 7 - This chapter provides summary and key findings, as well as recommendations for future research and practical applications.

CHAPTER 2. UPDATING ADVERSE WEATHER CONDITIONS LANE CHANGE PARAMETERS USING SHRP2 NATURALISTIC DRIVING DATA: DEEP LEARNING AND MICROSIMULATION APPROACH

2.1 DETECTION OF LANE CHANGE MANEUVERS USING SHRP2 NDS DATA USING DEEP LEARNING

2.1.1 Introduction

Lane change maneuvers are widely recognized as some of the most common yet intricate actions on roadways. Improper and unsafe lane changes can significantly jeopardize traffic safety. According to the annual motor vehicle crash data, the NHTSA revealed that in 2019, lane changes played a role in approximately 574,000 motor vehicle accidents in the US. Additionally, (Sen, Smith, and Najm 2003) estimated that lane change errors contribute to over 250,000 crashes each year. Furthermore, Feng et al. 2015 pointed out that lane change accidents account for nearly 5 percent of all reported crashes and a substantial 7 percent of crash-related fatalities. Moreover, (Li et al. 2014) argued that more than 60 percent of crashes can be attributed to lane changes, particularly on freeways. In general, these studies underscore the necessity for a comprehensive examination of lane change maneuvers, given their profound implications for traffic safety.

2.1.2 Background

The detection of lane change maneuvers using different approaches and data sets can be found in the literature. Thiemann, Treiber, and Kesting 2008 evaluated lane-changing dynamics from next generation simulation (NGSIM) trajectory data. To detect a lane change, they used vehicle dimension and position in addition to the lane index that the vehicle is currently occupying. Knoop et al. 2012 quantified the number of lane changes considering the traffic flow characteristics of the target and initial lane using loop detector data. Their lane change detection method is based on lane index, vehicle speed, and length recorded from the data. Using degree of curvature data, Koziol et al. 1999, proposed a lane change detection method where five parameters were considered to identify a lane change event including: complete lane change duration; mini- mum and maximum points on the degree of curvature and their duration; and variation of the degree of curvature. A study by Xuan and Coifman 2006 developed a lane change detection method using global positioning system (GPS) data, and

used vehicle lateral position and lateral velocity to identify lane change maneuvers. Considering a subjective approach adopted in a driving simulator, Salvucci and Liu, 2002, identified lane change maneuvers when the start and end-points of simulated highway seemed readily apparent based on the experimenter's decision. Although these studies used various data sources, the detection of lane changes in naturalistic settings is not well researched.

Machine learning (ML) techniques have recently found utility in the detection of lane change maneuvers when considering methodological approaches. In a study focused on freeway off-ramps, a lane change identification model based on a two-level CNN was developed, yielding an average detection accuracy of 94.6 percent (Xu 2021). Another investigation utilized a support vector machine (SVM) for lane change detection through instrumented vehicles, achieving an overall accuracy of 97.9 percent in maneuver identification (Mandalia and Salvucci 2005). Bakhit, Osman, and Ishak 2017 applied an artificial neural network (ANN) to identify imminent lane change maneuvers within connected vehicle environments, resulting in an approximate 80 percent detection accuracy. Yang et al. 2017 employed a random forest (RF) model to detect lane change decisions from NGSIM data, reporting detection accuracies of 88 percent and 91 percent for right and left lane changes, respectively. Furthermore, Zheng and Hansen 2017 directed their efforts towards detecting lane changes using steering angle signals obtained from the vehicle's CAN-bus. They incorporated K-nearest neighbor (KNN) and hidden Markov model (HMM) classifiers, achieving an accuracy exceeding 80 percent.

Although the aforementioned studies have indicated that ML methods offer potential for enhanced lane change detection performance in terms of overall accuracy, there is a pressing need to improve detection models to ensure balanced recall values. Recall, in this context, signifies the model's ability to accurately identify lane change maneuvers. In real-world scenarios, lane change events are significantly less frequent than instances of no lane change, leading to a highly imbalanced dataset. Consequently, a detection model with high overall accuracy may exhibit a lower recall value in detecting lane changes. Additionally, the literature review reveals a scarcity of studies addressing lane change maneuvers under naturalistic conditions. Moreover, there is a paucity of research examining the effectiveness of the ML approach, particularly within a deep learning (DL) framework. Consequently, there exists a need

for advancements in lane change detection models, encompassing both overall accuracy and balanced recall values to effectively identify lane changes.

Taking into consideration these research gaps and imperatives, the principal objective of this study was to formulate an efficient and resilient lane change detection model based on DL, utilizing trajectory-level SHRP2 NDS and Roadway Information Database (RID) datasets. Indeed, the study sought to leverage the extensive SHRP2 NDS dataset to incorporate additional variables, notably lane change data, which is absent in the existing SHRP2 database. By detecting lane change maneuvers using the NDS and RID datasets, it was possible to integrate lane change variables into the NDS time-series data. This integration holds great potential for researchers and practitioners engaged in lane change-related investigations, facilitating assessments of traffic safety and operations across diverse scenarios, including environmental, traffic, and roadway conditions. The research objectives were accomplished through the following research tasks:

- Generating a data set associated with lane changes and no lane changes by aggregating time-series data from the SHRP2 NDS trips and merging it with driver demographics and RID.
- Balancing the lane change database through the synthetic minority oversampling technique (SMOTE) and random majority under sampling (RMUS) techniques.
- Applying numeric-to-image transformation method to transform lane change data sets into images; and
- Training and validating a robust DL architecture named ResNet-18 and investigating the performance of the trained lane change detection models using test data sets.

The main contributions of this study can be summarized as follows: first, it leverages representative naturalistic data from the SHRP2 NDS and uses a comprehensive set of features, such as vehicle kinematics, machine vision, roadway geometries, and driver characteristics to develop reliable lane change detection models. Second, a cutting-edge technique named ‘‘DeepInsight’’ has been employed to convert numeric lane change and no lane change data to image data. To the best of the authors’ knowledge, this study is the first attempt to explicitly apply this technique in the lane change database. Third, wrapper-based Boruta and eXtreme

gradient boosting (XGBoost) algorithms are used to select relevant features from the data sets. Fourth, this study develops a novel DL-based approach concentrating on balanced recall values for detecting lane change maneuvers.

2.1.3 Data Description and Reduction

To accomplish the research objective, naturalistic data from the SHRP2 NDS database was utilized. This database contains an extensive dataset of trajectory-level information collected from over 3,400 drivers in six U.S. states during a three-year span, spanning from 2010 to 2013. All participating vehicles were equipped with a Data Acquisition System (DAS), which recorded a wide range of data, encompassing vehicle kinematics, machine vision, front-facing radar data, and front and rear video footage of roadways (Hankey, 2016). We also utilized data from the RID, which provides detailed roadway information for the six SHRP2 states. Furthermore, demographic data collected from self-reported questionnaires completed by the drivers were incorporated into our analysis, alongside NDS and RID data.

Trips from the NDS database occurred in diverse weather conditions and were obtained using two innovative data acquisition techniques developed by the research team. These methodologies were founded on supplementary weather data from the National Climatic Data Center (NCDC) and weather-related crash locations sourced from the RID database. A comprehensive description of these methods can be found in Ahmed et al 2018 and Ahmed et al 2022. Employing these approaches, we collected and processed a substantial number of trips that occurred under various weather conditions. Out of this dataset, we randomly selected 400 trips for further examination. Subsequently, we aggregated the NDS time-series databased on the duration of lane change events. Notably, lane change and no lane change events were distinguished based on time intervals. Additionally, each event was considered as a distinct discrete occurrence within the NDS database, without overlapping multiple samples. To detect lane change events, we devised an automated extraction algorithm that considered a lane offset variable. This variable was calculated by measuring the distance between the vehicle's position relative to the center of the lane and the center of the vehicle. A lane change event was identified when the NDS vehicle initiated a lateral movement from its current lane to an adjacent lane (Das, Khan, and Ahmed 2020; Das, Khan, and Ahmed 2022). Specifically, a lane

offset value exceeding 100 cm in the lateral direction was defined as a lane change event (Das, Khan, and Ahmed 2020).

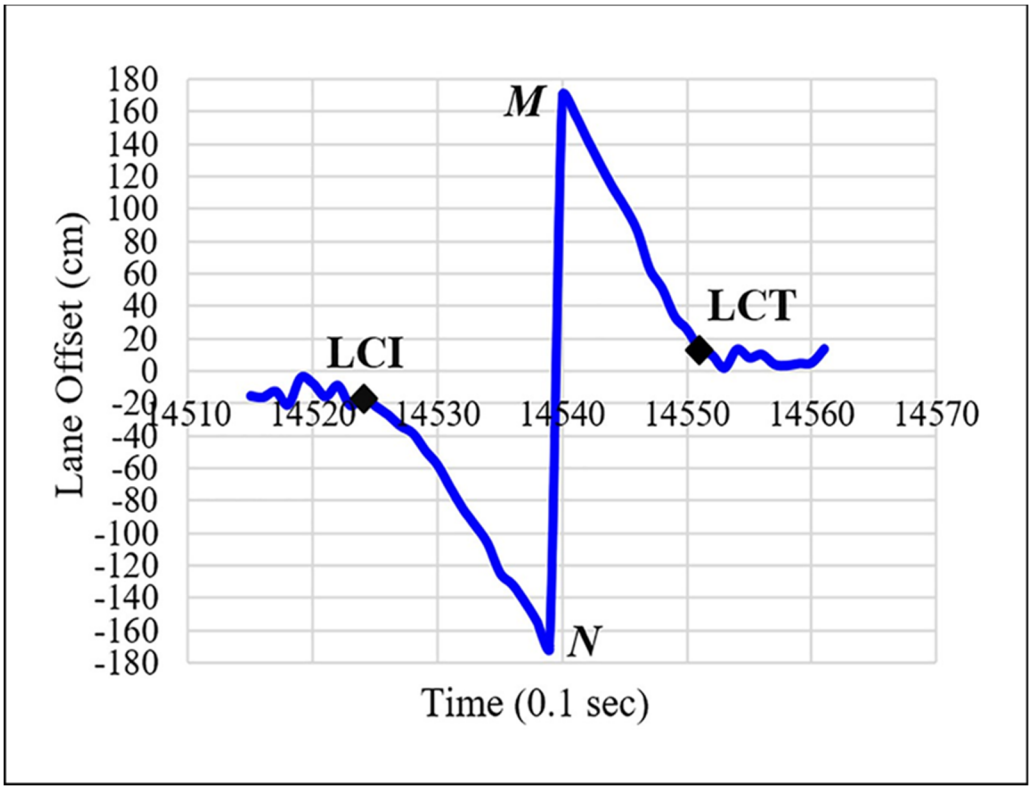

Figure 4 Demonstration of a lane change event from right to left via lane offset.

***Note*: LCI = lane change initiation; LCT = lane change termination.**

The automatic algorithm, depicted in Figure 4, initiated with the imputation of missing lane offsets within the dataset. Notably, during lane change events, the lane offset displayed distinct patterns with peaks either in the positive or negative directions. Subsequently, the identification of the positive lane offset peak, referred to as "M" in Figure 4, was undertaken. Following this, a continuous observation of the absolute change in lane offset between the positive peak and just before (termed "N" in Figure 4) timestamp occurred, utilizing a threshold of +/- 100 cm in the time-series data. This threshold equated to an absolute change of 200 cm (Das, Khan, and Ahmed 2020). Events with absolute changes less than 200 cm were categorized as 'no lane change,' while those exceeding 200 cm indicated a lane change event. Continuous reductions from point N in the backward direction and point M in the forward direction were monitored. The initiation (LCI) and termination (LCT) points of a lane change event were

identified when these reductions ceased, and the lane position offset stabilized within +/- 25 cm. Specifically, stability was determined when the lane position offset reached the +/- 25 cm threshold and remained within it for 1 second. Instances with unusual data patterns, particularly when the vehicle maintained a lane offset of zero for an extended period or exhibited back-and-forth movements, resulted in the exclusion of those lane offset values from the dataset, omitting them from the algorithm's consideration.

Utilizing the automatic algorithm, various time-series parameters (e.g., speed, acceleration, yaw rate, and lane offset) for each lane change event were efficiently extracted, including minimum, maximum, mean, and standard deviation values. Subsequently, the extracted lane change events were verified and annotated through the Wyoming NDS visualization and visibility identification tool. Conversely, for 'no lane change' events, a dynamic segmentation approach was adopted, where all trips were dynamically segmented based on lane change duration, ranging from 1 to 16 seconds. Lane change events within any dynamic segment(s) were excluded, ensuring that only 'no lane change' events remained. This approach was crucial as lane change maneuvers could occur over various segment lengths. To reduce bias in the detection of lane change events, the distribution of durations for 'no lane change' events was matched with that of lane change durations. A similar distribution approach was employed to minimize bias. Subsequently, the dynamic 'no lane change' events and the annotated and verified lane change data sets were merged with roadway characteristics data from the RID and driver demographics from SHRP2 questionnaire responses. The final dataset comprised 1,200 lane changes and 68,173 'no lane change' events. Table 1 provides an overview of the features corresponding to the various data sources considered in this study.

With the selected features from diverse sources, the analysis was conducted by combining these features into six distinct categories. These categories, coupled with vehicle kinematics and machine vision-based variables, were used to develop lane change detection models, as outlined in Table 2. Notably, machine vision-based lane offset measurements could be influenced by adverse environmental conditions, such as inclement weather obstructing lane markings. Therefore, the combination of various feature categories aimed to offer valuable insights into developing detection models based on data availability. Table 2 outlines the six

data categories corresponding to different data sources, facilitating the analysis of lane change events.

2.1.4 Methodology

Balancing the Lane Change Database in the lane change database, a substantial number of events correspond to "no lane change" (specifically, 68,173 instances), in contrast to actual lane change events. This significant imbalance within the dataset poses a challenge, as building detection models with imbalanced data may yield misleading results. While overall accuracy may appear higher, the detection model might accurately classify instances related to "no lane change" events but fail to accurately classify lane changes, which are of primary interest. To mitigate this issue, this study employed various data balancing techniques, including oversampling and under sampling, before commencing the analysis. The data was systematically balanced by testing different "lane change" to "no lane change" data ratios, ranging from 1:1 to 1:4.

The oversampling technique increases the number of samples associated with minority classes, but it also increases the risk of overfitting in the detection models. Conversely, the under sampling method balances the dataset by using a subset of the majority group, potentially introducing bias by neglecting valuable information from most samples. Studies have suggested that a combination of both oversampling and under sampling methods can lead to improved classification performance. Therefore, this study utilized two widely recognized data balancing methods, SMOTE and RMUS. SMOTE generates synthetic samples for the minority group by considering every minority sample and creating synthetic samples along line segments connecting some or all the K-nearest minority class neighbors. RMUS, on the other hand, was employed for under sampling, as it is a common approach in ML. Feature selection algorithms to identify relevant and significant features within the dataset, this study employed two robust feature extraction algorithms, Boruta and XGBoost.

Boruta is an all-relevant feature selection technique that utilizes a wrapper-based method with an embedded RF model. Notably, many feature selection methods introduce bias into the development of classification models, leading to unpredictable outcomes. Boruta addresses this issue by generating duplicates of each feature, known as shadow features, which are shuffled

to minimize biases and correlations among features. These shadow features are assigned to objects arbitrarily, and decision trees are constructed based on them. An iterative process follows, where the method calculates the highest/maximum Z score among shadow features (MZSF) and compares it to the Z score of the original features. The Z score serves as a measure of significance/importance in the Boruta method. Features with a higher Z score (indicating greater importance) than MZSF are identified as important, while those with a lower Z score (indicating lower importance) than MZSF are classified as unimportant.

Table 1 Overview of the considered features

Features	Definition	Categories
Vehicle Kinematics		
Speed *(Min., Max., Mean, Std. Dev.)* (mph)	Vehicle speed during lane change	-
Longitudinal Acceleration *(Min., Max., Mean, Std. Dev.)* (g)	Vehicle acceleration in the longitudinal direction versus time during lane change	-
Lateral Acceleration *(Min., Max., Mean, Std. Dev.)* (g)	Vehicle acceleration in the lateral direction versus time during lane change	-
Yaw Rate *(Min., Max., Mean, Std. Dev.)* (deg/sec)	Vehicle angular velocity of vehicle around the vertical axis during lane change	-
Machine Vision		
Lane Offset (*Min., Max., Mean, Std. Dev.)* (cm)	Distance to the left/right of the center of the lane and center of the vehicle during lane change	-
Roadway Geometries		
Presence of Curve	Whether the participants drove curve or tangent during lane change	1 = Curve
		2 = Tangent
Curve Radius (Feet)	Curve radius of segment in which participants drove during lane change	-
Curve Length (Feet)	Curve length of segment in which participants drove during lane change	-
Superelvation (Percent)	Average Cross Slope of the segment during lane change	-
Number of Freeway Lanes	Average number of lanes during lane change	-
Speed Limit (mph)	Speed limit during lane change	1 = ≤ 60 mph
		2 = > 60 mph
Driver Demographics		
Gender	The participant's gender	1 = Male
		2 = Female
Age	The participant's age	1 =Young (< 25 years)
		2 =Middle (25-55 years)
		3 =Old (> 55 years)
Education	The participant's highest completed education level	1=Low: High school diploma or G.E.D.
		2 = Medium (Some education beyond high school but no degree and College degree)
		3 = High (Some graduate or professional school, but no advanced degree and Advanced degree)
Marital Status	The participant's marital status	1 = Single
		2 = Married
		3 = Other (divorced, widow)
Vehicle Class	The participant's vehicle class	1 = Passenger Car/SUV
		2 = Minivan/Pick-up
Driving Experience	The participant's number of driving years	1 = ≤ 10 years
		2 = > 10 years
Driver Mileage Last year	The approximate number	1= < 10,000 miles

Table 2 Illustration of Six Data Categories

Categories	Data Set
Category 1	Vehicle Kinematics
Category 2	Machine Vision
Category 3	Vehicle Kinematics + Machine Vision
Category 4	Vehicle Kinematics + Machine Vision + Roadway geometry
Category 5	Vehicle Kinematics + Machine Vision + Driver Demographics
Category 6	Vehicle Kinematics + Machine Vision + Roadway geometry + Driver Demographics

XGBoost, a powerful technique for feature extraction, plays a pivotal role in discerning feature importance within a dataset. It accomplishes this by quantifying the significance of each feature through a metric known as "gain." The gain metric is calculated by estimating the improvement in accuracy achieved by introducing a new feature split within a decision tree branch. A higher gain value assigned to a feature signifies its greater importance in comparison to other features for the purpose of detection (Soleimani et al. 2019).

2.1.4.1 Numeric Data to Image transformation

The process of transforming numeric lane change data into image data begins with the application of an innovative technique named "DeepInsight," as devised by Sharma et al., 2019. This transformative approach converts a feature vector, denoted as x (representing lane change data), into a feature matrix A, which portrays the spatial relationships between features. These positions within the matrix are influenced by feature similarity. For instance, features like f1, f3, f6, and f7 are closer to each other in this matrix (Figure 5). Once feature positions are identified within the matrix, the corresponding feature values are mapped to generate individual images for each feature vector.

The entire transformation process of numeric lane change data into image data is elaborated in (Figure 6). Initially, the lane change data is transposed to meet input requirements. Subsequently, the t-distributed stochastic neighbor embedding (t-SNE), a nonlinear dimensionality reduction technique, is applied to project features onto a 2-D plane (Van Der Maaten and Hinton, 2008). Each point on this plane represents the Cartesian coordinates of a feature. Importantly, these coordinates only indicate feature positions. After projection, the convex hull algorithm is employed to identify the minimum rectangle encompassing all feature

points. Following this, a rotation is applied to orient the rectangle and feature points horizontally. Then, Cartesian coordinates are normalized and scaled to pixel frames based on a predetermined image height (Rahim and Hassan 2021).

The pixel frame contains feature locations for a sample xi, where i = 1, 2, 3, ..., n. As locations are defined, feature values are mapped to corresponding pixel positions (Sharma et al. 2019). During the mapping process, if any features overlap; their values are averaged and assigned to the same pixel location. To ensure precise image representation with minimal feature overlap, this study employs an image resolution of 50 x 50 pixels, based on the number of features in the lane change dataset.

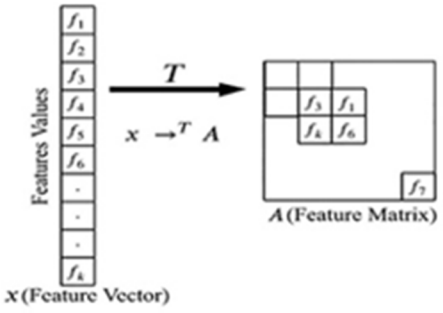

Figure 5 Conversion from feature vector to feature matrix

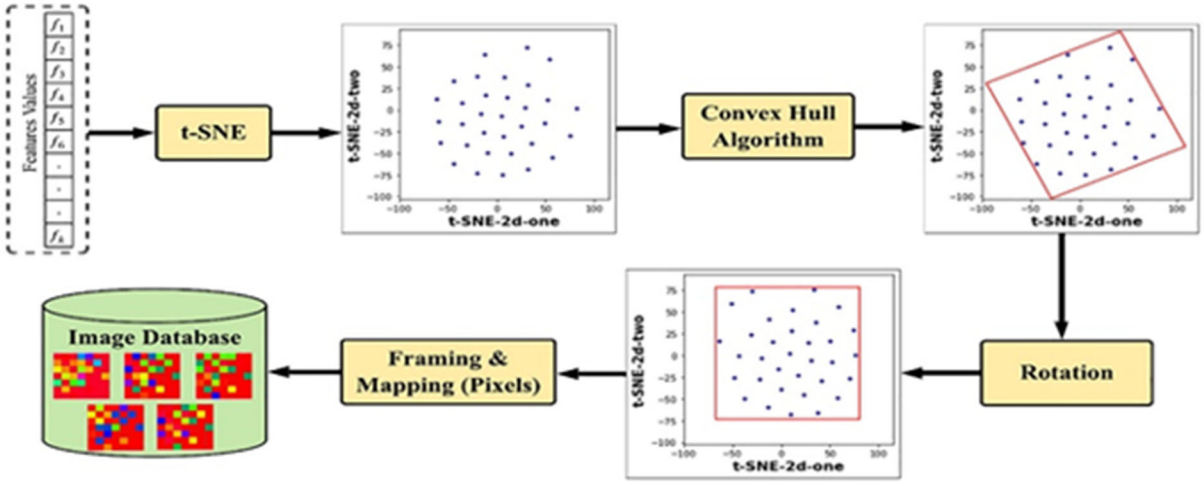

Figure 6 Demonstration of the ''DeepInsight'' method to convert feature vector to image pixels.

***Note*: t-distributed SNE = t-distributed stochastic neighbor embedding.**

2.1.4.2 Deep Learning Model

For training and validating lane change detection models, this study leverages ResNet-18, an advanced pre-trained deep CNN. Notably, training deep CNNs can be challenging due to convergence issues leading to reduced detection accuracy with increased layers. ResNet-18 addresses this challenge by incorporating a deep residual learning approach, delivering high accuracy while requiring comparatively less computational time and power than other similarly deep CNN models. The ResNet-18 architecture encompasses five convolutional blocks, featuring 17 convolutional layers and one fully connected (FC) layer, alongside parallel shortcut connections to each basic block (D. Li, Cong, and Guo 2019). Figure 7 illustrates the block diagram of the modified ResNet-18 architecture for lane change detection. In the initial convolutional operation (Conv1), a 7x7 kernel size and 64 feature map size are applied, with padding zeros added three times in every dimension. This results in an output volume of 112 x 112. Subsequently, the second convolutional layer (Conv2_x) employs a 3x3 kernel size and maintains a 64-feature map size, with padding zeros added once in each dimension, yielding an output size of 56 x 56 x 64. The subsequent three convolutional layers (Conv3_x, Conv4_x, and Conv5_x) each employ 128, 256, and 512 filters of the same size as the second convolutional layer, respectively. After Conv5_x, a pooling layer is applied, leading to an output size of 1 x 1 x 512 to reduce the information from the previous layer and to provide the most important ones to the following layer. This layer was then connected to the FC layer to generate an output vector of two dimensions considering the lane change/no lane change categories (Khan and Ahmed 2021). Thereafter, a softmax layer was added that allocates decimal probabilities to every output category (Khan, Das, and Ahmed 2020). Considering the probabilities, the last layer was an output layer that provided the final lane change/no lane change category.

The original ResNet-18 underwent training using a dataset of more than a million images sourced from the ImageNet database, which is organized based on the WordNet hierarchy. To provide further details, the model's training was performed on a subset of ImageNet, known as ImageNet large-scale visual recognition challenge (ILSVRC) (Russakovsky et al. 2015; He et al. 2016). This pre-trained iteration of ResNet-18 possesses the capability to classify images into a

diverse array of 1,000 object categories and can acquire a robust feature representation through the utilization of a method known as "transfer learning" (Mathworks-Resnet18; MathWorks- Pretrained Deep Neural Networks). Transfer learning stands as a widely recognized approach for training deep convolutional neural network (CNN) models, leveraging insights gleaned from well-established pre-trained CNN models (Khan and Ahmed 2021). By employing transfer learning, the pre-trained model consistently demonstrates remarkable accuracy in detection when compared to CNN models trained exclusively on a relatively limited number of training images. Previous research studies have also underscored the significant performance enhancement achievable through the application of transfer learning (T. Li et al. 2021; Gaweesh, Khan, and Ahmed 2021; Khan and Ahmed 2021). Figure 8 offers an illustrative depiction of the transfer learning process (conceived from MATLAB®) for retraining a pre-trained CNN model with the goal of classifying new sets of images.

In the present study, the pre-trained ResNet-18 model was harnessed for lane change detection tasks through the utilization of the transfer learning methodology. Specifically, certain layers within the model were adapted to align with the objectives of the study. This adaptation involved the replacement of the input layer and the final three layers with a fresh input layer, an FC layer, a softmax layer, and an output layer, respectively. Furthermore, adjustments were made to the input image size to conform to the specifications of the ResNet-18 model, which necessitated images of dimensions 224 x 224 pixels.

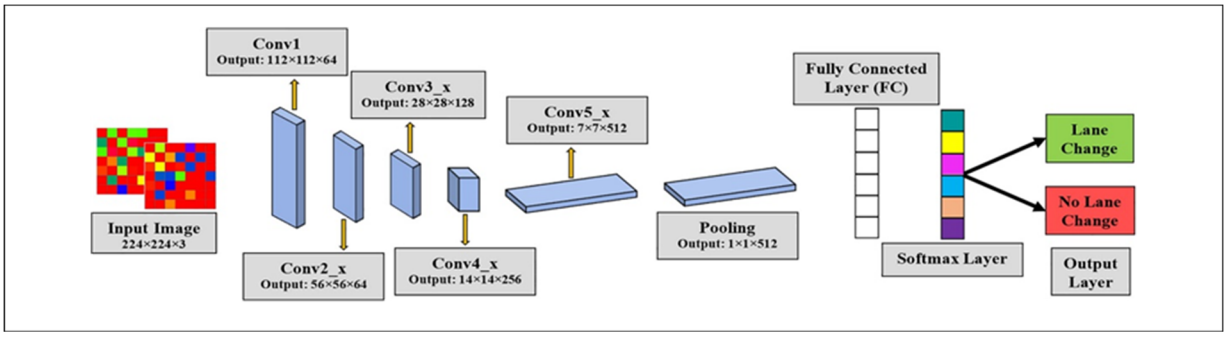

Figure 7 Descriptive block diagram of modified ResNet-18 architecture

***Note*: Conv = convolutional layer**

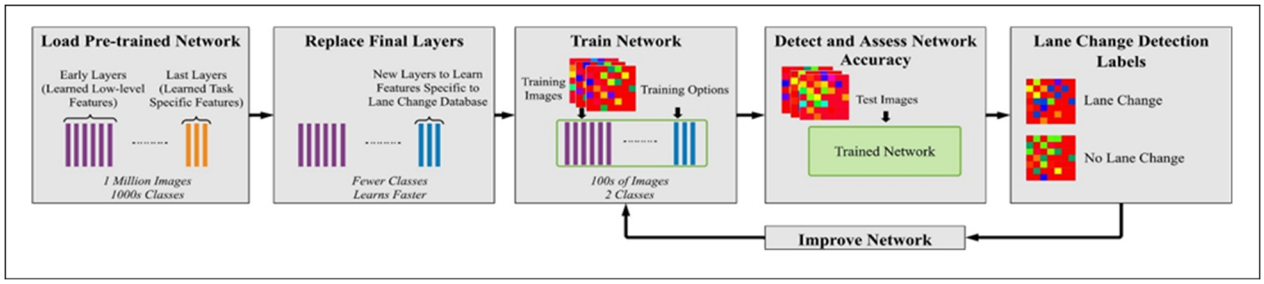

Figure 8 Example diagram of transfer learning in lane change detection

Following the modification of ResNet-18, the training and validation of detection models for lane change and no lane change scenarios were conducted using a dataset encompassing six distinct categories of features. Multiple models were evaluated for each category, with data balancing techniques and diverse sampling ratios applied in the process. Subsequently, the models underwent rigorous testing and assessment using a separate set of test images. It is noteworthy that, post-training, the proposed DL models possess the capability to promptly inspect and detect lane changes based on available features. As a result, all trained models, corresponding to different categories, are poised for real-time deployment in the context of lane change detection. Figure 9 provides an overview of the comprehensive methodology employed for detecting lane changes using a DL framework.

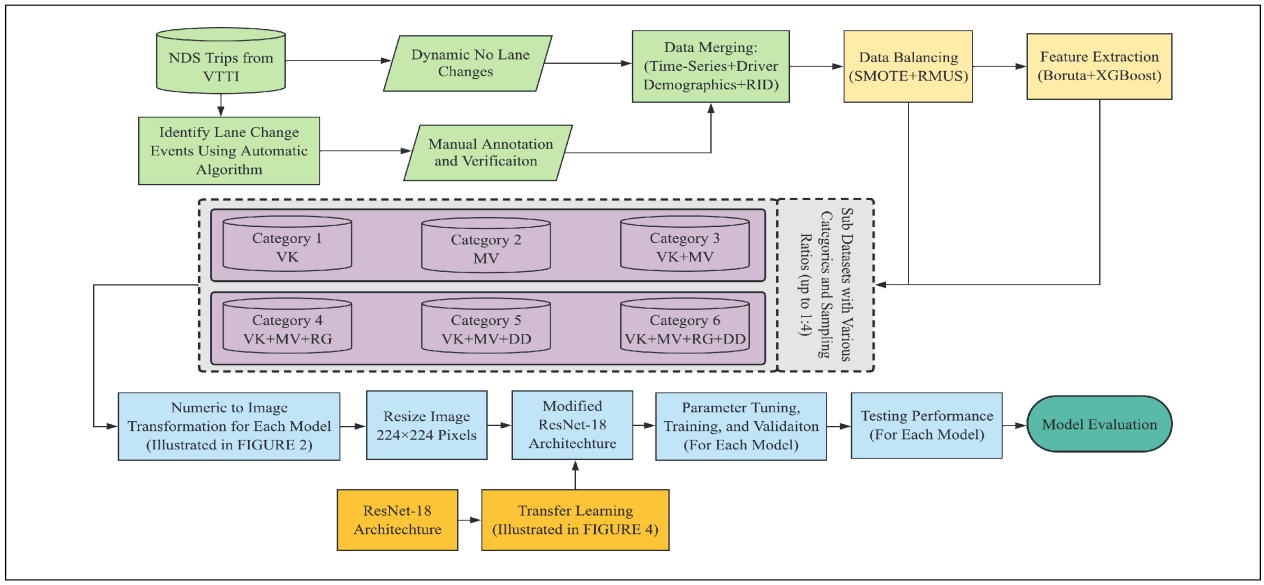

Figure 9 Flowchart illustrating overall methodology considered in this study.

Note: VTTI = Virginia Tech Transportation Institute; RID = roadway information database; SMOTE = synthetic minority oversampling technique; RMUS = random majority undersampling; XGBoost =

eXtreme gradient boosting; DD = driver demographics; VK = vehicle kinematics; RG = roadway geometry; MV = machine vision.

2.1.5 Results and Discussion

2.1.5.1 Relevant Feature Selection

To address potential overfitting in the dataset, we conducted a correlation analysis on the baseline data set. This analysis aimed to identify and remove highly correlated features. Features exhibiting a correlation value exceeding 0.7 were highly correlated among the parameters (Ratner 2009). It is important to note that the formation of categories was carried out after the elimination of these highly correlated features from the baseline dataset. As previously mentioned, this study employed both Boruta and XGBoost feature selection algorithms to assess the significance and contribution of various features associated with the six data categories in detecting lane change maneuvers. Figures 10 and 11 depict the significance of features as determined by the Boruta and XGBoost algorithms for each of the six data categories. The blue boxplots provide insight into the maximum, mean, and minimum Z scores of a shadow feature. Additionally, the Z scores of important and unimportant features for each category are represented by green and red boxplots, respectively, within the figures. Our analysis revealed that, for Category 1, the five most crucial features were 'minimum lateral acceleration,' 'maximum lateral acceleration,' 'standard deviation of yaw rate,' 'maximum speed,' and 'maximum yaw rate.' Conversely, when considering Categories 3 to 6, the most critical feature in detecting lane changes was 'standard deviation of lane offset,' followed by 'minimum lane offset,' 'maximum lane offset,' 'mean lane offset,' and 'standard deviation of yaw rate,' as determined by the Boruta algorithm.

It is important to highlight that the top four features linked with Categories 3 to 6 closely resemble the crucial features found in Category 2. These findings are unsurprising, given that Categories 2 to 6 incorporate a lane offset parameter exhibiting a specific pattern during lane change processes. Notably, in contrast to other categories, 'driver mileage last year details' emerged as the sole unimportant feature within Category 5 as indicated by the Boruta method. In terms of the XGBoost algorithm, the top five features largely align with those obtained through the Boruta algorithm for Category 1. However, for Categories 3 to 6, the five most

important features mirror those identified by Boruta. Additionally, similar to Boruta, all machine vision-based features were deemed important using XGBoost. Nonetheless, XGBoost identified only two features ('presence of curve' and 'speed limit') as unimportant (with zero gain value) in Category 4. Furthermore, in Category 5 and 6, several features, including 'driver mileage last year details,' 'age,' 'gender,' and 'marital status,' were categorized as unimportant by XGBoost.

Notably, in Category 1, where machine vision-based features were not considered, 'minimum lateral acceleration,' 'maximum lateral acceleration,' and 'standard deviation of yaw rate' emerged as the most crucial features based on both Boruta and XGBoost methodologies. The primary significance of these parameters was expected to be due to their association with lane change maneuvers. Specifically, both lateral acceleration and yaw rate play integral roles in such maneuvers.

Overall, it is evident that the importance and ranking of features, whether deemed important or unimportant, yielded by the two algorithms exhibit substantial similarities across all categories.

2.1.5.2 Training and Validation:

In this study, we developed lane change detection models using a pre-trained CNN, ResNet-18. To carry out the training, validation, and testing of our proposed model, we utilized the DL Toolbox™ in MATLAB® version 9.10 (R2021a). It is important to note that 80 percent of the original image data were allocated for the training and validation phases. Consequently, within this 80 percent, we used 80 percent for training the lane change detection models and reserved the remaining 20 percent for validation purposes.

During the validation process, we optimized the training cost of the ResNet-18 model using the stochastic gradient descent with momentum (SGDM) optimizer. Although we experimented with two additional optimizers, including root mean square propagation and Adam, it was evident that SGDM consistently outperformed the others across all categories. The initial hyperparameters of the ResNet-18 model underwent fine-tuning through close monitoring of the training progress and validation outcomes with various parameter sets. We employed a grid-search method to identify the optimal performance configurations.

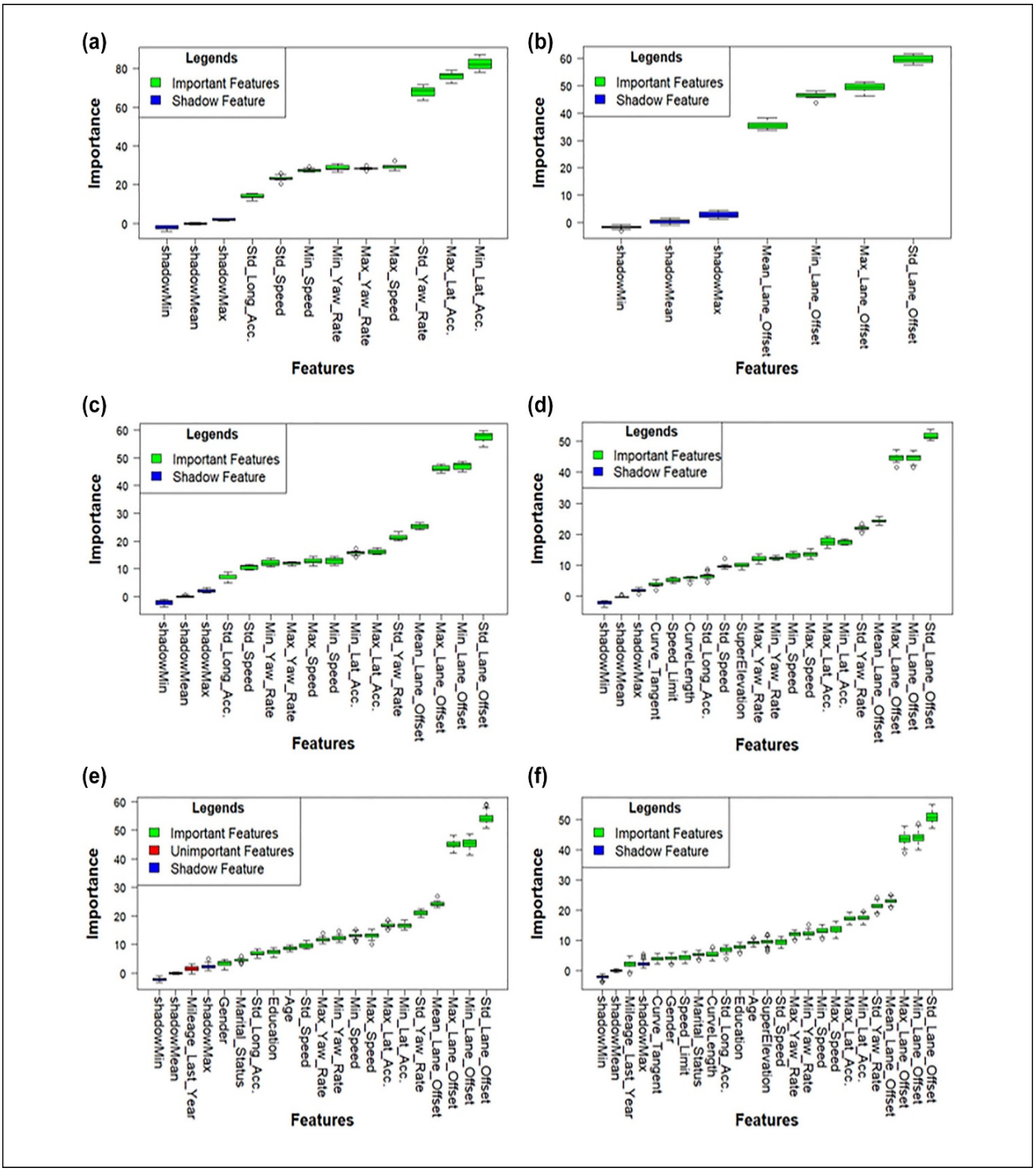

Figure 10 Plots of feature importance for six data categories using Boruta: (a) Category 1 (vehicle kinematics); (b) Category 2 (machine vision); (c) Category 3 (vehicle kinematics + machine vision); (d) Category 4 (vehicle kinematics + roadway geometry + machine vision)

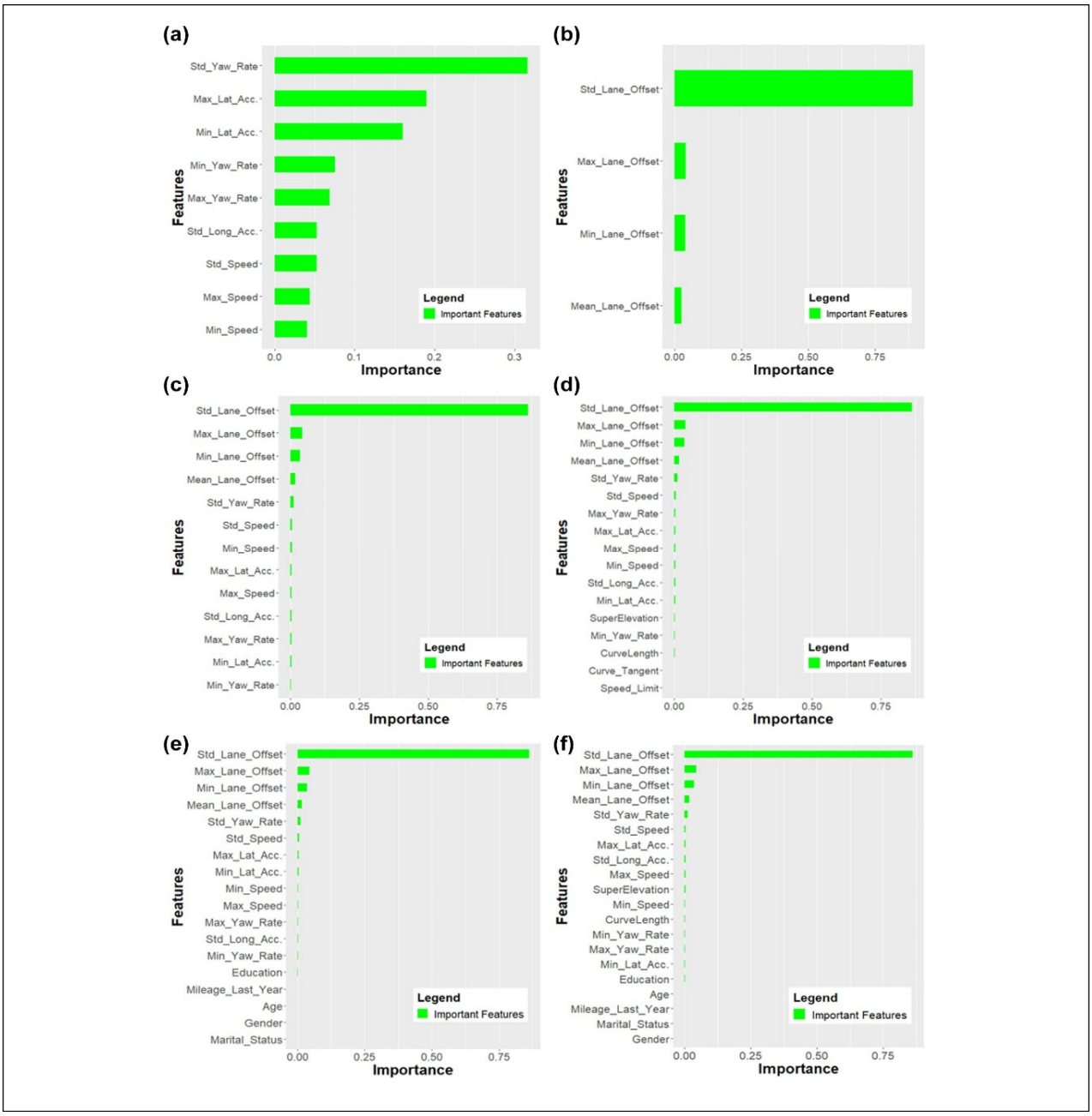

Figure 11 Plots of feature importance for six data categories using XGBoost: (a) Category 1 (vehicle kinematics); (b) Category 2 (machine vision); (c) Category 3 (vehicle kinematics + machine vision); (d) Category 4 (vehicle kinematics + roadway geometry + machine

It is noteworthy that some hyperparameters exhibited negligible impacts on model performance; hence, we excluded them from the grid-search to reduce computational costs during training and validation. For all six categories of lane change detection models, which were based on multiple features and data balancing ratios, hyperparameters were individually

tuned. However, the parameter values for the best-performing models were consistent across categories. Specifically, the optimized parameter values for these models were as follows: optimizer = SGDM, maximum epochs = 25, minimum batch size = 200, validation frequency = 10, initial learning rate = 0.001, learning rate drop factor = 0.5, learning rate drop period = 8, and L2 regularization = 0.004.

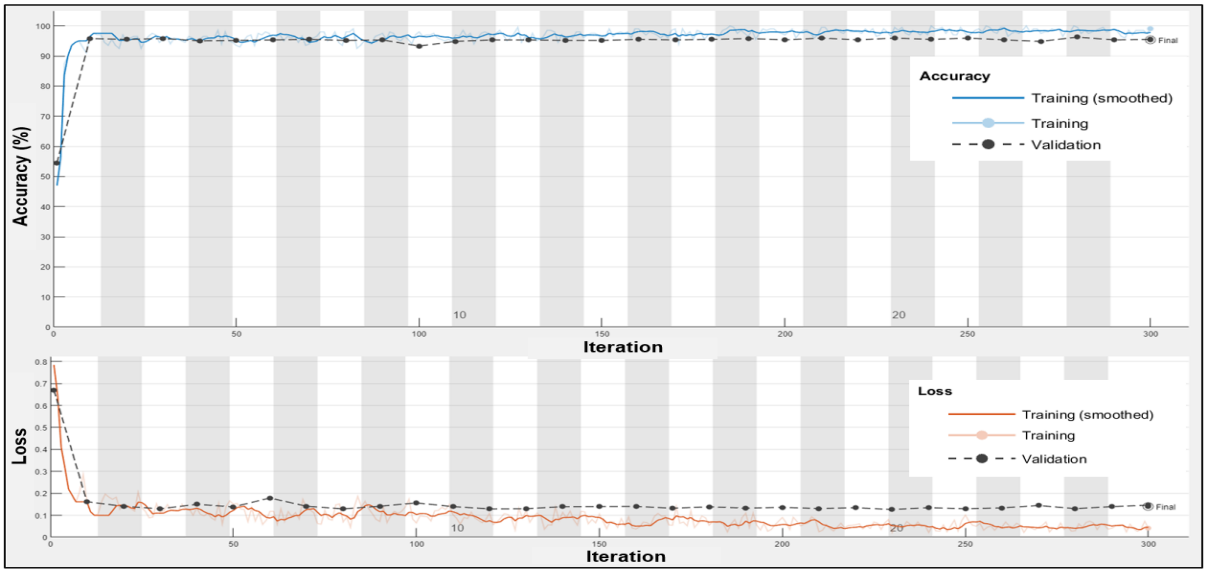

Figure 12 Example training progress of lane change detection models for kinematic features based in Category 1

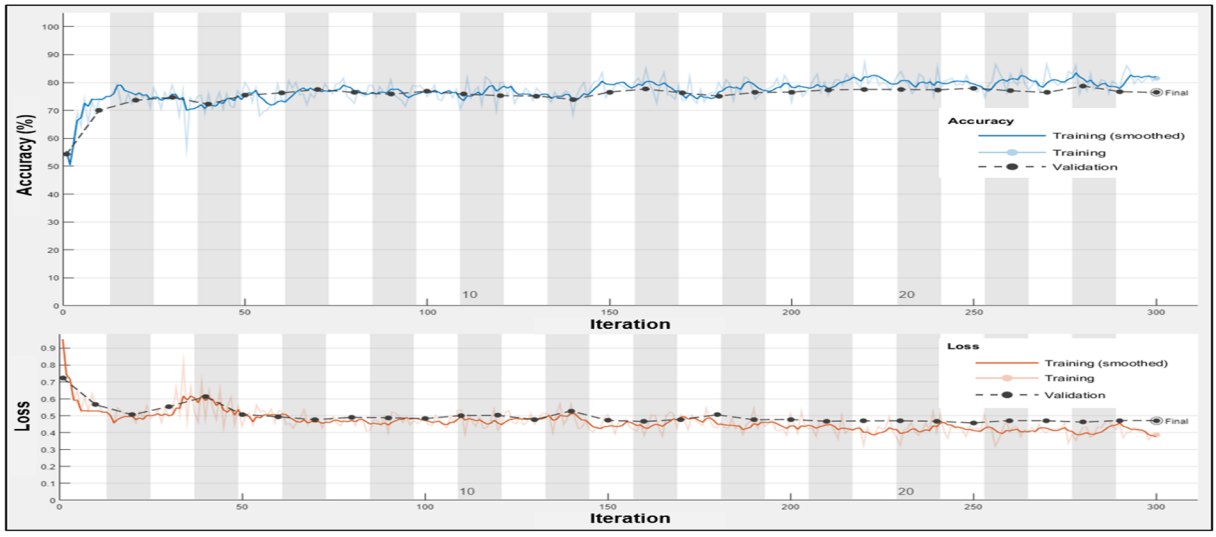

Figure 13 Example training progress for lane change detection models based on all features in Category 6

Figures 12 and 13 in this study illustrate the training progress of the best lane change detection models for two data categories: vehicle kinematics in Category 1 and all features in Category 6, using the modified parameter sets. This figure demonstrates the decreasing loss during validation across training iterations in both categories. As observed, the initial overall validation accuracy of ResNet-18 for vehicle kinematics-based features started at approximately 57 percent, gradually improving to an overall validation accuracy of about 75.5 percent after 25 epochs of training. The loss decreased from around 0.66 initially to approximately 0.50 at the final iteration. Similar improvements in accuracy and loss reduction were observed when considering all the features in Category 6. The training and validation of the best-performing models required approximately 142 minutes for vehicle kinematics and 140 minutes for all features.

2.1.6 Performance Evaluation

The assessment of the lane change detection models' performance involved utilizing a test dataset consisting of 20 percent of the original image data for each feature category. It is important to note that these DL models were specifically designed to detect lane changes, a critical aspect from both safety and operational standpoints. It is imperative to recognize that relying solely on detection accuracy, as a performance metric may not provide a comprehensive evaluation, especially in cases involving imbalanced data where certain image classes exhibit significantly higher recall rates compared to others. Therefore, this study employed a range of performance metrics; including recall/sensitivity, precision, F1-score, specificity, false positive rate (FPR), and false negative rate (FNR), in addition to overall accuracy.

Recall signifies the model's capability to correctly identify all instances of "lane change" within the test dataset. Precision, on the other hand, assesses the model's capacity to accurately classify instances as "lane change" without making false predictions. It is important to acknowledge that a model could exhibit high recall and low precision, or vice versa. The optimal performance is achieved when the model strikes a balance, demonstrating both high recall and precision values. This equilibrium can be quantified using the F1-score, which is the harmonic mean of recall and precision. A high F1-score is indicative of an effective detection model that strikes the right balance between high recall and precision values.

Specificity, meanwhile, measures the proportion of accurately classified negative cases, which, in the context of this study, refers to instances of "no lane change." The FPR and FNR serve as complements to specificity and recall, respectively. These performance measures were computed using Equations 1 to 7.

$$\text{Accuracy (A)} = \frac{TP+TN}{(TP+TN+FP+FN)} \quad (1)$$

$$\text{Recall (R)} = \frac{TP}{(TP+FN)} \quad (2)$$

$$\text{Precision (P)} = \frac{TP}{(TP+FP)} \quad (3)$$

$$\text{F1-Score} = 2 \text{ x } \frac{R\ x\ P}{(R+P)} \quad (4)$$

$$\text{Specificity (S)} = \frac{TN}{(TN+FP)} \quad (5)$$

$$\text{False Positive Rate (FPR)} = 1 - S \quad (6)$$

$$\text{False Negative Rate (FNR)} = 1 - R \quad (7)$$

In this context, True Positive (TP), signifies the number of accurately classified 'lane change' instances; True Negative (TN) pertains to the number of accurately classified 'no lane change' cases; False Negative (FN) refers to the instances where 'lane change' is misclassified as 'no lane change'; and False Positive (FP) refers to number of misclassified 'no lane change' to 'lane change'

In Table 3, the detection summary of the ResNet-18 DL model is presented concerning the performance measures for the six feature categories. The lane change database faced a severe class imbalance issue due to a significantly higher proportion of instances with no lane changes. To address this, a combination of the SMOTE and RMUS methods with varying ratios of 'lane change' to 'no lane change' was applied. Initially, for Category 1, which comprises vehicle kinematics-based features, a 1:1 ratio (lane change: no lane change) was used to train the

detection model. This resulted in an overall accuracy of 75.5 percent during validation and 77.9 percent during testing, with correct detection rates of 82 percent for 'lane change' and 73.8 percent for 'no lane change.' A F1-score of 78.8 percent was also achieved with this ratio, demonstrating good detection performance primarily due to the application of both data balancing techniques.

To explore if different ratios could improve detection performance, various 'lane change' to 'no lane change' ratios were tested while maintaining the use of both balancing methods. However, it was observed that although overall accuracy improved with increased sampling ratios, recall values did not see significant improvement, potentially exacerbating data imbalance. Consequently, to reduce computation costs and assess the impact of limited features on detection performance, several detection models were developed using selected features obtained from feature selection methods. Figures 10 and 11 show that all kinematic-based features were found to be crucial for Category 1. As such, the original model, which included all vehicle kinematic features with a 1:1 ratio, was determined to be the best performing model. Similarly, for Categories 2 and 3, which also found all features to be important, the best performing models were achieved with a 1:1 ratio. Conversely, for Category 4, which involved reduced features identified by the XGBoost algorithm, the original model with all features and a 1:1 ratio yielded better detection accuracy and F1-score compared to models with reduced features. Thus, the initial model was considered the best performing model for Category 4.

Table 3 Lane Change Detection Performance of the Developed ResNet-18 Models for Six Data Categories

Data categories	Data balancing technique	Data ratio (LC:NLC)	Features used	Class	Recall (%)	Precision (%)	Specificity (%)	FPR (%)	FNR (%)	F1-score (%)	Overall accuracy (%)
Category 1*	**SMOTE+RMUS**	**1:1**	**All**	**LC**	**82.0**	**75.8**	**73.8**	**26.2**	**18.0**	**78.8**	**77.9**
				NLC	**73.8**	**80.4**	**82.0**	**18.0**	**26.2**	**76.9**	
	SMOTE+RMUS	1:2	All	LC	59.8	74.0	89.5	10.5	40.2	66.1	79.6
				NLC	89.5	81.6	59.8	40.2	10.5	85.4	
	SMOTE+RMUS	1:3	All	LC	57.3	66.2	90.3	9.7	42.7	61.4	82.0
				NLC	90.3	86.4	57.3	42.7	9.7	88.3	
	SMOTE+RMUS	1:4	All	LC	50.5	70.4	94.7	5.3	49.5	58.8	85.9
				NLC	94.7	88.4	50.5	49.5	5.3	91.5	
Category 2*	**SMOTE+RMUS**	**1:1**	**All**	**LC**	**99.5**	**93.4**	**93.0**	**7.0**	**0.5**	**96.4**	**96.3**
				NLC	**93.0**	**99.5**	**99.5**	**0.5**	**7.0**	**96.1**	
	SMOTE+RMUS	1:2	All	LC	97.0	86.4	92.4	7.6	3.0	91.4	93.9
				NLC	92.4	98.4	97.0	3.0	7.6	95.3	
	SMOTE+RMUS	1:3	All	LC	90.5	88.5	96.1	3.9	9.5	89.5	94.7
				NLC	96.1	96.8	90.5	9.5	3.9	96.4	
	SMOTE+RMUS	1:4	All	LC	93.0	83.2	95.3	4.7	7.0	87.8	94.9
				NLC	95.3	98.2	93.0	7.0	4.7	96.7	
Category 3*	**SMOTE+RMUS**	**1:1**	**All**	**LC**	**98.2**	**93.3**	**93.0**	**7.0**	**1.8**	**95.7**	**95.6**
				NLC	**93.0**	**98.2**	**98.2**	**1.8**	**7.0**	**95.5**	
	SMOTE+RMUS	1:2	All	LC	94.8	89.8	94.6	5.4	5.2	92.2	94.7
				NLC	94.6	97.3	94.8	5.2	5.4	95.9	
	SMOTE+RMUS	1:3	All	LC	94.5	87.5	95.5	4.5	5.5	90.9	95.3
				NLC	95.5	98.1	94.5	5.5	4.5	96.8	
	SMOTE+RMUS	1:4	All	LC	90.8	90.1	97.5	2.5	9.2	90.4	96.2
				NLC	97.5	97.7	90.8	9.2	2.5	97.6	
Category 4	**SMOTE+RMUS**	**1:1**	**All**	**LC**	**98.5**	**96.3**	**96.3**	**3.7**	**1.5**	**97.4**	**97.4**
				NLC	**96.3**	**98.5**	**98.5**	**1.5**	**3.7**	**97.3**	
	SMOTE+RMUS	1:2	All	LC	92.8	95.4	97.8	2.2	7.2	94.0	96.1
				NLC	97.8	96.4	92.8	7.2	2.2	97.1	
	SMOTE+RMUS	1:3	All	LC	93.0	93.0	97.7	2.3	7.0	93.0	96.5
				NLC	97.7	97.7	93.0	7.0	2.3	97.7	
	SMOTE+RMUS	1:4	All	LC	90.3	92.8	98.3	1.7	9.7	91.5	96.7
				NLC	98.3	97.6	90.3	9.7	1.7	97.9	
	SMOTE+RMUS	1:1	From XGBoost	LC	98.5	93.1	92.8	7.2	1.5	95.7	95.6
				NLC	92.8	98.4	98.5	1.5	7.2	95.5	
Category 5	**SMOTE+RMUS**	**1:1**	**All**	**LC**	**98.2**	**95.2**	**95.0**	**5.0**	**1.8**	**96.7**	**96.6**
				NLC	**95.0**	**98.2**	**98.2**	**1.8**	**5.0**	**96.6**	
	SMOTE+RMUS	1:2	All	LC	96.5	91.7	95.6	4.4	3.5	94.0	95.9
				NLC	95.6	98.2	96.5	3.5	4.4	96.9	
	SMOTE+RMUS	1:3	All	LC	95.8	89.3	96.2	3.8	4.2	92.4	96.1
				NLC	96.2	98.5	95.8	4.2	3.8	97.3	
	SMOTE+RMUS	1:4	All	LC	95.0	91.8	97.9	2.1	5.0	93.4	97.3
				NLC	97.9	98.7	95.0	5.0	2.1	98.3	
	SMOTE+RMUS	1:1	From Boruta	LC	96.8	93.5	93.3	6.7	3.2	95.1	95.0
				NLC	93.3	96.6	96.8	3.2	6.7	94.9	
	SMOTE+RMUS	1:1	From XGBoost	LC	97.8	92.7	92.3	7.7	2.2	95.1	95.0
				NLC	92.3	97.6	97.8	2.2	7.7	94.9	
Category 6	SMOTE+RMUS	1:1	All	LC	98.3	95.2	95.0	5.0	1.7	96.7	96.6
				NLC	95.0	98.2	98.3	1.7	5.0	96.6	
	SMOTE+RMUS	1:2	All	LC	94.8	90.7	95.1	4.9	5.2	92.7	95.0
				NLC	95.1	97.3	94.8	5.2	4.9	96.2	
	SMOTE+RMUS	1:3	All	LC	95.5	91.6	97.1	2.9	4.5	93.5	96.7
				NLC	97.1	98.5	95.5	4.5	2.9	97.8	
	SMOTE+RMUS	1:4	All	LC	96.8	87.6	96.6	3.4	3.2	91.9	96.6
				NLC	96.6	99.2	96.8	3.2	3.4	97.8	
	SMOTE+RMUS	**1:1**	**From XGBoost**	**LC**	**98.8**	**91.9**	**91.2**	**8.8**	**1.2**	**95.2**	**95.0**
				NLC	**91.2**	**98.6**	**98.8**	**1.2**	**8.8**	**94.8**	

Note: **Category 1 = vehicle kinematics; Category 2 = machine vision; Category 3 = vehicle kinematics + machine vision; Category 4 = vehicle kinematics + machine vision + roadway geometry; Category 5 = vehicle kinematics + machine vision + driver demographics; Category 6 = vehicle kinematics + roadway geometry + machine vision + driver demographics; SMOTE = synthetic minority oversampling technique; RMUS = random majority undersampling; LC = lane change; NLC = no lane change; FPR = false positive rate; FNR = false negative rate. Bold and green color represents the best performing model in each category.**

*All the features were found to be important based on feature selection methods for the corresponding category.

Regarding Category 5, despite the development of additional detection models with reduced features, significant enhancements in detection performance remained elusive. Consequently, the optimal detection model was maintained at a 1:1 ratio, consistent with the approach applied to other categories. It is worth noting that for Category 6, the utilization of XGBoost led to the most notable improvement, achieving a remarkable recall value of 98.8 percent. This result, when compared to the original 1:1 ratio, suggests that limited features from the XGBoost algorithm played a significant role in effectively identifying lane change maneuvers, encompassing all features.

To delve deeper into the performance of the best-performing lane change detection models across the six categories (highlighted in Table 3), we present a visual representation in Figure 14 through test confusion matrices. These matrices also include recall, FNR, precision, and False Discovery Rate (FDR) metrics to offer comprehensive insights. Notably, FNR and FDR are inversely related to recall and precision, respectively. The green-marked diagonal elements in the matrix signify accurate detections of lane change and no lane change instances. Adjacent to the confusion matrix, aligned with the y-axis, are boxes denoting recall values for respective categories. Similarly, boxes positioned beside the confusion matrix along the x-axis represent precision values for corresponding categories.

For Category 1, which exclusively considers vehicle kinematic features, 72 out of 400 test instances labeled as 'lane change' were erroneously detected as 'no lane change' (resulting in a recall of 82 percent and precision of 75.8 percent). Consequently, the FNR and FPR stood at 18 percent and 26.2 percent, respectively, for the 'lane change' group. These statistics carry safety implications, as a higher FNR indicates an increased associated risk, where drivers may not receive alerts for 'lane change,' while a high FPR could lead to frequent false alarms, potentially eroding trust in the system.

As anticipated, substantial improvements in recall and precision were observed for 'lane change' instances in Categories 2 through 6, thanks to the inclusion of machine vision-based variables. In Category 2, where only machine vision-based features were considered, a mere 2 out of 400 test images were misclassified as 'no lane change,' resulting in an outstanding recall of 99.5 percent and a precision value of 93.4 percent. Categories 3 to 5 exhibited similar patterns, with

approximately 98 percent accuracy in identifying 'lane change' images. Notably, Category 6, encompassing all features, achieved the detection of 395 out of 400 test samples as 'lane change,' corresponding to a recall of 98.8 percent. Furthermore, Category 6 boasted a significantly lower FNR (1.2 percent) compared to the vehicle kinematic-based features in Category 1.

Additionally, Categories 3 to 6 consistently yielded excellent precision values, ranging from approximately 92 percent to 96 percent. In summary, the presented confusion matrices provide in-depth insights into the classification performance of 'lane change' and 'no lane change' instances within each data category.

Figure 14 Confusion matrices of the best performing lane change detection models using ResNet-18 for six data categories: (a) Category 1 (vehicle kinematics); (b) Category 2 (machine vision); (c) Category 3 (vehicle kinematics + machine vision); (d) Category 4 (vehicle kinematics + roadway geometry + machine vision); (e) Category 5 (vehicle kinematics + machine vision + driver demographics); and (f) Category 6 (vehicle kinematics + roadway geometry + machine vision + driver demographics).

***Note*: LC = lane change; NLC = no lane change; FDR = false discovery rate.**

2.1.7 Comparison of the Proposed ResNet-18 CNN with Traditional Machine Learning Models

Traditional ML models require data to be represented as a feature vector to facilitate detection. The feature vector is obtained through a feature extraction process, which is a prerequisite for ML models. In these models, the order of features is typically considered irrelevant, as they are assumed to be independent of one another. This renders the feature arrangement step redundant, especially in the context of conventional ML methods like RF and decision trees. Moreover, the effectiveness of ML methods heavily depends on the quality of the feature extraction technique.

In contrast, CNNs treat data samples as images. CNNs leverage the inherent characteristics of images to perform feature extraction and detection. They employ various hidden layers, including convolutional and max-pooling layers, to automatically generate features from raw attributes. CNNs also explore nonlinear correlations and higher-order statistics within images. Unlike traditional ML techniques and classic neural networks, CNNs consider the local spatial coherence of image pixels, meaning that adjacent pixels share similar information. Consequently, the arrangement of adjacent image pixels in CNNs is not arbitrary; it can significantly impact the feature extraction process and detection performance. CNNs capture information from neighboring pixels in a manner that is not achievable in traditional ML methods (Sharma et al. 2019).

It is important to note that ML methods find wide application across various domains, including the analysis of time-series driving behaviors, where the data is predominantly in non-image formats. However, CNN cannot be effectively applied to these datasets as they require image inputs. Given the advantages of CNN, it could potentially deliver superior detection performance if non-image driving behavior data, such as lane change or no lane change in this study, could be transformed into a structured image format. This is particularly challenging due to the need to discern subtle variations in the lane change database amid numerous randomly distributed features from various data sources. To address this challenge and facilitate better understanding of relationships among features, this study employs the DeepInsight method. This method transforms numeric data into images by performing three critical steps: feature arrangement, feature extraction, and classification, with the goal of enhancing lane change

detection rates. The method organizes similar features (clusters) and separates dissimilar ones to enable the combined utilization of adjacent features. Additionally, it provides insight into the relative importance of all features in relation to a target feature. Moreover, this method leverages the CNN architecture for feature extraction and classification, extending the applicability of CNN to numeric data (non-image samples) and delivering universal outcomes (Sharma et al. 2019).

To assess the hypothesis that CNN typically outperforms basic neural networks and other traditional ML models, this study investigates the detection performance of several ML models, including classic Artificial Neural Networks (ANN), XGBoost, Classification and Regression Trees (CART), SVM, RF, KNN, and Naïve Bayes (NB). These results are then compared to the proposed lane change detection models based on the ResNet-18 architecture for all six data categories. It is worth noting that the best-performing models in each category were selected for the comparison, and the evaluation utilized previously established performance metrics, as presented in Table 4. The comparison reveals that the pretrained ResNet-18 model consistently outperforms all the other models, especially in terms of recall, which is a key metric in this study (indicated in bold in Table 3-4). For example, in Category 1, the highest recall of 81.3 percent was achieved using the RF model, while ANN, XGBoost, SVM, and KNN also exhibited similar performances, each with a recall close to or exceeding 80 percent. The ResNet-18 model achieved the highest recall of 82 percent in detecting lane changes. The best performance in terms of recall, 97.7 percent, was observed in Category 6 using the RF and NB models based on all features. However, ResNet-18 surpassed these traditional ML models with a recall value of 98.8 percent. The lane change detection models employing traditional ML in other categories demonstrated a similar trend, as illustrated in Table 4.

Table 4 Comparison of the developed Res-18 models with the traditional machine learning models

Categories	Models	Class	Recall (%)	Precision (%)	Specificity (%)	FPR (%)	FNR (%)	F1-score (%)	Overall accuracy (%)
Category 1	ANN	LC	79.0	75.6	75.0	25.0	21.0	77.3	77.0
		NLC	75.0	78.5	79.0	21.0	25.0	76.7	
	XGBoost	LC	78.8	81.7	82.7	17.3	21.2	80.2	80.8
		NLC	82.7	79.9	78.8	21.2	17.3	81.3	
	CART	LC	70.7	73.9	75.5	24.5	29.3	72.3	73.1
		NLC	75.5	72.4	70.7	29.3	24.5	73.9	
	SVM	LC	78.3	79.3	80.0	20.0	21.7	78.8	79.1
		NLC	80.0	79.0	78.3	21.7	20.0	79.5	
	RF	LC	81.3	81.3	81.7	18.3	18.7	81.3	81.5
		NLC	81.7	81.7	81.3	18.7	18.3	81.7	
	KNN	LC	81.1	75.2	73.8	26.2	18.9	78.0	77.4
		NLC	73.8	79.9	81.1	18.9	26.2	76.7	
	NB	LC	76.3	73.5	73.0	27.0	23.7	74.8	74.6
		NLC	73.0	75.8	76.3	23.7	27.0	74.4	
	ResNet-18	**LC**	**82.0**	75.8	73.8	26.2	18.0	78.8	77.9
		NLC	73.8	80.4	82.0	18.0	26.2	76.9	
Category 2	ANN	LC	98.2	92.2	92.3	7.7	1.8	95.1	95.1
		NLC	92.3	98.2	98.2	1.8	7.7	95.2	
	XGBoost	LC	97.7	94.0	94.2	5.8	2.3	95.8	95.9
		NLC	94.2	97.8	97.7	2.3	5.8	96.0	
	CART	LC	97.9	92.6	92.8	7.2	2.1	95.2	95.3
		NLC	92.8	98.0	97.9	2.1	7.2	95.3	
	SVM	LC	98.7	92.7	92.8	7.2	1.3	95.6	95.6
		NLC	92.8	98.7	98.7	1.3	7.2	95.7	
	RF	LC	97.7	94.7	94.9	5.1	2.3	96.2	96.3
		NLC	94.9	97.8	97.7	2.3	5.1	96.3	
	KNN	LC	98.2	92.6	92.8	7.2	1.8	95.3	95.4
		NLC	92.8	98.2	98.2	1.8	7.2	95.4	
	NB	LC	96.9	93.5	93.7	6.3	3.1	95.2	95.3
		NLC	93.7	97.0	96.9	3.1	6.3	95.3	
	ResNet-18	**LC**	**99.5**	93.4	93.0	7.0	0.5	96.4	96.3
		NLC	93.0	99.5	99.5	0.5	7.0	96.1	
Category 3	ANN	LC	97.8	92.7	92.2	7.8	2.2	95.2	95.0
		NLC	92.2	97.6	97.8	2.2	7.8	94.8	
	XGBoost	LC	97.0	94.0	93.7	6.3	3.0	95.5	95.4
		NLC	93.7	96.9	97.0	3.0	6.3	95.3	
	CART	LC	96.8	93.1	92.7	7.3	3.2	94.9	94.8
		NLC	92.7	96.6	96.8	3.2	7.3	94.6	
	SVM	LC	97.5	93.6	93.2	6.8	2.5	95.5	95.4
		NLC	93.2	97.4	97.5	2.5	6.8	95.3	
	RF	LC	98.0	93.4	93.0	7.0	2.0	95.6	95.5
		NLC	93.0	97.9	98.0	2.0	7.0	95.4	
	KNN	LC	98.0	91.4	90.7	9.3	2.0	94.6	94.4
		NLC	90.7	97.8	98.0	2.0	9.3	94.1	
	NB	LC	95.8	92.8	92.5	7.5	4.2	94.2	94.1
		NLC	92.5	95.6	95.8	4.2	7.5	94.0	
	ResNet-18	**LC**	**98.2**	93.3	93.0	7.0	1.8	95.7	95.6
		NLC	93.0	98.2	98.2	1.8	7.0	95.5	

Categories	Models	Class	Recall (%)	Precision (%)	Specificity (%)	FPR (%)	FNR (%)	F1-score (%)	Overall accuracy (%)
Category 4	ANN	LC	96.8	93.4	92.8	7.2	3.2	95.1	94.9
		NLC	92.8	96.5	96.8	3.2	7.2	94.6	
	XGBoost	LC	97.1	95.2	94.9	5.1	2.9	96.1	96.0
		NLC	94.9	96.9	97.1	2.9	5.1	95.9	
	CART	LC	98.3	94.6	94.1	5.9	1.7	96.4	96.3
		NLC	94.1	98.1	98.3	1.7	5.9	96.1	
	SVM	LC	97.1	94.5	94.1	5.9	2.9	95.8	95.6
		NLC	94.1	96.8	97.1	2.9	5.9	95.4	
	RF	LC	98.0	95.3	94.9	5.1	2.0	96.6	96.5
		NLC	94.9	97.9	98.0	2.0	5.1	96.4	
	KNN	LC	95.9	91.6	90.8	9.2	4.1	93.7	93.4
		NLC	90.8	95.4	95.9	4.1	9.2	93.0	
	NB	LC	98.3	94.6	94.1	5.9	1.7	96.4	96.3
		NLC	94.1	98.1	98.3	1.7	5.9	96.1	
	ResNet-18	**LC**	**98.5**	96.3	96.3	3.7	1.5	97.4	97.4
		NLC	96.3	98.5	98.5	1.5	3.7	97.3	
Category 5	ANN	LC	95.9	93.3	93.4	6.6	4.1	94.6	94.6
		NLC	93.4	96.0	95.9	4.1	6.6	94.7	
	XGBoost	LC	97.4	92.9	92.9	7.1	2.6	95.1	95.1
		NLC	92.9	97.4	97.4	2.6	7.1	95.1	
	CART	LC	97.4	92.7	92.7	7.3	2.6	95.0	95.0
		NLC	92.7	97.4	97.4	2.6	7.3	95.0	
	SVM	LC	94.9	91.3	91.5	8.5	5.1	93.1	93.1
		NLC	91.5	94.9	94.9	5.1	8.5	93.2	
	RF	LC	97.2	93.8	93.9	6.1	2.8	95.5	95.5
		NLC	93.9	97.2	97.2	2.8	6.1	95.5	
	KNN	LC	95.6	90.7	90.8	9.2	4.4	93.1	93.1
		NLC	90.8	95.6	95.6	4.4	9.2	93.1	
	NB	LC	97.9	92.0	92.0	8.0	2.1	94.9	94.9
		NLC	92.0	97.9	97.9	2.1	8.0	94.9	
	ResNet-18	**LC**	**98.2**	95.2	95.0	5.0	1.8	96.7	96.6
		NLC	95.0	98.2	98.2	1.8	5.0	96.6	
Category 6	ANN	LC	95.4	90.4	90.2	9.8	4.6	92.8	92.8
		NLC	90.2	95.3	95.4	4.6	9.8	92.7	
	XGBoost	LC	97.5	94.6	94.6	5.4	2.5	96.0	96.0
		NLC	94.6	97.5	97.5	2.5	5.4	96.0	
	CART	LC	96.7	92.5	92.4	7.6	3.3	94.5	94.5
		NLC	92.4	96.7	96.7	3.3	7.6	94.5	
	SVM	LC	95.4	92.4	92.4	7.6	4.6	93.9	93.9
		NLC	92.4	95.4	95.4	4.6	7.6	93.9	
	RF	LC	97.7	93.9	93.9	6.1	2.3	95.8	95.8
		NLC	93.9	97.7	97.7	2.3	6.1	95.7	
	KNN	LC	95.4	89.7	89.4	10.6	4.6	92.5	92.4
		NLC	89.4	95.3	95.4	4.6	10.6	92.3	
	NB	LC	97.7	92.3	92.1	7.9	2.3	94.9	94.9
		NLC	92.1	97.7	97.7	2.3	7.9	94.8	
	ResNet-18	**LC**	**98.8**	91.9	91.2	8.8	1.2	95.2	95.0
		NLC	91.2	98.6	98.8	1.2	8.8	94.8	

2.2 OPTIMIZING KEY LANE CHANGE PARAMETERS TO DEVELOP MICROSIMULATION MODEL FOR ADVERSE WEATHER-BASED SAFETY ASSESSMENT

2.2.1 Introduction

Severe weather conditions, such as rain, snow, and fog, are widely recognized for their substantial influence on the safety and functionality of transportation systems. According to the Federal Highway Administration (FHWA), adverse weather is the primary factor behind approximately 1,235,000 vehicle accidents annually in the US, resulting in injuries to 418,000 individuals and the loss of 5,000 lives. Additionally, adverse weather conditions can lead to significant reductions in traffic efficiency, including decreases of up to 64 percent in free-flow speed, 44 percent in volume, and 30 percent in capacity (FHWA 2020). In a study utilizing Structural Equation Modeling (SEM) to analyze the factors influencing risky driving behavior in clear and adverse weather conditions, the results showed variations in risky behavior under different weather conditions and identified the significant role of "Human Factors." In this study that utilized the SHRP2 NDS database, the decreased driving skills were linked to increased risky behavior in adverse weather (Das and Ahmed 2022). As a result, transportation authorities allocate significant resources to develop proactive strategies and effective countermeasures to mitigate the impact of adverse weather on road users and transportation networks. One potential solution is the utilization of microsimulation models, which can replicate real-world traffic flow dynamics by simulating individual vehicle movements within the network (Hammit et al. 2019).

One of the key elements within the microsimulation model revolves around modeling driving behavior, aiming to accurately depict how drivers make decisions such as lane changes, following leading vehicles, or selecting optimal routes within the network. These driving behavior models encompass various parameters, each associated with default values. However, these default parameter values typically lack specificity regarding local conditions, as driver behavior exhibits significant variations across different geographic regions, environmental contexts, and traffic attributes. Consequently, it becomes imperative to adapt these default parameters to align with local conditions, ensuring the attainment of realistic results from microsimulation (Al-Ahmadi et al. 2019).

Adjusting the driving behavior models within microsimulation can be accomplished through the utilization of both macroscopic and microscopic data. Macroscopic data refers to aggregated traffic data sourced from spot sensors, loop detectors, and similar devices. In contrast, microscopic data involves detailed, disaggregated trajectory-level information pertaining to individual vehicles. When it comes to making adjustments, macroscopic data may not be the most suitable choice due to its limited resolution, which fails to capture the nuances of realistic driving behavior in microsimulation models. In recent years, the availability of high-resolution microscopic trajectory-level data has ushered in new opportunities for enhancing and fine-tuning driving behavior models within microsimulation (Hammit et al. 2019; Reiter 1994).

2.2.2 Background

Many studies have focused on updating and calibrating microsimulation models to account for different weather conditions and their effects on driving behavior. These assessments have primarily relied on macroscopic data. For instance, (Rakha, Arafeh, and Park 2012) developed an approach that calibrated non-steady-state car-following models using macroscopic field data. Their findings indicated that rainy conditions led to a 5 percent reduction in light-duty vehicle speeds and a 3 percent reduction in heavy-duty vehicle speeds. Moreover, they noted that speed reductions were even more pronounced in snowy conditions.

Khavas, Hellinga, and Masouleh 2017 introduced a method to assess the impact of adverse weather on the VISSIM microsimulation model. This method identified key driving behavior parameters, such as lane change and car-following, essential for capturing weather effects. Another study by Zhang, Holm, and Colyar 2004 evaluated the sensitivity of weather-related traffic parameters in the CORSIM microsimulation model. They explored how adverse weather affected traffic operations and identified parameters that were particularly sensitive to such conditions.

Zhao and Sadek 2012 developed a model using the TRANSIMS microsimulation system to assess the impact of snow on transportation networks. They adjusted parameters of the Cellular Automata (CA) model within TRANSIMS to account for adverse weather, finding that snowy conditions reduced the network's capacity to handle travel demand. Additionally, Jung, Qin, and Noyce 2011 fine-tuned microsimulation models to replicate weather effects on traffic

operations, with adjustments to desired deceleration rate and desired speed distribution proving effective in rainy weather.

C. Chen et al. 2019 assessed adverse weather's impact on traffic flow characteristics by incorporating weather-influenced driving behavior parameters into microsimulation models. They evaluated variations in traffic flow characteristics under different weather conditions. Hammit et al. 2019 adjusted car-following behavior using trajectory-level data from the NDS to study traffic flow predictions in adverse weather, highlighting behavioral differences among drivers in various weather events.

While most studies have used macroscopic traffic data to update microsimulation models for different weather conditions, few have utilized microscopic trajectory-level data, especially in naturalistic settings. Additionally, there is a lack of research specifically addressing the adjustment of key lane change parameters in microsimulation platforms across various weather conditions.

Recognizing these research gaps, this study aims to enhance and adapt lane change models for the development of realistic microsimulation models under diverse weather conditions. This objective will be accomplished by leveraging trajectory-level data from the SHRP2 NDS to assess the safety and operational impacts of adverse weather. This study has been divided into two sections. In the first section, the study focuses on finding the lane change parameters based on SHRP2 NDS database for adverse weather conditions and evaluating the parameter's performance on a custom freeway segment while section 2 will focus on using those parameters in a microsimulation model for the actual I-80 segments of Wyoming. The research goals of this study include:

- Developing a novel approach to identify, extract, and incorporate key lane change parameters into microsimulation models under varying weather conditions.
- Evaluating the safety impacts of adverse weather using the Surrogate Safety Assessment Model (SSAM) and considering vehicle trajectory data from the VISSIM microscopic simulation model.
- Assessing the network-wide impacts of adverse weather on traffic operations by applying the identified parameters.

- Insights into the potential applicability of this methodology for transportation agencies seeking to enhance their contemporary microsimulation modeling practices.

2.2.3 Methodology

The research objective in this study was achieved by employing trajectory-level naturalistic driving data obtained from the SHRP2 NDS. The Virginia Tech Transportation Institute (VTTI) was responsible for overseeing the comprehensive data collection process (Campbell 2012). For the purposes of this study, a subset of the extensive SHRP2 NDS data was utilized. The research team extracted NDS traversals occurring under various weather conditions, including clear, rain, snow, and fog, employing innovative data extraction methods outlined in Ahmed et al. 2018; Das, Ghasemzadeh, and Ahmed 2019; Ghasemzadeh et al. 2019; Khan, Ghasemzadeh, and Ahmed 2018. Identification of NDS trips in adverse weather was primarily based on supplementary weather data obtained from the National Climatic Data Center (NCDC), as well as weather-related crash reports. These data extraction techniques allowed for the collection of NDS trips conducted in both clear and various adverse weather conditions.

The subsequent data processing step involved the identification of lane change events within the collected SHRP2 NDS trips. The automated algorithm was developed, utilizing front-facing NDS radar data. It is worth noting that NDS vehicles were equipped with front-mounted radar systems that limited their ability to detect vehicles traveling behind them. Consequently, the algorithm focused on scenarios where vehicles performed lane changes from adjacent lanes to the lane of the NDS vehicle. In essence, the NDS vehicle acted as a following vehicle, and key information about the lane-changing vehicles, including speed, acceleration, and longitudinal and lateral positions, was recorded through the NDS forward radar. Additionally, vehicle kinematics and machine vision-based data from the NDS trips contributed to the development of this automated algorithm. Detailed information on the algorithm's development and formation can be found in Section 1 of this chapter (Das, Khan, and Ahmed 2020).

Following the algorithmic identification of lane changes, all such events were subject to manual verification using the Wyoming NDS Visualization and Visibility Identification Tool (Ahmed et al. 2018). During this manual verification process, the predominant weather conditions and

specific lane change maneuver types were annotated for each lane change event. Weather conditions were categorized into seven distinct classes, including clear, light rain, heavy rain, light snow, heavy snow, distant fog, and heavy fog. This categorization relied on several criteria, such as the visibility of roadside surroundings, road markings, readability of road signs, concentration of raindrops and snowflakes, and the horizon. To minimize potential biases and errors during the manual verification process, the research team received extensive training and detailed descriptions of various weather conditions, along with sample weather images as illustrated in Figure 15 and Table 5 (Khan, Das, and Ahmed 2020). In addition, lane change maneuver types were grouped as mandatory and discretionary considering different types of maneuvers identified from video observations as demonstrated in a previous study (Das and Ahmed 2019).

(a) Clear

(b) Light Rain

(c) Heavy Rain

(d) Light Snow

(e) Heavy Snow

(f) Distant Fog

(g) Heavy Fog

Figure 15 Sample Images of Various Weather Conditions

Table 5 Criteria for Annotating Predominant Weather Conditions (Khan et al., 2020)

Weather Categories	Criteria
Clear	• **High visibility** • **Road signs, markings, and surroundings are visible**
Light Rain	• **Clearly visible raindrops** • **Low swipe rate of wipers** • **Dry/Slightly wet road surfaces** • **Clear/Moderate visibility** • **Road markings and information on road signs and vehicle(s) ahead could be recognized**
Heavy Rain	• **Raindrops could be visible** • **High swipe rate of wipers** • **Wet road surface** • **Affected visibility** • **Road markings and information on road signs and vehicle(s) ahead could not be recognized**
Light Snow	• **Clearly visible snowflakes** • **Low swipe rate of wipers** • **No/Little snow on the road surface** • **Clear/Moderate visibility** • **Road markings and information on road signs and vehicle(s) ahead could be recognized**
Heavy Snow	• **Clearly visible snowflakes** • **High Wiper Status** • **Snow on the road surface** • **Affected visibility** • **Road markings and information on road signs and vehicle(s) ahead could not be recognized**
Distant Fog	• **The horizon cannot be defined** • **Roadside surroundings and traffic ahead are visible** • **Road markings and information on road signs could be easily recognized**
Heavy Fog	• **The horizon cannot be defined** • **Only a few road markings could be observed** • **Roadside surroundings, information on the road signs, and traffic ahead could not be easily recognized**

2.2.4 Generic Segment Microsimulation Analysis Implementation

A total of 439 lane changes corresponding to 314 trips were verified and considered for the analysis. Table 6 summarizes the final annotated number of lane changes associated with each weather event.

Table 6 Summary of Number of Lane Changes in Each Weather Condition

Weather Categories	Lane Change Maneuver Types		Total No. of Lane Changes	Number of Trips Associated with Lane Change
	Mandatory	Discretionary		
Clear	74	94	168	138
Light Rain	16	57	73	49
Heavy Rain	7	47	54	39
Light Snow	15	18	33	21
Heavy Snow	12	19	31	26
Distant Fog	8	38	46	39
Heavy Fog	8	26	34	30

2.2.4.1 Lane Change Model Parameter Extraction

In this research, PTV's VISSIM microsimulation software, a widely recognized platform among both practitioners and researchers, has been employed to fine-tune lane change parameters. The initial step in enhancing the microsimulation model involved the extraction of essential lane change parameters across various weather conditions. In the VISSIM environment, lane change events involve two distinct vehicles: the "Own Vehicle," denoting the lane-changing vehicle, and the "Trailing Vehicle," representing the vehicle trailing behind the lane-changing one (PTV Group, 2018).

A parallel situation was observed in the NDS dataset, where the NDS vehicle assumed the role of the "Trailing Vehicle," and the vehicle executing the lane change into the same lane as the NDS vehicle acted as the "Own Vehicle." As previously mentioned, the team devised an automated algorithm to identify these specific lane change scenarios and the associated parameters required for the microsimulation model update. Figure 16 provides a visual depiction of a typical lane change scenario occurring in clear weather conditions.

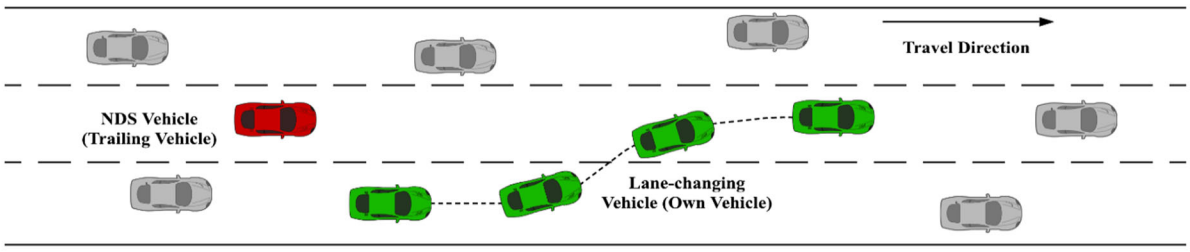

Figure 16 A Typical Lane Change Scenario Observed in the NDS Data

In VISSIM, the lane change maneuvers executed by vehicles can be categorized into two distinct groups: necessary lane changes and free lane changes. Necessary lane changes are driven by route considerations, primarily aimed at reaching the next connector of a designated route, such as exiting from a freeway. On the other hand, free lane changes are undertaken with the objective of improving driving conditions, which typically involve achieving higher speeds and maintaining greater following distances (Habtemichael and Santos 2012). Hence, these two categories correspond to mandatory and discretionary lane changes, respectively.

VISSIM defines a necessary lane change based on three critical parameters that govern deceleration, both for the vehicle initiating the lane change and any trailing vehicles (Habtemichael and Santos 2012; PTV Group 2018):

- Maximum Deceleration (Own/Trailing): This parameter denotes the maximum allowable deceleration for both the vehicle initiating the lane change and any trailing vehicles during the lane-changing process.
- Accepted Deceleration (Own/Trailing): It establishes the minimum acceptable deceleration for both the vehicle initiating the lane change and trailing vehicles involved in the maneuver.
- Reduction Rate of Acceleration: -1 ft/s2 per distance (Own/Trailing): This parameter operates linearly to reduce the maximum deceleration as the distance from the emergency stop position increases.

Conversely, for Free Lane changes in VISSIM, the following three parameters are considered of utmost importance (Habtemichael and Santos 2012; PTV Group 2018):

- Minimum Headway (Front/Rear): This parameter specifies the minimum allowable distance between two vehicles, encompassing the initiating vehicle and any trailing vehicles, following a lane change. Safety Distance Reduction Factor: It represents a

multiplicative factor that reduces the original safety distance during the execution of a lane change.

- Maximum Deceleration for Cooperative Braking: This parameter defines the cooperative deceleration level required for a trailing vehicle, allowing a lead vehicle (i.e., the initiating vehicle) to change lanes safely.

It is worth noting that within VISSIM, there may be other parameters that could potentially trigger lane change events. However, for the purpose of this study, we hypothesized that lane change maneuvers primarily rely on the key parameters associated with necessary and free lane changes. After identifying these critical parameters for necessary and free lane changes in VISSIM, we proceeded to extract feasible parameters using our developed identification algorithm. Specifically, we successfully extracted two parameters: "Maximum Deceleration (Own/Trailing)" and "Accepted Deceleration (Own/Trailing)," while the parameter "Reduction Rate of Acceleration" could not be extracted due to inherent limitations in the NDS data. Similarly, for free lane changes, the algorithm provided us with two relevant parameters: "Minimum Headway (Front/Rear)" and "Maximum Deceleration for Cooperative Breaking." It is worth noting that the adjustment process was performed manually to ensure reasonable and realistic parameter settings for lane changes under varying weather conditions, addressing the practical implementation challenge. In particular, the median value for each parameter was selected as the representative parameter in each weather condition, following the recommendation of a prior study (Hammit et al. 2019). This sampling technique was further validated through an optimization process employing a 10-fold cross-validation approach, which yielded the lowest mean absolute error.

However, for the extraction of the remaining free lane change parameter, "Safety Distance Reduction Factor," a different approach was employed. Drawing from previous study findings (Khan, Das, and Ahmed 2020), it was observed that drivers significantly reduced their speeds in adverse weather conditions. Consequently, we used the observed percentages of speed reduction in different adverse weather scenarios to calculate the "Safety Distance Reduction Factor," while retaining the default value for clear weather conditions.

In conclusion, all the lane change parameters, including those related to weather conditions, were documented for each weather scenario. These parameters were taken into consideration during the evaluation of the network-wide impacts of adverse weather on both traffic safety and operational efficiency.

2.2.4.2 Development of the VISSIM Model

The study proceeded by evaluating the obtained lane change parameters' performance within the VISSIM microsimulation platform, focusing on a straightforward freeway weaving segment. This choice of a weaving segment was made due to the prevalence of lane change events on such freeway sections and their substantial influence on both safety and traffic flow efficiency. The design of the freeway segment adhered to the guidelines outlined in the Highway Capacity Manual (HCM) and featured four lanes in one direction, complete with three on-ramps and three off-ramps, as depicted in Figure 17. To simulate real-world conditions, vehicles were introduced into the freeway via four entrances indicated by green arrows. Moreover, varying entering volumes were implemented at each of the four entrances to represent the overall network's loading. To enhance the realism of the simulation, essential routing decisions were assigned to the entering traffic at each of these four entrances.

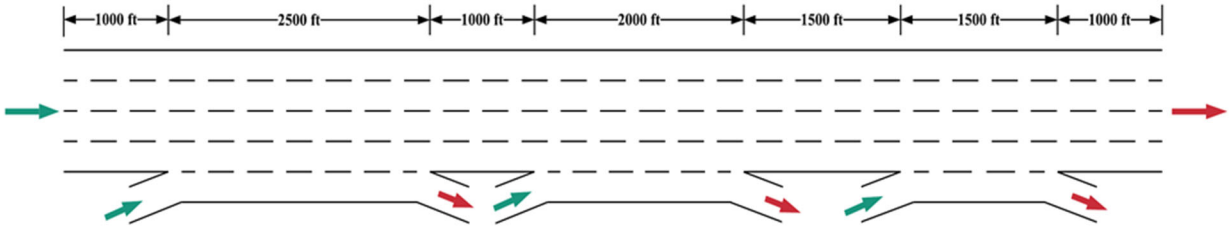

Figure 17 A Simple Freeway Segment Created in VISSIM Platform

It is important to note that constructing a microsimulation model involves significant time investment in establishing accurate roadway geometries and traffic volume inputs. Consequently, less emphasis is often placed on adjusting driving behavior parameters. However, in this study, a deliberate effort was made to fine-tune these parameters specifically for lane changes while keeping all other simulation variables constant. This adjustment aimed

to replicate the impacts of altered lane change parameters in various weather conditions, as extracted from the SHRP2 NDS data. Figure 18 provides a visual representation of where the modifications to driving behavior parameters for lane changes were applied.

Furthermore, adjustments were made to the desired speed distribution for a chosen freeway segment under different weather conditions. To achieve this, free-flow speeds corresponding to each weather condition were derived from a prior investigation, and the desired speed distribution in VISSIM was modified accordingly (Khan, Das, and Ahmed 2020). As an example, under heavy rain conditions, the 85th percentile and 15th percentile of vehicle free-flow speeds were identified as 68.92 mph and 51.07 mph, respectively. A cumulative distribution function was then created, encompassing free-flow speeds ranging from 25.26 mph to 79.87 mph. Figure 19 provides a visual illustration of the approach employed to establish the desired speed distribution in heavy rain conditions.

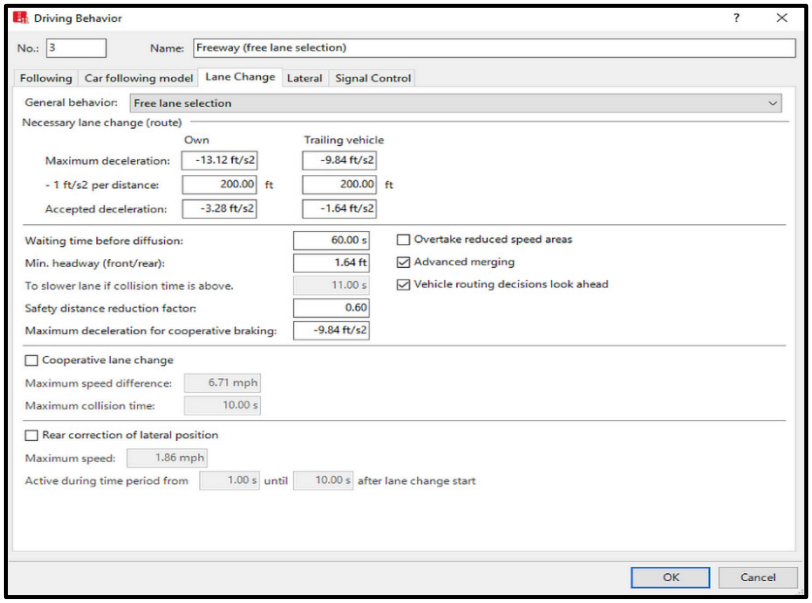

Figure 18 Snapshot of lane change parameters from VISSIM

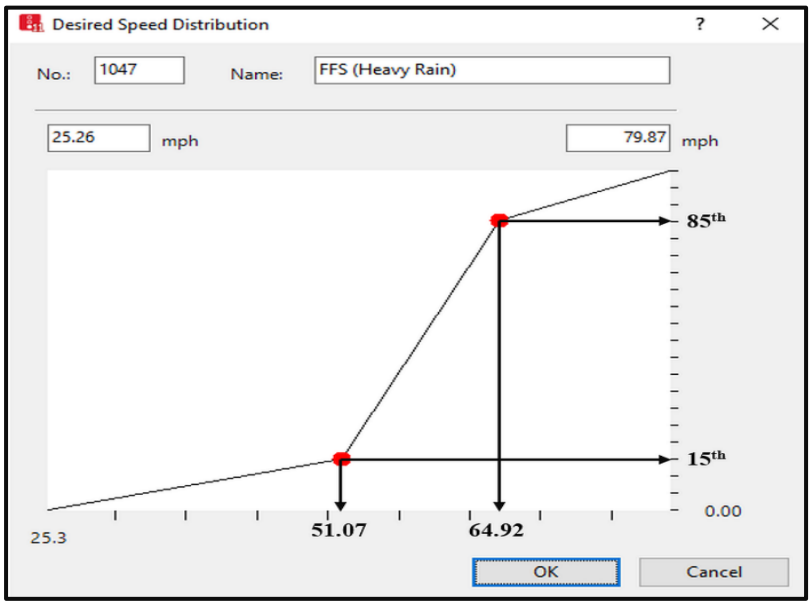

Figure 19 Snapshot of Desired Speed Distribution in VISSIM after adjustment for Heavy Rain

Taking this approach into consideration, simulation models were developed using VISSIM to simulate various weather conditions. Each weather condition was subjected to a 1-hour simulation run, preceded by a 10-minute warmup period. It is important to note that when working with simulation data, the aggregation of data at appropriate time and distance intervals is crucial for accurately defining traffic flow parameters. As such, we followed the recommendations of a prior study (Lu, Varaiya, and Horowitz 2009) and aggregated the data from each simulation run at 20-second time intervals and 500-foot distance intervals.

In total, 10 simulations were conducted for each distinct weather condition. The simulated data from each individual run were then compiled and analyzed to assess the safety implications of adverse weather. Additionally, this data made it possible to establish essential relationships among traffic flow parameters and other operational characteristics within the network for each weather condition. For a visual representation of this study's overall methodology, refer to Figure 20.

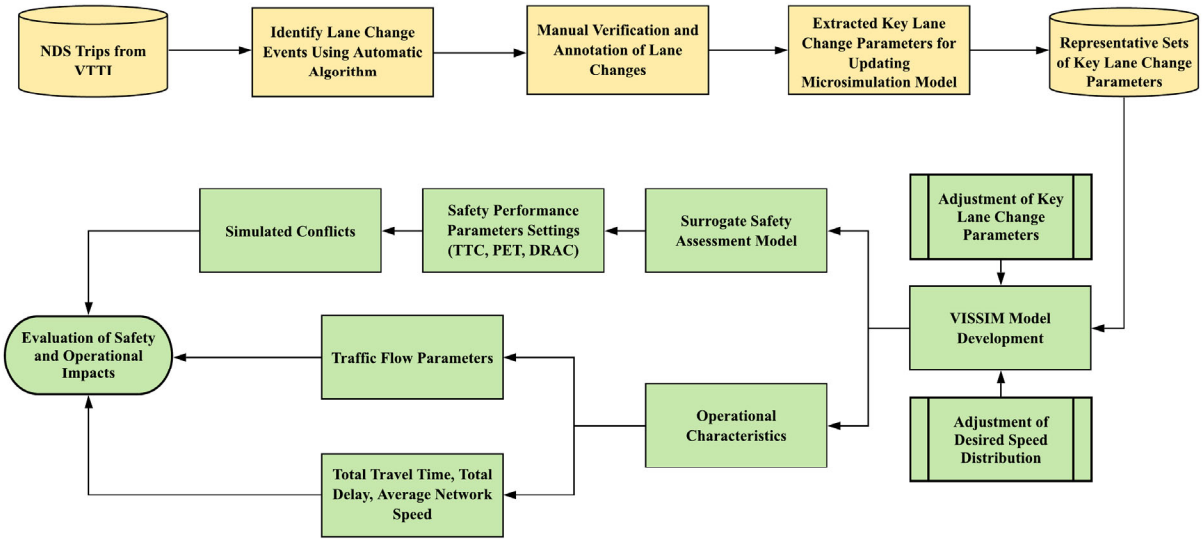

Figure 20 Flow Chart Summarizing the Overall Methodology to Adjust Key Lane Change Parameters in Microsimulation for Assessing Safety and Operational Impacts of Adverse Weather

2.2.4.3 Results and Discussions

2.2.4.3.1 Adjusted Key Lane Change Parameters

As previously mentioned, the median values of lane change parameters were considered to represent each weather condition effectively. Table 7 presents the adjusted lane change parameters in VISSIM for both the own vehicle and the trailing vehicle. While these values were adjusted separately, it is crucial to comprehend their interrelation and their influence on driving behavior. In Table 7, it can be observed that the maximum decelerations for the own vehicle in light rain, heavy rain, and distant fog are lower compared to clear weather. The highest value is attributed to heavy fog in clear contrast. Conversely, all maximum decelerations for the trailing vehicle in various weather conditions are lower when compared to clear weather, except for light rain. Regarding the adjusted accepted decelerations for the own vehicle, heavy snow presents the highest accepted deceleration, while light snow exhibits the lowest. However, relatively similar values are obtained for the adjusted accepted decelerations of the trailing vehicle across different weather conditions.

Table 7 also presents the adjusted free lane change parameters for different weather conditions. In light snow, it can be observed that the minimum rear headway is higher than in clear weather, followed by heavy rain and light rain conditions. It is noteworthy that the minimum rear headways in distant fog and heavy fog are comparatively lower than in clear

weather. In foggy weather, reduced visibility limits drivers' vision, causing them to perform lane changes more rapidly and resulting in shorter headways. As discussed earlier, the default safety distance reduction factor value for clear weather was kept the same while adjusting values for other weather conditions to simulate adverse weather effects. Consequently, all safety distance reduction factors are lower than those in clear weather, indicating a relatively higher reduction in safety distance during lane changes in adverse weather.

Lastly, the results of the adjusted maximum deceleration for cooperative braking show that rain and fog conditions are associated with lower deceleration values compared to clear weather. However, the highest deceleration value is observed in heavy snow, while the lowest is linked to light rain.

Table 7 Adjusted Necessary and Free Lane Change Parameters

Type of Lane Change	Parameters	Weather Conditions						
		Clear	Light Rain	Heavy Rain	Light Snow	Heavy Snow	Distant Fog	Heavy Fog
Necessary Lane Change	Maximum Deceleration-Own Vehicle (ft/s^2)	-11.38	-10.90	-5.74	-20.47	-15.21	-8.50	-26.36
	Accepted Deceleration- Own Vehicle (ft/s^2)	-0.11	-0.07	-0.04	-0.01	-0.21	-0.10	-0.02
	Maximum Deceleration-Trailing Vehicle (ft/s^2)	-1.78	-1.91	-1.31	-0.65	-0.64	-1.21	-1.21
	Accepted Deceleration-Trailing Vehicle (ft/s^2)	-0.09	-0.09	-0.09	-0.09	-0.06	-0.09	-0.09
Free Lane Change	Minimum Headway (Rear) (ft)	104.41	127.98	129.97	136.90	102.36	97.17	89.50
	Safety Distance Reduction Factor	0.6	0.58	0.54	0.51	0.42	0.59	0.56
	Maximum Deceleration for Cooperative Breaking (ft/s^2)	-1.70	-0.93	-1.40	-1.80	-2.05	-1.26	-1.31

2.2.4.3.2 Assessment of Safety Impacts of Adverse Weather

The examination focused on assessing the safety implications of adverse weather conditions for the adjusted parameters. It is important to note that microsimulation software cannot directly detect vehicle collisions. Instead, recent practice has advocated for the use of Surrogate Measures of Safety (SMoS) extracted from vehicle trajectory files (.trj files) as an effective method for safety evaluation (Fink, Kwigizile, and Oh 2016; Huang et al. 2013; Wu, Radwan, and Abou-Senna 2018). In this investigation, a safety assessment approach was employed, utilizing the SSAM. To gauge the severity of simulated conflicts, SSAM relies on safety assessment parameters such as Time-to-Collision (TTC), Post Encroachment Time (PET), and others. If the minimum values of these parameters between two vehicles exceed the default threshold values, SSAM identifies a conflict (Fan et al. 2013; Yang and Ahmed 2020).

Furthermore, this research incorporated three distinct types of SMoS—TTC, PET, and Deceleration Rate to Avoid Collision (DRAC)—to gauge the risk of crashes across varying weather conditions. According to Yang et al., TTC can be defined as the time required for two vehicles to collide if they maintain their current speeds and trajectories, which can be expressed mathematically as follows (Yang, Ahmed, and Adomah 2020):

$$TTC = \begin{cases} \frac{X_{1-2}}{V_2 - V_1}, & if V_2 > V_1 \\ \infty, & Otherwise \end{cases} \quad (8)$$

The first metric under consideration is the Time-to-Collision (TTC) parameter denoted as X(1-2), which signifies the gap distance between the leading and following vehicle. Concurrently, V1 and V2 represent the speeds of the leading and following vehicles, respectively. This parameter is not only commonly employed for safety analysis but also serves as a crucial warning measure in automobile collision avoidance systems and driving assistance systems (Mahmud et al. 2017). The vehicle trajectory data extracted from the VISSIM models were subsequently processed in the SSAM to identify simulated conflicts occurring in various weather conditions. To determine the total number of simulated conflicts, encompassing both lane change and rear-end conflicts, the default TTC threshold value of 1.5 seconds, a value frequently utilized in previous research (Gallelli et al. 2019; Xu et al., 2020), was employed. However, this study diverged by considering three distinct TTC thresholds: high risk (TTC = 1.5 s), medium risk (TTC = 3.5 s), and low risk (TTC = 9 s), aligning with the characteristics of the studied freeway segment and following the approach outlined in a prior study to qualitatively assess simulated conflicts across various weather conditions and conflict types (G. Yang, Ahmed, and Adomah 2020).

A second significant metric, Post Encroachment Time (PET), represents the time interval between the departure of the first vehicle from a conflict point and the approach of the second vehicle to that same point (Paul 2019). PET holds an advantage over TTC as it doesn't require speed estimation or distance measurements from the mutual conflict point. Moreover, PET is better suited for identifying critical conflicts compared to TTC (Mahmud et al. 2017; Paul 2019). In this study, PET thresholds, ranging from 0 to 10, were offered by SSAM to estimate conflict occurrences. However, critical conflicts were identified based on a PET threshold of less than 1 second, in accordance with AASHTO guidelines, in addition to tabulating the overall number of conflicts for each scenario (AASHTO 2001).

Lastly, the third significant metric considered is Deceleration Rate to Avoid Collision (DRAC), defined as the minimum deceleration rate that the following vehicle must achieve to prevent a potential collision with the leading vehicle. This metric can be mathematically expressed as follows (Wang and Stamatiadis 2013):

$$DRAC = \begin{cases} \frac{(V_2 - V_1)^2}{2X_{1-2}}, & if\ V_2 > V_1 \\ 0, & Otherwise \end{cases} \quad (9)$$

The evaluation of safety performance relies on a crucial indicator denoted as DRAC, where V1 and V2 represent the speeds of the leading and following vehicles, respectively, while X(1-2) signifies the net distance gap between these two vehicles. This indicator is valued for its ability to account for variations in speeds and decelerations within traffic flow, making it an effective measure. AASHTO has set a threshold, considering a DRAC value exceeding 3.4 m/s^2 as potentially critical (AASHTO 2001). To gauge the severity of conflicts in diverse weather conditions, this study employs the identified critical DRAC situations for analysis.

Table 8 presents the outcomes regarding the total number of conflicts, including lane change and rear-end conflicts, associated with different weather conditions and three TTC thresholds. A positive percentage in Table 8 indicates that a parameter's observed value was higher in comparison to clear weather conditions. The simulated results reveal a significant reduction in the number of conflicts as the TTC threshold increases, signifying a shift towards lower risk scenarios. Notably, under extreme adverse weather conditions, especially in heavy rain, heavy snow, and heavy fog, the total number of conflicts was found to be higher than clear weather for all three TTC thresholds. This outcome aligns with real-world observations, as adverse weather conditions, characterized by limited visibility, degraded vehicle performance, and poor road surface conditions, negatively influence driver behavior and performance, resulting in a higher number of conflicts.

Conversely, in light rain and distant fog, the simulated total number of conflicts, as well as lane change and rear-end conflicts, was lower than in clear weather, as shown in Table 8 for all three TTC thresholds. This trend may be attributed to drivers' heightened caution in these conditions, which offer relatively better visibility, reflecting their real-life driving behavior. Additionally, it's worth noting that the total number of conflicts remained consistently low when default

parameters were considered, highlighting their limitations in capturing representative scenarios across various weather conditions.

Table 8 Simulation Results of Conflicts Based on Three TTC Levels

Conditions	Total Conflicts Per hour	Increase in Risk from Clear (percentage)	Lane Change Conflicts Per hour	Increase in Risk from Clear (percentage)	Rear End Conflicts Per hour	Increase in Risk from Clear (percentage)
High Risk						
Default	316	-65.6	105	-57.7	211	-68.5
Clear	921	-	249	-	672	-
Light Rain	877	-4.8	226	-9.4	651	-3.1
Heavy Rain	1132	22.9	265	6.3	867	29.0
Light Snow	1196	29.8	263	5.4	933	38.8
Heavy Snow	1616	75.4	344	37.9	1272	89.3
Distant Fog	772	-16.2	217	-13.1	555	-17.3
Heavy Fog	954	3.6	259	3.9	695	3.5
Medium Risk						
Default	155	-49.7	39	-43.6	116	-51.5
Clear	308	-	69	-	239	-
Light Rain	305	-1.2	68	-2.0	237	-1.0
Heavy Rain	438	41.9	108	56.3	330	37.8
Light Snow	481	56.1	118	71.1	363	51.8
Heavy Snow	702	127.8	179	159.0	523	118.7
Distant Fog	267	-13.4	62	-10.9	205	-14.2
Heavy Fog	355	15.0	87	25.6	268	11.9
Low Risk						
Default	77	-50.0	20	-31.2	57	-54.4
Clear	153	-	29	-	124	-
Light Rain	148	-3.1	28	-4.1	120	-2.9
Heavy Rain	194	26.4	38	29.8	156	25.6
Light Snow	201	31.3	44	50.7	157	26.8
Heavy Snow	347	126.3	90	207.9	257	107.1
Distant Fog	126	-17.5	22	-24.0	104	-16.0
Heavy Fog	169	10.1	34	15.4	135	8.8

Table 9 presents the simulation results concerning conflicts and critical conflicts in relation to PET. Much like the TTC, severe adverse weather conditions yielded a notably higher count of overall conflicts and critical conflicts when compared to clear weather conditions. Furthermore, the simulated total count of estimated conflicts and critical conflicts was observed to be lower during episodes of light rain and distant fog than in clear weather. It's important to highlight

that the percentage increase in risk relative to clear weather conditions was consistent, particularly for the high-risk TTC category, across various scenarios, particularly for total and rear-end conflicts. Nevertheless, it's worth noting that a significant proportion of the simulated conflicts were flagged as critical conflicts under all conditions. For example, out of the 1,119 total conflicts recorded during clear weather conditions, a substantial 927 (82.8 percent) of these conflicts met the criteria for critical conflicts based on a specific PET threshold (i.e., less than 1 second).

Table 9 Simulation Results of Conflicts Based on PET

Conditions	Total Conflicts Per hour	Increase in Risk from Clear (percentage)	Lane Change Conflicts Per hour	Increase in Risk from Clear (percentage)	Rear End Conflicts Per hour	Increase in Risk from Clear (percentage)
Default	477	-57.3	134	-52.8	343	-58.9
Clear	1119	-	284	-	835	-
Light Rain	1071	-4.3	250	-12.2	821	-1.6
Heavy Rain	1364	21.8	285	0.1	1079	29.3
Light Snow	1437	28.4	289	1.6	1148	37.6
Heavy Snow	1993	78.1	425	49.3	1568	87.9
Distant Fog	942	-15.8	240	-15.5	702	-15.9
Heavy Fog	1176	5.1	287	0.8	889	6.6
Critical Conflicts (PET < 1 s)						
Default	388	-58.2	116	-44.1	272	-62.2
Clear	927	-	208	-	719	-
Light Rain	880	-5.1	180	-13.5	700	-2.7
Heavy Rain	1121	20.9	215	3.3	906	26.0
Light Snow	1157	24.7	208	-0.2	949	32.0
Heavy Snow	1592	71.7	318	52.9	1274	77.1
Distant Fog	791	-14.7	182	-12.7	609	-15.3
Heavy Fog	980	5.6	217	4.2	763	6.0

Table 10 presents the simulation results for conflicts generated by SSAM in scenarios where DRAC values exceed 3.4 m/s^2. As anticipated, these results align with the earlier findings derived from TTC and PET assessments, particularly regarding the total number of conflicts, including lane change and rear-end conflicts. The data in Table 10 reveals a clear trend: the risk of encountering potentially critical driving situations escalates significantly during severe adverse weather conditions, such as heavy rain, heavy snow, and heavy fog. Consequently, the number of simulated conflicts is notably higher under these adverse conditions compared to

clear weather. Furthermore, a consistent pattern emerges when examining the percentage change in risk from clear weather across various conditions. Therefore, we can draw parallel conclusions for the conflict results, mirroring the insights previously discussed for TTC and PET.

Table 10 Simulation Results of Conflicts with Potentially Critical Situations Based on DRAC

Conditions	Total Conflicts Per hour	Increase in Risk from Clear (percentage)	Lane Change Conflicts Per hour	Increase in Risk from Clear (percentage)	Rear End Conflicts Per hour	Increase in Risk from Clear (percentage)
Default	274	-64.7	85	-51.7	189	-68.5
Clear	776	-	176	-	600	-
Light Rain	731	-5.7	165	-6.5	566	-5.5
Heavy Rain	941	21.3	196	11.2	745	24.3
Light Snow	976	25.9	190	8.1	786	31.1
Heavy Snow	1305	68.3	247	40.3	1058	76.5
Distant Fog	665	-14.2	159	-9.8	506	-15.5
Heavy Fog	792	2.2	181	3.0	611	1.9

2.2.4.3.3 Operational Characteristics Evaluation

The VISSIM simulation results for operational assessments are presented in Table 11. To evaluate traffic flow characteristics under various weather conditions, we compared the default and updated parameters to clear weather conditions. We examined the maximum flow rate for each weather condition and measured the corresponding speed at that maximum flow rate. Subsequently, we calculated density based on the observed speed, utilizing the fundamental relationship between these factors. Given that the network included multiple weaving segments, we anticipated frequent lane changes near on-ramps and off-ramps (i.e., merge and diverge points). Consequently, we expected variations in lane changes across different weather conditions.

Table 11 reveals noteworthy enhancements in maximum flow rates during rainy and foggy conditions compared to clear weather, while snow conditions showed little to no improvement. The speed at the maximum flow rate for clear weather was recorded at 45.4 mph. Intriguingly, in most adverse weather scenarios, observed speeds at the maximum flow rate increased by approximately 14 percent to 30 percent, with an 11 percent decrease in heavy snow.

Correspondingly, density at the maximum flow rate decreased in all adverse weather conditions except for heavy snow, mirroring the speed pattern. The simulation results for jam density indicated that there were generally no density changes between clear and adverse weather conditions.

Furthermore, an examination of the simulation outcomes revealed that default parameters consistently yielded significantly higher speeds and lower densities at the maximum flow rate compared to the updated parameters. As a result, default parameters are not suitable for the development of microsimulation models.

Table 11 Simulation Results of Traffic Flow Characteristics

Conditions	Max. Flow Rate (veh/hr/ln)		Speed at Max. Flow Rate (mph)		Density at Max. Flow Rate (veh/mi/ln)		Jam Density (veh/mi/ln)	
	Observed	Percentage Change from Clear	Observed	Percentage Change from Clear	Observed	Percentage Change from Clear	Observed	Percentage Change from Clear
Default	1840	6.1	63.1	38.8	29	-23.6	84	-2.9
Clear	1734	-	45.4	-	38	-	86	-
Light Rain	1909	10.1	57.5	26.4	33	-12.9	86	0.0
Heavy Rain	1898	9.4	52.3	15.0	36	-4.8	86	0.0
Light Snow	1728	-0.4	51.7	13.8	33	-12.4	86	0.0
Heavy Snow	1736	0.1	40.3	-11.4	43	12.9	86	0.0
Distant Fog	1898	9.4	59.1	30.1	32	-15.9	85	0.9
Heavy Fog	1839	6.1	55.1	21.3	33	-12.6	86	0.0

Furthermore, various performance metrics were employed to assess and compare the operational characteristics of the simulated network under varying weather conditions, including clear and adverse conditions. Table 12 presents the simulated outcomes for total travel time, total delay, and average speed based on adjusted parameters for different weather scenarios, alongside default parameters for reference. When comparing clear weather with adverse weather conditions, the findings revealed a notable increase in total travel time ranging from 6 percent to 75 percent for all adverse weather situations except distant fog. Surprisingly, distant fog exhibited a 7 percent reduction in total travel time compared to clear weather.

Additionally, the analysis showed distinct patterns in total delay. Distant fog exhibited a 25 percent reduction in total delay, while other adverse weather conditions resulted in an 11

percent to 245 percent increase in total delay when compared to clear weather. Conversely, average speeds were consistently lower in all adverse weather scenarios, excluding distant fog, when compared to clear weather. Notably, heavy snow recorded the lowest average speed at 29.6 mph. These findings suggest that drivers proactively adjusted their behavior in response to reduced visibility during adverse weather, leading to lower average speeds and increased total travel time and total delay, as a general trend (Das, Ghasemzadeh, and Ahmed 2019). Moreover, an examination of the results related to default parameters indicated that these parameters should not serve as representative values. The data in Table 12 clearly illustrates that different outcomes were obtained for various weather conditions, reinforcing the necessity of tailored parameter settings for accurate simulations.

Table 12 Simulation Results of Total Travel Time, Total Delay, and Average Speed

Conditions	Total Travel Time (hr)	Percentage Change from Clear	Total Delay (hr)	Percentage Change from Clear	Average Speed (mph)	Percentage Change from Clear
Default	0.47	-5.0	0.04	-55.5	54.5	4.4
Clear	0.49	-	0.09	-	52.2	-
Light Rain	0.52	5.8	0.10	11.3	49.3	-5.6
Heavy Rain	0.62	24.7	0.15	77.8	41.6	-20.3
Light Snow	0.66	32.7	0.18	111.0	39.1	-25.1
Heavy Snow	0.86	74.8	0.30	245.2	29.6	-43.4
Distant Fog	0.46	-6.7	0.06	-24.6	55.9	7.0
Heavy Fog	0.55	10.6	0.11	23.5	47.3	-9.5

2.2.5 Wyoming-specific Segment Microsimulation Analysis

Results from previous study were extended to a 7-mile Wyoming-specific segment. Lane-change maneuvers occurring in freeway weaving segments (FWS) and basic freeway segments (BFS) were grouped using ArcGIS software.

In total, the study verified and utilized 723 lane-change events occurring in various weather conditions and freeway segments. Table 13 provides details regarding the number of lane-change events corresponding to different weather conditions and types of freeway facilities.

Table 13 Lane changes in each Weather and Freeway facility types

Weather	Freeway Facility Types		Total
	FWS	**BFS**	
Clear	168	290	458
Rain	54	71	125
Snow	32	30	62
Fog	44	34	78
Total	**298**	**425**	**723**

The initial section of this study aimed to identify lane-change parameters that accurately represent different weather conditions and could be employed to create weather-specific microsimulation models. Using the developed identification algorithm, potential parameters were extracted, while the remaining parameters were sourced from previous research findings. Among microsimulation tools, PTV VISSIM was chosen as the most suitable for adjusting these lane-change parameters.

Subsequently, a Geographic Information System (GIS)-based method was employed to categorize these representative lane-change events occurring in freeway weaving segments (FWS) and basic freeway segments (BFS). The latitude and longitude coordinates of the extracted lane-change events were imported into ArcGIS software, which allowed the identification of lane-change events occurring in specific freeway facilities, following guidelines outlined in the Highway Capacity Manual (HCM). For instance, Figure 21 illustrates the

procedure for identifying lane changes based on different facility types in GIS, showcasing lane-change events in clear weather on FWS (green symbols) and BFS (red symbols).

Figure 21 Identification of lane-change events occurring in various freeway facilities: (a) lane-change events in a freeway weaving segment (I-90, New York) and (b) lane-change events in a basic freeway segment (I-90, New York).

2.2.5.1 Development of VISSIM Models and Microsimulation Scenarios

The analysis in this study was centered on two distinct freeway segments situated along Interstate 80 (I-80) in Wyoming. The first segment, known as the Freeway Weaving Segment (FWS), spans a 2-mile stretch from milepost (MP) 357 to MP 359, comprising two eastbound lanes and featuring various on- and off-ramps. The second segment, referred to as the Basic Freeway Segment (BFS), covers an equivalent 2-mile distance, extending from MP 301 to MP 303, and consists of two eastbound lanes. It's noteworthy that the BFS was thoughtfully selected to be positioned far enough from the nearest exit, aligning with guidance from the Highway Capacity Manual (HCM), to eliminate direct interactions stemming from weaving traffic movements. A visual representation of these chosen freeway segments can be found in Figure 22 of the study, offering insights into their layout and configuration.

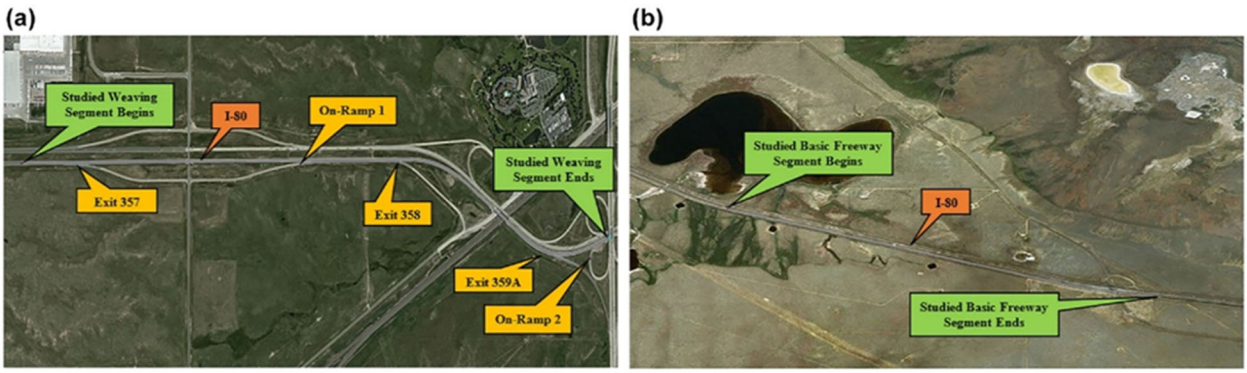

Figure 22 Layout of the considered I-80 freeway segments (images captured from VISSIM background map): (a) freeway weaving segment and (b) basic freeway segment

The essential traffic data for the chosen freeway segments were sourced from the WYDOT traffic database. These traffic volume statistics were extracted from the monthly hourly volume report for September 2020, chosen as a representative month for analysis. Peak hourly volume calculations were based on Thursdays, and the entering and exiting volumes were adjusted to ensure balance and accuracy for the specified freeway segments. It is important to note that the recorded traffic volume was relatively low because the selected segments are part of rural Interstate 80 in Wyoming, which typically experiences lower traffic volumes. Additionally, Google Earth Pro and Google Maps were utilized to gather information on roadway geometries, posted speed limits, and other network characteristics (Haq, Zlatkovic, and Ksaibati 2020).

To accurately represent the freeway segments in VISSIM, layouts were created using VISSIM's built-in background maps. The coded network's geometry, including lane counts, gradients, segment lengths, and the locations of on- and off-ramps, was further cross-checked through Google Street View to ensure that the developed models faithfully represented real-world field conditions. In VISSIM, traffic proportions were defined using two vehicle types: cars and trucks, with associated traffic compositions derived from existing data. The adjusted lane-change parameters from the SHRP2 NDS, alongside other general driving behavior parameters, were integrated into VISSIM to modify driving behavior. All other simulation parameters remained constant, ensuring that only the effect of the adjusted parameters for each weather condition was reflected in the simulation. Additionally, the desired speed distribution was adjusted based on observed free-flow speeds under various weather conditions from a prior study, and a cumulative distribution function was created, incorporating minimum, maximum, 15th, and

85th percentile free-flow speeds for each weather type (Khan, Das, and Ahmed 2020). Table 14 provides details on the adjusted lane-change parameters and other general parameters for both freeway segments. It's noteworthy that while both necessary (mandatory) and free (discretionary) lane changes were observed in the Freeway Weaving Segment (FWS), only free lane changes were found to occur in the Basic Freeway Segment (BFS).

Table 14 Adjusted Lane Change Parameters for Freeway Facility Types

Segment	Lane Change Parameters	Necessary Lane Change			
		Own Vehicle			
		Clear	Rain	Snow	Fog
FWS	Maximum Deceleration (ft/s²)	-11.38	-10.09	-18.70	-10.69
	Accepted Deceleration (ft/s²)	-0.11	-0.09	-0.07	-0.09
		Trailing Vehicle			
	Maximum Deceleration (ft/s²)	-1.78	-2.43	-0.75	-1.21
	Accepted Deceleration (ft/s²)	-0.09	-0.09	-0.06	-0.09
		Free Lane Change			
FWS	Minimum Headway (Rear) (ft)	104.41	130.81	132.57	92.39
	Safety Distance Reduction Factor	0.6	0.56	0.48	0.58
	Maximum Deceleration for Cooperative Breaking (ft/s²)	-1.70	-1.40	-1.91	-1.31
BFS	Minimum Headway (Rear) (ft)	128.29	125.25	119.37	104.46
	Safety Distance Reduction Factor	0.6	0.56	0.48	0.58
	Maximum Deceleration for Cooperative Breaking (ft/s²)	-1.12	-1.12	-1.82	-1.26
Additional Parameters					
Both Segments	Waiting Time Before Diffusion (s)	200	200	200	200
	Advanced Merging	No	No	No	No
	Cooperative Lane Change	No	No	No	No
	Lane Change Distance (ft)	1500	1500	1500	1500

As evident from Table 14, there is notable variability in the maximum and accepted decelerations for both own and trailing vehicles in different weather conditions within the Freeway Weaving Segment (FWS). It's important to clarify that these deceleration values represent the lower and upper limits within which decelerations for own and trailing vehicles will be assigned during simulation, as specified in Table 14. The variation in deceleration values stems from adjustments made based on real-world SHRP2 data, which encompassed participants from diverse driver demographics, including differences in age, gender, driving experience, and more. Additionally, the safety distance reduction factor was found to be lower

for adverse weather conditions, such as snowy conditions, compared to clear weather. This adjustment reflects the significant reduction in driver speeds during adverse weather conditions. Notably, the parameters "advanced merging" and "cooperative lane change" primarily pertain to connected and autonomous vehicles. Given that this study exclusively employed human-driven vehicles mimicking driver behavior from SHRP2 NDS and did not consider connected or automated vehicles, these two parameters were set to "OFF" during simulation (Yang, Ahmed, and Adomah 2020; Bakhshi and Ahmed 2021).

Furthermore, the study considered three different traffic volumes that could potentially occur in the selected freeway segments, considering field traffic flow conditions. These traffic volumes were designated as 600, 800, and 1000 vehicles per hour (vph). Each traffic demand level was tested across four distinct weather conditions and applied to the two different freeway segments. In total, 24 microsimulation modeling scenarios were developed within the VISSIM platform, representing the combinations of three traffic volumes, four weather conditions, and two freeway segments (i.e., 3 traffic volumes × 4 weather conditions × 2 freeway corridors = 24 scenarios). The simulation models were executed for a duration of 70 minutes, with the initial 10 minutes serving as a warm-up period. For each scenario, 10 simulation runs were conducted to account for the influence of various simulation seeds in the analysis. Simulated data were collected from each run to assess safety and operational characteristics under diverse weather conditions and demand levels for both freeway networks.

2.2.5.2 Calibration and Validation

Before delving into an investigation of existing freeway models, the study first focused on calibrating and validating the baseline models. Adjustments were made to VISSIM parameters to align them more closely with real-world driving scenarios. To establish realistic desired speeds for the two vehicle types, a custom cumulative distribution function was created based on available field speed data. This function considered the 85th percentile of speed, which corresponds to the posted speed limit. For each vehicle category, additional performance characteristics such as vehicle lengths, acceleration/deceleration capabilities, weight-to-power (W/P) ratios (particularly for trucks), and other relevant attributes were fine-tuned based on observations from the field.

Following the calibration of the existing models, validation procedures were conducted. The microsimulation models were validated by comparing real-life traffic volumes with simulated volumes, which were derived as an average of 10 simulation runs. To assess the accuracy of the simulation results, the Geoffrey E. Havers (GEH) statistic test was employed to evaluate the discrepancies between simulated and field-observed traffic volumes. This validation process aimed to ensure that the simulation models accurately replicated real-world traffic conditions, helping to establish their reliability for subsequent analyses as per Equation 10 (PTV Group 2018).

$$\text{GEH} = \sqrt{\frac{2(M_{obs}(n) - M_{sim}(n))^2}{(M_{obs}(n) + M_{sim}(n)}} \quad (10)$$

where $M_{obs}(n)$ is the observed volume from the field condition and $M_{sim}(n)$ is the simulated volume from the microsimulation modeling. The GEH statistic test results are valuable indicators of the calibration and validation quality for the baseline models. When the GEH value falls below 5, it signifies a strong match between the simulated and field-observed traffic volumes, indicating a well-calibrated model. Values ranging from 5 to 10 suggest that further investigation into calibration may be necessary, while values exceeding 10 raise concerns about the model's calibration accuracy. In Table 15, a detailed comparison is presented, showcasing the GEH statistics obtained from the comparison between simulated and real-life traffic volumes for the two freeway corridors. Notably, the GEH test results in this analysis remained within an acceptable range, indicating that the models were successfully calibrated and offering confidence in their reliability for subsequent assessments.

Table 15 GEH Test Statistics for Baseline Scenario

Segment	Location	GEH Statistic Test			
		Observed Volume (vph)	Simulated Volume (vph)	GEH Value	Acceptable (<5?)
FWS	Main Corridor	601	606	0.20	Yes
	On-Ramp 1	34	28	1.08	Yes
	On-Ramp 2	29	24	0.97	Yes
BFS	Main Corridor	630	634	0.16	Yes

Furthermore, travel times measured in the field by the WYDOT were compared with the travel

times obtained from the simulation model. The mean absolute percentage error (MAPE) statistic was used to quantify the difference between the observed travel time in the field and the simulated travel time in VISSIM. The MAPE statistic can be calculated using Equation 11 (Wu, Radwan, and Abou-Senna 2017; Moreno et al., 2013):

$$\text{MAPE} = \frac{100\%}{n}\sum_{t-1}^{n}\left|\frac{A_t - S_t}{A_t}\right| \quad (11)$$

where n represents the sample size, A_t is the actual travel time, and S_t is the simulated travel time. A lower MAPE indicates a smaller discrepancy between the observed and simulated travel times, reflecting a higher level of accuracy in the models. As shown in Table 16, the obtained MAPE values for the two freeway corridors were within an acceptable range. This outcome indicates that the baseline models for both the Freeway Weaving Segment (FWS) and the Basic Freeway Segment (BFS) were successfully validated based on travel times. With these calibrated models meeting the validation criteria, they were deemed suitable for further analysis in the study.

Table 16 MAPE Test Statistics for Baseline Scenario

Segment	MAPE Statistic Test			
	Observed Travel Time (hr)	Simulated Travel Time (hr)	MAPE Value (percent)	Acceptable?
FWS	0.0271	0.0280	3.19	Yes
BFS	0.0273	0.0279	2.18	Yes

2.2.5.3 Data Analysis

2.2.5.3.1 Safety Performance Evaluation

This study considered a safety assessment method through the SSAM to identify the potential traffic conflicts during simulations. Among various surrogate measures of safety (SMoS), three different ones, namely time-to-collision (TTC), deceleration rate to avoid collision (DRAC), and post encroachment time (PET), were utilized for assessing the risk of crashes in the two corridors under various weather. The simulated number of conflicts based on three TTC thresholds including high-risk (1.5 s), medium-risk (3.5 s), and low-risk (9 s) for each weather

condition under three demand levels are shown in Tables 17 to 19 for the two freeway segments. The results also include the relative risk ratio that was determined by dividing the number of conflicts in clear weather with the respective conflicts in adverse weather for each scenario. In general, the total number of conflicts, including lane-change and rear-end conflicts in adverse weather were found to be significantly higher than in clear weather in the majority of the scenarios. This should be attributed to driving behavior deteriorating under inclement weather, as can be experienced from real-world observation. As expected, FWS had higher conflicts than did BFS. In addition, it was observed that the number of conflicts significantly increased with the increase of demand levels.

The simulation results, specifically focusing on conflicts under the low-risk time-to-collision (TTC) threshold, are presented in Table 17. These results demonstrate that adverse weather conditions generally led to a higher number of conflicts compared to clear weather, and these differences were statistically significant based on Welch's t-test in most cases. However, it's worth noting that for the Basic Freeway Segment (BFS), especially under level 1 and level 2 demand, there were instances of insignificant differences between clear and adverse weather conditions, particularly for rear-end conflicts. This is primarily attributed to the low or zero conflict counts in these scenarios. Additionally, the number of conflicts was exceptionally low for BFS under level 1 traffic demand, which is a consequence of the microsimulation models being developed for a 2-mile BFS. Consequently, this resulted in insignificant differences in the numbers of total and lane-change conflicts in rainy and foggy conditions when compared to clear weather.

Table 18 provides simulation results for conflicts under medium-risk time-to-collision (TTC) conditions. Across all three demand levels, adverse weather conditions consistently resulted in significantly higher numbers of total conflicts and lane-change conflicts compared to clear weather. Notably, the highest conflict counts were observed under snowy weather conditions in both freeway segments. For example, in snowy conditions for the Basic Freeway Segment (BFS), the number of total conflicts indicated that the risks in snowy weather were approximately 29, 24, and 32 times higher than those in clear weather for the three demand levels.

Moving on to the simulation results for conflicts under high-risk/critical TTC conditions, Table 19 illustrates that the total number of conflicts in adverse conditions, particularly under level 3 traffic demand, was significantly higher than in clear weather for both freeway segments. This trend aligns with what was observed in the low and medium-risk TTC scenarios. However, it is worth noting that the increase in conflict counts in adverse weather for BFS, particularly in rain and snow conditions, was not as pronounced under level 1 and level 2 demand levels. This phenomenon can be attributed to the lower number of conflicts generated in such traffic demand scenarios. However, in the case of foggy weather conditions for BFS, a higher number of conflicts was observed under high-risk TTC conditions compared to other adverse weather conditions. This could be explained by the fact that driving on a Basic Freeway Segment (BFS) is less likely to result in speed reduction, especially when visibility is limited due to fog. In foggy weather, drivers tend to perceive speeds as slower than they actually are, leading to less significant speed reductions (as per reference 18). Higher speeds also increase the likelihood of encountering critical conflicts, which could account for the higher number of high-risk conflicts observed in BFS under foggy weather conditions.

Table 17 Simulation Results of Conflicts Considering Low-risk TTC Threshold (TTC = 9 s)

Volume	Segment	Weather	Total Conflicts	Relative Risk	t-Statistic	P-Value	Lane Change Conflicts	Relative Risk	t-Statistic	P-Value	Rear End Conflicts	Relative Risk	t-Statistic	P-Value
Level 1 (600 vph)	FWS	Clear	4	1.0	-	-	1	1.0	-	-	3	1.0	-	-
		Rain	10	2.5	-1.77	<0.05	1	1.0	0.00	0.50	9	3.0	-1.90	<0.05
		Snow	34	8.5	-4.97	<0.05	15	15.0	-3.93	<0.05	19	6.3	-3.92	<0.05
		Fog	13	3.3	-1.99	<0.05	7	7.0	-1.72	0.05	6	2.0	-1.34	0.10
	BFS	Clear	0	na	-	-	0	na	-	-	0	na	-	-
		Rain	2	na	-1.50	0.08	2	na	-1.50	0.08	0	na	0.00	0.50
		Snow	10	na	-4.74	<0.05	10	na	-4.74	<0.05	0	na	0.00	0.50
		Fog	2	na	-1.50	0.08	2	na	-1.50	0.07	0	na	0.00	0.50
Level 2 (800 vph)	FWS	Clear	21	1.0	-	-	4	1.0	-	-	17	1.0	-	-
		Rain	55	2.6	-2.79	<0.05	13	3.3	-2.10	<0.05	42	2.5	-2.73	<0.05
		Snow	102	4.9	-5.15	<0.05	28	7.0	-3.04	<0.05	74	4.4	-4.85	<0.05
		Fog	39	1.9	-1.47	0.08	15	3.8	-2.18	<0.05	24	1.4	-0.80	0.22
	BFS	Clear	0	na	-	-	0	na	-	-	0	na	-	-
		Rain	10	na	-3.87	<0.05	10	na	-3.87	<0.05	0	na	0.00	0.50
		Snow	27	na	-4.39	<0.05	27	na	-4.39	<0.05	0	na	0.00	0.50
		Fog	13	na	-4.99	<0.05	12	na	-6.00	<0.05	1	na	-1.00	0.17
Level 3 (1000 vph)	FWS	Clear	49	1.0	-	-	6	1.0	-	-	43	1.0	-	-
		Rain	134	2.7	-4.16	<0.05	28	4.7	-4.92	<0.05	106	2.5	-3.52	<0.05
		Snow	225	4.6	-5.85	<0.05	71	11.8	-6.53	<0.05	154	3.6	-4.87	<0.05
		Fog	122	2.5	-3.43	<0.05	41	6.8	-4.05	<0.05	81	1.9	-2.59	<0.05
	BFS	Clear	0	na	-	-	0	na	-	-	0	na	-	-
		Rain	24	na	-3.67	<0.05	22	na	-3.40	<0.05	2	na	-1.50	0.08
		Snow	70	na	-14.16	<0.05	56	na	-9.97	<0.05	14	na	-4.58	<0.05
		Fog	31	na	-4.49	<0.05	26	na	-4.63	<0.05	5	na	-1.63	0.06

Note: na = not applicable

Table 18 Simulation Results of Conflicts Considering Medium-risk TTC Threshold (TTC = 3.5 s)

Volume	Segment	Weather	Total Conflicts	Relative Risk	t-Statistic	P-Value	Lane Change Conflicts	Relative Risk	t-Statistic	P-Value	Rear End Conflicts	Relative Risk	t-Statistic	P-Value
Level 1 (600 vph)	FWS	Clear	27	1.0	-	-	16	1.0	-	-	11	1.0	-	-
		Rain	70	2.6	-3.37	<0.05	35	2.2	2.75	<0.05	35	3.2	-2.02	<0.05
		Snow	121	4.5	-6.78	<0.05	70	4.4	-9.97	<0.05	51	4.6	-2.83	<0.05
		Fog	75	2.8	-3.04	<0.05	37	2.3	-2.41	<0.05	38	3.5	-2.85	<0.05
	BFS	Clear	2	1.0	-	-	2	1.0	-	-	0	na	-	-
		Rain	7	3.5	-1.99	<0.05	7	3.5	-1.99	<0.05	0	na	0.00	0.50
		Snow	58	29.0	-8.71	<0.05	58	29.0	-8.71	<0.05	0	na	0.00	0.50
		Fog	21	10.5	-3.64	<0.05	19	9.5	-3.26	<0.05	2	na	-1.50	0.08
Level 2 (800 vph)	FWS	Clear	100	1.0	-	-	45	1.0	-	-	55	1.0	-	-
		Rain	222	2.2	-3.35	<0.05	99	2.2	-2.75	<0.05	123	2.2	-3.48	<0.05
		Snow	357	3.6	-6.46	<0.05	187	4.2	-7.52	<0.05	170	3.1	-4.53	<0.05
		Fog	144	1.4	-2.11	<0.05	88	2.0	-3.35	<0.05	56	1.0	-0.07	0.47
	BFS	Clear	4	1.0	-	-	4	1.0	-	-	0	na	-	-
		Rain	51	12.8	-6.48	<0.05	49	12.3	-6.64	<0.05	2	na	-1.50	0.08
		Snow	96	24.0	-8.87	<0.05	91	22.8	-8.28	<0.05	5	na	-3.00	<0.05
		Fog	70	17.5	-9.19	<0.05	69	17.3	-8.61	<0.05	1	na	-1.00	0.17
Level 3 (1000 vph)	FWS	Clear	204	1.0	-	-	85	1.0	-	-	119	1.0	-	-
		Rain	505	2.5	-6.43	<0.05	249	2.9	-8.07	<0.05	256	2.2	-4.44	<0.05
		Snow	800	3.9	-12.08	<0.05	414	4.9	-14.83	<0.05	386	3.2	-6.76	<0.05
		Fog	459	2.3	-3.93	<0.05	241	2.8	-4.90	<0.05	218	1.8	-2.67	<0.05
	BFS	Clear	6	1.0	-	-	6	1.0	-	-	0	na	-	-
		Rain	93	15.5	-9.97	<0.05	91	15.2	-9.83	<0.05	2	na	-1.50	0.08
		Snow	191	31.8	-14.56	<0.05	186	31.0	-14.49	<0.05	5	na	-2.24	<0.05
		Fog	176	29.3	-11.86	<0.05	164	27.3	-11.09	<0.05	12	na	-3.67	<0.05

Note: na = not applicable

Table 19 Simulation Results of Conflicts Considering High-risk/Critical TTC Threshold (TTC = 1.5 s)

Volume	Segment	Weather	Total Conflicts	Relative Risk	t-Statistic	P-Value	Lane Change Conflicts	Relative Risk	t-Statistic	P-Value	Rear End Conflicts	Relative Risk	t-Statistic	P-Value
Level 1 (600 vph)	FWS	Clear	14	1.0	-	-	3	1.0	-	-	11	1.0	-	-
		Rain	27	1.9	-1.59	0.07	6	2.0	-0.80	0.22	21	1.9	-1.74	<0.05
		Snow	52	3.7	-3.84	<0.05	15	5.0	-2.207	<0.05	37	3.4	-3.33	<0.05
		Fog	33	2.4	-2.54	<0.05	8	2.7	-1.39	0.09	25	2.3	-9.97	<0.05
	BFS	Clear	0	na	-	-	0	na	-	-	0	na	-	-
		Rain	1	na	-1.00	0.17	1	na	-1.00	0.17	0	na	0.00	0.50
		Snow	6	na	-2.71	<0.05	4	na	-2.45	<0.05	2	na	-1.50	0.08
		Fog	9	na	-3.86	<0.05	5	na	-3.00	<0.05	4	na	-2.45	<0.05
Level 2 (800 vph)	FWS	Clear	41	1.0	-	-	12	1.0	-	-	29	1.0	-	-
		Rain	104	2.5	-3.71	<0.05	28	2.3	-2.49	<0.05	76	2.6	-3.35	<0.05
		Snow	139	3.4	-5.44	<0.05	35	2.9	-3.15	<0.05	104	3.6	-5.34	<0.05
		Fog	69	1.7	-1.87	<0.05	20	1.7	-1.44	0.08	49	1.7	-1.81	<0.05
	BFS	Clear	3	1.0	-	-	2	1.0	-	-	1	1.0	-	-
		Rain	7	2.3	-1.33	0.10	5	2.5	-1.41	0.09	2	2.0	-0.60	0.28
		Snow	8	2.7	-1.39	0.09	6	3.0	-1.549	0.07	2	2.0	-0.60	0.28
		Fog	22	7.3	-3.10	<0.05	14	7.0	-2.68	<0.05	8	8.0	-2.05	<0.05
Level 3 (1000 vph)	FWS	Clear	109	1.0	-	-	42	1.0	-	-	67	1.0	-	-
		Rain	246	2.3	-3.78	<0.05	79	1.9	-1.99	<0.05	167	2.5	-4.54	<0.05
		Snow	382	3.5	-5.06	<0.05	98	2.3	-3.02	<0.05	284	4.2	-5.17	<0.05
		Fog	216	2.0	-2.99	<0.05	59	1.4	-1.27	0.11	157	2.3	-3.19	<0.05
	BFS	Clear	2	1.0	-	-	1	1.0	-	-	1	1.0	-	-
		Rain	16	8.0	-3.32	<0.05	10	10.0	-2.59	<0.05	6	6.0	-2.06	<0.05
		Snow	12	6.0	-3.54	<0.05	9	9.0	-3.15	<0.05	3	3.0	-1.10	0.14
		Fog	61	30.5	-6.48	<0.05	30	30.0	-4.53	<0.05	31	31.0	-6.10	<0.05

Note: na = not applicable

The second safety performance measure considered in the study was the Deceleration Rate to Avoid Collision (DRAC) in each scenario. Table 20 presents the simulation results, specifically highlighting scenarios with DRAC values exceeding 3.4 m/s^2 (indicative of possibly critical situations) for the two studied freeway segments. Consistent with the evaluation based on Time-to-Collision (TTC), the results show an increase in the risk of possibly critical driving conditions in various adverse weather scenarios when assessing DRAC. In other words, adverse weather conditions led to a higher number of critical conflicts, as indicated by DRAC values, compared to clear conditions. It is worth noting that the Basic Freeway Segment (BFS) produced a relatively lower number of critical conflicts when compared to the Freeway Weaving Segment (FWS). As expected, foggy conditions in BFS exhibited relatively higher numbers of critical conflicts, similar to the high-risk TTC level, across all three traffic demand levels. For instance, in foggy weather for BFS, the total critical conflicts were 16 and 46, respectively, which were approximately 5 and 46 times significantly higher than those in clear weather for level 2 and 3 demands. Conversely, snowy conditions resulted in a higher number of critical conflicts in FWS. Moreover, the increase in risk from clear weather to adverse weather was notably higher in BFS when compared to FWS, particularly for total and rear-end conflicts under level 3 traffic demand conditions.

The final safety performance measure considered in the study was Post-Encroachment Time (PET). Table 21 provides the simulation results, specifically focusing on conflicts where PET is critical (i.e., PET < 1 second). In general, the results pertaining to total conflicts, as well as lane-change and rear-end conflicts, in adverse weather conditions align with the findings obtained based on Time-to-Collision (TTC) and Deceleration Rate to Avoid Collision (DRAC) assessments. According to Table 21, critical conflicts were more prevalent in snowy weather for the Freeway Weaving Segment (FWS) and foggy weather for the Basic Freeway Segment (BFS), consistent with the observations from high-risk TTC and DRAC scenarios. Similarly, the analysis revealed that an increase in the number of conflicts corresponded to higher traffic volumes, consistent with the findings from the TTC and DRAC evaluations.

Table 20 Simulation Results of Conflicts Considering DRAC (DRAC > 3.4 m/s2)

Volume	Segment	Weather	Total Conflicts	Relative Risk	t-Statistic	P-Value	Lane Change Conflicts	Relative Risk	t-Statistic	P-Value	Rear End Conflicts	Relative Risk	t-Statistic	P-Value
Level 1 (600 vph)	FWS	Clear	12	1.0	-	-	2	1.0	-	-	10	1.0	-	-
		Rain	21	1.8	-1.28	0.11	3	1.5	-0.40	0.35	18	1.8	-1.39	0.09
		Snow	43	3.6	-3.81	<0.05	12	6.0	-2.61	<0.05	31	3.1	-3.19	<0.05
		Fog	29	2.4	-2.92	<0.05	7	3.5	-1.71	0.05	22	2.2	-2.71	<0.05
	BFS	Clear	0	na	-	-	0	na	-	-	0	na	-	-
		Rain	1	na	-1.00	0.17	1	na	-1.00	0.17	0	na	0.00	0.50
		Snow	5	na	-2.24	<0.05	3	na	-1.96	<0.05	2	na	-1.50	0.08
		Fog	9	na	-3.86	<0.05	5	na	-3.00	<0.05	4	na	-2.45	<0.05
Level 2 (800 vph)	FWS	Clear	35	1.0	-	-	10	1.0	-	-	25	1.0	-	-
		Rain	89	2.5	-3.27	<0.05	23	2.3	-2.25	<0.05	66	2.6	-2.83	<0.05
		Snow	114	3.3	-5.37	<0.05	26	2.6	-2.23	<0.05	88	3.5	-5.41	<0.05
		Fog	50	1.4	-1.31	0.10	13	1.3	-0.63	0.27	37	1.5	-1.39	0.09
	BFS	Clear	3	1.0	-	-	2	1.0	-	-	1	1.0	-	-
		Rain	2	0.7	0.40	0.35	1	0.5	0.60	0.28	1	1.0	0.00	0.50
		Snow	3	1.0	0.00	0.50	2	1.0	0.00	0.50	1	1.0	0.00	0.50
		Fog	16	5.3	-2.87	<0.05	9	4.5	-2.60	<0.05	7	7.0	-1.90	<0.05
Level 3 (1000 vph)	FWS	Clear	90	1.0	-	-	35	1.0	-	-	55	1.0	-	-
		Rain	213	2.4	-3.92	<0.05	62	1.8	-1.73	<0.05	151	2.7	-5.03	<0.05
		Snow	327	3.6	-4.84	<0.05	80	2.3	-2.59	<0.05	247	4.5	-5.25	<0.05
		Fog	185	2.1	-3.10	<0.05	43	1.2	-0.72	0.24	142	2.6	3.56	<0.05
	BFS	Clear	1	1.0	-	-	0	na	-	-	1	1.0	-	-
		Rain	11	11.0	-3.94	<0.05	6	na	-3.67	<0.05	5	5.0	1.63	<0.05
		Snow	9	9.0	-2.72	<0.05	6	na	-2.25	<0.05	3	3.0	-1.10	0.14
		Fog	46	46.0	-5.96	<0.05	18	na	-4.07	<0.05	28	28.0	-5.96	<0.05

Note: na = not applicable

Volume	Segment	Weather	Total Conflicts	Relative Risk	t-Statistic	P-Value	Lane Change Conflicts	Relative Risk	t-Statistic	P-Value	Rear End Conflicts	Relative Risk	t-Statistic	P-Value
Level 1 (600 vph)	FWS	Clear	19	1.0	-	-	2	1.0	-	-	17	1.0	-	-
		Rain	47	2.5	-2.19	<0.05	13	6.5	-2.35	<0.05	34	2.0	-1.80	<0.05
		Snow	78	4.1	-5.58	<0.05	32	16.0	-5.46	<0.05	46	2.7	-3.73	<0.05
		Fog	58	3.1	-3.69	<0.05	20	10.0	-3.14	<0.05	38	2.2	-3.0137	<0.05
	BFS	Clear	8	1.0	-	-	1	1.0	-	-	7	1.0	-	-
		Rain	18	2.3	-2.17	<0.05	10	10.0	-3.25	<0.05	8	1.1	-0.30	0.38
		Snow	18	2.3	-2.29	<0.05	9	9.0	-3.89	<0.05	9	1.3	-0.57	0.29
		Fog	23	2.9	-2.53	<0.05	12	12.0	-2.95	<0.05	11	1.6	-0.98	0.17
Level 2 (800 vph)	FWS	Clear	79	1.0	-	-	26	1.0	-	-	53	1.0	-	-
		Rain	137	1.7	-2.92	<0.05	45	1.7	-1.89	<0.05	91	1.7	-2.58	<0.05
		Snow	187	2.4	-4.88	<0.05	61	2.3	-3.44	<0.05	126	2.4	-4.31	<0.05
		Fog	118	1.5	-2.27	<0.05	48	1.8	-2.39	<0.05	70	1.3	-1.39	0.09
	BFS	Clear	18	1.0	-	-	4	1.0	-	-	14	1.0		
		Rain	39	2.2	-4.20	<0.05	18	4.5	-3.55	<0.05	21	1.5	-1.70	<0.05
		Snow	38	2.1	-2.47	<0.05	23	5.8	-3.16	<0.05	15	1.1	-0.23	0.41
		Fog	63	3.5	-3.54	<0.05	31	7.8	-3.12	<0.05	32	2.3	-2.70	<0.05
Level 3 (1000 vph)	FWS	Clear	145	1.0	-	-	57	1.0	-	-	87	1.0	-	-
		Rain	306	2.1	-4.81	<0.05	99	1.7	-2.44	<0.05	207	2.4	-5.03	<0.05
		Snow	473	3.3	-5.84	<0.05	136	2.4	-5.12	<0.05	337	3.9	-4.97	<0.05
		Fog	325	2.2	-4.73	<0.05	122	2.1	-4.05	<0.05	202	2.3	-3.64	<0.05
	BFS	Clear	25	1.0	-	-	8	1.0	-	-	17	1.0	-	-
		Rain	51	2.0	-2.64	<0.05	21	2.6	-2.87	<0.05	30	1.8	-1.59	<0.05
		Snow	62	2.5	-3.62	<0.05	37	4.6	-3.50	<0.05	25	1.5	-1.14	0.14
		Fog	127	5.1	-6.68	<0.05	61	7.6	-5.34	<0.05	66	3.9	-5.18	0.00

Table 21 Simulation Results of Conflicts Considering PET (PET < 1 s)

Volume	Segment	Weather	Total Conflicts	Relative Risk	t-Statistic	P-Value	Lane Change Conflicts	Relative Risk	t-Statistic	P-Value	Rear End Conflicts	Relative Risk	t-Statistic	P-Value
Level 1 (600 vph)	FWS	Clear	19	1.0	-	-	2	1.0	-	-	17	1.0	-	-
		Rain	47	2.5	-2.19	<0.05	13	6.5	-2.35	<0.05	34	2.0	-1.80	<0.05
		Snow	78	4.1	-5.58	<0.05	32	16.0	-5.46	<0.05	46	2.7	-3.73	<0.05
		Fog	58	3.1	-3.69	<0.05	20	10.0	-3.14	<0.05	38	2.2	-3.0137	<0.05
	BFS	Clear	8	1.0	-	-	1	1.0	-	-	7	1.0	-	-
		Rain	18	2.3	-2.17	<0.05	10	10.0	-3.25	<0.05	8	1.1	-0.30	0.38
		Snow	18	2.3	-2.29	<0.05	9	9.0	-3.89	<0.05	9	1.3	-0.57	0.29
		Fog	23	2.9	-2.53	<0.05	12	12.0	-2.95	<0.05	11	1.6	-0.98	0.17
Level 2 (800 vph)	FWS	Clear	79	1.0	-	-	26	1.0	-	-	53	1.0	-	-
		Rain	137	1.7	-2.92	<0.05	45	1.7	-1.89	<0.05	91	1.7	-2.58	<0.05
		Snow	187	2.4	-4.88	<0.05	61	2.3	-3.44	<0.05	126	2.4	-4.31	<0.05
		Fog	118	1.5	-2.27	<0.05	48	1.8	-2.39	<0.05	70	1.3	-1.39	0.09
	BFS	Clear	18	1.0	-	-	4	1.0	-	-	14	1.0		
		Rain	39	2.2	-4.20	<0.05	18	4.5	-3.55	<0.05	21	1.5	-1.70	<0.05
		Snow	38	2.1	-2.47	<0.05	23	5.8	-3.16	<0.05	15	1.1	-0.23	0.41
		Fog	63	3.5	-3.54	<0.05	31	7.8	-3.12	<0.05	32	2.3	-2.70	<0.05
Level 3 (1000 vph)	FWS	Clear	145	1.0	-	-	57	1.0	-	-	87	1.0	-	-
		Rain	306	2.1	-4.81	<0.05	99	1.7	-2.44	<0.05	207	2.4	-5.03	<0.05
		Snow	473	3.3	-5.84	<0.05	136	2.4	-5.12	<0.05	337	3.9	-4.97	<0.05
		Fog	325	2.2	-4.73	<0.05	122	2.1	-4.05	<0.05	202	2.3	-3.64	<0.05
	BFS	Clear	25	1.0	-	-	8	1.0	-	-	17	1.0	-	-
		Rain	51	2.0	-2.64	<0.05	21	2.6	-2.87	<0.05	30	1.8	-1.59	<0.05
		Snow	62	2.5	-3.62	<0.05	37	4.6	-3.50	<0.05	25	1.5	-1.14	0.14
		Fog	127	5.1	-6.68	<0.05	61	7.6	-5.34	<0.05	66	3.9	-5.18	0.00

2.2.5.3.2 Operational Performance Investigation

The operational performance of the two simulated freeway networks with adjusted parameters was evaluated using various performance measures, including average speed, total travel time, and total delay. The simulation results for these performance measures under different scenarios are summarized in Table 22.

Notably, adverse weather conditions consistently resulted in significant reductions in average speeds for both freeway facilities when compared to clear weather. The most substantial reduction in speed was observed in snowy conditions across all scenarios. Furthermore, adverse weather led to a significant increase in both total travel time and total delay.

For example, in the case of the Freeway Weaving Segment (FWS) under level 2 traffic demands, total travel time increased by approximately 18 percent for rain, 45 percent for snow, and 10 percent for fog compared to clear weather. Correspondingly, the total delay increased by 113 percent, 303 percent, and 90 percent for rain, snow, and fog, respectively. These results highlight the considerable impact of adverse weather conditions on driver behavior and the subsequent effect on operational performance.

In terms of a comparison between the two freeway facilities, it was consistently observed that the Freeway Weaving Segment (FWS) exhibited higher total travel time and total delay than the Basic Freeway Segment (BFS) across various weather and traffic demand scenarios.

Table 22 Simulation Results of Operational Characteristics

Volume	Segment	Weather	Average Speed (mph)	Percentage Change from Clear	t-Statistic	P-Value	Total Travel Time (hr)	Percentage Change from Clear	t-Statistic	P-Value	Total Delay (hr)	Percentage Change from Clear	t-Statistic	P-Value
Level 1 (600 vph)	FWS	Clear	63.2	-	-	-	0.63	-	-	-	0.01	-	-	-
		Rain	54.3	-14.0	28.55	<0.05	0.73	16.8	-6.44	<0.05	0.03	116.8	-4.94	<0.05
		Snow	44.7	-29.2	64.88	<0.05	0.89	42.1	-13.75	<0.05	0.06	329.0	-9.58	<0.05
		Fog	58.3	-7.7	14.51	<0.05	0.68	8.8	-3.50	<0.05	0.03	98.0	-4.67	<0.05
	BFS	Clear	63.4	-	-	-	0.53	-	-	-	0.01	-	-	-
		Rain	54.5	-14.0	31.71	<0.05	0.62	16.7	-5.48	<0.05	0.02	142.1	-5.47	<0.05
		Snow	44.7	-29.5	64.88	<0.05	0.75	42.8	-11.82	<0.05	0.05	439.8	-10.18	<0.05
		Fog	58.4	-8.0	14.91	<0.05	0.58	9.2	-3.12	<0.05	0.02	144.9	-5.48	<0.05
Level 2 (800 vph)	FWS	Clear	62.2	-	-	-	0.85	-	-	-	0.03	-	-	-
		Rain	52.9	-14.9	26.83	<0.05	1.00	18.0	-6.97	<0.05	0.07	113.4	-5.36	<0.05
		Snow	43.1	-30.7	71.26	<0.05	1.23	45.1	-15.08	<0.05	0.13	303.4	-11.27	<0.05
		Fog	56.9	-8.5	14.73	<0.05	0.93	9.7	-3.92	<0.05	0.06	89.9	-4.74	<0.05
	BFS	Clear	62.7	-	-	-	0.71	-	-	-	0.02	-	-	-
		Rain	53.2	-15.1	35.02	<0.05	0.84	18.3	-6.93	<0.05	0.05	146.6	-6.69	<0.05
		Snow	43.2	-31.2	80.08	<0.05	1.04	46.2	-14.70	<0.05	0.11	396.0	-11.60	<0.05
		Fog	56.8	-9.5	17.98	<0.05	0.79	11.1	-4.22	<0.05	0.06	154.8	-6.37	<0.05
Level 3 (1000 vph)	FWS	Clear	61.1	-	-	-	1.08	-	-	-	0.06	-	-	-
		Rain	51.2	-16.2	24.66	<0.05	1.29	19.8	-7.07	<0.05	0.13	116.6	-5.84	<0.05
		Snow	41.2	-32.6	59.11	<0.05	1.60	49.1	-15.04	<0.05	0.23	292.7	-11.25	<0.05
		Fog	54.8	-10.3	12.60	<0.05	1.21	12.1	-4.33	<0.05	0.12	109.1	-5.05	<0.05
	BFS	Clear	61.8	-	-	-	0.90	-	-	-	0.04	-	-	-
		Rain	51.6	-16.6	30.22	<0.05	1.09	20.4	-7.49	<0.05	0.10	156.4	-6.97	<0.05
		Snow	41.4	-33.1	72.90	<0.05	1.35	50.2	-15.89	<0.05	0.19	381.7	-12.82	<0.05
		Fog	54.8	-11.3	19.94	<0.05	1.02	13.4	-5.26	<0.05	0.10	165.4	-8.40	<0.05

CHAPTER 3. MODELING CAT AT VARYING MARKET PENETRATION AND LEVEL OF AUTONOMY ON FREEWAY

3.1 Introduction

The technology of CAVs holds great promise in reducing accidents and potential disputes on road networks. This is achieved by improving drivers' understanding of their surroundings and eliminating human errors through the continuous delivery of real-time environmental data to road users, thereby enhancing their situational awareness (Amini, Omidvar, and Elefteriadou 2021; Virdi et al., 2019). A key aspect of this emerging approach to traffic safety involves recognizing the importance of changing driver behavior. Human factors play a significant role in ensuring road safety, accounting for over 90 percent of all road accidents (Hosseinzadeh, Moeinaddini, and Ghasemzadeh 2021; Mousavi et al. 2021; Singh 2015; Shirani-Bidabadi, Ma, and Anderson 2021). CAVs can perform certain functions such as steering, acceleration, and braking without direct human intervention. The Society of Automotive Engineers (SAE) has defined six levels of driving automation, ranging from level zero, which offers no driver assistance, to level 5, where the driver is entirely uninvolved in the driving process (SAE International 2018). Currently, technologies corresponding to levels 1 and 2 are widely available, while levels 3 to 5 are still in testing phases in different regions. Most existing studies in the CAV field focus primarily on market penetration in terms of one-dimensional aspects, neglecting the level of autonomy (Mousavi et al. 2021; Adomah, Bakhshi, and Ahmed 2021; Liu and Fan 2020; Yu et al. 2019). Market research surveys have been employed to predict the expected market adoption of various CAV levels based on the SAE classification. Factors such as the year of initiation, which marks the commercial introduction and public use of Level 4 and Level 5 CAV operations, as well as their initial market shares and subsequent growth patterns, are crucial for infrastructure planning and CAV-related operations. Consequently, understanding the impact of mixed vehicles with different levels of autonomy on traffic is of equal importance (Gkartzonikas and Gkritza 2019; Saeed et al. 2020).

3.2 Background

Microscopic traffic simulation models have been widely used to assess the effects of CAVs. Extensive efforts have gone into modeling the integration of CAVs into mixed traffic flow. Prior

research has employed various simulation software platforms, including VISSIM, AIMSUN, PARAMICS, and SUMO, to simulate CAV behavior within broader traffic contexts. These tools have proven valuable for studying how CAVs impact traffic flow, efficiency, and safety (Fountoulakis et al. 2017; Shi, He, and Huang 2019; H. Yang, Wang, and Xie 2017).

Notably, a groundbreaking study by Morando et al. was the first to investigate the influence of autonomous vehicles on traffic safety (Morando et al. 2018). Morando used VISSIM software to simulate AVs and employed the Surrogate Safety Assessment Model (SSAM) to assess crash potential. The study explored different scenarios with varying levels of AV penetration, revealing a significant reduction in the average number of crashes at signalized intersections and roundabouts as AV penetration increased.

Hartmann et al. used VISSIM to assess the impact of automated vehicles on freeway capacity. Their simulations showed a decrease in capacity of up to 7 percent as the proportion of partially and highly automated vehicles increased. However, a high penetration of CAVs, promoting cooperative driving and reduced spacing between vehicles, resulted in a substantial capacity increase of up to 30 percent (Hartmann et al. 2017).

Mousavi et al. conducted a study on the safety of an unsignalized three-way intersection under various levels of service with autonomous vehicles. VISSIM was used for simulation, and safety analysis employed the SSAM with Time to Collision (TTC) measurements. The results suggested that autonomous vehicles have the potential to reduce conflicts near intersections, whether on minor streets or major arterials (Mousavi, Osman, and Lord 2019)

Arvin et al. considered two types of Autonomous Vehicles (AVs) with different automation levels, employing the open-source software VENTOS for simulation. They introduced a novel safety assessment indicator called "driving volatility" and found a significant decrease in accidents as the number of AVs increased (Arvin, Khattak, and Torres 2019).

Ye and Yamamoto found that dedicating lanes for Connected and Automated Vehicles (CAVs) improved traffic flow throughput when the Market Penetration Rate (MPR) exceeded 40 percent (Ye and Yamamoto 2018).

Deluka Tibljas et al. used VISSIM microsimulation to assess the safety effects of CAVs at roundabouts, observing a slight increase in conflicts with the introduction of CAVs (Deluka-

Tibljaš et al. 2018). Stanek et al. also examined CAV behavior using the Wiedemann 99 model parameters and studied potential impacts (Stanek et al. 2017). Rahman and Abdel-Aty focused on platooning autonomous vehicles on expressways using VISSIM software, showing that forming platoons could enhance safety by reducing the time vehicles spent below the TTC threshold by 19 percent to 28 percent (Rahman and Abdel-Aty 2018).

Prior research has explored the efficiency and safety of highway segments and large-scale networks in the context of CAV traffic. These studies have investigated factors like truck ratios and exclusive lane policies on CAV operations. While most of these studies have focused on varying CAV market penetration, there is limited research considering both Market Penetration and Level of Autonomy simultaneously. This underscores a gap in the literature and underscores the need for further research to examine the combined effects of market penetration and level of autonomy on CAV performance and outcomes. Subsequent sections will provide details on the methodology and data analysis employed in this regard.

3.3 Methodology and Simulation Framework

The VISSIM software is employed to create a simulation of the transportation network under study, while the SSAM is used to assess the safety implications of Connected and Automated Vehicles (CAVs) within the specific section being investigated.

The freeway segment selected for this study is the same as used in the previous chapter, it is located along Interstate 80 (I-80) in Wyoming, spanning from milepost (MP) 357 to MP 359. This eastbound segment covers 2 miles and includes two lanes, along with various on- and off-ramps. This particular freeway segment was chosen due to its characteristic features, including significant merging and diverging traffic patterns that often require drivers to make frequent lane changes. Additionally, the study utilized lane change parameters derived using the automated algorithm from the SHRP2 NDS data and given in chapter 4. Consequently, it was more appropriate to select this segment over a Basic Freeway Segment (BFS) which typically involves fewer lane change maneuvers. The layout of the chosen freeway segment is depicted in Figure 23.

Figure 23 Layout of Selected Study Segment (captured from VISSIM background map)

To obtain details about roadway geometries, posted speed limits, and other network attributes, Google Earth Pro and Google Maps were employed as supplementary data sources. In this study, several initial assumptions have been set to delineate the scope and context of the research goals. These assumptions serve to clarify the particular focus and conditions being examined.

3.3.1 Simulation Assumptions

As time progresses, the level of autonomy in Connected and Automated Vehicles (CAVs) is expected to evolve, along with their market penetration rate. Initially, with increasing automation levels, CAVs are anticipated to exhibit more assertive behaviors and maintain shorter following distances. Additionally, as their communication capabilities improve, they are likely to engage in cooperative lane changes, advanced merging, platoon formation, predictive collision avoidance, and cooperative speed harmonization.

To ensure consistency in the simulation, CAVs are categorized into three levels: Low-Level CAVs, Mid-Level CAVs, and High-Level CAVs. These levels are defined using parameters from the CoExist project (CoExist, 2020), which encompass different degrees of automation, ranging from Cautious to Normal to Aggressive levels. Low-Level CAVs aim to replicate SAE Level 1 automation, where they are automated but lack advanced communication abilities, relying heavily on human drivers for control and decision-making. Mid-Level CAVs represent

automation levels characterized by robust connectivity while still incorporating some degree of human control, akin to the combined attributes of SAE automation Levels 2 and 3. In contrast, High-Level CAVs possess advanced automation capabilities, demonstrating assertive behavior, maintaining shorter following distances, and possessing superior communication abilities. These vehicles rely significantly less on human control, resembling the combined functionalities of SAE automation Levels 4 and 5.

However, Human Driven Vehicles (HDVs) in the simulation are represented using real-time traffic data from the Wyoming Department of Transportation (WYDOT) traffic database, as well as lane change parameters and desired speed distribution for clear weather conditions from chapter 4. Conversely, the speed distribution for CAVs adheres to the CoExist project (CoExist 2020) guidelines and is set to align with the posted speed limits of Interstate 80 (I-80). Figure 24 illustrates the desired speed distribution of HDVs and different levels of CAVs. Furthermore, unless there are no HDVs present in the network, Low-Level CAVs follow the speed distribution of HDVs, and when HDVs are absent, they align with the speed distribution of Mid-Level CAVs. A mixed traffic environment is established, including both Non-CAV and CAV cars and trucks. To simplify the simulation and focus on the primary study objectives, platooning, which involves coordinated travel of multiple vehicles closely together, is intentionally omitted. This decision eliminates complexities associated with platooning and allows the study to precisely analyze how changing MPLA affects traffic behavior and performance.

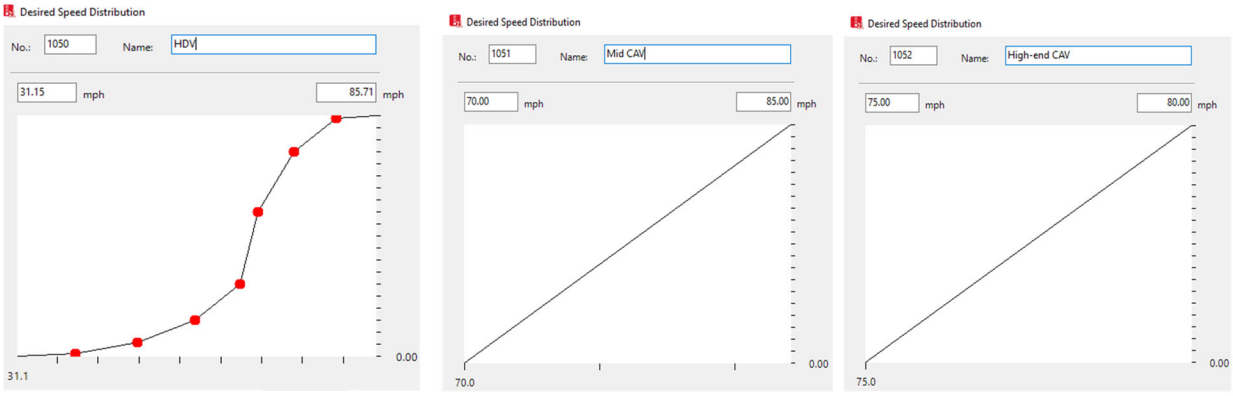

Figure 24 Desired speed distribution for different CAV levels

3.3.2 Simulation Parameters

When it comes to modeling Connected and Automated Vehicle (CAV) behavior within VISSIM, there are two approaches available: the internal and external methods (CoExist 2020). For simplicity, this research adopts the internal approach, which entails adjusting the default driving behavior settings within VISSIM.

VISSIM typically employs the Wiedemann car-following model (Higgs et al., 2011), which comes in two versions: Wiedemann 1974 for urban scenarios and Wiedemann 1999 for freeway conditions. To simulate both human drivers and CAVs comprehensively, this study opted to use the Wiedemann 99 model, which includes ten parameters denoted as CC0 to CC9. Detailed documentation on these parameters can be found in the PTV VISSIM User Manual. The PTV Group offers recommendations for configuring the internal model in VISSIM specifically for CAVs, which involve making adjustments to car-following and lane-changing behavior parameters (Sukennik 2020). The specific modifications made to the internal models in VISSIM for this study are summarized in Table 23.

Table 23 Car-following and lane-change parameters of HDVs and CAVs

Driving Behavior	Parameters	HDVs	Low-Level CAVs	Mid-Level CAVs	High-Level CAVs
Following Parameters	Look-ahead distance (ft)	0-820.21	0-820.21	0-820.21	0-984.25
	Look-back distance (ft)	0-492.13	0-492.13	0-492.13	0-492.13
	Number of interacting objects	2	2	2	10
Car following Parameters	CC0, Standstill distance (ft)	4.92	4.92	4.92	3.28
	CC1, Gap time distribution (s)	0.9	1.5	0.9	0.6
	CC2, 'Following' distance oscillation (ft)	13.12	0	0	0
	CC3, Threshold for entering 'following' (s)	-8	-10	-8	-6
	CC4, Negative speed difference (ft/s)	-0.35	-0.1	-0.1	-0.1
	CC5, Positive speed difference (ft/s)	0.35	0.1	0.1	0.1
	CC6, Distance dependency of oscillation	11.44	0	0	0
	CC7, Oscillation acceleration (ft/s^2)	0.82	0.33	0.33	0.33
	CC8, Acceleration from standstill (ft/s^2)	11.48	9.84	11.48	13.12
	CC9, Acceleration at 50 mph (ft/s^2)	4.92	3.94	4.92	6.56
lane change Parameters	Maximum deceleration, own vehicle (ft/s^2)	-11.38	-11.48	-13.12	-13.12
	Maximum deceleration, trailing vehicle (ft/s^2)	-1.78	-8.2	-9.84	-13.12
	−1 ft/s^2 per distance, own vehicle and trailing vehicle (ft)	200	80	100	100
	Accepted deceleration, own vehicle (ft/s^2)	-0.11	-3.28	-3.28	-3.28
	Accepted deceleration, trailing vehicle (ft/s^2)	-0.09	-3.28	-3.28	-4.92
	Waiting time before diffusion (s)	200	60	60	60
	Minimum Clearance, front/rear (ft)	104.41	1.64	1.64	1.64
	Safety distance reduction factor	0.6	1	0.6	0.75
	Maximum deceleration for cooperative braking (ft/s^2)	-1.7	-8.2	-9.84	-19.69
	Advanced Merging	No	Yes	Yes	Yes
	Cooperative lane change	No	No	Yes	Yes
	Maximum speed difference (mph)	-	-	6.71	6.71
	Maximum collision time (s)	-	-	10	10
Autonomous Driving Parameters	Enforce absolute braking distance	No	Yes	No	No
	Use implicit stochastics	Yes	No	No	No
	Platooning	No	No	No	No

3.4 Simulation Scenarios

Using the built-in background maps in VISSIM, the freeway segments' layout was created. The coded network was designed to reflect real-world conditions, including the number of lanes, grades, segment lengths, and locations of on- and off-ramps. To ensure accuracy, the geometry of the developed models was verified by cross-checking with Google Street View to confirm that it accurately represented the actual field conditions. A total of 27 microsimulation modeling scenarios were developed in the VISSIM platform. These scenarios included three

different traffic volumes of 600, 800, and 1000 vehicles per hour (vph). Each traffic volume was tested with nine different scenarios representing varying levels of market penetration and level of autonomy (MPLA). This resulted in a combination of three traffic volumes and nine MPLA scenarios, as shown in (Table 24). The simulation models were executed for a total duration of 70 minutes, with the first 10 minutes designated as the warm-up time to stabilize the simulation. For each scenario, 10 simulation runs were performed to account for the influence of different simulation seeds on the analysis. Data were collected from each run to assess the safety and operational aspects under various MPLA conditions across the network.

Table 24 Simulation Scenarios

SN	Scenario	Proportion of vehicles			
		HDV	L-CAV	M-CAV	H-CAV
1	All vehicles are human-driven	100	0	0	0
2	Low-Level CAVs are introduced alongside HDV	75	25	0	0
3	Mid-Level CAVs are introduced with HDV and Low-Level CAV has a higher percentage	25	50	25	0
4	Mid-Level CAV takes over in the presence of Low-Level CAV and some HDV	25	25	50	0
5	High-Level CAV is introduced, Low-Level CAVs speed follows HDVs speed	0	25	50	25
6	High-Level CAV is introduced, Low-Level CAVs speed follows Mid-Level CAVs speed	0	25	50	25
7	High-Level CAV alongside Mid-Level CAV	0	0	50	50
8	High-Level CAV takes over Mid-Level CAV	0	0	25	75
9	All vehicles are High-Level CAVs	0	0	0	100

L-CAV = Low-Level CAV, M-CAV= Mid-Level CAV and H-CAV = High-Level CAV.

3.5 Calibration and validation

The baseline model was calibrated and validated before examining existing freeway models. VISSIM parameters were fine-tuned to represent real-life driving scenarios accurately. A custom cumulative distribution function was used to establish desired speeds for human-driven vehicles (HDVs) based on field speed data. Other vehicle characteristics, such as lengths, acceleration/deceleration capabilities, weight-to-power (W/P) ratio (especially for trucks), and additional attributes, were adjusted based on field observations to ensure accurate representation of real-world driving conditions. After calibration, microsimulation models were validated by comparing the simulated traffic volumes (averaged over 10 runs) with real-life traffic volumes. This validation step ensured that the models accurately replicated the real-world traffic conditions. The validation involved using the Geoffrey E. Havers (GEH) statistic test

(PTV Group 2018), which helped assess the discrepancies between the simulated and field-observed traffic volumes based on Equation 10.

The GEH test results indicate that the model was calibrated successfully, as the obtained values fell within an acceptable range.

Furthermore, travel times measured in the field by the WYDOT were compared with the travel times obtained from the simulation model. The MAPE statistic was used to quantify the difference between the observed travel time in the field and the simulated travel time in VISSIM. The MAPE statistic can be calculated using Equation 11 (Wu, Radwan, and Abou-Senna 2017; Moreno et al. 2013).

The MAPE value for the study segment, as shown in (Table 25), indicates the difference between the observed and simulated travel times (the lower the MAPE, the smaller the difference). It was found that the MAPE values met the acceptable threshold, indicating successful validation of the baseline model for the freeway segment based on travel times.

Table 25 GEH and MAPE Statistics for Baseline Scenario

Location	Observed Volume (vph)	Simulated Volume (vph)	Observed Travel Time (h)	Simulated Travel Time (h)	GEH value	MAPE (percent)	Acceptable
Main Corridor	601	552	-	-	2.04	-	Yes
On-ramp 1	34	27	-	-	1.27	-	Yes
On-ramp 2	29	25	-	-	0.77	-	Yes
Study Segment	-	-	0.0271	0.0279	-	2.95	Yes

3.6 Safety Performance Assessment

This study used the SSAM to evaluate the safety of simulated scenarios. SSAM analyzed trajectory data from the microsimulation model's output to identify potential conflicts that might result in near-crash collisions in vehicular traffic. Time-To-Collision (TTC) served as a surrogate measure of safety, assessing crash risk in the study segment across various scenarios. The selection of an appropriate threshold for TTC is still an area of ongoing research, and there is no definitive consensus on the ideal value. Typically, the threshold for TTC falls within the range of 1 to 5 seconds, with 1.5 seconds being commonly used (Lu, Grembek, and Hansen 2022; Jiang et al. 2020; Essa and Sayed 2015). In this study, three specific thresholds for TTC were used to categorize different levels of collision risk. The high-risk threshold was set at 1.5

seconds, the medium-risk threshold at 3 seconds, and the low-risk threshold at 5 seconds. These thresholds provided a means to classify and analyze the potential collision risk levels in the simulated scenarios. By applying these thresholds, the study aimed to assess the safety implications of different traffic conditions and evaluate the effectiveness of the implemented measures in reducing collision risk.

3.7 Results and Discussion

3.7.1 Traffic conflict Analysis

Table 26 presents conflict summaries from SSAM for MPLA scenarios and various TTC thresholds. Scenario 1 (baseline) with only HDVs had very few conflicts at the rural freeway's low volume condition, indicating good network performance. The number of conflicts were found to be increased for Scenario 1 as the volume was increased. Safety improved at low volumes in scenario 2 (mixed traffic with low-level CAVs) but worsened at higher volumes, possibly due to low-level CAVs' limited communication and HDV-like behavior, impeding traffic flow. Scenario 3 and 4 (Mid-Level CAVs, Low-Level CAVs, and HDVs) performed slightly better than the baseline for all TTC thresholds and volumes, showing a trend of improved safety with higher automation and market penetration. Scenarios 5 and 6 examined Low-Level CAVs with different speed distributions. Scenario 6 (matching Mid-Level CAVs speed) demonstrated better safety, emphasizing the benefits of uniform vehicle speeds of CAVs as compared to Scenario 5 which followed the speed distribution of HDVs. Scenarios 4 and 5 showed about 50 percent conflict reduction with 50 percent market penetration of Mid to High-Level CAVs, especially at higher volumes. Scenarios 7, 8 and 9 showed the best results as they comprised of only the Mid and High-Level CAVs. A saturation spot was attained as scenarios 8 and 9 were reached and the conflict values were almost similar at both these scenarios but for higher threshold levels of TTC, it was seen that the conflicts were slightly higher for Scenario 9 which comprised of only High-Level CAVs as compared to scenario 8 which had both High-Level and Mid-Level CAVs. This might be due to the fact that High-Level CAVs used short following distances between each other and were aggressive in nature when performing lane changes as compared to Mid-Level CAVs which were less aggressive than them.

From the results, it can also be seen that the MPLA does not have much effect on the number of conflicts at the initial stages for a low volume and this clearly shows that the Low-Level CAVs are better suited for urban networks so that they can handle the huge traffic in an effective manner. For a rural network with low traffic, Low-Level CAVs do not make much of a difference because the network has a very low volume and the drivers are not generally impeded by other vehicles and since Low-Level CAVs lack advanced communication capabilities and were made to follow speed distribution of HDVs, this mix traffic environment would still act as if all vehicles were human-driven. In almost all volumes and TTC thresholds, it can be clearly seen that Scenarios 7, 8, and 9 comprising Mid and High-Level CAVs performed exceptionally well in reducing the number of conflicts. It was reduced by more than 85 percent during these scenarios. In general, both the rear-end and lane change conflicts followed a similar trend with the lane change conflict always being less than or equal to the rear-end conflicts.

Table 26 Simulation results of conflicts for TTC threshold of 1.5, 3, and 5 s

Volume	Scenario	TTC = 1.5s			TTC = 3s			TTC = 5s		
		Total	rear end	lane change	Total	rear end	lane change	Total	rear end	lane change
Low (600 vph)	1	28	23	5	60	37	23	91	52	39
	2	25	23	2	51	31	20	87	50	37
	3	23	13	10	44	23	21	77	50	27
	4	25	17	8	46	28	18	83	54	29
	5	27	20	7	44	25	19	68	37	31
	6	7	4	3	16	9	7	14	8	6
	7	3	3	0	5	5	0	8	4	4
	8	4	4	0	3	3	0	9	6	3
	9	4	3	1	2	2	0	9	6	3
Medium (800 vph)	1	90	57	33	180	96	84	315	160	155
	2	110	67	43	170	103	67	286	164	122
	3	57	30	27	88	51	37	195	100	95
	4	56	32	24	92	49	43	179	95	84
	5	41	24	17	53	29	24	138	85	53
	6	17	8	9	36	21	15	47	32	15
	7	8	6	2	12	8	4	19	14	5
	8	5	4	1	6	4	2	11	8	3
	9	2	1	1	11	8	3	17	10	7
High (1000 vph)	1	197	115	82	398	215	183	793	448	345
	2	243	148	95	422	240	182	763	468	295
	3	146	94	52	221	135	86	447	275	172
	4	100	51	49	155	75	80	379	201	178
	5	96	60	36	153	88	65	352	217	135
	6	44	26	18	88	60	28	119	84	35
	7	15	12	3	19	15	4	26	19	7
	8	7	6	1	13	8	5	26	18	8
	9	5	4	1	19	12	7	33	23	10

1: HDV = 100percent ; 2: L-CAV =25percent , HDV = 75percent ; 3: M-CAV=25percent , L-CAV= 50percent , HDV=25percent ; 4: M-CAV= 50percent , L-CAV=25percent , HDV= 25percent ; 5: H-CAV= 25percent , M-CAV= 50percent , L-CAV= 50percent (L-CAV speed follows HDVs speed); 6: H-CAV= 25percent , M-CAV= 50percent , L-CAV= 50percent (L-CAVs speed follows M-CAVs speed); 7: H-CAV= 50percent , M-CAV=50percent ; 8: H-CAV= 75percent , M-CAV= 25percent ; 9: H-CAV= 100percent

3.7.2 Operational Characteristics Analysis

Table 27 presents the various performance measures including the average speed, total travel time, and total delay used for investigating the operational performance of the simulated network. Based on the Table, a significant increase in the Average Speed of vehicles was seen as the MPLA increased except for scenario 2 where it was slightly decreased. And this might be due to the fact that the Low-Level CAVs were made to follow the speed distribution of HDVs, and they also lacked sophisticated communication and cooperative lane changes abilities, unlike the Mid and High-Level CAVs. As Scenario 5 was reached which comprised just the CAVs, the Average Speed was already higher by more than 12 percent than the baseline scenario for all volumes. Furthermore, the Average Speed of the vehicles reached around 77 mph at later stages of the scenario irrespective of the volume. A similar trend was observed in both Total Travel Time and Total Delay, whereby they improved with higher MPLA values but experienced slight degradation during the initial stages. The Total Travel Time increased with the increasing volume whereas the Total Delay was almost the same at the highest MPLA scenario. The results clearly show that CAVs are highly efficient in improving the operational characteristics of the freeway and the best results are seen when the level of automation is high (high-level to Medium-level CAV) alongside the higher market penetration. Furthermore, it can be noticed that the Low-Level CAVs with low market penetration are clearly not very effective and communication technology is quite vital in the performance of an automated vehicle.

Table 27 Simulation Results of Operational Characteristics

Volume	Scenario	Average Speed (mph)	Total Travel Time (h)	Total Delay (h)
	1	63.15	0.629	0.014
	2	62.89	0.632	0.017
	3	65.22	0.609	0.019
	4	68.59	0.577	0.015
Low (600 vph)	5	72.44	0.546	0.009
	6	76.62	0.517	0.005
	7	76.96	0.515	0.003
	8	77.12	0.514	0.002
	9	77.18	0.513	0.002
	1	62.25	0.844	0.031
	2	61.91	0.849	0.035
	3	64.31	0.817	0.037
	4	67.74	0.775	0.028
Medium (800 vph)	5	71.91	0.729	0.017
	6	76.36	0.687	0.008
	7	76.82	0.683	0.004
	8	77.01	0.681	0.003
	9	77.11	0.680	0.003
	1	61.16	1.075	0.058
	2	60.77	1.082	0.065
	3	63.18	1.039	0.065
	4	66.92	0.980	0.048
High (1000 vph)	5	71.11	0.921	0.031
	6	75.82	0.864	0.016
	7	76.63	0.855	0.007
	8	76.87	0.852	0.005
	9	77.01	0.851	0.004

1: HDV = 100percent ; 2: L-CAV =25percent , HDV = 75percent ; 3: M-CAV=25percent , L-CAV= 50percent , HDV=25percent ; 4: M-CAV= 50percent , L-CAV=25percent , HDV= 25percent ; 5: H-CAV= 25percent , M-CAV= 50percent , L-CAV= 50percent (L-CAV speed follows HDVs speed); 6: H-CAV= 25percent , M-CAV= 50percent , L-CAV= 50percent (L-CAVs speed follows M-CAVs speed); 7: H-CAV= 50percent , M-CAV=50percent ; 8: H-CAV= 75percent , M-CAV= 25percent ; 9: H-CAV= 100percent

CHAPTER 4. MODELING THE IMPACT OF INFRASTRUCTURE ON CAT PERFORMANCE AND SAFETY

4.1 Introduction

In recent years, the rapid advancement of technology has propelled the automotive industry into a new era, marked by the emergence of Connected Automated Vehicles (CAVs). These vehicles, integrated with sophisticated sensors, communication systems, and autonomous capabilities, hold immense potential to revolutionize the transportation landscape. With a primary focus on enhancing road safety and reducing collisions, CAVs utilize advanced technologies to improve drivers' comprehension of their surroundings and eliminate human errors. Real-time information dissemination enables road users to have heightened situational awareness, paving the way for a safer and more efficient road network (Amini, Omidvar, and Elefteriadou 2021; Virdi et al. 2019).

A critical element in this evolving approach to traffic safety involves recognizing the significance of modifying driver behavior, as the Human Factor remains responsible for over 90 percent of all road crashes (Hosseinzadeh, Moeinaddini, and Ghasemzadeh 2021; Mousavi et al. 2021; Singh, 2015; Shirani-Bidabadi, Ma, and Anderson 2021). CAV technology addresses this concern by empowering vehicles to perform certain functions autonomously, such as steering control, acceleration, and braking, without the need for direct driver intervention. The Society of Automotive Engineers (SAE) has established a classification comprising six levels of driving automation, ranging from Level 0 with no driver assistance to Level 5, where the driver is entirely disengaged from the driving task (SAE International 2018).

As CAVs continue to reshape the transportation landscape, it is essential to recognize the pivotal role of the infrastructure industry in enabling automation. At present, the responsibilities in the transportation sector are largely divided between the vehicle and telecommunications industries. However, with the evolution of CAVs, the infrastructure industry is expected to play an increasingly crucial role in facilitating automation in the future (Gopalakrishna 2021). As we delve into the intricacies of automation levels, it becomes evident that a one-size-fits-all approach is insufficient, especially given the diverse road infrastructure and geometric configurations encountered in the real world. Road infrastructure and geometry

play a pivotal role in influencing the performance and safety of CAVs. A broad spectrum of factors, such as road type, design, curvature, signage, lane markings, and traffic patterns, contribute to the complexity of driving environments. It is, therefore, essential to ascertain the optimal automation level for CAVs in various scenarios, ensuring seamless integration and maximal benefits (Carreras et al. 2018).

4.2 Background

Over the years, microscopic traffic simulation models have seen extensive utilization for conducting impact analyses of CAVs. In light of the scarcity of crash data, researchers worldwide have employed microsimulation methods to assess the impact of AVs on traffic safety at varying levels of adoption. Some studies adjusted car-following and lane-change models to represent AVs. Key metrics such as conflict frequency, conflict rate (the ratio of potential conflicts/collisions to throughput), and crash rate were employed to quantify the effect of AVs on traffic safety. Considerable efforts have been dedicated to modeling mixed traffic flow incorporating CAVs. Various simulation software platforms have been employed in previous studies for CAV simulation, including VISSIM®, AIMSUN, PARAMICS, and SUMO. These software tools have proven useful in simulating and analyzing the behavior and interactions of CAVs within a broader traffic context, enabling researchers to explore the potential impacts of CAVs on traffic flow, efficiency, and safety (Fountoulakis et al. 2017; Shi, He, and Huang 2019; H. Yang, Wang, and Xie 2017). Rahman et al. examined the influence of connected vehicles (CVs) both with and without platooning and found a substantial safety improvement with a minimum penetration rate of 30 percent. They also noted that CVs with platooning outperformed those without, particularly at penetration rates of 50 percent or higher (Rahman et al. 2019). A pioneering study conducted by Morando et al. examined the influence of autonomous vehicles on traffic safety (Morando et al. 2018). Utilizing VISSIM® software to simulate AVs and employing the Surrogate Safety Assessment Model (SSAM) to evaluate potential crashes, the study involved five scenarios representing different AV penetration rates within the network using VISSIM®. The results revealed a significant decrease in the average number of crashes at simulated signalized intersections and four-legged roundabouts as the penetration rate of AVs increased. Hartmann et al. also utilized VISSIM® to evaluate the effects

of automated vehicles on freeway capacity (Hartmann et al. 2017). Their simulation findings demonstrated that as the proportion of partially and highly automated vehicles increased, there was a decrease in capacity of up to 7 percent. However, with a high penetration rate of CAVs promoting cooperative maneuvering and reduced headways, a substantial increase in road capacity of up to 30 percent was observed. Mousavi et al. conducted a study investigating the impact of autonomous vehicles on the safety of an unsignalized three-way intersection across different levels of service (Mousavi, Osman, and Lord 2019). Utilizing VISSIM® software and the SSAM with Time to Collision (TTC) measurement, the results indicated that autonomous vehicles have the potential to decrease the number of conflicts near intersections, whether they occur on minor streets or major arterials. Arvin et al. considered two types of Autonomous Vehicles (AVs) with different automation levels (Arvin, Khattak, and Torres 2019). To model AVs with low automation levels, the Wiedemann 74 model was employed, while highly automated vehicles were represented using the Adaptive Cruise Control (ACC) model. The simulation was conducted using the open-source software VENTOS, and the study introduced a new safety assessment indicator called "driving volatility." The results demonstrated a significant reduction in the number of accidents as the number of AVs increased. Ye and Yamamoto found that dedicating lanes for Connected and Automated Vehicles (CAVs) could improve traffic flow throughput when the Market Penetration Rate (MPR) exceeded 40 percent (Ye and Yamamoto 2018). Deluka Tibljas et al. conducted a study using VISSIM® microsimulation to quantify the safety effects of Connected and Automated Vehicles (CAVs) at roundabouts (Deluka-Tibljaš et al. 2018). To replicate CAV behavior, they modified the Wiedemann 99 car-following model parameters and observed a slight increase in conflicts with the introduction of CAVs. Similarly, Stanek et al. simulated CAV behavior using the Wiedemann 99 model parameters obtained from existing literature and examined potential impacts (Stanek et al. 2017). Another study by Rahman and Abdel-Aty focused on the impact of platooning autonomous vehicles on expressways using VISSIM® software (Rahman and Abdel-Aty 2018). By utilizing Time to Collision (TTC) as one of the Surrogate Measures of Safety, they observed a noteworthy improvement in safety with platooning resulting in a reduction of 19 percent to 28 percent in the total time that vehicles spent running below the TTC threshold.

Prior research has extensively investigated the efficiency and safety of highway segments and large-scale networks concerning Connected and Automated Vehicle (CAV) traffic. These studies have examined various factors, such as market penetration, truck ratios and exclusive lane policies, and their impact on CAV operations. As we explore the intricacies of automation levels, it becomes evident that a standardized approach of using same automation level throughout the network is insufficient, particularly when considering the diverse road infrastructure and geometric configurations encountered in real-world settings. A critical research gap lies in limited consideration of the crucial role that road infrastructure and geometry play in influencing the performance and safety of CAVs. This gap highlights the need for further investigations that explore the implications of adapting automation levels of CAVs in response to varying road infrastructure and geometry. Understanding this interplay is vital for tailoring automation strategies that optimize CAV operations on different road types. To address this research gap comprehensively, this study aims to investigate the benefits of adapting automation levels of CAVs in response to varying road infrastructure and geometry on the safety and operation of the Interstate freeway (I-80 corridor) in Wyoming. This research utilizes the lane change parameters from the SHRP2 NDS database in conjunction with the Coexist project parameters (Sukennik, 2020) for VISSIM® microsimulation. The investigation centers on examining the impact of varying CAV automation levels based on road infrastructure and geometry, utilizing Time to Collision (TTC) as a Surrogate Measure of Safety (SMoS). The subsequent sections outline the details on the methodology and data analysis employed in this regard.

4.3 Methodology and Simulation Framework

The transportation network simulation in this study is conducted through VISSIM® software. To assess the safety impact of Connected and Automated Vehicles (CAVs) on specific segments, predefined scenarios are introduced into the simulation. The Safety Assessment Model (SSAM) is then employed to evaluate the safety outcomes. This study utilizes the same segment as the previous study which focuses on the Freeway Segment along Interstate 80 (I-80) in Wyoming, covering a 2-mile eastbound segment from milepost (MP) 357 to MP 359. The selected Freeway Segment comprises two lanes with multiple on- and off-ramps, making it suitable for the study

due to its significant merging and diverging traffic movements, involving frequent lane changes. Since the study used lane change parameters leveraged from the SHRP2 data, this particular segment was preferred over a Basic Freeway Segment (BFS) which has fewer lane change maneuvers. The traffic volume observed in this segment is relatively low. This is attributed to the selection of a segment on Interstate 80 in Wyoming, a rural freeway with low traffic volume. In this study, we conducted simulations using three distinct traffic volumes: 800 vehicles per hour (vph), 1000 vph, and 1400 vph. The first two traffic volumes were acquired from real-time field data available in the WYDOT database. As for the 1400 vph volume, it represents a projected future traffic scenario that could potentially manifest in this corridor. Maintaining a higher traffic volume is crucial for effectively observing the impacts of Connected and Automated Vehicles (CAV) implementation on highways. Higher volumes allow for a more pronounced evaluation of CAV behavior and their interactions with other vehicles. This is especially beneficial when assessing the safety and efficiency implications of CAVs, as their influence on traffic dynamics becomes more discernible in denser traffic conditions. To obtain data on roadway geometries, posted speed limits, and other network characteristics, Google Earth Pro and Google Maps were utilized as additional data sources. Figure 25 displays the layout of the chosen freeway segment.

Figure 25 Layout of the Selected Study Segment taken from google earth

The simulation methodology used in this study enables the investigation of mixed traffic conditions, considering different levels of CAVs based on roadway segments. Understanding the impact of various CAV automation levels on traffic and the benefits of adopting automation based on roadway infrastructure is crucial. To define the scope and context of the research objectives, certain initial assumptions are established. These assumptions clarify the specific focus and conditions being studied, ensuring a clear framework for the research.

4.3.1 Simulation Settings

Accurate representation of real-world conditions in a VISSIM® network is crucial for the microsimulation-based study. Consequently, the simulations were conducted using PTV VISSIM®, 2021 version.

4.3.1.1 Assumptions

In the present context, the CAV industry and CAVs account for the overall performance of CAV transportation but as it is bound to change in the future the infrastructure industry and Infrastructure Owners and Operators (IOOs) will account for a higher responsibility. As time progresses, the connectivity development of CAVs will be rapid and it is understandable that they will be heavily communicating with the Roadside Units (RSUs) and be able to manage their Automation level based on the information provided by these RSUs. It is evident that all the road segments and geometry won't be uniform and road segments are found to be changing frequently thus it is vital to understand whether it is beneficial to run the CAVs with the same automation level throughout the network or if one should change the CAV level as per the road geometry and other road infrastructure parameters. At these future stages, the roads are likely to be predominantly used by the mid to high-level CAVs with effective communication with the RSUs. They are expected to make cooperative lane changes, advanced merging, platoon formation, predictive collision avoidance, and cooperative speed harmonization and be able to vary their automation level based on the approaching roadway geometry. For this to replicate, the CAVs in this study are represented in two automation levels: Mid-Level CAVs and High-Level CAVs. Mid-Level CAVs are intended to simulate automation levels with good connectivity while still involving some human control. These correspond to the combination of SAE Level 2 and 3,

where the system assists the driver, but the driver remains partially responsible for vehicle control. High-Level CAVs, on the other hand, represent higher automation capabilities with aggressive behavior, shorter following distances, and superior communication capabilities, similar to the combined functionalities of SAE automation Levels 4 and 5. These levels are simulated using parameters from the CoExist project (CoExist 2020). On the other hand, the Human-Driven Vehicles (HDVs) were simulated based on the real-time traffic data obtained from the Wyoming Department of Transportation (WYDOT) traffic database alongside the lane change parameters and findings from previous chapter which utilized SHRP2 database. The desired speed distribution for HDVs was adjusted based on the values from chapter 3 for clear weather conditions while the speed distribution for CAVs followed the guidelines from the CoExist project (CoExist 2020) and was set to align with the posted speed limits of I-80. (Figure 26) showcases the speed distribution of HDVs and CAVs as desired in the study. The simulation involves a mixed traffic scenario, incorporating both cars and trucks. For the CAV scenarios, the market penetration is kept at 100 percent to better understand the effect of changing level of automation throughout the segments. However, the research excludes platooning, and it was intentionally deactivated in the simulation software. The deliberate exclusion of platooning was aimed at avoiding added complexities that arise when multiple vehicles travel closely together in a coordinated manner. This distinctive behavior introduces additional variables and dynamics that could overshadow or interact with the study's main focus on the effects of varying automation levels of CAVs within segments. By deactivating platooning in the simulation software, the study ensures a clear and distinct examination of how adapting automation levels based on approaching infrastructure influence traffic behavior and performance.

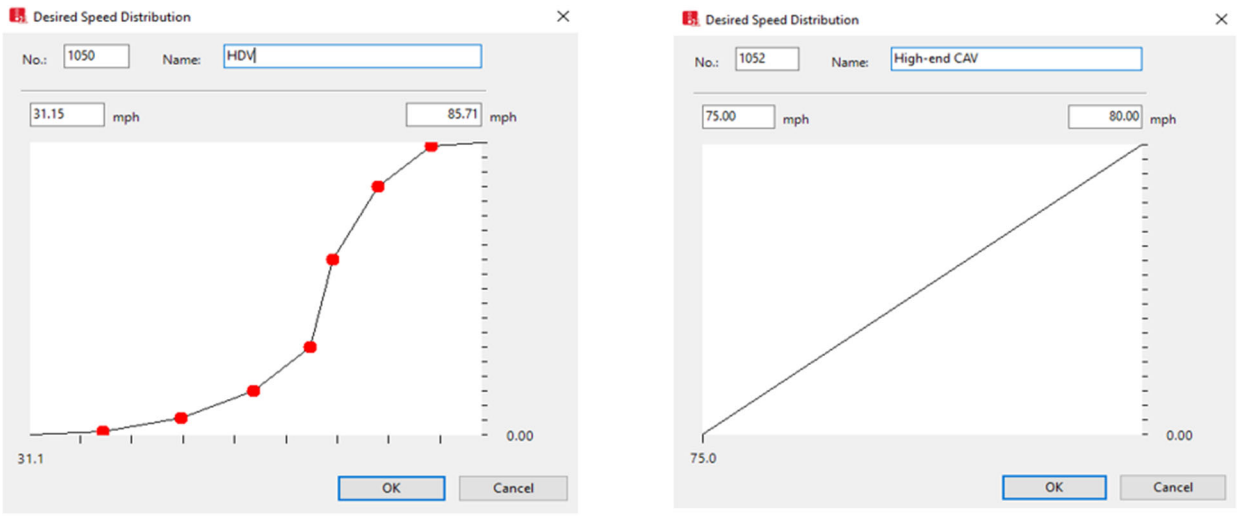

Figure 26 Screenshots of Desired Speed Distribution in VISSIM for (a) HDV (b) CAV

4.3.1.2 Simulation Parameters

According to the PTV Group, there are two approaches to model Connected and Automated Vehicle (CAV) behavior in VISSIM®: internal and external (Sukennik, 2020). This study adopts the internal approach, which involves modifying the default driving behavior parameters within VISSIM®. The internal approach is considered more straightforward and convenient compared to the external one, used when researchers aim to define their driving behavior models.

In this study, the Wiedemann 99 model was employed to simulate both human drivers and CAVs, as it captures behavioral characteristics comprehensively compared to the Wiedemann 74 model (Higgs et al 2011). The Wiedemann 99 model in VISSIM® consists of ten parameters (CC0 to CC9), and the PTV VISSIM® User Manual provides detailed documentation on their implications within the model.

The PTV Group recommends configuring the internal model in VISSIM® by adjusting car-following and lane-changing behavior parameters specifically for CAVs (Sukennik 2020). Different studies have made specific adjustments to the default values, commonalities include allowing CAVs to maintain shorter distances with the leading vehicle, exhibiting faster and smoother reactions, greater awareness of surrounding vehicles, and engaging in cooperative lane-changing behavior. These adjustments aim to represent the unique characteristics and capabilities of CAVs

in the simulation environment. This study made specific modifications to the internal models in VISSIM®, as shown in Table 28.

Table 28 Car-following and lane-change parameters of HDVs and CAVs

Driving Behavior	Parameters	HDVs	Mid-Level CAVs	High-Level CAVs
Following Parameters	Look-ahead distance (ft)	0-820.21	0-820.21	0-984.25
	Look-back distance (ft)	0-492.13	0-492.13	0-492.13
	Number of interacting objects	2	2	10
Car following Parameters	CC0, Standstill distance (ft)	4.92	4.92	3.28
	CC1, Gap time distribution (s)	0.9	0.9	0.6
	CC2, 'Following' distance oscillation (ft)	13.12	0	0
	CC3, Threshold for entering 'following' (s)	-8	-8	-6
	CC4, Negative speed difference (ft/s)	-0.35	-0.1	-0.1
	CC5, Positive speed difference (ft/s)	0.35	0.1	0.1
	CC6, Distance dependency of oscillation	11.44	0	0
	CC7, Oscillation acceleration (ft/s^2)	0.82	0.33	0.33
	CC8, Acceleration from standstill (ft/s^2)	11.48	11.48	13.12
	CC9, Acceleration at 50 mph (ft/s^2)	4.92	4.92	6.56
lane change Parameters	Maximum deceleration, own vehicle (ft/s^2)	-11.38	-13.12	-13.12
	Maximum deceleration, trailing vehicle (ft/s^2)	-1.78	-9.84	-13.12
	-1 ft/s^2 per distance, own vehicle and trailing vehicle (ft)	200	100	100
	Accepted deceleration, own vehicle (ft/s^2)	-0.11	-3.28	-3.28
	Accepted deceleration, trailing vehicle (ft/s^2)	-0.09	-3.28	-4.92
	Waiting time before diffusion (s)	200	60	60
	Minimum Clearance, front/rear (ft)	104.41	1.64	1.64
	Safety distance reduction factor	0.6	0.6	0.75
	Maximum deceleration for cooperative braking (ft/s^2)	-1.7	-9.84	-19.69
	Advanced Merging	No	Yes	Yes
	Cooperative lane change	No	Yes	Yes
	Maximum speed difference (mph)	-	6.71	6.71
	Maximum collision time (s)	-	10	10
Autonomous Driving Parameters	Enforce absolute braking distance	No	No	No
	Use implicit stochastics	Yes	No	No
	Platooning	No	No	No

4.3.2 Simulation Scenarios

The VISSIM platform's built-in background maps were used to create the layout of the freeway segments. The coded network was designed to accurately reflect real-world conditions, considering factors like the number of lanes, grades, segment lengths, and on- and off-ramp locations. To ensure precision, the geometry of the models was cross verified with Google Street View, confirming its representation of actual field conditions.

A total of 15 microsimulation modeling scenarios were developed in VISSIM®, comprising three different traffic volumes: 800, 1000, and 1400 vehicles per hour (vph). Each traffic volume was

tested with five different conditions representing various autonomy levels for different road segments, as detailed in (Figure 27).

The simulation models were executed for a duration of 70 minutes, with the first 10 minutes designated as warm-up time to stabilize the simulation. For each scenario, ten simulation runs were conducted to account for variations in simulation seeds and their impact on the analysis. Data were collected from each run to evaluate safety and operational aspects under different Infrastructure-based Automation conditions across the network.

Scenario 1: Baseline Condition with Only HDVs

Scenario 2: Mid-Level Automation Network

Scenario 3: Mixed Automation Network: High-Level on Junctions/Ramps, Mid-Level on Straight Segments

Scenario 4: Mixed Automation Network: Mid-Level on Junctions/Ramps, High-Level on Straight Segments

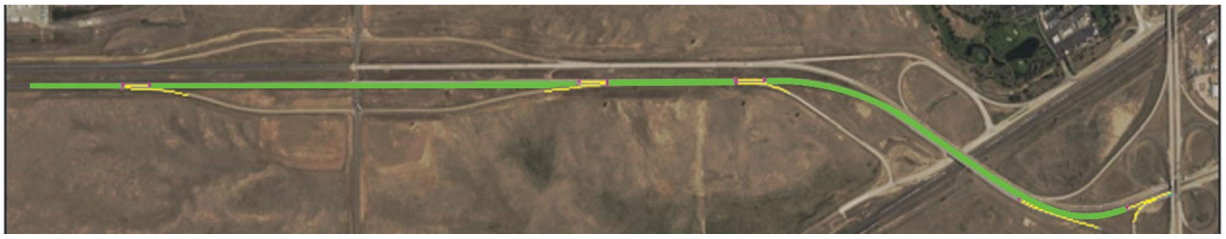

Scenario 5: High-Level Automation Network

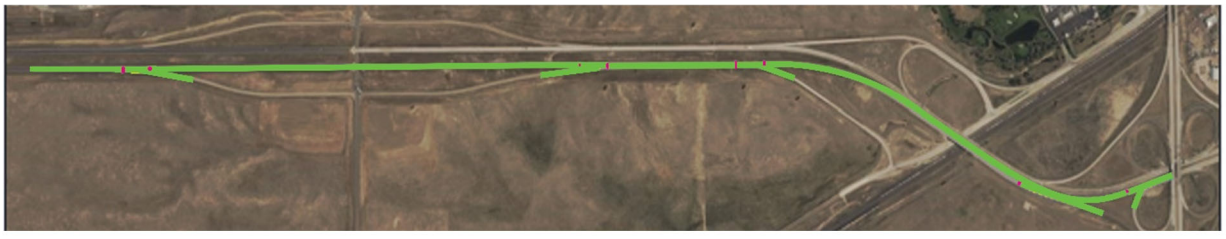

= HDV = Mid-Level CAV = High-Level CAV

Figure 27 Simulation Scenarios in VISSIM

4.3.3 Safety Performance Assessment

This study used the SSAM to evaluate the safety of simulated scenarios. SSAM analyzed trajectory data from the microsimulation model's output to identify potential conflicts that might result in near-crash collisions in vehicular traffic. Time-To-Collision (TTC) served as a surrogate measure of safety, assessing crash risk in the study segment across various scenarios. Similar to the previous chapter, this study employed three specific thresholds for TTC to categorize different levels of collision risk. The high-risk threshold was set at 1.5 seconds, the medium-risk threshold at 3 seconds, and the low-risk threshold at 5 seconds. By applying these thresholds, the study aimed to assess the safety implications of different traffic conditions and evaluate the effectiveness of the implemented measures in reducing collision risk.

4.4 Results and Discussion

4.4.1 Traffic conflict Analysis

The summary of conflicts from SSAM for all volumes and simulation scenarios is presented in Table 29. The baseline scenario consists only of HDVs running through the selected network, resulting in higher conflict numbers compared to other volumes. This baseline scenario was implemented to assess the effectiveness of CAV technology, and it is evident that scenarios involving CAVs performed exceptionally better in reducing conflicts.

At a low volume of 800 vph and a threshold of 1.5 seconds, all CAV scenarios performed almost equally, likely due to the lower conflict volume. However, at medium and high thresholds of 3 and 5 seconds, a distinct trend emerged. Scenario 2, with medium-level automation throughout the network, and Scenario 3, which featured mid-level automation on straight segments and high-level automation on junctions and ramps, outperformed Scenario 4 (high-level automation on straight segments and mid-level on junctions and ramps) and Scenario 5 (all segments as high-level automation).

This trend was more pronounced at higher volumes of 1000 vph and 1400 vph. Across scenarios, it was evident that Scenario 3, with mid-level automation on straight segments and

high-level automation at junctions and ramps, performed the best at moderate to high volumes, closely followed by Scenario 2 with all medium-level automation.
Scenarios 4 and 5 had similar performances, with reduced conflicts, but they were not as effective as Scenarios 2 and 3. Overall, the results indicate that mid-level automation on straight segments and high-level automation at junctions and ramps significantly outperformed other scenarios, reducing conflicts by approximately 30 percent or more compared to an all-high automation setup.

Table 29 Simulation results of conflicts for TTC threshold of 1.5, 3, and 5 s

TTC		1.5			3			5		
Volume (vph)	Scenario	T	R-E	L-C	T	R-E	L-C	T	R-E	L-C
800	1) HDVs on all segments	72	44	28	149	75	74	275	134	141
	2) Mid-Level CAVs on all segments	3	2	1	5	5	0	7	6	1
	3) Mid-Level CAVs on straight segments and High-Level CAVs on Junctions and Ramps	6	3	3	9	7	2	10	8	2
	4) High-Level CAVs on straight segments and Mid-Level CAVs on Junctions and Ramps	4	0	4	14	11	3	18	10	8
	5) High-Level CAVs on all segments	3	1	2	13	10	3	16	8	8
1000	1) HDVs on all segments	105	55	50	244	112	132	569	286	283
	2) Mid-Level CAVs on all segments	7	7	0	10	8	2	16	13	3
	3) Mid-Level CAVs on straight segments and High-Level CAVs on Junctions and Ramps	5	5	0	8	6	2	14	11	3
	4) High-Level CAVs on straight segments and Mid-Level CAVs on Junctions and Ramps	10	6	4	12	6	6	37	28	9
	5) High-Level CAVs on all segments	10	6	4	15	9	6	37	29	8
1400	1) HDVs on all segments	382	210	172	1028	579	449	2301	1421	880
	2) Mid-Level CAVs on all segments	18	10	8	54	37	17	116	85	31
	3) Mid-Level CAVs on straight segments and High-Level CAVs on Junctions and Ramps	19	15	4	44	29	15	107	79	28
	4) High-Level CAVs on straight segments and Mid-Level CAVs on Junctions and Ramps	40	31	9	70	54	16	140	96	44
	5) All high	37	27	10	76	52	24	149	103	46

T = Total Conflicts; R-E = Rear End Conflicts; L-C = Lane Change Conflicts

4.4.2 Operational Characteristics Analysis

Table 30 depicts a variety of performance measures utilized to assess the operational performance of the simulated network. These measures include Average Speed, Total Travel Time, and Total Delay. Evaluating these metrics under different scenarios provides valuable

insights into the efficiency and effectiveness of the transportation system, enabling a comprehensive understanding of its overall performance. The data from Table 30 clearly indicates that scenarios involving CAVs outperformed the baseline scenario with only HDVs. Additionally, as the traffic volume increased, the operational performance of HDVs was found to decline, and a similar trend, albeit with less magnitude, was observed for CAV scenarios. The CAV scenarios demonstrated excellent operational performance, with speeds consistently around 76 mph regardless of the traffic volume or scenario.

While Total Travel Time and Total Delay for CAV scenarios increased with higher volumes, the magnitude of this increase was lower compared to the all-HDV setup. Overall, all the CAV scenarios exhibited similarly improved operational characteristics for traffic, showcasing their potential in enhancing the efficiency of the transportation system.

Table 30 Simulation Results of Operational Characteristics

Volume (vph)	Scenario	Avg speed (mph)	Total Travel Time (h)	Total Delay (h)
800	1) HDVs on all segments	62.3870	0.8427	0.0290
	2) Mid-Level CAVs on all segments	77.0156	0.6811	0.0034
	3) Mid-Level CAVs on straight segments and High-Level CAVs on Junctions and Ramps	77.0163	0.6811	0.0034
	4) High-Level CAVs on straight segments and Mid-Level CAVs on Junctions and Ramps	76.9665	0.6815	0.0037
	5) All high	76.9761	0.6814	0.0037
1000	1) HDVs on all segments	61.5539	1.0676	0.0510
	2) Mid-Level CAVs on all segments	76.9264	0.8516	0.0050
	3) Mid-Level CAVs on straight segments and High-Level CAVs on Junctions and Ramps	76.9467	0.8514	0.0047
	4) High-Level CAVs on straight segments and Mid-Level CAVs on Junctions and Ramps	76.8649	0.8523	0.0055
	5) All high	76.8914	0.8520	0.0052
1400	1) HDVs on all segments	58.6474	1.5664	0.1475
	2) Mid-Level CAVs on all segments	76.6094	1.1932	0.0116
	3) Mid-Level CAVs on straight segments and High-Level CAVs on Junctions and Ramps	76.6578	1.1923	0.0108
	4) High-Level CAVs on straight segments and Mid-Level CAVs on Junctions and Ramps	76.6020	1.1933	0.0115
	5) All high	76.6257	1.1929	0.0112

CHAPTER 5. IMPACT OF COOPERATIVE AUTOMATED TRANSPORTATION ON WORK ZONE SAFETY AND OPERATION

5.1 Introduction and Background

The prevalence of roadway Work Zones (WZs) across the US has surged due to the growing demand for roadway expansion and the maintenance of aging infrastructure. Recent statistics from the Federal Highway Administration (FHWA) indicate that WZs are now found on approximately 20 percent of U.S. highways, particularly during peak seasons (H. Yang et al., 2015). For drivers, encountering a WZ has become a frequent occurrence, with the average expectation of encountering one every 100 miles driven (Khoda Bakhshi and Ahmed 2021). However, this proliferation of WZs presents a significant safety concern, both for the drivers navigating the complex array of signs, signals, markings, drums, and cones, and for the workers involved in new construction and roadway maintenance within or near these zones. According to crash statistics from the National Safety Council (NSC) in 2020, WZs were responsible for approximately 102,000 crashes, resulting in 44,240 injuries and 857 fatalities (NSC 2020a). The Bureau of Labor Statistics (BLS) also reported 57 worker fatalities resulting from vehicle strikes in WZs (NSC 2020b). Additionally, the presence of WZs exerts a substantial adverse impact on roadway operations and mobility, accounting for 10 percent of national congestion and causing $4.6 billion in user cost delays and 1.75 billion hours of vehicle delay, as reported by the American Road and Transportation Builders Association (ARTBA 2022).

Furthermore, the influence of inclement weather conditions can exacerbate the risk of accidents within WZs (Ghasemzadeh and Ahmed 2018). Driving under adverse weather conditions, particularly within WZs, is inherently challenging due to reduced visibility, compromised roadway surface friction, and significant disruptions in driver behavior and vehicle performance. Data collected by the FHWA from 2007 to 2016 revealed that adverse weather contributes to approximately 5,400 fatal crashes, 418,000 injury crashes, and 1,235,000 property damage-only (PDO) crashes annually in the U.S. (Federal Highway Administration 2020). Furthermore, crashes that occur in adverse weather conditions tend to result in more severe injuries, as indicated by studies conducted by Khan et al. (2018). Numerous research studies have concurred that adverse weather conditions can intensify the

severity of crashes, often involving multiple vehicles (Ahmed et al. 2011). Consequently, the adverse impact of inclement weather on traffic safety and operation, particularly within WZs, underscores the pressing need for an in-depth understanding of WZ operations and crash characteristics, with a focus on enhancing preventive measures.

In efforts to address the safety concerns associated with Work Zones (WZs), the Department of Transportation (DOTs), transportation agencies, and road safety practitioners have traditionally relied on conventional countermeasures, including the use of static signs to disseminate information related to WZs. However, researchers have raised concerns that these traditional safety measures may not be sufficient in enhancing safety and operations within WZs in the era of emerging Cooperative Automated Transportation (CAT) (Khoda Bakhshi and Ahmed 2021). CAT, encompassing Connected Vehicles (CV), Autonomous Vehicles (AV), and Connected and Automated Vehicles (CAV), has garnered significant attention in recent years and is heralded as a transformative force in the current transportation landscape. Connected Vehicles (CV) technology comprises advanced wireless communication systems enabling vehicles to share real-time transportation data through vehicle-to-vehicle (V2V) and vehicle-to-infrastructure (V2I) communications (Intelligent Transportation Systems Joint Program Office (ITSJPO) 2020). Autonomous Vehicles (AV) encompass various technologies, such as video cameras, radar sensors, and light detection, which are integrated into vehicles to enable them to operate autonomously at different hierarchy levels (Anderson et al. 2016). CAV combines the capabilities of CV and AV, operating with various levels of connectivity and automation. Implementing these cutting-edge technologies has the potential to significantly enhance the complex longitudinal and lateral behaviors of drivers in WZs. This enhancement can be achieved through CV notifications like Work Zone Warning (WZW) and Rear Collision Warning (RCW), as well as assistance in selecting appropriate headway, acceleration, steering, and speed in accordance with weather conditions.

Alternatively, the platooning of heavy trucks equipped with CAV technologies has gained momentum over the past few years (Hoque et al. 2021; Haque, Rilett, and Zhao 2023). Specifically, the concept of Cooperative Adaptive Cruise Control (CACC) has been extensively studied in real-time scenarios. Building upon the foundation of Adaptive Cruise Control (ACC),

CACC introduces a cooperative approach through vehicle-to-vehicle (V2V) communication. This transformative shift from a reactive system to a cooperative system enables CACC-equipped vehicles to maintain shorter inter-vehicle and intra-vehicle distances, facilitated by communication and signaling. By utilizing this technology, CACC vehicles can achieve a higher lane capacity, optimizing the utilization of roadway infrastructure. Prominent projects, such as the California PATH project, have dedicated substantial efforts to exploring the potential of CACC technology, particularly in the context of trucks. With a primary focus on level 1 automation, these initiatives have aimed to demonstrate the feasibility and benefits of CACC implementation in real-world scenarios. The primary objective of level 1 automation is to support drivers in performing specific driving tasks, enhancing safety and efficiency on the road. Additionally, research efforts have extended to encompass both level 1-2 and level 4-5 automation of CACC trucks, further examining their potential benefits and operational implications.

This study is centered around two primary objectives. The first objective involves conducting a comprehensive analysis of various driving behaviors, including High-Visibility (HV), Connected Vehicles (CV), and Autonomous Vehicles (AV), within work zones. Subsequently, the focus shifts to an in-depth exploration of Truck Platooning, with specific attention to two distinct levels of automation. For the initial study, a 403-mile section of I-80 in Wyoming was selected due to its exposure to adverse weather conditions, sharp curves, and steep grades, making it an ideal testing segment in PTV VISSIM. In the context of Truck Platooning, a dedicated segment within VISSIM, featuring a continuous series of weaving sections and concluding with a work zone was modelled. This segmented approach, tailored to each study, allows us to capture a more comprehensive range of factors, providing richer insights than a one-size-fits-all approach.

This study has contributed significantly to the field of CAT research in the following ways: Firstly, it introduces an innovative analytical approach for investigating the impacts of different CAT scenarios, utilizing a specialized microsimulation model customized for both a work zone segment on I-80 and a general four-lane segment. Secondly, it refines driving behavior parameters, aligning them with human-driven vehicles (HV), connected vehicles (CV), and three categories of autonomous vehicles (AV) - cautious, normal, and aggressive, along with two

distinct levels of automation utilizing Cooperative Adaptive Cruise Control (CACC) trucks based on data from the SHRP 2 NDS, WYDOT CV Pilot, and the CoExist project. Thirdly, it demonstrates the utility of microsimulation modeling in evaluating the safety and operational performance of various CAT scenarios under foggy weather conditions and varying Market Penetration Rates (MPRs). Lastly, it assesses the performance of different merge strategies, including early and late merges, within the context of truck platooning.

5.2 INVESTIGATING THE EFFECT OF DIFFERENT DRIVING BEHAVIORS (HV, CV and AV) ON WORK ZONES

5.2.1 Data Acquisition and Processing

To achieve the study's objectives, a comprehensive array of data sources was systematically collected and processed. Initially, crucial traffic performance data, encompassing traffic flow characteristics and speed data, were procured from the Wyoming Department of Transportation (WYDOT) through the use of roadside Wavetronix speed sensors installed along the I-80 corridor, offering real-time traffic observations. Furthermore, corresponding weather information was sourced from WYDOT's Road Weather Information System (RWIS) sensors. It is important to note that the weather conditions were determined by the RWIS sensor associated with the specific speed observation, taking into account the proximity of that RWIS sensor. In light of the available dataset, traffic performance data linked to a specific sensor, Sensor #2178, were selected for analysis. Moreover, the nearest RWIS sensor, identified as #KVDW, corresponding to the speed sensors, was also considered. Subsequently, comprehensive traffic compositions, traffic volumes, and speed-time profiles were gathered at each sensor location (G. Yang, Ahmed, and Adomah 2020).

Additionally, micro-level driving behavior data under the Cooperative Automated Transportation (CAT) environment were sourced from a motion-based, high-fidelity University of Wyoming Driving Simulator Lab, known as WyoSafeSim, as a component of the WYDOT CV Pilot. To replicate a driving environment akin to a Work Zone (WZ) area, the InternetSceneAssembler (ISA) was employed. The scenarios were programmed based on

JavaScript, and vehicle kinematics were meticulously recorded using a software named SimObserver at a frequency of 60 Hz. This allowed for the observation of how driving behavior of the participants was influenced by various Work Zone Warning (WZW) notifications from the Human Machine Interface (HMI) within the context of foggy weather under the CAT environment. For the driving simulator experiment, 23 participants were recruited by WYDOT. Before the experiment, each participant received E-training pertaining to the WYDOT CV Pilot and various CAT notifications. Additionally, two mini-scenarios and warm-up driving sessions were provided to each participant to familiarize them with the operation of the driving simulator. Further information regarding the simulated WZ scenarios in foggy weather and associated details can be found in (Adomah, Bakhshi, and Ahmed 2021).

5.2.2 Extraction and Adjustment of Driving Behavior

In the initial section of this study, meticulously identification and fine-tuning of essential driving behavior parameters were performed to suit Human-Driven Vehicles (HV), Connected Vehicles (CV), and Autonomous Vehicles (AV). In the subsequent section, the driving behaviors of CACC trucks were adapted for two different levels, namely stage 1 platooning utilizing Level 1 automation (L1) and stage 2 platooning utilizing Level 4 automation (L4). It is worth emphasizing that driving behavior parameters cannot be directly extrapolated from weather and road surface conditions in microsimulation. Hence, the meticulous adjustment of these parameters was crucial to accurately represent real-world driving behavior, especially under specific weather conditions.

For HV, the research team calibrated the default Wiedemann-99 (W99) car-following parameters for driving in foggy weather, followed by further adjustments for Work Zone (WZ) scenarios. This was achieved by utilizing trajectory-level naturalistic data from the SHRP 2 NDS. A systematic calibration methodology was employed to determine optimal W99 car-following parameters (Hammit et al. 2019). In addition to car-following parameters, default lane change parameters in VISSIM were also fine-tuned. To facilitate this, the research team developed an automated algorithm for identifying lane change events (Das, Khan, and Ahmed 2022). These lane change events in VISSIM were categorized into necessary and free lane changes, and

parameters related to these were obtained through the algorithm, alongside other relevant parameters to ensure a realistic representation of driving behavior in foggy weather within a WZ.

Regarding CV, driving behavior within WZ areas under foggy conditions was calibrated by updating both W99 car-following and lane change parameters, with additional changes made to CV driver behavior based on various considerations, as discussed in (Khoda Bakhshi and Ahmed 2021). Notably, cooperative lane change parameters for CV were activated, reflecting their capacity for cooperative lane changes and the speed distribution associated with CV was characterized as more harmonized compared to HV, a feature observed in the driving simulator. In the case of AV, real-world data from the CoEXist project were employed and three distinct driving logics, namely Cautious, Normal, and Aggressive were utilized This European project, conducted from 2017 to 2020, focused on preparing for the transitional phase when automated and human-driven vehicles coexist on roadways (Sukennik 2019). The Cautious AVs consistently adopt safe driving behavior and adhere to traffic regulations, the normal driving logic emulates human driving, with the ability to assess gaps and speeds of surrounding vehicles based on in-vehicle sensors while the Aggressive AVs predict the maneuvers and behaviors of other road users, exhibiting a form of cooperative behavior. Each of these AV driving logics has specific driving parameters and behaviors which were integrated into PTV VISSIM 11 version, based on the W99 car-following parameters (PTV Group 2022; Sukennik 2019). It is important to note that while this study covers various scenarios, it might necessitate making assumptions for certain recommended AV driving behavior parameters, as mentioned by Sukennik (Sukennik 2018). This study utilized the recommended parameters associated with the three AV driving logics, making some minor adjustments to account for foggy weather and WZ conditions. Table 31 provides an overview of the driving behavior parameters, as well as other general parameters for HV, CV, and AV.

Table 31 Adjusted Driving Behavior Parameters for Human Vehicle, Connected Vehicle, and Automated Vehicle

Driving Behavior Parameters	Human Vehicle	Connected Vehicle	Automated Vehicle		
			Cautious	Normal	Aggressive
Car-following Parameters					
CC0: Standstill Distance (ft)	13.78	7.00	4.92	4.92	3.28
CC1: Spacing Time (s)	1.00	4.00	1.50	0.90	0.6
CC2: Following Variation (ft)	42.32	17.00	0.00	0.00	0.00
CC3: Threshold for Entering Following (s)	-21.90	-8.00	-10.00	-8.00	-6.00
CC4: Negative Following Threshold (ft/s)	0.00	-0.35	-0.10	-0.10	-0.10
CC5: Positive Following Threshold (ft/s)	1.10	0.35	0.10	0.10	0.10
CC6: Speed Dependency of Oscillation (10^{-4} rad/s)	2.20	11.44	0.00	0.00	0.00
CC7: Oscillation Acceleration (ft/s^2)	5.25	0.82	0.33	0.33	0.33
CC8: Standstill Acceleration (ft/s^2)	9.51	7.30	9.84	11.48	13.12
CC9: Acceleration at 50 mph (ft/s^2)	0.66	3.00	3.94	4.92	6.56
Lane Change Parameters					
Necessary Lane Change					
Maximum Deceleration (Own Vehicle) (ft/s^2)	-13.12	-13.12	-11.48	-13.12	-13.12
Accepted Deceleration (Own Vehicle) (ft/s^2)	-3.28	-3.28	-3.28	-3.28	-3.28
Maximum Deceleration (Trailing Vehicle) (ft/s^2)	-9.84	-9.84	-8.20	-9.84	-13.12
Accepted Deceleration (Trailing Vehicle) (ft/s^2)	-1.64	-3.28	-3.28	-3.28	-4.92
Free Lane Change					
Safety Distance Reduction Factor	0.58	0.70	1.00	0.60	0.75
Maximum Deceleration for Cooperative Breaking (ft/s^2)	-1.26	-9.84	-8.20	-9.84	-19.69
Additional Parameters					
Maximum Look Ahead Distance	820.21	1000	820.21	820.21	984.25
Minimum Look Ahead Distance	492.13	492.13	492.13	492.13	492.13
Observed Vehicle	2	3	2	2	10
Waiting Time Before Diffusion (s)	200	200	200	200	200
Advanced Merging	No	Yes	Yes	Yes	Yes
Cooperative Lane Change	No	Yes	No	Yes	Yes
Vehicle Routing Decisions Look Ahead	No	Yes	Yes	Yes	Yes
Enforce Absolute Braking Distance	No	No	Yes	No	No

5.2.3 VISSIM model

A 7- miles two lane basic freeway segment in eastbound direction encompassing a span from milepost (MP) 323 to MP 330 along I-80 was considered for the analysis. The selected segment symbolizes the most challenging traffic conditions due to significantly high elevation (i.e., summit at MP 325), steep vertical grades, and extreme weather situations (e.g., heavy fog).

Since this study concentrated on evaluating the performance of CAT in WZ safety and operations under foggy conditions, it is essential to develop the microsimulation model considering segments with high altitudes. Figure 28 displays the layout of the selected freeway segments.

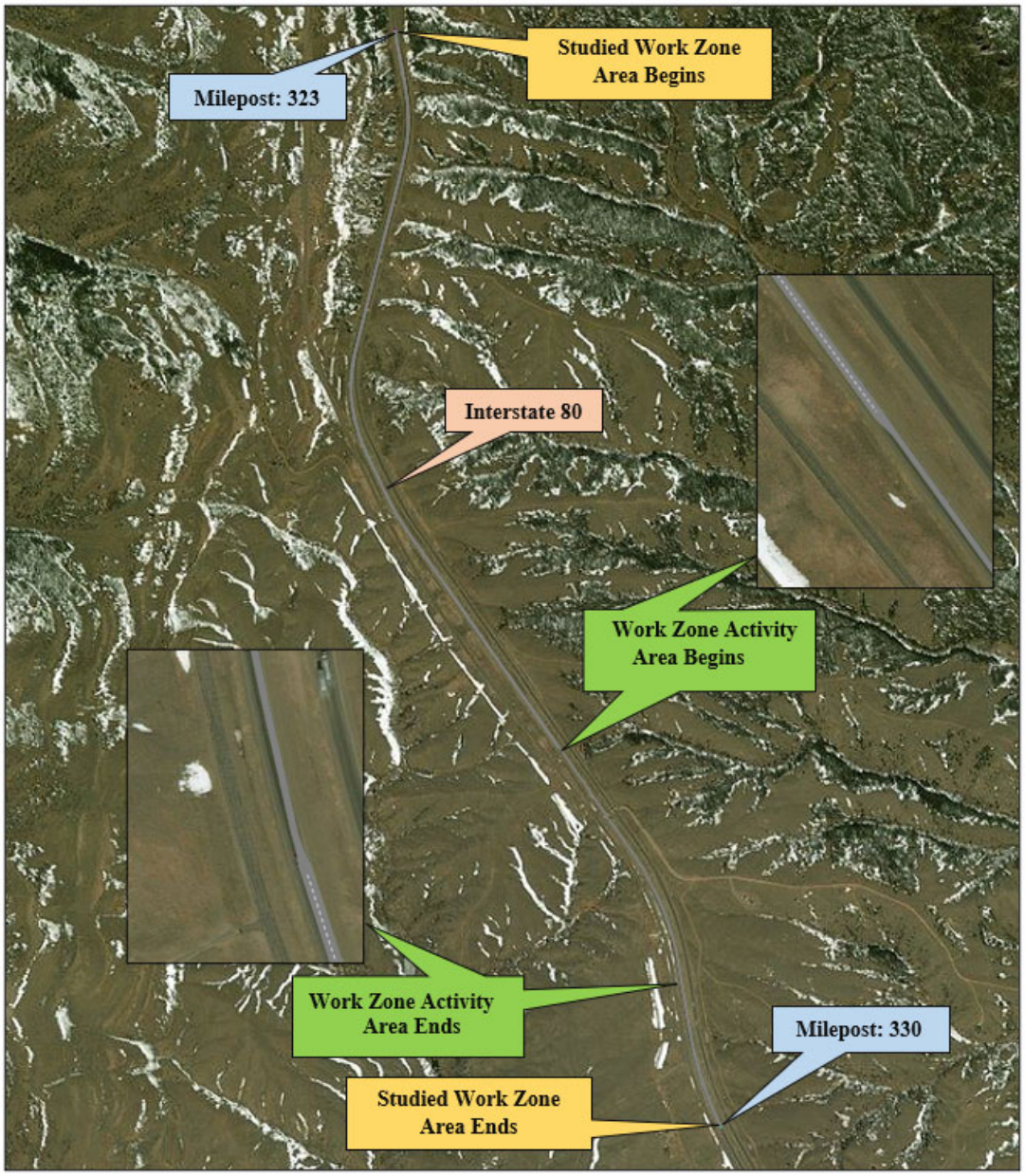

Figure 28 Layout of the Selected I-80 Freeway Segment (Image acquired from VISSIM background map)

Furthermore, required traffic data associated with the segment was collected from the WYDOT traffic database for calibration purposes. Considering September 2021 as a representative

month, traffic volume data were obtained from the WYDOT Monthly Hourly Volume report. Then, the peak hourly volume was calculated for Wednesday and necessary tuning and adjustment of arriving and departing traffic volume were conducted for the selected segment. To identify the appropriate geometric features, posted speed limits, and additional roadway characteristics, Google Earth Pro and Google Maps were utilized.

Next, the layout of the freeway segment was constructed in VISSIM via its own background maps. To verify whether the created model exemplified the actual field situations, additional inspection was performed by Google Street View software for the geometry of the coded network such as length of the segment, number of lanes, grades, etc. The next step was to define traffic compositions in VISSIM. For this purpose, two vehicle categories, car and truck, were considered and their corresponding proportions were collected from the existing data. Subsequently, a WZ that consists of four sequential areas namely Advance Warning, Transition, Activity, and Termination were created in the coded network in VISSIM following the Manual on Union Traffic Control Devices (MUTCD) guidelines. The developed network with WZ was then used to evaluate the impact of HV, CV, AV, and different combinations on traffic safety and operations.

Besides, six levels of CAT MPRs, including 0 percent, 10 percent, 25 percent, 50 percent, 75 percent, and 100 percent were considered by altering the proportion of HV, CV, and AV in VISSIM, as shown in Table 32. Except for 0 percent MPR, HV was included with CV, three types of AV, and a combination of both CV and AV for each MPR resulting in seven different combinations that generated mixed traffic situations. It is worth mentioning that an equal share for both CV and AV for a specific MPR was regarded when both of them were included with HV. The 0 percent MPR represents the baseline condition reflecting a fully traditional vehicle (i.e., only HV) whereas 100 percent MPR indicates a completely connected and/or automated environment (i.e., CV, AV, and combination of both). The adjusted driving behavior parameters along with additional general behavior corresponding to HV, CV, and AV were utilized to modify respective driving behavior during simulation in VISSIM. In addition, desired speed distribution was updated for HV by generating a cumulative distribution function through minimum, maximum, $15^{th,}$ and 85^{th} percentile of free-flow speeds in WZ under foggy weather (Xu et al.,

2021). Similarly, speed distributions for CV and AV were modified based on the insights from previous studies (Khoda Bakhshi and Ahmed 2021; Papadoulis, Quddus, and Imprialou 2019).

Table 32 Microsimulation Scenarios in Each Market Penetration Rate

MPR (percent)	Share for HV (percent)	Total Share for CV and AV (percent)	Microsimulation Scenarios							
0	-	-	Only HV	-	-	-	-	-	-	-
10	90	10	-	HV+CV	HV+AV(C)	HV+AV(N)	HV+AV(A)	HV+CV+AV(C)	HV+CV+AV(N)	HV+CV+AV(A)
25	75	25	-	HV+CV	HV+AV(C)	HV+AV(N)	HV+AV(A)	HV+CV+AV(C)	HV+CV+AV(N)	HV+CV+AV(A)
50	50	50	-	HV+CV	HV+AV(C)	HV+AV(N)	HV+AV(A)	HV+CV+AV(C)	HV+CV+AV(N)	HV+CV+AV(A)
75	25	75	-	HV+CV	HV+AV(C)	HV+AV(N)	HV+AV(A)	HV+CV+AV(C)	HV+CV+AV(N)	HV+CV+AV(A)
100	0	100	-	CV	AV(C)	AV(N)	AV(A)	CV+AV(C)	CV+AV(N)	CV+AV(A)

Note: MPR=Market Penetration Rate, HV=Human Vehicles, CV= Connected Vehicles, AV= Automated Vehicles, C=Cautious, N=Normal, A=Aggressive

A total of 36 microsimulation scenarios (i.e., five MPR × seven combinations + only HV at 0 percent MPR = 36 scenarios) were developed in the VISSIM. Each simulation run lasted for 4200 seconds (70 minutes) with the first 600 seconds (10 minutes) warm-up period to let the freeway segment be completely occupied. Ten simulation runs were performed for each scenario to integrate the effect of different simulation seeds and simulated data associated with each run were compiled to investigate the safety and operational attributes under various MPRs and vehicle combinations across the network.

5.2.4 Baseline Model Calibration and Validation

The baseline model with only HV was calibrated and validated before evaluating the prevailing freeway model. In this regard, the parameters in VISSIM were adjusted in such a way that represented real-world driving situations. Utilizing the available field speed data, a custom cumulative probability function was generated for vehicular speeds where 85^{th} percentile of speed was considered as the posted speed limit. In addition, other performance characteristics including vehicular length, weight-to-power ratio, acceleration abilities along with additional features were modified following field observation for each vehicle class.

Once the calibration of the existing model was completed, validation was performed. The model was validated by comparing the real-world traffic to the simulated traffic (i.e., mean of ten runs). In order to do that, GEH statistic formula was employed to verify the errors between simulated and field volume.

The GEH value was found to be 0.16 (i.e., less than 5) demonstrating that the baseline model was successfully validated. The validated model was then considered for further analysis.

5.2.5 Results and Discussions

5.2.5.1 Assessment of Safety Performance

The study's primary objective was to assess the safety implications of various Cooperative Automated Transportation (CAT) scenarios, including Human-Driven Vehicles (HV), Connected Vehicles (CV), Autonomous Vehicles (AV), and combinations thereof, under different Market Penetration Rates (MPRs) for rural Work Zones (WZs) in foggy weather. To evaluate safety, the study adopted a technique using Surrogate Measures of Safety (SMoS), which are derived from traffic conflicts observed in the VISSIM simulation outputs (G. Yang et al., 2020). The Surrogate Safety Assessment Model (SSAM), developed by the Federal Highway Administration (FHWA), was utilized to identify potential conflicts during simulations based on two SMoSs: Time-To-Collision (TTC) and Post Encroachment Time (PET). These measures were employed to assess the crash risks in the WZ corridor under different MPRs.

The default TTC threshold in SSAM is 1.5 s; however, since this study considered rural freeway corridors with comparatively lower traffic volumes and higher headways, three different TTC thresholds were employed including high-risk (1.5 s), medium-risk (3.5 s), and low-risk (9 s) based on the findings from a previous study (G. Yang, Ahmed, and Adomah 2020).

The final quantitative SMoS was PET, which was used to detect traffic conflict situations. It is the time difference between the moment when a vehicle departs the potential conflict area, and the other vehicle reaches that area (Mahmud et al. 2017). To predict the number of conflicts, SSAM utilizes PET thresholds from 1 to 10. A PET threshold of less than 1 s is considered a critical conflict (AASHTO 2001). This study calculated overall conflicts as well as critical conflicts using the recommended threshold from various simulation scenarios.

The number of simulated conflicts associated with three TTC levels namely high-risk (1.5 s), medium-risk (3.5 s), and low-risk (9 s) for each CAT scenario are shown in Table 33 to Table 35. A relative risk ratio was included in the analysis that was defined by dividing the number of conflicts in baseline scenario (i.e., only HV at 0 percent MPR) with the respective conflicts in other scenarios. For each TTC level, the number of conflicts in different CAT scenarios was compared to the baseline scenario. Note that most of the simulated conflicts were rear-end conflicts. This should be attributed to the fact that most of the vehicles were driving in the left lane due to the WZ area under foggy condition with a minimal number of lane changes. Additionally, the studied corridor was a basic freeway segment with no on/off ramps resulting in a very lower number of lane change maneuvers. Overall, the total number of conflicts, including the rear-end conflicts significantly decreased with the increase of MPRs in most of the scenarios. However, the reductions in conflicts were not significant for lower MPRs in some cases.

As shown in Table 33, the results of simulated conflicts with respect to high-risk TTC level represented that introducing CAT scenarios generated a lower total number of conflicts, including lane change and rear-end conflicts compared to non-CAT scenario (i.e., baseline). The differences in conflicts were statistically significant based on Welch's t-test, especially for total and rear-end conflicts. For this TTC level, relative risks corresponding to different CAT scenarios were decreased with the increase of MPRs. In addition, it was observed that the reduction in the number of lane change conflicts was not significant for 10 percent MPR. However, the reductions in lane change conflict were significant for 25 percent to 75 percent MPR, except for a few scenarios. Moreover, the highest reductions in total conflicts, including lane change and rear-end conflicts reached more than 80 percent on average for MPR 75 percent and MPR 100 percent (i.e., fully connected/cooperative scenario). In addition, the number of total and rear-end conflicts were found to increase for the combination of HV, CV, and AV compared to other individual scenarios.

Table 34 presents the results of simulated conflicts with respect to medium-risk TTC level. Interestingly, the number of conflicts for different CAT scenarios were decreased in general compared to baseline; however, the conflicts were tended to increase in some scenarios. For

instance, total conflicts and rear-end conflicts were found to be higher, especially for MPR 50 percent and 75 percent. The results of simulated conflicts based on low-risk TTC level demonstrated that the total number of conflicts in various CAT scenarios for MPR 100 percent were significantly lower than the baseline, as observed in high and medium-risk levels (Table 35). Also, it was found that the number of conflicts were decreased for other MPRs, except for a few scenarios. It is worth pointing out that scenarios containing AV(A) (i.e., AV having aggressive driving logic) produced relatively higher conflicts than other two AV logics in low and medium TTC levels under MPR 10 percent to 75 percent. AV(A) maintained smaller gaps in relation to other vehicles. This could be the probable reason for the higher number of conflicts for AV(A) at those levels.

Table 33 Simulation Results of Traffic Conflicts based on High-risk TTC

MPR (Percentage)	Scenario	Total Conflicts				Lane Change Conflicts				Rear End Conflicts			
		No. of Conflicts	Relative Risk	t Statistic	P-value	No. of Conflicts	Relative Risk	t Statistic	P-value	No. of Conflicts	Relative Risk	t Statistic	P-value
0	Only HV (Baseline)	752	1.00	-	-	80	1.00	-	-	672	1.00	-	-
10	HV+CV	610	0.81	5.59	<0.05	77	0.96	0.19	0.42	533	0.79	6.36	<0.05
	HV+AV(C)	696	0.93	1.74	<0.05	73	0.91	0.38	0.35	623	0.93	2.04	<0.05
	HV+AV(N)	582	0.77	6.35	<0.05	56	0.70	1.46	0.08	526	0.78	6.49	<0.05
	HV+AV(A)	625	0.83	3.98	<0.05	66	0.83	0.76	0.23	559	0.83	4.35	<0.05
	HV+CV+AV(C)	688	0.91	2.08	<0.05	67	0.84	0.73	0.24	621	0.92	2.03	<0.05
	HV+CV+AV(N)	664	0.88	3.24	<0.05	50	0.63	1.88	<0.05	614	0.91	2.67	<0.05
	HV+CV+AV(A)	683	0.91	2.53	<0.05	51	0.64	1.80	<0.05	632	0.94	1.79	<0.05
25	HV+CV	415	0.55	11.35	<0.05	52	0.65	1.66	0.06	363	0.54	12.48	<0.05
	HV+AV(C)	422	0.56	11.72	<0.05	26	0.33	3.42	<0.05	396	0.59	10.52	<0.05
	HV+AV(N)	354	0.47	14.95	<0.05	27	0.34	3.45	<0.05	327	0.49	15.37	<0.05
	HV+AV(A)	387	0.51	12.85	<0.05	32	0.40	2.98	<0.05	355	0.53	14.50	<0.05
	HV+CV+AV(C)	523	0.70	8.54	<0.05	38	0.48	2.61	<0.05	485	0.72	8.68	<0.05
	HV+CV+AV(N)	545	0.72	6.71	<0.05	30	0.38	3.34	<0.05	515	0.77	5.54	<0.05
	HV+CV+AV(A)	555	0.74	7.53	<0.05	33	0.41	2.75	<0.05	522	0.78	7.05	<0.05
50	HV+CV	204	0.27	19.59	<0.05	22	0.28	3.86	<0.05	182	0.27	18.86	<0.05
	HV+AV(C)	249	0.33	18.86	<0.05	75	0.94	0.31	0.38	174	0.26	22.89	<0.05
	HV+AV(N)	194	0.26	22.10	<0.05	18	0.23	4.10	<0.05	176	0.26	23.30	<0.05
	HV+AV(A)	332	0.44	11.02	<0.05	40	0.50	2.48	<0.05	292	0.43	11.39	<0.05
	HV+CV+AV(C)	312	0.41	15.17	<0.05	14	0.18	4.36	<0.05	298	0.44	14.62	<0.05
	HV+CV+AV(N)	310	0.41	15.36	<0.05	12	0.15	4.64	<0.05	298	0.44	14.72	<0.05
	HV+CV+AV(A)	370	0.49	11.09	<0.05	24	0.30	3.65	<0.05	346	0.51	10.65	<0.05
75	HV+CV	101	0.13	28.47	<0.05	9	0.11	4.78	<0.05	92	0.14	30.14	<0.05
	HV+AV(C)	141	0.19	26.39	<0.05	73	0.91	0.46	0.33	68	0.10	32.59	<0.05
	HV+AV(N)	43	0.06	32.68	<0.05	1	0.01	5.40	<0.05	42	0.06	35.52	<0.05
	HV+AV(A)	207	0.28	21.15	<0.05	15	0.19	4.33	<0.05	192	0.29	20.34	<0.05
	HV+CV+AV(C)	170	0.23	23.59	<0.05	29	0.36	3.36	<0.05	141	0.21	26.24	<0.05
	HV+CV+AV(N)	150	0.20	26.64	<0.05	12	0.15	4.57	<0.05	138	0.21	27.11	<0.05
	HV+CV+AV(A)	195	0.26	18.59	<0.05	22	0.28	3.80	<0.05	173	0.26	18.43	<0.05
100	HV+CV	2	0.00	35.09	<0.05	0	0.00	25.99	<0.05	2	0.00	38.46	<0.05
	HV+AV(C)	32	0.04	33.36	<0.05	25	0.31	5.48	<0.05	7	0.01	37.59	<0.05
	HV+AV(N)	0	0.00	35.25	<0.05	0	0.00	3.63	<0.05	0	0.00	38.68	<0.05
	HV+AV(A)	0	0.00	35.25	<0.05	0	0.00	5.48	<0.05	0	0.00	38.68	<0.05
	HV+CV+AV(C)	32	0.04	33.52	<0.05	9	0.11	4.80	<0.05	23	0.03	36.95	<0.05
	HV+CV+AV(N)	4	0.01	34.96	<0.05	0	0.00	5.48	<0.05	4	0.01	38.28	<0.05
	HV+CV+AV(A)	6	0.01	34.78	<0.05	0	0.00	5.48	<0.05	6	0.01	38.03	<0.05

Table 34 Simulation Results of Traffic Conflicts based on Medium-risk TTC

MPR (Percentage)	Scenario	Total Conflicts				Lane Change Conflicts				Rear End Conflicts			
		No. of Conflicts	Relative Risk	t Statistic	P-value	No. of Conflicts	Relative Risk	t Statistic	P-value	No. of Conflicts	Relative Risk	t Statistic	P-value
0	Only HV (Baseline)	163	1.00	-	-	27	1.00	-	-	136	1.00	-	-
10	HV+CV	182	1.12	-1.28	0.11	31	1.15	-0.47	0.32	151	1.11	-1.32	0.10
	HV+AV(C)	136	0.83	1.80	<0.05	36	1.33	-1.89	<0.05	100	0.74	2.39	<0.05
	HV+AV(N)	144	0.88	1.13	0.14	36	1.33	-1.28	0.11	108	0.79	1.86	<0.05
	HV+AV(A)	195	1.20	-2.04	<0.05	28	1.04	-0.19	0.43	167	1.23	-2.28	<0.05
	HV+CV+AV(C)	162	0.99	0.08	0.47	34	1.26	-1.47	0.08	128	0.94	0.74	0.23
	HV+CV+AV(N)	130	0.80	2.15	<0.05	24	0.89	0.53	0.30	106	0.78	2.17	<0.05
	HV+CV+AV(A)	154	0.94	0.48	0.32	20	0.74	1.25	0.11	134	0.99	0.13	0.45
25	HV+CV	193	1.18	-2.48	<0.05	36	1.33	-1.18	0.13	157	1.15	-1.93	<0.05
	HV+AV(C)	114	0.70	3.60	<0.05	24	0.89	0.49	0.31	90	0.66	3.56	<0.05
	HV+AV(N)	125	0.77	3.60	<0.05	13	0.48	2.82	<0.05	112	0.82	1.38	0.09
	HV+AV(A)	212	1.30	-1.94	<0.05	5	0.19	4.84	<0.05	207	1.52	-2.83	<0.05
	HV+CV+AV(C)	134	0.82	1.85	<0.05	27	1.00	0.00	0.50	107	0.79	2.01	<0.05
	HV+CV+AV(N)	115	0.71	3.71	<0.05	20	0.74	1.35	0.09	95	0.70	2.01	<0.05
	HV+CV+AV(A)	186	1.14	-1.37	0.09	21	0.78	1.19	0.13	165	1.21	-1.87	<0.05
50	HV+CV	202	1.24	-1.87	<0.05	22	0.81	0.84	0.21	180	1.32	-2.46	<0.05
	HV+AV(C)	180	1.10	-0.80	0.22	35	1.30	-1.03	0.16	145	1.07	-0.56	0.29
	HV+AV(N)	80	0.49	6.04	<0.05	15	0.56	2.30	<0.05	65	0.48	6.40	<0.05
	HV+AV(A)	479	2.94	-6.00	<0.05	44	1.63	-2.75	<0.05	435	3.20	-5.65	<0.05
	HV+CV+AV(C)	225	1.38	-2.6	<0.05	42	1.56	-2.20	<0.05	183	1.35	-2.44	<0.05
	HV+CV+AV(N)	184	1.13	-1.13	0.14	18	0.67	1.57	0.07	166	1.22	-2.01	<0.05
	HV+CV+AV(A)	359	2.20	-5.21	<0.05	36	1.33	-1.80	<0.05	323	2.38	-4.86	<0.05
75	HV+CV	212	1.30	-1.81	<0.05	43	1.59	-1.92	<0.05	169	1.24	-1.36	0.09
	HV+AV(C)	205	1.26	-3.23	<0.05	49	1.81	-3.63	<0.05	156	1.15	-1.62	0.06
	HV+AV(N)	130	0.80	2.24	<0.05	22	0.81	0.94	0.18	108	0.79	2.26	<0.05
	HV+AV(A)	483	2.96	-10.52	<0.05	32	1.19	-0.94	0.18	451	3.32	-10.69	<0.05
	HV+CV+AV(C)	391	2.40	-4.28	<0.05	58	2.15	-3.43	<0.05	333	2.45	-4.27	<0.05
	HV+CV+AV(N)	253	1.55	-2.72	<0.05	23	0.85	0.77	0.23	230	1.69	-2.99	<0.05
	HV+CV+AV(A)	368	2.26	-4.39	<0.05	38	1.41	-1.23	0.12	330	2.43	-4.93	<0.05
100	HV+CV	12	0.07	15.47	<0.05	4	0.15	5.37	<0.05	8	0.06	15.42	<0.05
	HV+AV(C)	132	0.81	2.71	<0.05	47	1.74	-2.85	<0.05	85	0.63	5.45	<0.05
	HV+AV(N)	0	0.00	17.73	<0.05	0	0.00	6.82	<0.05	0	0.00	16.88	<0.05
	HV+AV(A)	0	0.00	17.73	<0.05	0	0.00	6.82	<0.05	0	0.00	16.88	<0.05
	HV+CV+AV(C)	106	0.65	3.02	<0.05	22	0.81	0.87	0.20	84	0.62	3.34	<0.05
	HV+CV+AV(N)	8	0.05	15.53	<0.05	1	0.04	6.37	<0.05	7	0.05	15.01	<0.05
	HV+CV+AV(A)	30	0.18	11.61	<0.05	0	0.00	6.82	<0.05	30	0.22	10.04	<0.05

Note: MPR=Market Penetration Rate, HV=Human Vehicles, CV= Connected Vehicles, AV= Automated Vehicles, C=Cautious, N=Normal, A=Aggressive

Table 35 Simulation Results of Traffic Conflicts based on Low-risk TTC

MPR (Percentage)	Scenario	Total Conflicts				Lane Change Conflicts				Rear End Conflicts			
		No. of Conflicts	Relative Risk	t Statistic	P-value	No. of Conflicts	Relative Risk	t Statistic	P-value	No. of Conflicts	Relative Risk	t Statistic	P-value
0	Only HV (Baseline)	176	1.00	-	-	16	1.00	-	-	160	1.00	-	-
10	HV+CV	175	0.99	0.07	0.47	30	1.88	-2.09	<0.05	145	0.91	1.13	0.14
	HV+AV(C)	154	0.88	1.45	0.08	23	1.44	-1.29	0.11	131	0.82	1.93	<0.05
	HV+AV(N)	129	0.73	3.01	<0.05	14	0.88	0.38	0.35	115	0.72	2.90	<0.05
	HV+AV(A)	178	1.01	-0.10	0.46	12	0.75	0.69	0.25	166	1.04	-0.31	0.38
	HV+CV+AV(C)	153	0.87	1.39	0.09	23	1.44	-1.47	0.08	130	0.81	1.77	<0.05
	HV+CV+AV(N)	158	0.90	1.21	0.12	20	1.25	-0.77	0.23	138	0.86	1.46	0.08
	HV+CV+AV(A)	204	1.16	-1.98	<0.05	20	1.25	-0.65	0.26	184	1.15	-1.60	0.06
25	HV+CV	117	0.66	4.94	<0.05	17	1.06	-0.17	0.43	100	0.63	4.92	<0.05
	HV+AV(C)	139	0.79	2.44	<0.05	22	1.38	-1.07	0.15	117	0.73	2.65	<0.05
	HV+AV(N)	144	0.82	2.11	<0.05	8	0.50	1.90	<0.05	136	0.85	1.42	0.09
	HV+AV(A)	184	1.05	-0.48	0.32	23	1.44	-1.40	0.09	161	1.01	-0.05	0.48
	HV+CV+AV(C)	159	0.90	1.07	0.15	24	1.50	-1.33	0.10	135	0.84	1.58	0.07
	HV+CV+AV(N)	116	0.66	4.14	<0.05	4	0.25	2.78	<0.05	112	0.70	2.88	<0.05
	HV+CV+AV(A)	142	0.81	1.91	<0.05	7	0.44	2.10	<0.05	135	0.84	1.29	0.11
50	HV+CV	119	0.68	3.04	<0.05	18	1.13	-0.34	0.37	101	0.63	3.41	<0.05
	HV+AV(C)	153	0.87	1.31	0.10	14	0.88	0.42	0.34	139	0.87	1.09	0.15
	HV+AV(N)	68	0.39	19.15	<0.05	12	0.75	-4.64	<0.05	56	0.35	7.14	<0.05
	HV+AV(A)	240	1.36	-1.42	0.09	11	0.69	1.03	0.16	229	1.43	-1.52	0.07
	HV+CV+AV(C)	157	0.89	0.99	0.17	7	0.44	1.72	<0.05	150	0.94	0.54	0.30
	HV+CV+AV(N)	124	0.70	3.77	<0.05	4	0.25	2.38	<0.05	120	0.75	2.68	<0.05
	HV+CV+AV(A)	210	1.19	-1.57	0.07	5	0.31	2.40	<0.05	205	1.28	-1.93	<0.05
75	HV+CV	151	0.86	1.45	0.08	34	2.13	-3.43	<0.05	117	0.73	2.27	<0.05
	HV+AV(C)	134	0.76	3.01	<0.05	14	0.88	0.34	0.37	120	0.75	2.84	<0.05
	HV+AV(N)	74	0.42	7.24	<0.05	6	0.38	2.19	<0.05	68	0.43	5.89	<0.05
	HV+AV(A)	426	2.42	-3.70	<0.05	4	0.25	2.63	<0.05	422	2.64	-3.80	<0.05
	HV+CV+AV(C)	216	1.23	-1.25	0.11	17	1.06	-0.19	0.43	199	1.24	1.21	0.12
	HV+CV+AV(N)	153	0.87	1.14	0.13	15	0.94	0.18	0.43	138	0.86	1.00	0.16
	HV+CV+AV(A)	248	1.41	-1.77	<0.05	10	0.63	1.11	0.14	238	1.49	-2.03	<0.05
100	HV+CV	0	0.00	21.14	<0.05	0	0.00	4.00	<0.05	0	0.00	15.18	<0.05
	HV+AV(C)	38	0.22	14.64	<0.05	18	1.13	-0.40	0.35	20	0.13	12.12	<0.05
	HV+AV(N)	0	0.00	21.14	<0.05	0	0.00	4.00	<0.05	0	0.00	15.18	<0.05
	HV+AV(A)	0	0.00	21.14	<0.05	0	0.00	4.00	<0.05	0	0.00	15.18	<0.05
	HV+CV+AV(C)	82	0.47	7.48	<0.05	14	0.88	0.46	0.32	68	0.43	6.70	<0.05
	HV+CV+AV(N)	7	0.04	18.33	<0.05	0	0.00	4.00	<0.05	7	0.04	13.59	<0.05
	HV+CV+AV(A)	27	0.15	16.60	<0.05	0	0.00	4.00	<0.05	27	0.17	12.02	<0.05

Note: MPR=Market Penetration Rate, HV=Human Vehicles, CV= Connected Vehicles, AV= Automated Vehicles, C=Cautious, N=Normal, A=Aggressive

The final measure for assessing safety performance was PET. Table 36 and Table 37 show the results of simulated conflicts and critical conflicts based on PET. The findings of total conflicts along with rear-end conflicts corresponding to various CAT scenarios are in agreement with results from the TTC, especially high-risk level. In other words, the risk of WZ crashes in fog conditions decreased in different CAT scenarios than baseline with the increase of MPRs. Based on Table 36 and Table 37, the highest reduction in conflicts and critical conflicts were observed in 100 percent MPR, as per the findings from all three TTC levels.

5.2.6 Evaluation of Operational Performance

To evaluate the operational performance of the Work Zone (WZ) corridor in foggy weather for various Cooperative Automated Transportation (CAT) scenarios at different Market Penetration Rates (MPRs), two critical performance measures, average speed, and total travel time, were analyzed. The results, as detailed in Table 38, revealed that each CAT scenario consistently yielded significantly higher average speeds compared to the baseline scenario of Human-Driven Vehicles (HVs) at 0 percent MPR. As MPRs increased, average speeds increased, with the most substantial increments observed at 100 percent MPR. Furthermore, total travel times for all CAT scenarios were notably reduced compared to the fully conventional vehicle scenario, with the most significant reductions occurring as MPRs approached 100 percent. Specifically, for MPRs exceeding 50 percent, total travel times decreased by a range of approximately 15 percent to 39 percent across all CAT scenarios. These findings indicate smoother traffic operations with higher average speeds and reduced total travel times as MPRs increased, without inducing congestion. Notably, in mixed traffic scenarios combining Connected Vehicles (CV) and Autonomous Vehicles (AV), the rate of average speed increase declined as MPRs increased, likely due to the increased interaction and complexities among the three vehicle types in mixed traffic conditions.

Table 36 Simulation Results of Traffic Conflicts based on PET

MPR (Percentage)	Scenario	Total Conflicts				Lane Change Conflicts				Rear End Conflicts			
		No. of Conflicts	Relative Risk	t Statistic	P-value	No. of Conflicts	Relative Risk	t Statistic	P-value	No. of Conflicts	Relative Risk	t Statistic	P-value
0	Only HV (Baseline)	1359	1.00	-	-	34	1.00	-	-	1325	1.00	-	-
10	HV+CV	1111	0.82	3.71	<0.05	49	1.44	-2.21	<0.05	1062	0.80	3.89	<0.05
	HV+AV(C)	1150	0.85	3.19	<0.05	38	1.12	-0.56	0.29	1112	0.84	3.33	<0.05
	HV+AV(N)	1079	0.79	4.44	<0.05	37	1.09	-0.42	0.34	1042	0.79	4.52	<0.05
	HV+AV(A)	1108	0.82	4.05	<0.05	47	1.38	-1.59	0.07	1061	0.80	4.24	<0.05
	HV+CV+AV(C)	1183	0.87	2.83	<0.05	49	1.44	-2.21	<0.05	1134	0.86	3.06	<0.05
	HV+CV+AV(N)	1162	0.86	3.19	<0.05	31	0.91	0.45	0.33	1131	0.85	3.13	<0.05
	HV+CV+AV(A)	1190	0.88	2.60	<0.05	30	0.88	0.61	0.27	1160	0.88	2.55	<0.05
25	HV+CV	719	0.53	10.43	<0.05	40	1.18	-0.83	0.21	679	0.51	10.66	<0.05
	HV+AV(C)	756	0.56	9.98	<0.05	29	0.85	0.64	0.27	727	0.55	9.76	<0.05
	HV+AV(N)	624	0.46	12.57	<0.05	14	0.41	2.97	<0.05	610	0.46	12.07	<0.05
	HV+AV(A)	681	0.50	11.02	<0.05	36	1.06	-0.22	0.41	645	0.49	11.32	<0.05
	HV+CV+AV(C)	894	0.66	7.25	<0.05	31	0.91	0.51	0.31	863	0.65	7.22	<0.05
	HV+CV+AV(N)	950	0.70	5.56	<0.05	32	0.94	0.34	0.37	918	0.69	5.54	<0.05
	HV+CV+AV(A)	987	0.73	5.14	<0.05	54	1.59	-2.97	<0.05	933	0.70	5.47	<0.05
50	HV+CV	394	0.29	15.85	<0.05	35	1.03	-0.14	0.45	359	0.27	15.51	<0.05
	HV+AV(C)	419	0.31	15.35	<0.05	82	2.41	-5.22	<0.05	337	0.25	16.47	<0.05
	HV+AV(N)	344	0.25	16.09	<0.05	33	0.97	0.13	0.45	311	0.23	16.25	<0.05
	HV+AV(A)	627	0.46	8.76	<0.05	57	1.68	-2.90	<0.05	570	0.43	9.19	<0.05
	HV+CV+AV(C)	559	0.41	13.34	<0.05	22	0.65	2.01	<0.05	537	0.41	12.96	<0.05
	HV+CV+AV(N)	595	0.44	12.28	<0.05	26	0.76	1.29	0.11	569	0.43	12.05	<0.05
	HV+CV+AV(A)	695	0.51	9.96	<0.05	38	1.12	-0.49	0.32	657	0.50	9.89	<0.05
75	HV+CV	206	0.15	19.78	<0.05	17	0.50	2.15	<0.05	189	0.14	19.16	<0.05
	HV+AV(C)	213	0.16	20.50	<0.05	71	2.09	-4.56	<0.05	142	0.11	21.04	<0.05
	HV+AV(N)	170	0.13	21.09	<0.05	6	0.18	4.79	<0.05	164	0.12	20.44	<0.05
	HV+AV(A)	351	0.26	17.51	<0.05	30	0.88	0.67	0.26	321	0.24	17.33	<0.05
	HV+CV+AV(C)	321	0.24	16.17	<0.05	28	0.82	0.88	0.19	293	0.22	15.90	<0.05
	HV+CV+AV(N)	289	0.21	18.89	<0.05	4	0.12	5.50	<0.05	285	0.22	18.10	<0.05
	HV+CV+AV(A)	347	0.26	15.57	<0.05	20	0.59	2.33	<0.05	327	0.25	15.37	<0.05
100	HV+CV	14	0.01	24.11	<0.05	0	0.00	6.53	<0.05	14	0.01	23.24	<0.05
	HV+AV(C)	73	0.05	22.99	<0.05	25	0.74	1.37	<0.05	48	0.04	22.53	<0.05
	HV+AV(N)	66	0.05	23.13	<0.05	2	0.06	5.95	<0.05	64	0.05	22.33	<0.05
	HV+AV(A)	78	0.06	22.89	<0.05	1	0.03	6.22	<0.05	77	0.06	22.07	<0.05
	HV+CV+AV(C)	97	0.07	22.57	<0.05	6	0.18	4.95	<0.05	91	0.07	21.81	<0.05
	HV+CV+AV(N)	79	0.06	22.64	<0.05	2	0.06	5.95	<0.05	77	0.06	21.81	<0.05
	HV+CV+AV(A)	89	0.07	22.60	<0.05	8	0.24	4.66	<0.05	81	0.06	21.89	<0.05

Note: MPR=Market Penetration Rate, HV=Human Vehicles, CV= Connected Vehicles, AV= Automated Vehicles, C=Cautious, N=Normal, A=Aggressive

Table 37 Simulation Results of Traffic Conflicts based on Critical PET

MPR (Percentage)	Scenario	Total Conflicts				Lane Change Conflicts				Rear End Conflicts			
		No. of Conflicts	Relative Risk	t Statistic	P-value	No. of Conflicts	Relative Risk	t Statistic	P-value	No. of Conflicts	Relative Risk	t Statistic	P-value
0	Only HV (Baseline)	1287	1.00	-	-	33	1.00	-	-	1254	1.00	-	-
10	HV+CV	1075	0.84	3.19	<0.05	49	1.48	-2.57	<0.05	1026	0.82	3.37	<0.05
	HV+AV(C)	1077	0.84	3.38	<0.05	38	1.15	-0.75	0.23	1039	0.83	3.50	<0.05
	HV+AV(N)	1003	0.78	4.49	<0.05	37	1.12	-0.60	0.28	966	0.77	4.51	<0.05
	HV+AV(A)	1048	0.81	3.79	<0.05	46	1.39	-1.64	0.59	1002	0.80	3.90	<0.05
	HV+CV+AV(C)	1122	0.87	2.53	<0.05	49	1.48	-2.57	<0.05	1073	0.86	2.78	<0.05
	HV+CV+AV(N)	1100	0.85	2.94	<0.05	31	0.94	0.33	0.37	1069	0.85	2.87	<0.05
	HV+CV+AV(A)	1112	0.86	2.75	<0.05	30	0.91	0.50	0.31	1082	0.86	2.70	<0.05
25	HV+CV	688	0.53	9.59	<0.05	40	1.21	-1.05	0.15	648	0.52	9.77	<0.05
	HV+AV(C)	701	0.54	9.88	<0.05	29	0.88	0.54	0.30	672	0.54	9.68	<0.05
	HV+AV(N)	582	0.45	11.88	<0.05	14	0.42	3.07	<0.05	568	0.45	11.35	<0.05
	HV+AV(A)	608	0.47	11.13	<0.05	34	1.03	-0.12	0.45	574	0.46	11.13	<0.05
	HV+CV+AV(C)	837	0.65	7.15	<0.05	30	0.91	0.54	0.30	807	0.64	7.07	<0.05
	HV+CV+AV(N)	913	0.71	5.20	<0.05	32	0.97	0.19	0.43	881	0.70	5.16	<0.05
	HV+CV+AV(A)	922	0.72	5.09	<0.05	45	1.36	-1.63	0.06	877	0.70	5.40	<0.05
50	HV+CV	310	0.24	16.10	<0.05	33	1.00	0.00	0.50	277	0.22	15.62	<0.05
	HV+AV(C)	364	0.28	14.65	<0.05	81	2.45	-5.12	<0.05	283	0.23	15.76	<0.05
	HV+AV(N)	319	0.25	15.07	<0.05	33	1.00	0.00	0.50	286	0.23	15.16	<0.05
	HV+AV(A)	434	0.34	15.07	<0.05	50	1.52	-2.68	<0.05	384	0.31	12.77	<0.05
	HV+CV+AV(C)	512	0.40	12.93	<0.05	22	0.67	2.06	<0.05	490	0.39	12.52	<0.05
	HV+CV+AV(N)	528	0.41	12.04	<0.05	26	0.79	1.24	0.11	502	0.40	11.80	<0.05
	HV+CV+AV(A)	554	0.43	11.91	<0.05	33	1.00	0.00	0.50	521	0.42	11.69	<0.05
75	HV+CV	114	0.09	20.27	<0.05	15	0.45	2.82	<0.05	99	0.08	19.69	<0.05
	HV+AV(C)	176	0.14	19.60	<0.05	64	1.94	-3.78	<0.05	112	0.09	19.85	<0.05
	HV+AV(N)	156	0.12	19.82	<0.05	6	0.18	5.17	<0.05	150	0.12	19.11	<0.05
	HV+AV(A)	210	0.16	18.74	<0.05	11	0.33	3.88	<0.05	199	0.16	18.19	<0.05
	HV+CV+AV(C)	232	0.18	17.27	<0.05	27	0.82	0.97	0.17	205	0.16	16.81	<0.05
	HV+CV+AV(N)	242	0.19	18.02	<0.05	4	0.12	6.08	<0.05	238	0.19	17.23	<0.05
	HV+CV+AV(A)	222	0.17	17.92	<0.05	13	0.39	4.22	<0.05	209	0.17	17.34	<0.05
100	HV+CV	5	0.00	22.72	<0.05	0	0.00	7.36	<0.05	5	0.00	21.79	<0.05
	HV+AV(C)	72	0.06	21.37	<0.05	25	0.76	1.33	0.10	47	0.04	20.86	<0.05
	HV+AV(N)	66	0.05	21.49	<0.05	2	0.06	6.63	<0.05	64	0.05	20.64	<0.05
	HV+AV(A)	78	0.06	21.26	<0.05	1	0.03	6.96	<0.05	77	0.06	20.39	<0.05
	HV+CV+AV(C)	63	0.05	21.62	<0.05	6	0.18	5.40	<0.05	57	0.05	20.80	<0.05
	HV+CV+AV(N)	71	0.06	21.18	<0.05	2	0.06	6.63	<0.05	69	0.06	20.32	<0.05
	HV+CV+AV(A)	76	0.06	21.24	<0.05	4	0.12	6.08	<0.05	72	0.06	20.38	<0.05

Note: MPR=Market Penetration Rate, HV=Human Vehicles, CV= Connected Vehicles, AV= Automated Vehicles, C=Cautious, N=Normal, A=Aggressive

Table 38 Simulation Results of Traffic Operations based on Average Speed and Total Travel Time

MPR (Percentage)	Conditions	Avg Speed (mph)	percent Change from Only HV	t Statistic	P-value	Total Travel Time (hr)	percent Change from Only HV	t Statistic	P-value
0	Only HV (Baseline)	38.76	-	-	-	56.15	-	-	-
10	HV+CV	39.10	0.9percent	-1.49	0.06	55.70	-0.8percent	1.00	0.17
	HV+AV(C)	39.42	1.7percent	-2.49	<0.05	55.18	-1.7percent	1.76	<0.05
	HV+AV(N)	39.48	1.9percent	-2.58	<0.05	55.12	-1.8percent	1.80	<0.05
	HV+AV(A)	39.45	1.8percent	-2.34	<0.05	55.17	-1.7percent	1.66	0.06
	HV+CV+AV(C)	39.43	1.7percent	-3.37	<0.05	55.21	-1.7percent	2.24	<0.05
	HV+CV+AV(N)	39.62	2.2percent	-4.31	<0.05	54.95	-2.1percent	2.80	<0.05
	HV+CV+AV(A)	39.60	2.2percent	-4.22	<0.05	54.98	-2.1percent	2.71	<0.05
25	HV+CV	39.92	3.0percent	-3.93	<0.05	54.60	-2.8percent	3.01	<0.05
	HV+AV(C)	40.15	3.6percent	-5.39	<0.05	54.17	-3.5percent	3.78	<0.05
	HV+AV(N)	40.28	3.9percent	-5.69	<0.05	53.99	-3.8percent	3.98	<0.05
	HV+AV(A)	40.32	4.0percent	-5.41	<0.05	53.95	-3.9percent	3.82	<0.05
	HV+CV+AV(C)	40.23	3.8percent	-6.20	<0.05	54.09	-3.7percent	4.38	<0.05
	HV+CV+AV(N)	40.26	3.9percent	-6.20	<0.05	54.02	-3.8percent	4.39	<0.05
	HV+CV+AV(A)	40.23	3.8percent	-6.03	<0.05	54.08	-3.7percent	4.21	<0.05
50	HV+CV	41.83	7.9percent	-7.18	<0.05	52.12	-7.2percent	6.06	<0.05
	HV+AV(C)	41.97	8.3percent	-12.06	<0.05	51.93	-7.5percent	8.19	<0.05
	HV+AV(N)	42.76	10.3percent	-15.19	<0.05	50.95	-9.3percent	10.44	<0.05
	HV+AV(A)	42.63	10.0percent	-13.61	<0.05	51.12	-9.0percent	9.41	<0.05
	HV+CV+AV(C)	42.08	8.6percent	-9.81	<0.05	51.75	-7.8percent	1.99	<0.05
	HV+CV+AV(N)	42.12	8.7percent	-14.74	<0.05	51.69	-7.9percent	9.66	<0.05
	HV+CV+AV(A)	41.91	8.1percent	-13.29	<0.05	52.00	-7.4percent	9.07	<0.05
75	HV+CV	45.48	17.3percent	-17.33	<0.05	48.00	-14.5percent	16.61	<0.05
	HV+AV(C)	47.03	21.3percent	-22.24	<0.05	46.41	-17.3percent	18.80	<0.05
	HV+AV(N)	48.25	24.5percent	-28.28	<0.05	45.18	-19.5percent	24.06	<0.05
	HV+AV(A)	48.29	24.6percent	-22.30	<0.05	45.17	-19.6percent	20.88	<0.05
	HV+CV+AV(C)	45.70	17.9percent	-20.65	<0.05	47.71	-15.0percent	18.72	<0.05
	HV+CV+AV(N)	46.62	20.3percent	-22.48	<0.05	46.71	-16.8percent	19.80	<0.05
	HV+CV+AV(A)	46.73	20.5percent	-20.68	<0.05	46.66	-16.9percent	17.67	<0.05
100	HV+CV	56.77	46.5percent	-95.52	<0.05	38.31	-31.8percent	46.12	<0.05
	HV+AV(C)	61.39	58.4percent	-122.14	<0.05	35.37	-37.0percent	56.0358	<0.05
	HV+AV(N)	62.99	62.5percent	-134.40	<0.05	34.46	-38.6percent	58.91	<0.05
	HV+AV(A)	63.02	62.6percent	-134.62	<0.05	34.44	-38.7percent	58.99	<0.05
	HV+CV+AV(C)	58.12	50.0percent	-104.66	<0.05	37.41	-33.4percent	50.10	<0.05
	HV+CV+AV(N)	59.63	53.9percent	-106.09	<0.05	36.45	-35.1percent	52.05	<0.05
	HV+CV+AV(A)	59.61	53.8percent	-100.13	<0.05	36.47	-35.1percent	51.32	<0.05

Note: MPR=Market Penetration Rate, HV=Human Vehicles, CV= Connected Vehicles, AV= Automated Vehicles, C=Cautious, N=Normal, A=Aggressive

5.3 INVESTIGATING THE IMPACT OF CACC TRUCK PLATOONS ON WORK ZONES

5.3.1 Driving Behavior

According to the Society of Automotive Engineers (SAE), there are six levels of automation that are possible for vehicles. This study mainly focuses on level 1 automation for stage 1 platooning and level 4 automation for stage 2 platooning. In the case of stage 1 automation, only longitudinal distances and speeds are automated while steering is performed manually while stage 2 automation has both longitudinal and lateral control and maneuvers are done in a cautious mode. These automation levels are possible for Adaptive Cruise Control (ACC) vehicles. Cooperative Adaptive Cruise Control (CACC) is a special case where ACC vehicles are equipped with on board devices that can communicate with each other and thus aid the process of platoon formation. A key benefit of this approach is that there is little to no time lapse between the communication of vehicles and that every decision change occurs in a more cooperative and organized manner as opposed to the reactive approach observed in vehicles equipped with ACC. To investigate the effects of platoons on work zones, all trucks are assumed to have been equipped with CACC level 1 and CACC level 2 technology and other conventional vehicles are assumed to be human driven. The lane change parameters for HV vehicles were updated based on lane change parameters values extracted from previous chapters and research paper (Das and Ahmed 2022) and for stage 1 and 2 CACC they were based on parameters defined CoExist for cautious mode (Micro-Simulation Guide for Automated Vehicles 2020). Table 39 presents the lane change parameters for different driving behaviors.

In the stage 1 CACC scenario, it is assumed that all trucks are equipped with CACC technology, maintaining a time gap of 1.5 seconds between each other. However, upon encountering other trucks that meet specific conditions, they can form platoons where the gap time is reduced to 0.6 seconds. The platoons disperse when a lane change is initiated, and the vehicles execute the lane change based on their individual behavior. Contrastingly, the results from stage 1 CACC and stage 2 CACC scenarios are extracted and juxtaposed to discern the disparities in their respective outcomes.

Table 39 Lane change Parameters for different driving behaviors

Parameters	CACC stage 1	CACC stage 2
	Own vehicle	
Maximum deceleration(ft/s^2)	-11.38	-11.48
Accepted deceleration(ft/s^2)	-0.11	-3.28
	Trailing vehicle	
Maximum deceleration(ft/s^2)	-1.78	-8.2
Accepted deceleration(ft/s^2)	-0.09	-0.33
	Other Parameters	
Minimum clearance(ft)	104.41	1.64
Cooperative Lane change	Yes	Yes
Advanced merging	Yes	Yes

5.3.2 VISSIM Model Preparation

The VISSIM traffic simulation tool was utilized to create a freeway segment that consists of a combination of a basic freeway and weaving segments as shown in Figure 29. The vehicle inputs were programmed at the beginning of the basic freeway segment, with vehicles traveling from the basic freeway segment (2.5 miles) to the freeway weaving section. At the end of the freeway weaving section (Figure 29), a work zone section was introduced. The entire analysis segment had a total length of 4.5 miles. Within the configured segment, the rightmost lane was designated as the priority lane for trucks, while the middle lane served as the priority lane for other conventional vehicles. Given that the truck composition accounted for 40 percent of the total vehicles, the rightmost two lanes were predominantly occupied by trucks.

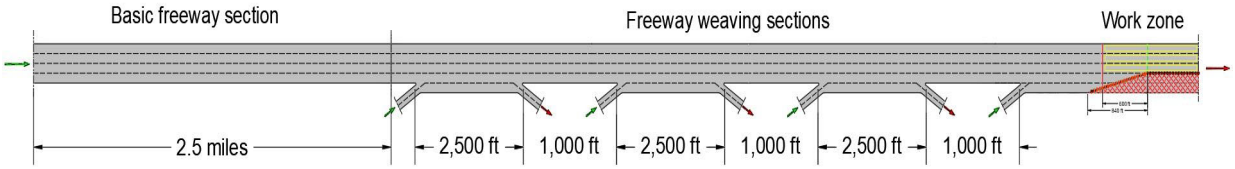

Figure 29 Basic Freeway and Weaving Segments Modeled in VISSIM

The weaving segments were mainly included to capture the effects of conflicting movements that occur between necessary lane changes performed by vehicles due to work zone condition and lane changes by vehicles that exit the freeway, and the distances between each interchange are maintained at 1000 ft and length of interchange is 2500 ft as per guidelines

provided by the Highway Capacity Manual (HCM). The freeway weaving section compromises of four entry ramps and three exit ramps, and the work zone segment is modelled at the end of the fourth entry point.

Given that the upstream area of a work zone necessitates a substantial number of lane changes, a situation that is particularly hazardous when truck platoons are involved, this study focuses specifically on the impact of such platoons on work zone merge areas. Therefore, this study focuses specifically on the upstream of work zone and other regions were ignored as they have less significant impact on safety compared to merge section on the upstream of Work zone area.

Initially, early merge condition is simulated where advanced warning area begins from one mile upstream of transition zone. In the simulation, the lane change decision for CACC trucks was activated one mile upstream from the start of the transition zone. This allowed platoons to disperse and merge early within the work zones. The activation of lane change decisions for platoons at this specific distance was facilitated by the provision of work zone information and vehicle-to-infrastructure communication. Since the study is interested in rural interstates, specific parameters such as speed distributions and vehicle composition are coded based on field observations and conditions on Interstate 80 (I80) in Wyoming. The study acknowledges that truck percentages can reach as high as 50 percent on I-80 in Wyoming, and therefore, a truck percentage of 40 percent is assumed for all scenarios in the simulations.

The primary focus of this section is to investigate the significance of truck platooning on the freeway weaving segment with work zones. This study places particular emphasis on updating the lane change parameters and comparing them across different sizes of platoons. Traffic volume was determined based on preliminary runs and density calculations, with specific volumes set to ensure they did not surpass a Level of Service B (LOS B) within the freeway weaving section, as defined by the Highway Capacity Manual (HCM). The traffic input assumptions are based on the premise that rural I-80, known for adverse weather conditions and high truck composition, does not experience extremely high traffic volumes. It is worth noting that a higher percentage of trucks is a characteristic feature of this route. Three different volume levels: 1700 vph, 2100 vph, and 2500 vph were selected after preliminary analysis.

5.3.3 Speed distribution

Figure 30 provides the speed distribution profile for road users in free flow condition in I-80. The speed distribution profile was modelled based on real time speeds observed on I-80 for clear weather condition and the maximum desired speed of platoon was limited to 75 mph.

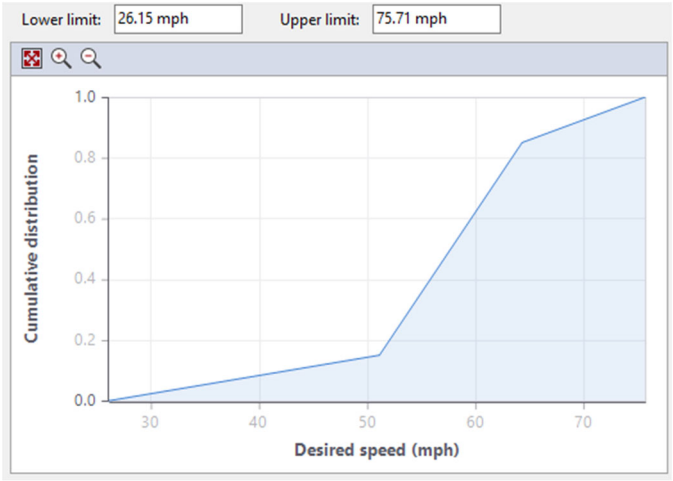

Figure 30 Speed distribution for road users in free flow condition in I-80

5.3.4 Data Analysis and Results

5.3.4.1 Effect of market penetration rate of CACC level 1 automation of trucks in Work zones

This section presents simulation results of a mixed-case scenario with varying Market Penetration Rates (MPRs) for heavy vehicles, while other conventional vehicles are human-driven. As only longitudinal direction is automated, the lane change parameters are identical for all vehicles. The key distinction between CACC trucks and conventional trucks lies in the lane change distance from the work zone. The maximum platoon size was capped at five, and the volume was maintained at 2100 vehicles per hour. Using SSAM software, the average number of conflicts observed per hour was extracted and are presented in Table 40.

Table 40 Effect of different MPR's on safety performance on Work zone

MPR of trucks (Percentage)	Total no. of conflicts (1 hr.)	Rear end	Lane change	Mean (TTC)
0	372	227	144	0.41
25	296	174	121	0.36
50	340	212	127	0.3623
75	274	174	100	0.436
100	248	165	83	0.49

The number of conflicts exhibits fluctuating patterns before showing a decline as the Market Penetration Rate (MPR) increases. However, this decrease is not linear, probably due to two primary factors. Firstly, the level of automation is confined to Level 1, focusing only on longitudinal control. Secondly, while trucks are automated, other conventional vehicles remain human-operated. As a result, there is no substantial reduction in the number of conflicts until the MPR reaches 75 percent. Interestingly, the average Time-to-Collision (TTC) begins to climb only when the MPR of trucks surpasses 50 percent. This analysis indicates that the safety advantages associated with platooning become evident at higher MPRs in this specific scenario.

5.3.4.2 Exploring the Influence of Traffic Volume, Platoon Length, and Driving Behavior on Safety in Work Zones

This study's primary objective is to scrutinize the influence of Cooperative Adaptive Cruise Control (CACC) trucks on traffic safety. As previously established, significant safety enhancements are only attained at higher Market Penetration Rates (MPR) of trucks. This section, however, explores the effects of other parameters—volume, maximum platoon size, and driving behavior—on work zone safety, with a constant truck MPR of 100 percent. (Table 41) offers a detailed summary of the number of conflicts under varied volumes, platoon sizes, and driving behaviors. Each scenario is evaluated against the base case without platooning, determining statistical significance through t-tests with a critical value derived from a significance value (p-value) of 0.05.

Analyzing the table, several patterns emerge correlating volume and conflicts within work zones. As the volume escalates, so does the number of conflicts in all scenarios. However, the benefits of CACC-based platooning become increasingly prominent with volume escalation. In scenarios of low volume and automation (CACC1), conflict numbers rise by 20 percent as the maximum platoon size extends to seven. However, in high-volume situations, this trend reverses dramatically, showing a 50 percent decrease in conflicts when the maximum platoon size reaches seven. This suggests that in high-volume conditions, platooning significantly bolsters safety by effectively mitigating conflicts.

Conversely, in scenarios with Level 2 CACC automation where platooning is permitted, the conflict numbers consistently remained below those of the base scenario. The safety benefits of platooning in this case grow progressively more pronounced with increasing volume, leading to a larger reduction in conflicts relative to the base scenario.

Table 42 presents the comparison of mean TTC and Delta-V parameters for various scenarios. An important observation from the table is the rising mean Time-to-Collision (TTC) as platoon length extends, while Delta V (change in velocity) recedes. This pattern indicates a decrease in conflict severity with platooning implementation, becoming more substantial at higher traffic volumes.

These insights underscore the safety benefits related to platooning, as it aids in lowering conflict severity. Furthermore, the results suggest these safety advantages are amplified as traffic volumes rise, indicating platooning's efficacy in managing conflicts in high-volume situations.

Table 41 Conflict frequency and risk comparison for various platoon configurations

CACC Level 1 Automation											
Volume (vph)	Max. Platoon size	Avg no. of conflicts (1 hr.)	Relative risk	t-statistic	Rear end Conflicts	Relative risk	t-statistic	Lane change Conflicts	Relative risk	t-statistic	t-critical
1700	zero	129	1	-	71.25	1	-	48	1	-	-
	two	128	1.26	2.41	97.6	1.37	3.21	53	1.1	0.92	1.89
	five	139.4	1.17	3.84	95.4	1.34	4.78	44	0.92	-1.82	1.89
	seven	146	1.22	3.74	97.6	1.37	5.38	47.4	0.99	-0.14	1.89
2100	zero	256.6	1	-	167.6	1	-	89	1	-	-
	two	282.2	1.1	1.79	185.2	1.11	1.77	97	1.09	1.5	1.86
	five	248.2	0.97	-0.62	165.4	0.99	-0.2	82.6	0.93	-1.41	1.86
	seven	254.6	0.99	-0.13	169	1.01	0.13	85.6	0.96	-0.62	1.86
2500	zero	542	1		542.25	1		181.75	1		-
	two	506	0.93	-0.56	494.5	0.91	-0.6	176	0.97	-0.32	1.94
	five	383	0.66	-2.74	339.5	0.63	-2.81	141.5	0.78	-2.2	1.94
	seven	339	0.54	-3.87	309	0.57	-3.27	84.75	0.47	-6.27	1.94
CACC Level 2 Automation											
1700	zero	92.75	1	-	55.5	1	-	37.25	1	-	-
	two	91.25	0.98	-0.34	56.75	1.02	0.25	34.5	0.93	-1.07	1.94
	five	86.25	0.93	-1.24	59.5	1.07	0.78	26.75	0.72	-3.26	1.94
	seven	82.25	0.89	-1.77	54	0.97	-0.23	28.25	0.76	-3.31	1.94
2100	zero	180	1	-	109.5	1	-	70.5	1	-	-
	two	150.25	0.83	-2.37	98.75	0.9	-0.83	50.75	0.72	-8.13	1.94
	five	146.75	0.82	-2.62	101.75	0.93	-0.64	45	0.64	-14.06	1.94
	seven	131.5	0.73	-4.33	90	0.82	-1.78	41.5	0.59	-9.17	1.94
2500	zero	375.25	1	-	251.5	1	-	123.75	1	-	-
	two	301.25	0.8	-3.35	214.5	0.85	-2.33	86.5	0.7	-4.15	1.94
	five	226.25	0.6	-6.31	152.75	0.61	-6.42	73.5	0.59	-4.83	1.94

Table 42 Comparison of Mean TTC and Delta V parameters for various scenarios

CACC stage 1 Automation						
Volume (vph)	Max. Platoon size	Mean TTC(s)	t-statistic	Delta V (ft/s)	t-statistic	t-critical
1700	zero	0.42	-	5.93	-	-
	two	0.46	1.21	6.1	0.49	1.66
	five	0.49	2.13	4.64	-3.78	1.66
	seven	0.48	1.72	4.28	-4.97	1.66
2100	zero	0.41	-	5.64	-	-
	two	0.45	1.67	5.27	-1.7	1.66
	five	0.49	3.4	4.58	-4.86	1.66
	seven	0.46	1.67	5.48	-0.51	1.66
2500	zero	0.62	-	3.89	-	-
	two	0.63	0.59	4.23	2.88	1.66
	five	0.56	-3.16	4.52	4.51	1.66
	seven	0.71	4.78	2.85	-8.89	1.66
CACC stage 2 Automation						
1700	zero	0.44	-	6.72	-	-
	two	0.62	3.82	5.22	-3.79	1.66
	five	0.64	4.33	3.99	-7.4	1.66
	seven	0.64	4.23	3.92	-7.31	1.66
2100	zero	0.48	-	5.32	-	-
	two	0.59	3.01	4.61	-2.63	1.66
	five	0.64	4.53	4.05	-4.89	1.66
	seven	0.63	4.06	4.2	-4.12	1.66
2500	zero	0.5	-	5.09	-	-
	two	0.63	5.08	4.21	-4.93	1.66
	five	0.6	3.79	4.22	-4.49	1.66
	seven	0.72	8.73	3.45	-9.63	1.66

5.3.4.3 Distribution of speeds along the Upstream of Work zone

To comprehend the variations in speed across the upstream work zone, a heatmap is generated for each individual scenario, capturing data from every timestamp as shown in Figure 31. This visual representation illustrates speed changes along the length of different zones observed upstream of the work zone.

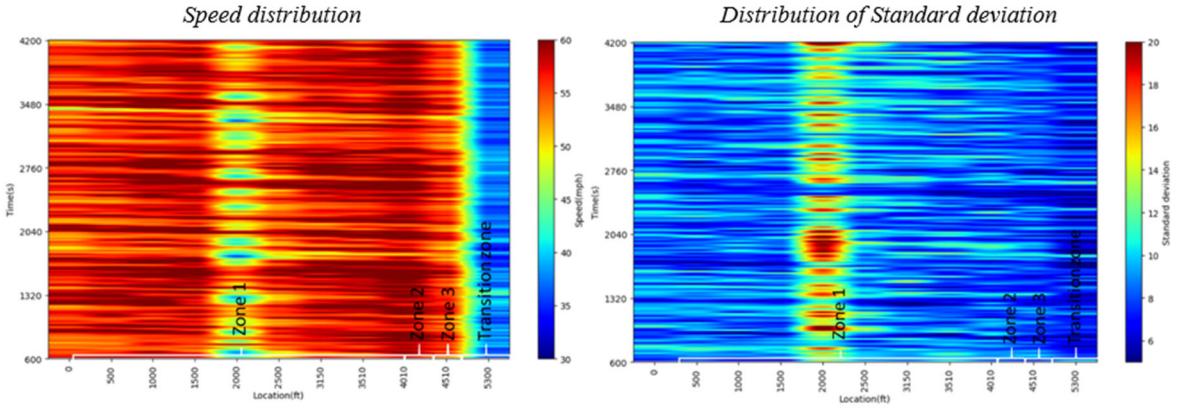

Figure 31 Spatiotemporal distribution for no platoon case with Low volume (1700 vph)

Heatmap analysis identifies two prominent regions where speed significantly reduces. The first region is approximately 2000 feet from the beginning of Zone 1(an interchange) and this decrease might be due to the concurrent lane changes involving CACC trucks shifting left and other vehicles exiting the freeway that necessitate right lane changes. These simultaneous lane alterations result in speed reductions as vehicles adjust to these transitions. The second region with speed reduction manifests in the transition zone, where the areas of reduced speed begin. The presence of these speed deceleration zones consequently leads to slower speeds.

In addition, the study generated distinct heatmaps to visually compare the effects of two driving behaviors across various scenarios as shown in Figure 32 and 33. Particularly, heatmaps were created for a high-volume scenario and a maximum platoon size of seven. These were then contrasted with the base scenario—low volume without platooning.

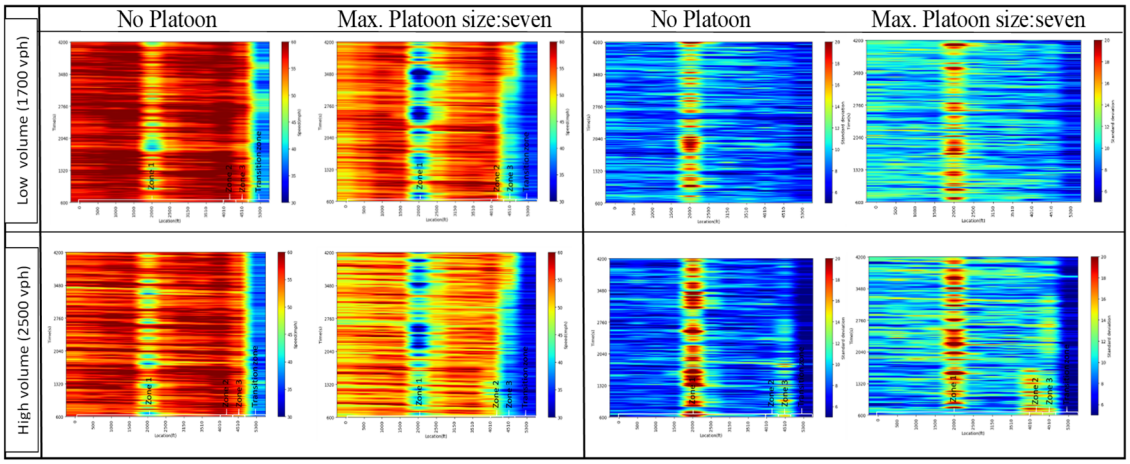

Figure 32 Spatiotemporal distribution of speeds and standard deviation for CACC stage 1 Automation

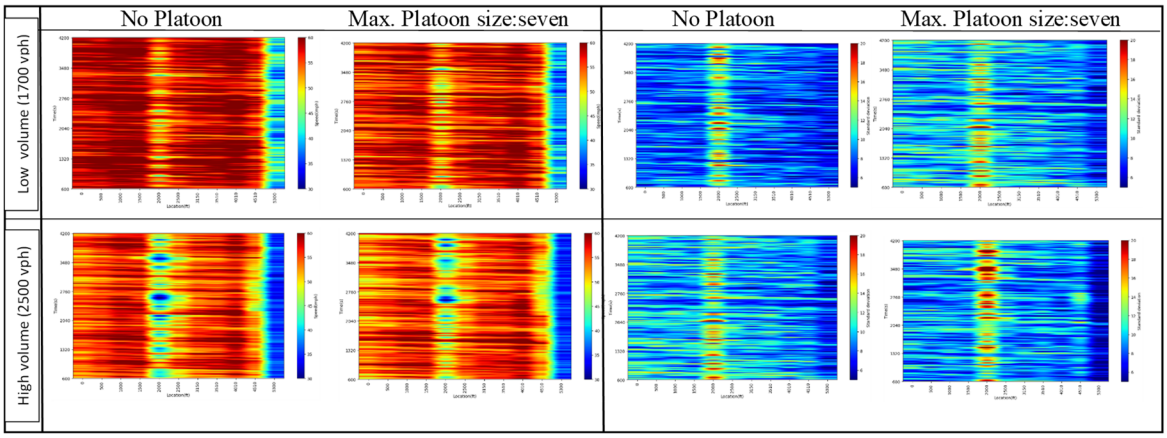

Figure 33 Spatiotemporal distribution of speeds and standard deviation for CACC stage 2 Automation

The speed distribution plots provide clear evidence that platooning has a significant impact on reducing speeds. Notably, in the regions where speed decreases are observed, the lower speeds are more widely distributed in the case of platooning. This can be attributed to the cohesive nature of vehicles within platoons. When encountering other vehicles changing lanes in front of them, the vehicles within a platoon act as a unit, collectively slowing down and gradually picking up speed. In contrast, in the base case without platooning, trucks act independently and make maneuvers to maintain their speed, resulting in narrower speed reduction regions compared to the platooning scenario. This trend is particularly observed in the case of CACC stage 1 automation, where operational speeds are decreased but safety is improved. On the other hand, in the case of CACC stage 2 automation, the speed distribution within platoons is almost similar to the base case without platooning. However, safety

advantages are still observed without compromising the operational speed on the freeway. These findings indicate that as the automation level increases, both safety and operational performance can be improved.

5.3.4.4 Effect of early merge and late merging of platoons in work zones

This investigation aims to understand how platoon-required lane changes affect the upstream area of a work zone. Simulations were conducted using various lane merge distances: 2 miles, 1 mile, 0.5 mile, and immediately before the transition zone (0.2 miles from the lane closure connector). All trucks participating in the study were automated with CACC stage 1, implementing advanced merge and cooperative lane change behaviors during the lane change process. Rather than being distributed values, lane change distances were treated as fixed points, as trucks initiated their lane change decisions at these specific locations, adapting to the traffic conditions on other lanes.

Moreover, this study probed the combined influence of traffic volume and platoon sizes on safety during lane changes, considering two volume levels (high and low) and two platoon sizes (short and long platoons). Shorter platoons were modeled by setting the maximum platoon size to two, while longer platoons were depicted by increasing the maximum platoon size to seven in the VISSIM software. This examination of these factors provides pivotal insights into the behavior of platoons and their lane-changing maneuvers in work zone areas.

Table 43 presents the conflict distribution under various lane change configurations. From the table, it can be observed that traffic safety is critical when platoons merge near the transition zone as the no. of conflicts increased by 300 percent to 400 percent as compared to the case when there were no platoons. On the other hand, the longer truck platoons improved safety along the freeway weaving section during early merge situations. Furthermore, the no. of conflicts decreased by 40 percent at high traffic volumes with respect to base case scenario without platoons.

The results reveal that the location of advanced warning signs up to one mile upstream does not significantly impact safety outcomes. However, after the lane change signs were placed at distances of 0.5 miles for platoons, and more significantly at 0.2 miles just before the transition zone, the total number of conflicts increased noticeably. This is due to huge increase in number

of Rear end conflicts as lane changes happen closer to work zone area and this led to shockwave development just before the transition zone. This result suggests that while platooning can be advantageous in controlled flow conditions, it poses a considerable risk to traffic safety when sudden lane changes or merges are involved.

To understand the traffic flow variation on upstream of work zones, the speed distribution was plotted for various lane merge scenarios as shown in Figure 34.

Table 43 Conflict distribution under various Lane change configurations

Volume (1700 vph)				
	Lane change sign distance from work zone activity area (mile)	Total No. of conflicts (1 hr.)	No. of Rear end Conflicts	No. of Lane change Conflicts
No platoon	2	104	64	40
	1	129	85	44
	0.5	156	103	53
	0.2	214	150	64
Platoon size 2	2	122	72	50
	1	128	87	41
	0.5	119	86	32
	0.2	421	367	53
Platoon size 7	2	118	81	37
	1	146	101	45
	0.5	125	87	38
	0.2	594	535	59
Volume (2500 vph)				
	Lane change sign distance from work zone activity area (mile)	Total (1 hr.) No. of Conflicts	No. of Rear end Conflicts	No. of Lane change Conflicts
No platoon	2	520	367	153
	1	542	390	152
	0.5	681	527	154
	0.2	701	526	175
Platoon size 2	2	421	312	109
	1	506	387	119
	0.5	724	628	96
	0.2	1533	1390	143
Platoon size 7	2	383	290	93
	1	339	253	86
	0.5	617	542	75
	0.2	1586	1480	105

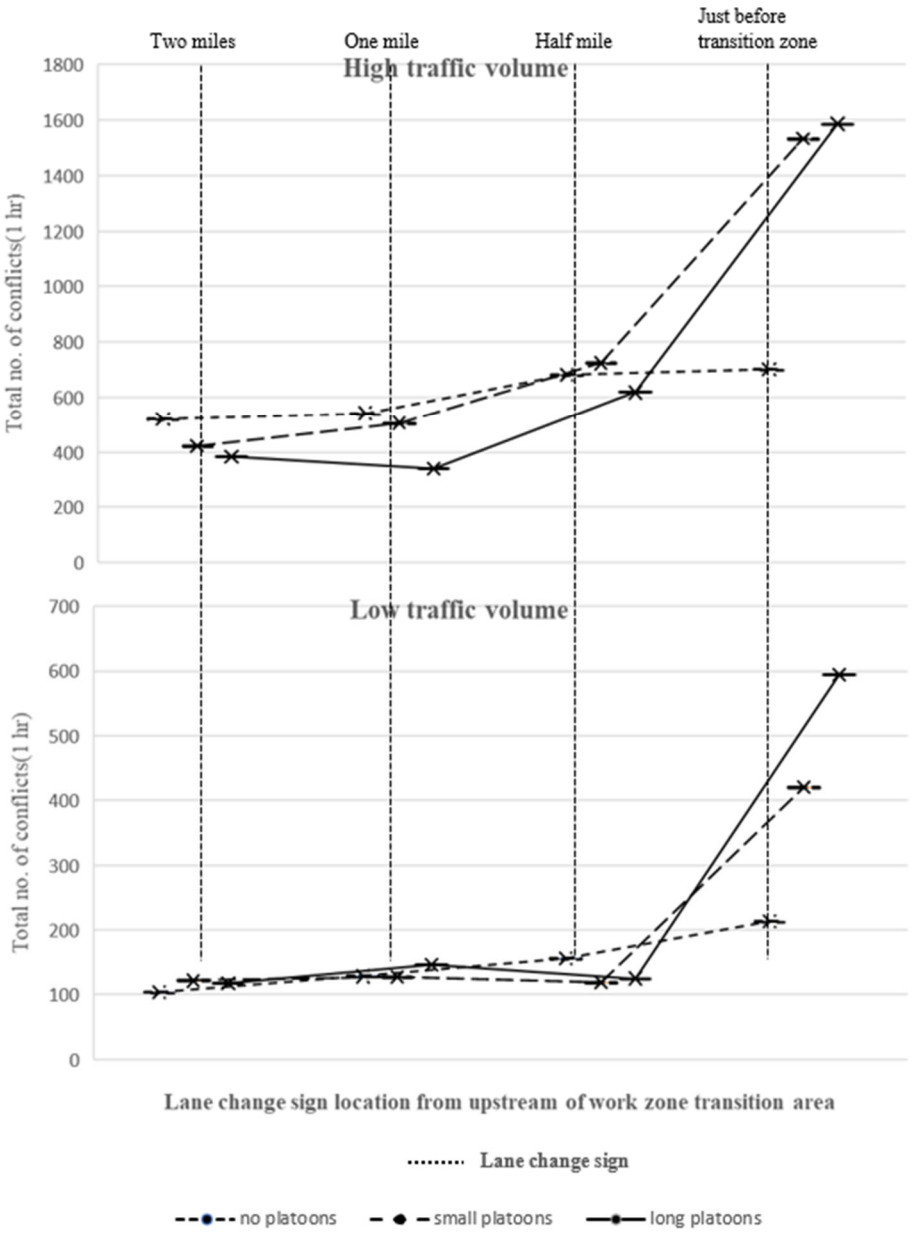

Figure 34 conflict frequency distribution with various lane change configurations

5.3.5 Operational performance Evaluation

Average speeds for all vehicles were computed every 500 feet from an upstream distance of two miles from the transition zone for each early and late merge case scenario. The resulting upstream speeds for each case have been illustrated in Figure 35.

The upstream location is considered from the point just before the activity area commences, encompassing the advanced warning area and the transition zone. The transition zone extends from 0.2 miles upstream to its termination point.

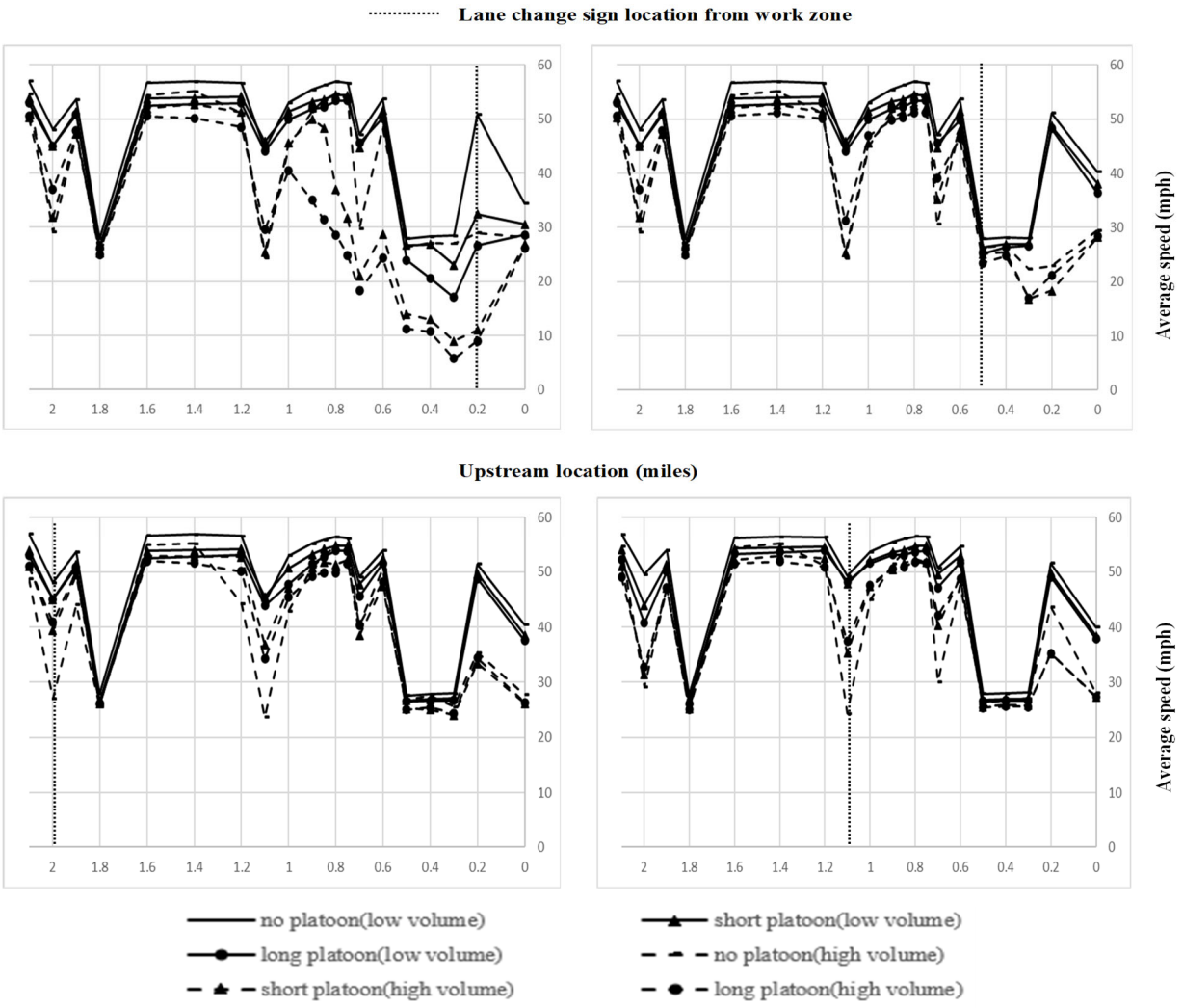

Figure 35 Speed distribution on upstream of work zone area

From the simulation results, it was observed that in Late merge cases, when the Lane change signal distances were 0.5 miles upstream and just before Transition zone (0.2 miles), there was a significant decrease in speeds and this was drastic for longer platoons as the speeds reached less than 10 mph at high traffic volumes in comparison to scenario without platooning the speeds were maintained above 20 mph before the Transition zone even at high volumes.

CHAPTER 6. OPTIMIZING LANE CONFIGURATION FOR EFFICIENT PLATOON CONTROL DURING LANE CLOSURES

6.1 Introduction

In recent years, the field of transportation has witnessed rapid technological advancements, marked by successive revolutionary innovations. While intelligent transportation systems (ITS), such as automated vehicles, have been in development for several decades, recent initiatives indicate an accelerated timeline for widespread implementation. Researchers have shown considerable interest in various applications of vehicle automation, seeking to identify those with the most profound implications for the future of transportation (Fagnant and Kockelman 2015; Wadud, MacKenzie, and Leiby 2016). Fundamentally, connected and automated vehicles (CAV) are poised to assist drivers by delegating some or all driving tasks to computerized systems. Additionally, CAVs leverage vehicle-to-vehicle (V2V) connectivity to exchange information with nearby vehicles and adapt their behavior accordingly. The Society of Automotive Engineers has established a framework comprising six levels of vehicle automation, ranging from level zero (no automation) to level five (full automation) (SAE 2018). These levels categorize vehicles based on their implementation of various advanced driving assistance (ADA) technologies, with level five designating vehicles capable of executing all driving functions without human intervention.

During the early phases of Connected and Automated Vehicle (CAV) deployment, when both CAVs and human-driven vehicles share the same lanes, several concerns arise. Given that CAV platoons tend to follow shorter headways, this can potentially create significant challenges for other vehicles when encountering platoons or attempting lane changes nearby. To effectively address these challenges, it is imperative to conduct a comprehensive assessment of platoon behavior across different freeway sections. This assessment encompasses the implementation of various lane-based configurations and strategies aimed at managing CAV operations and fostering a safer traffic environment. One frequently considered approach is the allocation of Dedicated Lanes (DLs) exclusively for CAVs, which reduces interactions between CAV platoons and human-driven vehicles while improving the possibility of platoon formation (Dehman and Farooq 2021), leading to a higher prevalence of CAV platoons in these lanes. Nonetheless, it is

crucial to recognize that Dedicated Lanes may become less efficient when the Market Penetration Rate (MPR) is very low (Razmi Rad et al. 2020). A proposed solution could be Human-Driven Vehicles (HDVs) sharing dedicated lanes with CAVs during periods of very low MPR, with a subsequent transition to fully dedicated CAV lanes once a predetermined MPR threshold is reached (Razmi Rad et al. 2020)

While the driver's behavior is improved with CAV's, it is still not clear on how these vehicles when forming platoons react to work zones. It was reported that a work zone fatality occurs every 15 hours and this also involved construction workers. Although many studies have utilized microsimulation to assess the impacts of CAVs near work zones. Most of them focused on operational advantages and safety improvements due to better communication V2I and V2V. Nonetheless, there has been a lack of studies that specifically consider lane configurations as a critical factor in evaluations. Additionally, there is a need for comparative analysis between mixed lanes, shared lanes, and dedicated lanes at various MPRs. This chapter aims to fulfill this gap by focusing on different lane configurations and their role in improving both safety and operations of platoons near work zones, this in a way helps to provide more insights for Infrastructure Owners and Operators, Traffic agencies for coming up with better ways to adopt the upcoming advances in CAT technology

6.2 Background

Extensive research efforts have been dedicated to the exploration of Connected and Autonomous Vehicles (CAVs) with a specific emphasis on platooning, aiming to enhance infrastructure for the benefit of both conventional and autonomous vehicles, ultimately leading to improvements in overall traffic flow. This section provides a comprehensive overview of these studies, shedding light on their specific objectives, noteworthy findings, and the research gaps that have been identified in the pursuit of advancing CAV technology and its integration into the transportation system

Table 44 Relevant literature on key factors affecting platooning

Study	Objectives	Key findings	Gaps
The impact of a dedicated lane for connected and automated vehicles on the behavior of drivers of manual vehicles (Razmi Rad et al. 2021)	Investigating the effect that platoons in dedicated lanes and mixed scenarios pose to other human driven vehicles	MV drivers drove closer to their leaders specially when driving on the middle lane next to the platoons and accepted shorter gaps (up to 12.7 percent shorter at on-ramps)	Although platooning behavior has improved in other lanes, the safety aspect was missing
Platoon Intensity of Connected Automated Vehicles: Definition, Formulas, Examples, and Applications (Jiang et al. 2023)	Evaluating the effect of platoon intensity and MPR on operational characteristics of freeways	An optimal platoon size of 5 vehicles was suggested for the CAV platoon. CAV platoon intensity has a low impact on the characteristics of mixed traffic flow with the low penetration rate	There is no consideration of traffic safety with relevance to traffic intensity
Impact of connected and autonomous vehicles on traffic safety of mixed traffic flow: from the perspective of connectivity and spatial distribution (Dong et al. 2022)	Investigate the impact of CAV on traffic safety with respect to connectivity (communication level)	Increase in MPR of CAV improved safety performance. No improvement at low MPR	-
A Review of Truck Platooning Projects for Energy Savings (Tsugawa et al. 2016)	Investigating the effect of Truck platoon from environmental and operational perspective	Platooning aerodynamic drag and allows vehicles to use energy efficiently reducing fuel emissions	-
Safety Impact of Connected Vehicles on Driver Behavior in Rural Work Zones under Foggy Weather Conditions (Adomah et al. 2022)	Investigating the safety benefits of CV Work Zone Warning (WZW) applications on driver behavior during foggy weather conditions	The advanced warning area had large no. of conflicts as compared to other areas of work zones. An increase in MPR of up to 60 percent on I-80 resulted in reduced speeds which led to speed harmonization and decreased crash risk	-
Impacts of advanced driver assistance systems on commercial truck driver behavior performance using naturalistic data (Wu et al. 2023)	Study the impacts of ADAS with respect to various collision warning systems, and speed limit indicators on commercial truck drivers' behaviors using naturalistic data	Analysis suggested that these warnings had positive effect on driver behavior as they made them more alert	-
Exploring work zone late merge strategies	Comparing the performance of late merge strategies with	The late merge strategy worked best with a CV	-

Study	Objectives	Key findings	Gaps
with and without enabling connected vehicles technologies (Algomaiah and Li 2021)	CV enabled and without CV technology	enabled environment in terms of operations. The advantages of late merge strategy were lost when heavy vehicle percentage is more than 20 percent	
Benefits and Risks of Truck Platooning on Freeway Operations Near Entrance Ramp (M. Wang et al. 2019)	Studying the effects of truck platoons near entrance ramp with varying MPR	Simulation results show that at high MPRs of truck platooning, the system mitigates congestion and increases throughput but at the expense of merging failures.	-
Impact of Platooning Connected and Automated Heavy Vehicles on Interstate Freeway Work Zone Operations (Haque et al. 2023)	Impact of CAHV on the operational performance of freeway work zones. Analyzing work zone performance as a function of CAHV market penetration rate, traffic demand, truck percentage values, and lane restriction.	The average flow rate increased by 67 percent. Maximum queue size and average delay decrease by approximately 97 percent. Queue and delay reduced as CAHV MPR increased (used 100 percent MPR CAHV)	Utilized aggressive driving logic and only full automation level parameters (Co-Exist) for Heavy vehicles. No safety evaluation was performed
Are work zone and connected automated vehicles ready for a harmonious coexistence? A scoping review and research agenda (Dehman and Farooq 2021)	A comprehensive study utilizing all aspects related to CAV near work zones	Findings suggest that platooning in closed lanes might not perform well near work zones and in open lanes just near closed lanes	No analysis was performed to evaluate the suggestions made. Suggestions were based on multilane freeway (five lane highway)
Evaluating the safety impact of connected and autonomous vehicles on motorways (Papadoulis et al. 2019)	Investigating safety evaluation using SSAM and External driver model in VISSIM	Traffic conflicts were reduced by 12 to 47 percent, 50 to 80 percent, 82 to 92 percent and 90 to 94 percent for 25 percent, 50 percent, 75 percent and 100 percent CAV penetration rates respectively	Didn't look at problematic sections (ramps, work zones). Did not have platooning
Safety analysis of freeway on-ramp merging with the presence of autonomous vehicles (Zhu and Tasic 2021)	Evaluating the safety of AVs on ramps using new indicator Conflicting Merge Headway (CMH)	Severity and frequency of conflicts reduced	No comparison of new conflict indicator with traditional indicators like TTC, PET

Study	Objectives	Key findings	Gaps
Dedicated Lane for Connected and Automated Vehicle: How Much Does A Homogeneous 23 Traffic Flow Contribute? (Zhong et al. 2020)	Investigating the change in the traffic flow characteristics with different configurations of dedicated CAV lane across various levels of market penetration	Observed a 90 percent increase in capacity of the lane at higher volumes	-
Design and operation of dedicated lanes for connected and automated vehicles on motorways: A conceptual framework and research agenda (Razmi Rad et al. 2020)	Develop a conceptual framework accounting for the factors that could affect the safety and efficiency of Dedicated lanes	Suggests a minimum MPR of 20 percent to implement a dedicated CAV lane. Combined effects of traffic safety and efficiency must be considered while designing DLs in transition period	-
A mixed traffic speed harmonization model with connected autonomous vehicles (Ghiasi et al. 2019)	Developing CAV-based trajectory-smoothing concept to harmonize traffic, improve fuel-efficiency and reduce environmental impacts	CAVs have harmonized speeds even at low MPR	-
Cooperative Adaptive Cruise Control Definitions and Operating Concepts (Shladover et al. 2015)	Reviewing studies related to CACC platoons	Making CAV vehicles to follow each other increased chances of platooning	-

Some research indicates that reserving the leftmost lane exclusively for Connected and Autonomous Vehicles (CAVs) can effectively reduce interactions between CAVs and on-ramps, potentially enhancing overall traffic flow. However, this configuration may present challenges for CAVs needing to exit or merge into CAV platoons from the left, requiring multiple lane changes to execute these maneuvers. Nonetheless, it's worth noting that a dedicated lane, shielded from disruptions, can achieve an impressive capacity of 3,400 vehicles per hour per lane at a 90 percent Market Penetration Rate (MPR) (Zhong et al., 2020). Additionally, studies suggest that a minimum MPR of 20 percent is necessary to justify the allocation of a dedicated CAV lane in a four-lane basic freeway segment (Rad et al. 2020; Chen et al. 2016).

6.3 Methodology

This section provides a comprehensive overview of the VISSIM model's development, including the underlying assumptions, the creation of various scenarios, and the presentation of

simulation results. The driver behavior parameters for car following were derived from Weidemann 99, while lane parameters remain consistent with those obtained from the NDS SHRP2 project, as discussed in the previous chapter. Given the focus of this study on the initial stages of CAV platooning, the analysis primarily employs CACC level 1 automation for platooning vehicles. Furthermore, certain assumptions have been made regarding platooning formation and dissolution.

6.3.1 Platooning logic

This study extensively explores lane configuration strategies aimed at mitigating safety issues resulting from mandatory lane merges involving conventional vehicles and CACC platoons. This will place greater emphasis on the development of various scenarios and assumptions, all of which are informed by the internal platooning logic in PTV VISSIM. The flowchart for internal platooning logic is presented in Figure 36.

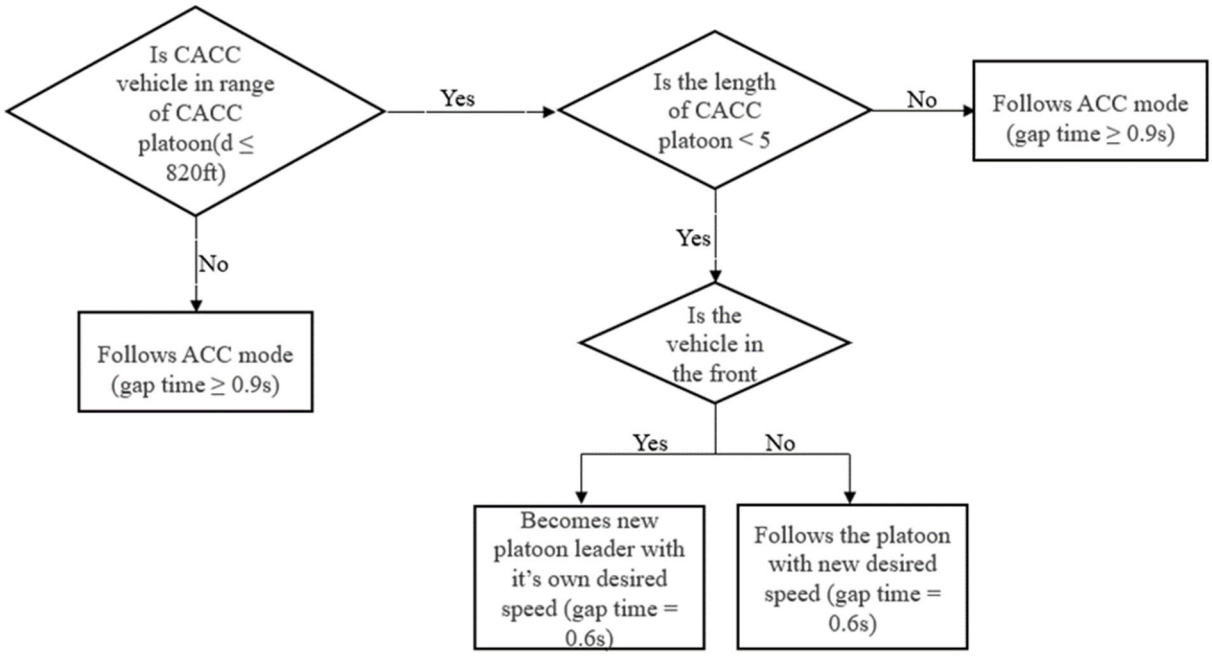

Figure 36 Internal platooning logic (PTV VISSIM 2021)

The maximum platoon size is limited to five vehicles, with a gap time of 0.6 seconds between CACC vehicles in a platoon. This aggressive following behavior assumption aims to emphasize

safety concerns in platoons while preserving their operational and environmental advantages through close spacing.

6.3.2 VISSIM model

The simulations were conducted on a two-lane section of a standard freeway. This segment consisted of an unobstructed freeway stretch spanning three miles, followed by an upstream work zone extending for one mile, and then the actual work zone, also covering one mile in length. The parameters for vehicle inputs were established at the freeway's entry point, with a traffic volume of 1000 vehicles per hour. The composition of vehicles in this flow was modeled after that of rural freeway I-80, with 40 percent heavy goods vehicles (HGVs) and 60 percent passenger cars.

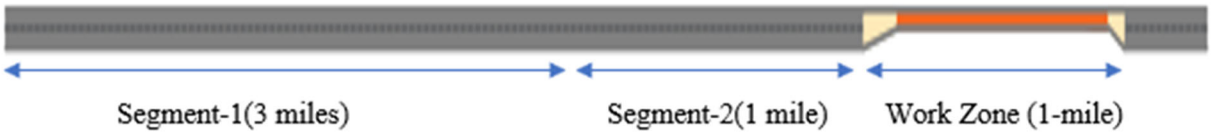

Figure 37 Freeway section modelled in VISSIM

6.3.3 Simulation parameters and other settings

The study adheres to the car-following parameters established by Wiedemann in 1999, utilizing internal settings within VISSIM. Additionally, lane-change parameters have been refined and updated based on the insights gained from the SHRP2 project (chapter 3). A comprehensive summary of these modifications is provided in Table 45.

Table 45 Driver behavior parameters

Car following parameters		**Lane change parameters**	
CC0 (Standstill distance (ft))	4.92	**Own vehicle**	
CC1 (Gap time distribution (s))	0.9	Maximum deceleration(ft/s2)	-11.38
CC2 ('Following' distance oscillation (ft))	0	Accepted deceleration(ft/s2)	-0.11
CC3 (Threshold for entering 'following' (s))	-8	**Trailing vehicle**	
CC4 (Negative speed difference (ft/s))	-0.1	Maximum deceleration(ft/s2)	-1.78
CC5 (Positive speed difference (ft/s))	0.1	Accepted deceleration(ft/s2)	-0.09
CC6 (Distance dependency of oscillation)	0	**Other lane change Parameters**	
CC7 (Oscillation acceleration (ft/s^2))	0.33	Minimum clearance(ft)	104.41
CC8 (Acceleration from standstill (ft/s^2))	11.48	Cooperative Lane change	Yes
CC9 (Acceleration at 50 mph (ft/s^2))	4.92	Advanced merging	Yes

The number of simulation runs for each scenario were kept to 10 with different seeds and simulation resolution was 20 timesteps/simulation sec.

6.3.4 Scenario Development

This study implemented work zone warnings one mile ahead of the transition zone, prompting vehicles to follow conventional early merge strategies. Platoons were examined under six conditions, based on three lane configurations. The first condition allowed platoons to use both lanes on the freeway without restrictions. In the second and third conditions, platoons were confined to a single lane due to one lane being closed in the work zone, resulting in platoons using either the open or closed lane. Within these three conditions, the study also considered whether platoons were permitted to merge upstream, resulting in six distinct conditions for a two-lane freeway with one lane closed.

A) **Base case scenario:** All the vehicles are human driven with right lane closure at the work zone
B) **Platooning allowed on both lanes:** (Two scenarios – platooning allowed upstream (✓), not allowed on one mile upstream (✗) of lane closure)

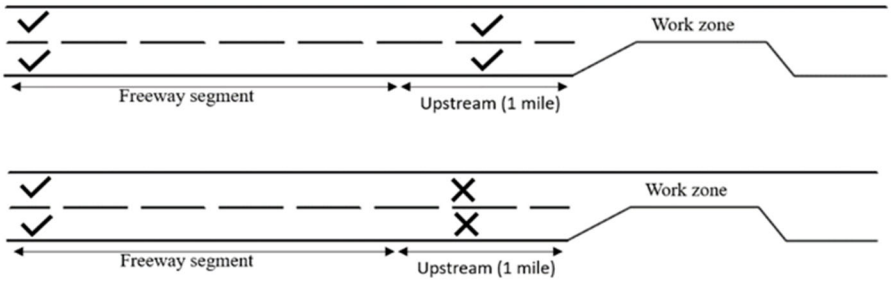

Figure 38 No restriction for platooning scenario

C) **Platooning allowed only on open lane:** (Two scenarios – platooning allowed upstream (✓), not allowed on one mile upstream (✗) of lane closure)

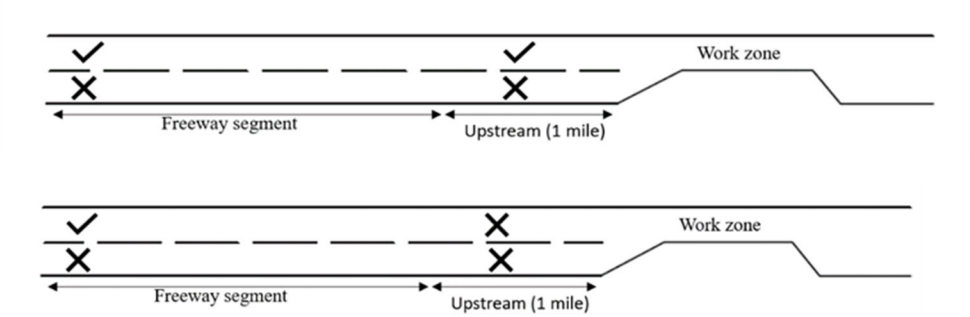

Figure 39 Open Lane utilized by platoons

D) **Platooning allowed only on closed lane:** (Two scenarios – platooning allowed upstream (✓), not allowed on one mile upstream (✗) of lane closure)

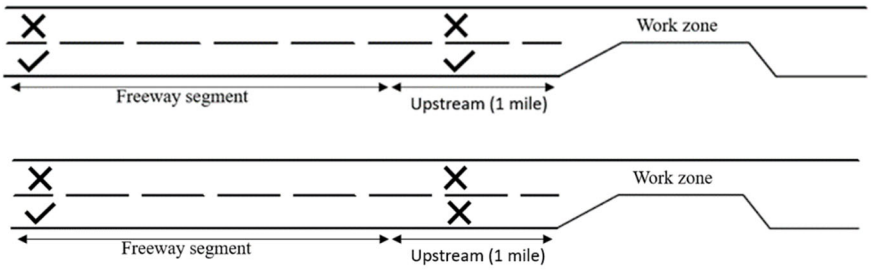

Figure 40 Closed Lane utilized by platoons

6.4 Results and discussion

6.4.1 Traffic conflict analysis

This study utilized TTC threshold of 1.5 s and traffic conflicts were extracted using SSAM tool based on the trajectory outputs from microsimulation. Table 46 and Figure 41 demonstrate the traffic conflict frequency distributions for various scenarios.

Table 46 Traffic conflict frequency distribution for various MPR (percent CACC)

Lanes used by platoons, upstream (1-mile) condition for platooning	Average no. of conflicts(hr) for different MPR (percentage of CACC)				
	0	**20**	**40**	**60**	**80**
Both lanes, Yes (B(Y))	149.4	109	158	198	303
Both lanes, No (B(N))	149.4	170.4	166.2	181.4	268.8
Open lane, Yes (O(Y))	149.4	139	112.2	104.6	114
Open lane, No (O(N))	149.4	163.8	131.6	125.2	126.6
Closed lane, Yes (C(Y))	149.4	136.2	137.5	138.6	158.3
Closed lane, No (C(N))	149.4	136	137	129	142.5

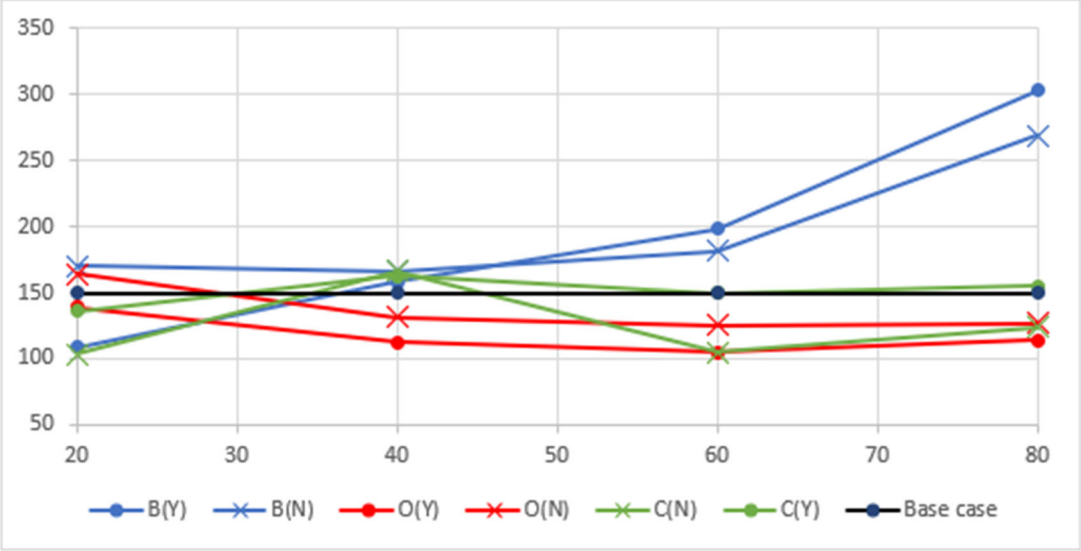

Figure 41 Traffic conflict frequency distribution vs MPR (percent CACC)

The results indicate that utilizing both lanes for platooning may compromise safety as the Minimum Platoon Ratio (MPR) increases, primarily due to increased interactions between Heavy-Duty Vehicles with Cooperative Adaptive Cruise Control (HDV-CACC) and Cooperative Adaptive Cruise Control with Cooperative Adaptive Cruise Control (CACC-CACC) vehicles during lane merges. Interestingly, in both open and closed lanes, there was no significant increase in traffic conflicts with increasing MPR, likely because platooning in a single lane reduced interactions between CACC-CACC vehicles. Among the scenarios considered, platooning in open lanes during lane closures was the most suitable, as conflicts decreased, suggesting fewer interactions between CACC vehicles and HDV, thus improving safety.

To determine the overall percentage of CACC vehicles participating in platoons across these scenarios, we processed the raw ".fzp" files from VISSIM using Python's PANDAS library. This involved calculating the percentage of CACC vehicles involved in platooning at each time step and subsequently computing the average platoon percentage across all time steps. The results have been presented in Table 47.

Table 47 Total percentage of CACC vehicles involved in platooning for various MPR (percent CACC)

Lane configuration and platooning condition	percent of CACC vehicles in platooning for different MPR (percentage CACC)			
	20	**40**	**60**	**80**
B(Y)	23.4	37.4	53.1	59.6
B(N)	11.0	17.3	27.7	33.2
O(Y)	13.7	17.3	25.9	30.2
O(N)	7.1	8.4	13.2	14.8
C(Y)	9.3	17.4	20.8	25.4
C(N)	7.7	10.2	13.1	16.0

Analysis of the results from both tables reveals a clear trend: a higher percentage of platoons occurs when both lanes are utilized for platooning, especially at higher Minimum Platoon Ratios (MPR), compared to using a single lane. Notably, an intriguing finding emerges; in the open lane condition at 80 MPR, there is a greater number of Cooperative Adaptive Cruise Control (CACC) platoons (30.2 percent) than in the closed lane condition (25.4 percent), while the number of

conflicts is notably lower by 28 percent. This suggests that the open lane configuration for platooning is the most favorable scenario in terms of safety near work zones.

6.4.2 Operational characteristics evaluation

From the simulation runs, Average speeds, and Delay were calculated and to monitor the Queue characteristics, a Queue detector was placed at 600 ft before complete lane closure in the transition zone where vehicles unable to merge on upstream must stop and make necessary lane changes. All these results were observed for various MPR of CACC vehicles in different lane configurations. Table 48, Table 49 and Figure 42 present the results from operational evaluation.

Table 48 Avg. speed, Total Avg. delay for different MPR (percent CACC)

Lane configuration and platooning condition	Average speed(mph) for different MPR (percent CACC)					Total Avg. delay(hr) for different MPR (percent CACC)				
	0	20	40	60	80	0	20	40	60	80
B(Y)	55.9	58.6	59.6	61.4	61.8	71.6	57.6	52.1	42.6	39.5
B(N)	55.9	55.9	56.3	57.9	58.5	71.6	72	70.0	61.4	58.7
O(Y)	55.9	56.9	58.9	60.5	61.4	71.6	67.2	56.8	48.6	44.6
O(N)	55.9	56.2	57.6	58.6	59.2	71.6	71	64.0	59.6	56.8
C(Y)	55.9	57.9	59.3	60.1	61.1	71.6	62.1	55.2	51.9	47.2
C(N)	55.9	57.9	59.1	59.1	59.9	71.6	62	56.9	57.1	53.6

Table 49 Avg. Queue length observed in transition zone vs MPR (percent CACC)

Lane configuration and platooning condition	Avg. Queue length observed before lane closure segment for different MPR(percent CACC)				
	0	**20**	**40**	**60**	**80**
B(Y)	346	167.5	71	27.4	8.7
B(N)	346	307.8	245.6	156.3	121.5
O(Y)	346	273.4	133.7	47.9	23.6
O(N)	346	315.1	207.7	135.8	109.4
C(Y)	346	239.4	118.3	115.7	84.5
C(N)	346	220.7	137	119.5	102.9

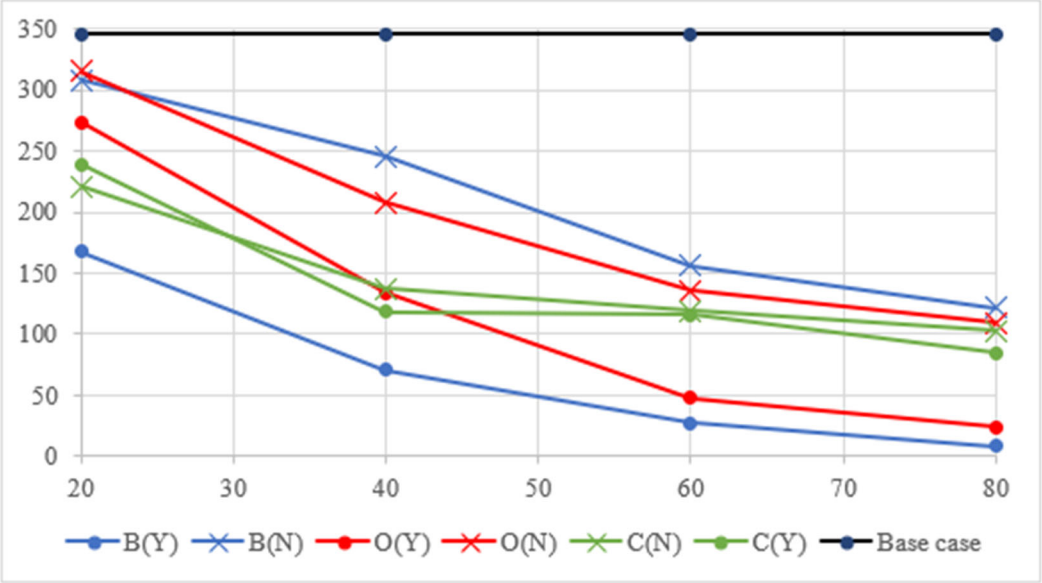

Figure 42 Avg. queue length (ft) vs MPR (percent CACC)

Analysis of the tables and Figures indicate that as the Market Penetration Rate (MPR) increases, operational performance also sees improvements. The scenario allowing platooning on both lanes, including the upstream approach, exhibits the best operational results, but at the compromise of safety performance as it has resulted in the highest number of traffic conflicts. Surprisingly, the open lane scenario closely follows the former in terms of operational performance, with marginal differences. At the same time, the open lane scenario consistently excels in safety compared to all other scenarios. These results suggest that permitting platooning on open lanes near work zones is not problematic. However, for any other lane

configurations, it is recommended that vehicles disengage from platooning at least one mile upstream of the work zone to ensure improved safety. Remarkably, platoons allowed on open lanes demonstrate superior performance in both operational and safety aspects compared to other alternate scenarios.

CHAPTER 7. CONCLUSIONS AND RECOMMENDATIONS

7.1 Research Summary and Key Findings

The primary objective of this study was to leverage SHRP2 NDS data for updating essential parameters necessary for modeling HV-CAT interaction and microsimulation. This update was crucial for gaining insights into the potential safety and operational advantages of CAT in the future. The approach employed in this study involved:

- The development of a DLalgorithm to extract lane change parameters from SHRP2 data, which, in turn, aided in updating parameters for microsimulation modeling.
- The utilization of this algorithm to analyze various adverse weather conditions typical in Wyoming, enabling the extraction of associated lane change parameters. These parameters were then applied to a real segment of Wyoming.
- Combining the parameters derived from SHRP2 NDS data with simulation parameters from various research and literature sources for conducting diverse microsimulation studies involving CAT, with a focus on assessing its safety and operational impacts.

SHRP2 NDS data plays a crucial role in facilitating the study involving CAT and for updating the microsimulation parameters. In the current scenario, CAT technology is still in a stage of mixed traffic adoption, and its full development is yet to be realized before achieving substantial safety and operational benefits. Leveraging SHRP2 data not only assists in modeling these parameters but also enhances the simulation environment, enabling it to closely mirror real-world conditions.

7.1.1 Updating lane change parameters from SHRP2 naturalistic driving data using deep learning and optimizing the parameters to develop microsimulation model for adverse weather

The main objective of this study was to enhance lane change models under varying weather conditions, utilizing the second-by-second trajectory-level dataset from the SHRP2 NDS. For the first time, this study sought to adjust lane change parameters specifically for distinct weather conditions in order to create realistic microsimulation models applicable in real-world scenarios. The adjustment of the lane change model was performed using a set of manually verified lane change events, identified through a developed automatic algorithm. The lane

change events were leveraged to derive the necessary lane change parameters, encompassing both Necessary and Free Lane changes that account for various weather conditions.

This involved automatically detecting lane change events, generating non-lane change instances, and extracting various feature categories. The study explored different sampling ratios and assessed model performance across feature categories, highlighting the significance of vehicle kinematics in detecting lane changes. The developed approach not only had the potential to enhance the SHRP2 dataset but could be extended to other trajectory-level datasets. The study's DL-based models have practical applications in Connected Vehicle (CV) environments, enabling real-time traffic pattern anomaly detection and facilitating timely control strategies. Furthermore, the model offered valuable information on lane change behavior, which was applied to microsimulation platform to assess and validate safety and operational treatments.

The adapted parameter values underwent a comprehensive examination to assess their interrelationships and understand their influences on predicted driving behavior. To facilitate this analysis, a freeway weaving segment was constructed within the VISSIM microsimulation platform, following the guidelines from the HCM. The adjusted lane change parameters corresponding to each distinct weather condition were then employed to simulate traffic flow. The study's systematic approach in second section, which includes the calibration and validation of baseline models and the assessment of safety and operational performance, provides valuable insights into the impact of adverse weather on roadway behavior.

Safety assessments under adverse weather conditions were conducted by analyzing vehicle trajectory data generated from the updated VISSIM models, considering three widely recognized safety measures: TTC, PET, and DRAC.

Furthermore, the study also explored the effects of adverse weather on traffic operations by evaluating traffic flow characteristics, total travel time, total delay, and average network speed. The investigation into the adjusted parameter values indicated that weather-specific lane changes exhibited unique characteristics distinct from one another. According to TTC, the total number of simulated conflicts, encompassing both lane change and rear-end conflicts, was notably higher in extreme adverse weather conditions such as heavy rain, heavy snow, and

heavy fog compared to clear weather. This finding suggests that inclement weather conditions negatively impact driver behavior and performance, especially in situations of poor visibility and hazardous road surfaces.

Consistently, similar results were obtained from PET and DRAC assessments. Considering the operational aspects of the simulated network, adverse weather conditions generally resulted in lower average speeds, higher total travel times, and increased total delays when compared to clear weather. These observations suggest that drivers adjust their behavior in response to limited visibility during adverse weather conditions. Additionally, the examination of safety and operational assessments related to default parameters emphasized the importance of developing microsimulation models based on weather-specific parameters rather than default ones.

This study's unique findings have the potential to enhance the field of weather-specific microsimulation modeling within the transportation industry. As Connected Vehicle (CV) deployment continues to advance, trajectory-level data, akin to the National Data Set (NDS), will become readily available. The methodology employed in this study offers the flexibility to be applied in investigating various research questions using CV data. This approach can extend to assessing different CV applications related to lane change, such as Lane Change Warning systems, in terms of their safety and operational impact within microsimulation platforms. These evaluations can be based on adjusted lane change behavior during adverse weather conditions. Furthermore, with access to similar trajectory-level data, this developed methodology can be adapted to explore a range of research areas pertaining to driver behavior and performance, accounting for demographics, geographic characteristics, and variations in environmental and driving conditions. Subsequently, microsimulation models can be tailored to reflect the specific behavior and performance characteristics (Hammit et al., 2019).

In addition to its contributions, the study also acknowledges certain limitations. Notably, it was observed that the number of lane changes in adverse weather conditions was relatively lower compared to clear weather conditions. In specific freeway facilities, there were instances where no lane changes were detected during adverse weather conditions. Consequently, the microsimulation models were not updated to account for different freeway facilities, such as

basic freeways or ramp junctions, under varying weather conditions. Furthermore, the study's assumption was that lane change maneuvers in VISSIM were primarily influenced by Necessary and Free Lane change parameters. However, it was acknowledged that there might be additional parameters governing lane changes, which could not be extracted and utilized due to limitations in the NDS data. To further enhance the understanding of driver behavior, future research should involve a comparison between driver behavioral responses within microsimulation models and real-life scenarios.

7.1.2 Modeling CAT at Varying Market Penetration and Level of autonomy on Freeway

It is highly likely that in the near future, Connected and Automated Vehicles (CAVs) will be introduced to the market and share the roads with conventional vehicles (HDVs). Initially, the proportion of CAVs on the roads will be low, and their level of autonomy will be limited. However, over time, the number of CAVs and their level of autonomy is expected to increase. This study aimed to investigate the effects of this mixed traffic environment, considering different levels of CAV market penetration and autonomy, alongside HDVs. To conduct the study, a microsimulation platform using VISSIM® was set up to model the mixed traffic flow. A total of 27 simulation scenarios were created, varying the CAV market penetration, level of autonomy, and traffic volume. The simulation results were then analyzed to understand the traffic conditions and characteristics at different stages of CAV integration.

The focus of this study was to evaluate the safety and operational impacts of varying CAV market penetration and level of autonomy (MPLA) on freeways. By analyzing the simulation data, the study aimed to gain insights into how these factors affect traffic dynamics and identify any potential challenges or benefits associated with the introduction of CAVs. Operational performance in this study was assessed by analyzing parameters such as average speed, total travel time, and total delay. Safety analysis, on the other hand, utilized Time-to-Collision (TTC) as a surrogate measure to evaluate the number of conflicts. Results show that, in the long term, as the market penetration and level of autonomy of CAVs increase, they are expected to have positive effects on the highway's traffic system, including increased average speed, decreased travel time, reduced delay, and fewer conflicts. However, during the transitional phase of mixed operation of manual vehicles and low-end CAVs, there may be negative effects to consider. The

findings of this study have implications for traffic engineers, car manufacturers, and stakeholders, as they provide insights into how different levels of connectivity and autonomy in vehicles can affect both operational and safety characteristics. This knowledge can be valuable in improving the manufacturing processes of connected and autonomous vehicles and enhancing traffic management strategies. It is important to note that this study specifically focuses on the impact of Connected and Automated Vehicles (CAVs) on a rural freeway segment and does not consider other roadway sections or the concept of platooning. Future research will aim to investigate more complex road sections, such as urban freeways and other roadway facility types, while also considering the integration of platooning into the traffic system.

7.1.3 Modeling the impact of Infrastructure on CAT Performance and Safety

The impending integration of Connected and Automated Vehicles (CAVs) into the market, along with their presence on regular roads, is an inevitable development in the near future. However, it is plausible that the existing road infrastructure may initially prove insufficient to accommodate these advanced CAVs, leading to a heavy reliance on the CAV industry for adaptation. Consequently, the infrastructure sector is expected to play a pivotal role in facilitating the adoption of automation technology in the future. Roads are likely to be designated with specific capabilities to handle varying levels of CAV automation based on their own geometric features and automation capabilities. Consequently, CAVs are anticipated to adapt their automation levels as they encounter different road segments.

This study was undertaken to explore the potential advantages of implementing different automation levels across various road segments. A microsimulation platform was created using VISSIM to simulate mixed traffic flows of trucks and cars. Five distinct automation conditions were introduced for the selected segment, including a baseline condition featuring only human-driven vehicles and four other conditions with varying automation capabilities on the road segment. These simulations encompassed three different traffic volumes: 800 vehicles per hour (vph), 1000 vph, and 1400 vph, resulting in a total of 15 simulated scenarios. Subsequently, the simulation results were analyzed to gain insights into traffic conditions and characteristics under different scenarios.

The findings of this study suggest that, especially for higher traffic volumes, the implementation of varying levels of CAV automation based on road segment type, geometry, and capability is preferable. Although all CAV conditions demonstrated similar operational benefits, the scenario where vehicles operated with mid-level automation on straight segments and high-level automation on junctions and ramps stood out. This combination significantly outperformed other scenarios, leading to a reduction in conflicts of approximately 30 percent or more compared to an all-high automation setup. One potential explanation for this result is that the frequent use of high-level automation, following the guidelines of the coexist project and relying on aggressive AV behavior with shorter following distances, resulted in rear-end conflicts during the simulations.

These findings aim to offer evidence-based recommendations for Infrastructure Owners and Operators (IOOs), policymakers, automotive manufacturers, and transportation authorities. These recommendations can be instrumental in harnessing the full potential of CAVs and in establishing a safer, more efficient, and sustainable future of transportation. They provide valuable insights into how varying levels of connectivity and autonomy in vehicles can impact operational and safety characteristics. These insights hold significant implications for IOOs, as they play a critical role in enhancing CAV safety by providing high-quality and consistent traffic control devices (TCD) and maintaining overall infrastructure conditions. IOOs can leverage this knowledge to maximize the safety potential of Connected and Automated Vehicles (CAVs) by gaining a better understanding of current technology requirements and anticipating future technological advancements. This understanding will enable them to strategically plan and design their infrastructure networks accordingly. Additionally, this knowledge can be valuable for improving the manufacturing processes of Connected and Automated Vehicles (CAVs) and enhancing traffic management strategies. In summary, the study contributes to the integration of CAVs into the transportation system, with a particular emphasis on safety and operational efficiency.

7.1.4 Investigating the Impact of CAT on work zone safety and operations

The two sections in this chapter represent two studies and they presented offer valuable insights into the evolving landscape of transportation technologies and their impact on safety

and operational performance, particularly in challenging road conditions. The first study delves into the world of Cooperative Automated Transportation (CAT) and its influence on a freeway work zone (WZ) corridor, specifically when confronted with adverse weather. It employs a comprehensive approach, utilizing weather-sensitive microsimulation modeling. The study's innovation lies in its systematic analytical methodology for assessing safety and operational performance in specific roadway situations under adverse weather conditions, a challenge often constrained by the lack of real-life traffic data in a CAT environment.

In this first study, three categories of vehicles are considered: Human-Driven Vehicles (HV), Connected Vehicles (CV), and Autonomous Vehicles (AV). These vehicle types are combined in various CAT scenarios, and real-world data sources, such as the SHRP 2 NDS and high-fidelity driving simulator experiments, are used to optimize parameters. The study's findings suggest that CAT scenarios consistently result in higher average speeds and reduced total travel times, with the most significant improvements observed at higher Market Penetration Rates (MPRs). This signifies an enhancement in overall traffic operations and a decrease in congestion. The study underlines the critical importance of understanding the implications of CAT technology, particularly in challenging driving conditions, and emphasizes the need for effective strategies throughout the different phases of CAT deployment.

In the second section, the focus shifts to truck platooning, an exciting technology with the potential to revolutionize the trucking industry by reducing fuel consumption and environmental pollution. The analysis centers on low automation but also includes some high automation scenarios for truck platooning, replicating real-life conditions where trucks may become connected and automated before other conventional vehicles. The study explores the safety aspects of truck platooning in work zones on freeway segments, with a specific focus on early merge scenarios. It investigates various levels of automation and their impact on safety and operational performance, demonstrating clear safety advantages as automation levels increase, especially in higher traffic volumes.

The study highlights the potential for truck platooning to enhance safety and operational performance, particularly in early merge situations. It underscores the importance of considering automation levels and traffic volumes when planning and implementing platooning

strategies in work zones, as these factors influence both safety and traffic flow. However, the study also reveals a contrasting outcome in late merge scenarios, where platooning can lead to adverse effects, including a significant increase in critical conflicts and speed reductions. This phenomenon is particularly pronounced in high-traffic scenarios, underscoring the importance of carefully tailoring platooning strategies to work zones to avoid undesirable outcomes.
In conclusion, these studies collectively stress the significance of conducting in-depth assessments of emerging transportation technologies and automation levels, particularly in complex scenarios like work zones and adverse weather. Such assessments are essential for informed decision-making and the development of strategies that maximize the benefits of these technologies while mitigating potential risks.

7.1.5 Studying various Lane Configurations for Efficient Platoon Control during Lane Closures

This study aimed to determine the optimal lane configurations for enhancing the adoption of platoons on two-lane freeways, focusing on both safety and operational efficiency. Given the forthcoming challenge of accommodating low automation Cooperative Adaptive Cruise Control (CACC) platoons on freeways, this investigation assumed Level 1 platooning, wherein only longitudinal behavior was automated. Lane parameters were derived from NDS SHRP2 data (Chapter 3) for clear weather conditions to update lateral behavior. To simulate interactions between CACC-equipped vehicles and conventional vehicles, a work zone was introduced at the end of the freeway, necessitating mandatory lane changes for merging into a single lane. The simulations encompassed three distinct lane configurations (both lanes open, open lane, closed lane) for platooning, each with two scenarios based on upstream platooning conditions (1-mile), resulting in six possible scenarios. Initial safety evaluations revealed that the open lane condition for platooning exhibited the lowest number of conflicts, outperforming other scenarios. Conversely, when platooning was unrestricted across all lanes and upstream (1-mile), it yielded the highest conflict count. Operational performance improved across all scenarios with increasing Market Penetration Rate (MPR). The best operational performance was observed when platooning was allowed on both lanes and upstream, followed closely by the open lane condition. Overall, the analysis indicated that the open lane scenario offered the best combination of safety and operational performance. Unrestricted platooning enhanced

operations but compromised safety, while the closed lane condition proved beneficial when platooning was dissolved before reaching the upstream work zone.

The findings from this study highlight the benefits of utilizing lane specific platooning and could benefit traffic agencies, Infrastructure Owners and Operators (IOOs) in planning efficient strategies for adopting CAT infrastructure in the near future.

References

AASHTO. (2001). A Policy on Geometric Design of Highways and Streets. Washington, DC.

Adomah, E., A. K. Bakhshi, and M. M. Ahmed. Safety Impact of Connected Vehicles on Driver Behavior in Rural Work Zones under Foggy Weather Conditions. Transportation Research Record: Journal of the Transportation Research, Vol. 2676, No. 3, 2022, pp. 88–107. https://doi.org/10.1177/03611981211049147.

Ahmed, M. M., Ghasemzadeh, A., Hammit, B., Khan, N., Das, A., Ali, E. Eldeeb, H. (2018). Driver Performance and Behavior in Adverse Weather Conditions: An Investigation Using the SHRP2 Naturalistic Driving Study Data-Phase 2. Final Report WY-18/05F, U.S. Department of Transportation.

Ahmed, M., H. Huang, M. Abdel-Aty, and B. Guevara. Exploring a Bayesian Hierarchical Approach for Developing Safety Performance Functions for a Mountainous Freeway. Accident Analysis and Prevention, Vol. 43, No. 4, 2011, pp. 1581–1589. https://doi.org/10.1016/J.AAP.2011.03.021.

Ahmed, M. M., Khan, M. N., Das, A., and Dadvar, S. E. (2022). Global lessons learned from naturalistic driving studies to advance traffic safety and operation research: A systematic review. Accident Analysis and Prevention, 167, 106568.

Al-Ahmadi, H. M., Jamal, A., Reza, I., Assi, K. J., and Ahmed, S. A. (2019). Using microscopic simulation-based analysis to model driving behavior: A case study of Khobar-Dammam in Saudi Arabia. Sustainability, 11(11). https://doi.org/10.3390/su11113018

Algomaiah, M., and Li, Z. (2021). Exploring work zone late merge strategies with and without enabling connected vehicles technologies. Transportation Research Interdisciplinary Perspectives, 9. https://doi.org/10.1016/j.trip.2021.100316

American Road and Transportation Builders Association (ARTBA). Work Zone Data — Work Zone Safety Information Clearinghouse.

Amini, E., A. Omidvar, and L. Elefteriadou. Optimizing Operations at Freeway Weaves with Connected and Automated Vehicles. Transportation Research Part C: Emerging Technologies, Vol. 126, 2021. https://doi.org/10.1016/J.TRC.2021.103072.

Anderson, J.M., Kalra, N., Stanley, K.D., Sorensen, P., Samaras, C., Oluwatola, O.A., 2016. Autonomous Vehicle Technology: A Guide for Policymakers. RAND Corp. doi:10.7249/rr443-2

Aoude, G.S., Desaraju, V.R., Stephens, L.H., How, J.P., 2012. Driver behavior classification at intersections and validation on large naturalistic data set. IEEE Trans. Intell. Transp. Syst. 13 2, 724–736. doi:10.1109/TITS.2011.2179537

Arvin, R., A. Khattak, and J. R. Torres. Evaluating Safety with Automated Vehicles at Signalized Intersections: Application of Adaptive Cruise Control in Mixed Traffic. 2019.

Bakhshi, A. K., and M. M. Ahmed. Practical Advantage of Crossed Random Intercepts under Bayesian Hierarchical Modeling to Tackle Unobserved Heterogeneity in Clustering Critical versus Non-Critical Crashes. Accident Analysis and Prevention, Vol. 149, 2021, p. 105855. https://doi.org/10.1016/j.aap.2020.105855.

Bakhit, P. R., O. A. Osman, and S. Ishak. "Detecting Imminent Lane Change Maneuvers in Connected Vehicle Environments." Transportation Research Record: Journal of the Transportation Research Board, 2017. 2645: 168–175.

Bakhshi, A. K., and M. M. Ahmed. Utilizing Black-Box Visualization Tools to Interpret Non-Parametric Real-Time Risk Assessment Models. Transportmetrica, Vol. 17, No. 4, 2020, pp. 739–765. https://doi.org/10.1080/23249935.2020.1810169.

Bidkar, O., Arkatkar, S., Joshi, G., and Easa, S. M. (2023a). Effect of Construction Work Zone on Rear-End Conflicts by Vehicle Type under Heterogeneous Traffic Conditions. Journal of Transportation Engineering, Part A: Systems, 149(4). https://doi.org/10.1061/jtepbs.teeng-7275

Bruno, J. L., J. M. Baker, A. Gundran, L. K. Harbott, Z. Stuart, A. M. Piccirilli, S. M. H. Hosseini, J. C. Gerdes, and A. L. Reiss. "Mind Over Motor Mapping: Driver Response to Changing Vehicle Dynamics." Human Brain Mapping, Vol. 39, No. 10, 2018, pp. 3915–3927.

Caliendo, C., and Guida, M. (2012). Microsimulation approach for predicting crashes at unsignalized intersections using traffic conflicts. Journal of Transportation Engineering, 138(12), 1453–1467. https://doi.org/10.1061/(ASCE)TE.1943-5436.0000473

Campbell, K. L. (2012). The SHRP2 Naturalistic Driving Study. Transportation Research News, 30–35.

Carreras, A., X. Daura, J. Erhart, and S. Ruehrup. Road Infrastructure Support Levels for Automated Driving. 2018.

Chambless, J., G. A. M., L. J. K., and M. J. (2002). Multistate work-zone crash characteristics. Institute of Transportation Engineers, ITE Journal, 5(46), 72.

Chawla, N. V., K. W. Bowyer, L. O. Hall, and W. P. Kegelmeyer. "SMOTE: Synthetic Minority Over-Sampling Technique." Journal of Artificial Intelligence Research, Vol. 16, 2002, pp. 321–357.

Chen, C., Zhao, X., Liu, H., Ren, G., Zhang, Y., and Liu, X. (2019). Assessing the influence of adverse weather on traffic flow characteristics using a driving simulator and VISSIM. Sustainability, 11(3). https://doi.org/10.3390/su11030830

Dai, Y., Wang, C., and Xie, Y. (2023). Explicitly incorporating surrogate safety measures into connected and automated vehicle longitudinal control objectives for enhancing platoon safety. Accident Analysis and Prevention, 183. https://doi.org/10.1016/j.aap.2023.106975

Das, A and Ahmed (2019). Exploring the effect of fog on lane-changing characteristics utilizing the SHRP2 naturalistic driving study data. Journal of Transportation Safety and Security, 1–26. https://doi.org/10.1080/19439962.2019.1645777

Das, A., and M. M. Ahmed. "Machine Learning Approach for Predicting Lane-Change Maneuvers Using the SHRP2 Naturalistic Driving Study Data." Transportation Research Record: Journal of the Transportation Research Board, 2021. 2675: 574–594.

Das, A., and Ahmed, M. M. (2022). Adjustment of key lane change parameters to develop microsimulation models for representative assessment of safety and operational impacts of adverse weather using SHRP2 naturalistic driving data. Journal of Safety Research, 81, 9–20. https://doi.org/10.1016/j.jsr.2022.01.002

Das, A., and Ahmed, M. M. (2022). Structural equation modeling approach for investigating drivers' risky behavior in clear and adverse weather using SHRP2 naturalistic driving data. Journal of Transportation Safety and Security, 1–32. https://doi.org/10.1080/19439962.2022.2155744

Das, A., M. N. Khan, and M. M. Ahmed. Deep Learning Approach for Detecting Lane Change Maneuvers Using SHRP2 Naturalistic Driving Data. Transportation Research Record: Journal of the Transportation Research Board, 2022, pp. 1–22. https://doi.org/10.1177/03611981221103229.

Das, A., M. N. Khan, and M. M. Ahmed. "Detecting Lane Change Maneuvers Using SHRP2 Naturalistic Driving Data: A Comparative Study Machine Learning Techniques." Accident Analysis and Prevention, Vol. 142, 2020, pp. 1–17.

Das, A., Ghasemzadeh, A., and Ahmed, M. M. (2019). Analyzing the effect of fog weather conditions on driver lane-keeping performance using the SHRP2 naturalistic driving study data. Journal of Safety Research, 68(February), 71–80. https://doi.org/10.1016/j.jsr.2018.12.015

Das, A., Khan, M. N., and Ahmed, M. M. (2020). Nonparametric Multivariate Adaptive Regression Splines Models for Investigating Lane-Changing Gap Acceptance Behavior Utilizing Strategic Highway Research Program 2 Naturalistic Driving Data. Transportation Research Record: Journal of the Transportation Research Board, 2674(5), 223–238. https://doi.org/10.1177/0361198120914293

Das, A., and M. M. Ahmed. Weather-Based Lane-Change Microsimulation Parameters for Safety and Operational Performance Evaluation of Weaving and Basic Freeway Segments. In Transportation Research Record, SAGE Publications Ltd, pp. 550–563.

Das A., Khan M. N., Ahmed M. M., Wulff S. S. Cluster Analysis and Multi-level Modeling for Evaluating the Impact of Rain on Aggressive Lane-changing Characteristics Utilizing Naturalistic Driving Data. Journal of Transportation Safety and Security, 2022.

Dehman, A., and Farooq, B. (2021). Are work zones and connected automated vehicles ready for a harmonious coexistence? A scoping review and research agenda. Transportation Research Part C: Emerging Technologies, 133. https://doi.org/10.1016/j.trc.2021.103422

Deluka-Tibljaš, A., T. Giuffrè, S. Šurdonja, and S. Trubia. Introduction of Autonomous Vehicles: Roundabouts Design and Safety Performance Evaluation. Sustainability, Vol. 10, No. 4, 2018, p. 1060. https://doi.org/10.3390/su10041060.

Dong J., Houchin A. J., Shafieirad N., Lu C., Hawkins N. R., Knickerbocker S. VISSIM Calibration for Urban Freeways. Center for Transportation Research and Education, Institute for Transportation, Iowa State University, Ames, IA, 2015, pp. 1–106.

Dong, J., Wang, J., and Luo, D. (2022). Impact of connected and autonomous vehicles on traffic safety of mixed traffic flow: From the perspective of connectivity and spatial distribution. Transportation Safety and Environment, 4(3). https://doi.org/10.1093/tse/tdac021

Eftekharzadeh, S. F., and A. K. Bakhshi. Safety Evaluation of Highway Geometric Design Criteria in Horizontal Curves at Downgrades. ResearchGate, 2014.

Essa, M., and T. Sayed. Simulated Traffic Conflicts Do They Accurately Represent Field-Measured Conflicts? Transportation Research Record: Journal of Transportation Research, Vol. 2514, 2015, pp. 48–57. https://doi.org/10.3141/2514-06.

Fan, R., Yu, H., Liu, P., and Wang, W. (2013). Using VISSIM simulation model and Surrogate Safety Assessment Model for estimating field measured traffic conflicts at freeway merge areas. IET Intelligent Transport Systems, 7(1), 68–77. https://doi.org/10.1049/iet-its.2011.0232

FHWA. (2020). How Do Weather Events Impact Roads? https://ops.fhwa.dot.gov/weather/q1_roadimpact.htm

FHWA. FHWA-HRT-21-015: Impacts of Automated Vehicles on Highway Infrastructure. 2021.

FHWA Work Zone Facts and Statistics - FHWA Office of Operations. (2023).

Fink, J., Kwigizile, V., and Oh, J. S. (2016). Quantifying the impact of adaptive traffic control systems on crash frequency and severity: Evidence from Oakland County, Michigan. Journal of Safety Research, 57, 1–7. https://doi.org/10.1016/j.jsr.2016.01.001

Gallelli, V., Guido, G., Vitale, A., and Vaiana, R. (2019). Effects of calibration process on the simulation of rear-end conflicts at roundabouts. Journal of Traffic and Transportation Engineering (English Edition), 6(2), 175–184. https://doi.org/10.1016/j.jtte.2018.03.006

Ganganwar, V. "An Overview of Classification Algorithms for Imbalanced Datasets." International Journal of Emerging Technology and Advanced Engineering, Vol. 2, No. 4, 2012, pp. 42–47.

Garber, N. J., Zhao, M., and Garber, N. J. (n.d.). Work zones tend to cause hazardous conditions for drivers and construction workers Distribution and Characteristics of Crashes at Different Work Zone Locations in Virginia.

Gaweesh, S., A. K. Bakhshi, and M. M. Ahmed. Safety Performance Assessment of Connected Vehicles in Mitigating the Risk of Secondary Crashes: A Driving Simulator Study. Transportation Research Record, Vol. 2675, No. 12, 2021, pp. 117–129. https://doi.org/10.1177/03611981211027881.

Gaweesh, S. M., M. N. Khan, and M. M. Ahmed. "Development of a Novel Framework for Hazardous Materials Placard Recognition System to Conduct Commodity Flow Studies Using Artificial Intelligence AlexNet Convolutional Neural Network." Transportation Research Record: Journal of the Transportation Research Board, 2021. 2675: 1357–1371.

Ghasemzadeh, A., Hammit, B. E., Ahmed, M. M., and Eldeeb, H. (2019). Complementary methodologies to identify weather conditions in naturalistic driving study trips: Lessons learned from the SHRP2 naturalistic driving study and roadway information database. Safety Science, 119(November), 21–28. https://doi.org/10.1016/j.ssci.2019.01.006

Ghasemzadeh, A., and M. M. Ahmed. Exploring Factors Contributing to Injury Severity at Work Zones Considering Adverse Weather Conditions. IATSS Research, 2018. https://doi.org/10.1016/j.iatssr.2018.11.002.

Ghiasi, A., Li, X., and Ma, J. (2019). A mixed traffic speed harmonization model with connected autonomous vehicles. Transportation Research Part C: Emerging Technologies, 104, 210–233. https://doi.org/10.1016/j.trc.2019.05.005

Gkartzonikas, C., and K. Gkritza. What Have We Learned? A Review of Stated Preference and Choice Studies on Autonomous Vehicles. Transportation Research Part C: Emerging Technologies, Vol. 98, 2019, pp. 323–337. https://doi.org/10.1016/J.TRC.2018.12.003.

Goh, Y. M., and C. U. Ubeynarayana. "Construction Accident Narrative Classification: An Evaluation of Text Mining Techniques." Accident Analysis and Prevention, Vol. 108, 2017, pp. 122–130.

Golshan Khavas, R., Hellinga, B., and Zarinbal Masouleh, A. (2017). Identifying parameters for microsimulation modeling of traffic in inclement weather. Transportation Research Record: Journal of the Transportation Research Board, 2613(1), 52–60. https://doi.org/10.3141/2613-07

Goyani, J., Paul, A. B., Gore, N., Arkatkar, S., and Joshi, G. (2021). Investigation of Crossing Conflicts by Vehicle Type at Unsignalized T-Intersections under Varying Roadway and Traffic Conditions in India. Journal of Transportation Engineering, Part A: Systems, 147(2). https://doi.org/10.1061/jtepbs.0000479

Goyani, J., Vallabhbhai, S., Pawar, N. M., Shrikant, S., Vallabhbhai, A. S., Pawar, N., Gore, N., Jain, M., and Arkatkar, S. (2019). Investigation of Traffic Conflicts at Unsignalized Intersection for Reckoning Crash Probability Under Mixed Traffic Conditions. Journal of the Eastern Asia Society for Transportation Studies, 13. https://doi.org/10.11175/easts.13.2091

Guanetti, J., Kim, Y., and Borrelli, F. (2018). Control of connected and automated vehicles: State of the art and future challenges. In Annual Reviews in Control (Vol. 45, pp. 18–40). Elsevier Ltd. https://doi.org/10.1016/j.arcontrol.2018.04.011

Guo, Y., Li, Z., Liu, P., and Wu, Y. (2019). Modeling correlation and heterogeneity in crash rates by collision types using full bayesian random parameters multivariate Tobit model. Accident Analysis and Prevention, 128, 164–174. https://doi.org/10.1016/j.aap.2019.04.013

Habtemichael, F. G., and Santos, L. D. P. (2012). Sensitivity Analysis of VISSIM Driver Behavior Parameters on Safety of Simulated Vehicles and Their Interaction with Operations of Simulated Traffic. Proceedings of the 92nd Transportation Research Board Annual Meeting, (January), 1–17.

Hallmark, S. (2019). Preparing Local Agencies for the Future of Connected and Autonomous Vehicles. http://mndot.gov/research/reports/2019/201918.pdf

Hammit, B. E., James, R., Ahmed, M., and Young, R. (2019). Toward the Development of Weather-dependent Microsimulation Models. Transportation Research Record: Journal of the Transportation Research Board, 2673(7), 143–156. Retrieved from https://doi.org/10.1177/0361198119844743

Hankey J. M., Perez M. A., McClafferty J. A. Description of the SHRP2 Naturalistic Database and the Crash, Near-Crash, and Baseline Data Sets. Virginia Tech Transportation Institute, Blacksburg, VA, 2016.

Haq M. T., Zlatkovic M., Ksaibati K. Benefit-Cost Assessment of Truck Climbing Lanes: A Case Study of I-80 in Wyoming, Transportation Letters, Vol. 14, No. 2, 2022, pp. 94–103.

Haque, M. S., Rilett, L. R., and Zhao, L. (2023a). Impact of Platooning Connected and Automated Heavy Vehicles on Interstate Freeway Work Zone Operations. Journal of Transportation Engineering, Part A: Systems, 149(3). https://doi.org/10.1061/jtepbs.teeng-7434

Hartmann, M., S. Krause, S. Hoffmann, N. Motamedidehkordi, P. Vortisch, and F. Busch. Impact of Automated Vehicles on Capacity of the German Freeway Network. researchgate.net, 2017.

Hayward, J. C. (1972). NEAR-MISS DETERMINATION THROUGH USE OF A SCALE OF DANGER.

He, K., X. Zhang, S. Ren, and J. Sun. "Deep Residual Learning for Image Recognition." Proceedings of the IEEE Conference on Computer Vision and Pattern Recognition (CVPR), IEEE, New York, 2016, pp. 770–778

Higgs, B., V. Tech, vtedu M. Montasir Abbas, and A. Medina. Analysis of the Wiedemann Car Following Model Over Different Speeds Using Naturalistic Data.

Hoque, Md. M., Lu, Q., Ghiasi, A., and Xin, C. (2021). Highway Cost Analysis for Platooning of Connected and Autonomous Trucks. Journal of Transportation Engineering, Part A: Systems, 147(1). https://doi.org/10.1061/jtepbs.0000474

Hosseinzadeh, A., A. Moeinaddini, and A. Ghasemzadeh. Investigating Factors Affecting Severity of Large Truck-Involved Crashes: Comparison of the SVM and Random Parameter Logit Model. Journal of Safety Research, Vol. 77, 2021, pp. 151–160. https://doi.org/10.1016/J.JSR.2021.02.012.

Hou T., Mahmassani H., Alfelor R., Kim J., Saberi M. Calibration of Traffic Flow Models under Adverse Weather and Application in Mesoscopic Network Simulation. Transportation Research Record: Journal of the Transportation Research Board, 2013. 2391: 92–104.

Huang, F., Liu, P., Yu, H., and Wang, W. (2013). Identifying if VISSIM simulation model and SSAM provide reasonable estimates for field measured traffic conflicts at signalized intersections. Accident Analysis and Prevention, 50, 1014–1024. https://doi.org/10.1016/j.aap.2012.08.018

Huynh, B. Q., H. Li, and M. L. Giger. "Digital Mammographic Tumor Classification Using Transfer Learning from Deep Convolutional Neural Networks." Journal of Medical Imaging, Vol. 3, No. 3, 2016, pp. 1–5.

InSight Website. "SHRP2 NDS Data Access." https://insight.shrp2nds.us/

Intelligent Transportation Systems Joint Program Office (ITSJPO), 2020. Connected Vehicles [WWW Document]. URL https://www.its.dot.gov/cv_basics/cv_basics_how.htm

J3016_202104: Taxonomy and Definitions for Terms Related to Driving Automation Systems for On-Road Motor Vehicles - SAE International. https://www.sae.org/standards/content/j3016_202104/. Accessed Jun. 14, 2023.

Jameis, Y. (, Tsai,), Turochy, R., and Jehn, N. (n.d.). Quantitatively Evaluate Work Zone! Driver Behavior using 2D Imaging, 3-D Lidar and Artificial Intelligence in Support of Congestion Mitigation IV1odel Calibration and Validation.

Jiang, R., S. Zhu, P. Wang, Q. C. Chen, H. Zou, S. Kuang, and Z. Cheng. In Search of the Consequence Severity of Traffic Conflict. Journal of Advanced Transportation, Vol. 2020, 2020. https://doi.org/10.1155/2020/9089817.

Jiang, Y., Zhu, F., Yao, Z., Gu, Q., and Ran, B. (2023). Platoon Intensity of Connected Automated Vehicles: Definition, Formulas, Examples, and Applications. Journal of Advanced Transportation, 2023. https://doi.org/10.1155/2023/3325530

Jolovic D., Stevanovic A. Evaluation of VISSIM and FREEVAL to Assess an Oversaturated Freeway Weaving Segment. Presented at 92nd Annual Meeting of the Transportation Research Board, Washington, D.C., 2013, pp. 1–17. https://doi.org/10.13140/2.1.4780.0963.

Jung, S., Qin, X., and Noyce, D. A. (2011). Modeling highway safety and simulation in rainy weather. Transportation Research Record: Journal of the Transportation Research Board, (2237), 134–143. https://doi.org/10.3141/2237-15

Kang, S., Asce, S. M., Ozer, H., Asce, M., and Al-Qadi, I. L. (n.d.). Benefit Cost Analysis (BCA) of Autonomous and Connected Truck (ACT) Technology and Platooning.

Khan, M. N., and M. M. Ahmed. "Development of a Novel Convolutional Neural Network Architecture Named RoadweatherNet for Trajectory-Level Weather Detection Using SHRP2 Naturalistic Driving Data." Transportation Research Record: Journal of the Transportation Research Board, 2021. 2675: 1016–1030

Khan, M. N., and M. M. Ahmed. "Trajectory-Level Fog Detection Based on In-Vehicle Video Camera with TensorFlow Deep Learning Utilizing SHRP2 Naturalistic Driving Data." Accident Analysis and Prevention, Vol. 142, 2020, pp. 1–12.

Khan, M. N., Das, A., and Ahmed, M. M. (2020). Non-Parametric Association Rules Mining and Parametric Ordinal Logistic Regression for an In-Depth Investigation of Driver Speed Selection Behavior in Adverse Weather using SHRP2 Naturalistic Driving Study Data. Transportation Research Record: Journal of the Transportation Research Board, 2674(11), 101–119.

Khan, M. N., Ghasemzadeh, A., and Ahmed, M. M. (2018). Investigating the Impact of Fog on Freeway Speed Selection Using the SHRP2 Naturalistic Driving Study Data. Transportation Research Record: Journal of the Transportation Research Board, 2672(16), 93–104. Retrieved from https://trid.trb.org/view/1497201

Khattak, A. J., Khattak, A. J., and Council, F. M. (2002). Effects of work zone presence on injury and non-injury crashes. In Accident Analysis and Prevention (Vol. 34). www.elsevier.com/locate/aap

Khoda Bakhshi A., Ahmed M. M. Accounting for Human-Related Unobserved Heterogeneity in the Safety Performance of Connected Vehicles: An Incorporation of Bayesian Hierarchical Negative Binomial into Simulated Work Zone Warning Application. IATSS Research, Vol. 45, No. 4, 2021, pp. 539–550. https://doi.org/10.1016/j.iatssr.2021.06.005.

Kitchener, F., R. Young, M. Ahmed, G. Yang, S. Gaweesh, T. English, V. Garcia, A. Ragan, N. Urena Serulle, and D. Gopalakrishna. Connected Vehicle Pilot Deployment Program: Phase 2 Final System Performance Report, Baseline Conditions – WYDOT CV Pilot. FHWA-JPO-17-474, 2018.

Learn, S., Ma, J., Raboy, K., Zhou, F., and Guo, Y. (2018). Freeway speed harmonisation experiment using connected and automated vehicles. IET Intelligent Transport Systems, 12(5), 319–326. https://doi.org/10.1049/iet-its.2017.0149

Li, D., A. Cong, and S. Guo. "Sewer Damage Detection from Imbalanced CCTV Inspection Data Using Deep Convolutional Neural Networks with Hierarchical Classification." Automation in Construction, Vol. 101, 2019, pp. 199–208.

Li, S., Y. Wu, Z. Xu, and X. Lin. "Improved Lane-Changing Model for Vanets in SUMO." Proc., IEEE 7th International Conference on Advanced Infocomm Technology, IEEE/ICAIT 2014, Fuzhou, China, IEEE, New York, 2015, pp. 260–266.

Liu, P., and W. Fan. Exploring the Impact of Connected and Autonomous Vehicles on Freeway Capacity Using a Revised Intelligent Driver Model. Transportation Planning and Technology, Vol. 43, No. 3, 2020, pp. 279–292. https://doi.org/10.1080/03081060.2020.1735746.

Li, Y., and Bai, Y. (2008). Comparison of characteristics between fatal and injury accidents in the highway construction zones. Safety Science, 46(4), 646–660. https://doi.org/10.1016/j.ssci.2007.06.019

Lu, J., O. Grembek, and M. Hansen. Learning the Representation of Surrogate Safety Measures to Identify Traffic Conflict. Accident Analysis and Prevention, Vol. 174, 2022, p. 106755. https://doi.org/10.1016/J.AAP.2022.106755.

Lu, X. Y., Varaiya, P., and Horowitz, R. (2009). Fundamental Diagram modelling and analysis based NGSIM data. Proceedings of the 12th IFAC Symposium on Transportation Systems, 42(15), 367–374. https://doi.org/10.3182/20090902-3-US-2007.0068

Mahdi A. Development of Freeway Weaving Areas Microsimulation Model (FWASIM). Civil Engineering and Architecture, Vol. 8, No. 5, 2020, pp. 1006–1018. https://doi.org/10.13189/cea.2020.080527.

Mahmud, S. M. S., Ferreira, L., Hoque, M. S., and Tavassoli, A. (2017). Application of proximal surrogate indicators for safety evaluation: A review of recent developments and research needs. IATSS Research, 41(4), 153–163. https://doi.org/10.1016/j.iatssr.2017.02.001

Ma, J., Li, X., Shladover, S., Rakha, H. A., Lu, X. Y., Jagannathan, R., and Dailey, D. J. (2016). Freeway speed harmonization. IEEE Transactions on Intelligent Vehicles, 1(1), 78–89. https://doi.org/10.1109/TIV.2016.2551540

Mandalia, H. M., and D. D. Salvucci. "Using Support Vector Machines for Lane-Change Detection." Proceedings of the Human Factors and Ergonomics Society, Vol. 49, 2005, pp. 1965–1969

Markos, F., N. Bekiaris-Liberis, C. Roncoli, I. Papamichail, and M. Papageorgiou. Highway Traffic State Estimation with Mixed Connected and Conventional Vehicles: Microscopic Simulation-Based Testing. Transportation Research Part C-emerging Technologies, Vol. 78, 2017, pp. 13–33. https://doi.org/10.1016/j.trc.2017.02.015.

Martínez-Díaz, M., Soriguera, F., Pérez, I., 2019. Autonomous driving: A bird's eye view. IET Intell. Transp. Syst. 13 4, 563–579. doi:10.1049/iet-its.2018.5061

MathWorks. "Resnet18." https://www.mathworks.com/help/deeplearning/ref/resnet18.html.

MathWorks. "Pretrained Deep Neural Networks." https://www.mathworks.com/help/deeplearning/ug/pretrained-convolutional-neural-networks.html

Miller, L., Mannering, F., and Abraham, D. M. (2009). Effectiveness of Speed Control Measures on Nighttime Construction and Maintenance Projects. https://doi.org/10.1061/ASCECO.1943-7862.0000018

Mitigating Work Zone Safety and Mobility Challenges through Intelligent Transportation Systems Case Studies. (2014).

Mobileye. "Mobileye 5-Series. User Manual." 2021.

Montaño Moreno, J. J., A. Palmer Pol, A. Sesé Abad, and B. Cajal Blasco. Using the R-MAPE Index as a Resistant Measure of Forecast Accuracy. Psicothema, Vol. 25, No. 4, 2013, pp. 500–506. https://doi.org/10.7334/PSICOTHEMA2013.23.

Morando, M. M., Q. Tian, L. T. Truong, and H. L. Vu. Studying the Safety Impact of Autonomous Vehicles Using Simulation-Based Surrogate Safety Measures. Journal of Advanced Transportation, Vol. 2018, 2018, pp. 1–11. https://doi.org/10.1155/2018/6135183.

Mousavi, S. M., O. A. Osman, and D. Lord. Impact of Urban Arterial Traffic LOS on the Vehicle Density of Different Lanes of the Arterial in Proximity of an Unsignalized Intersection for Autonomous Vehicle vs. Conventional Vehicle Environments. International Conference on Transportation and Development 2019: Smarter and Safer Mobility and Cities - Selected Papers from the International Conference on Transportation and Development 2019, 2019, pp. 303–314. https://doi.org/10.1061/9780784482575.029.

Mousavi, S. M., O. A. Osman, D. Lord, K. K. Dixon, and B. Dadashova. Investigating the Safety and Operational Benefits of Mixed Traffic Environments with Different Automated Vehicle Market

NHTSA, 2018. Automated Vehicles 3.0: Preparing for the Future of Transportation, National Highway Traffic Safety Administration, U.S. Department of Transportation.

NHTSA. "Traffic Safety Facts: A Compilation of Motor Vehicle Crash Data. From the Fatality Analysis Reporting System and the General Estimates System. U.S. Department of Transportation, Washington, D.C., 2019.

Nilsson, G. Traffic Safety Dimensions and the Power Model to Describe the Effect of Speed on Safety. 2004.

NSC. Work Zones - Injury Facts.

Papadoulis, A., Quddus, M., and Imprialou, M. (2019). Evaluating the safety impact of connected and autonomous vehicles on motorways. Accident Analysis and Prevention, 124, 12–22. https://doi.org/10.1016/j.aap.2018.12.019

Paul, M. (2019). Safety Assessment at Unsignalized Intersections Using Post-Encroachment Time's Threshold—A Sustainable Solution for Developing Countries. Advances in Transportation Engineering, 117–131.

Penetration Rates in the Proximity of a Driveway on an Urban Arterial. Accident Analysis and Prevention, Vol. 152, 2021, p. 105982. https://doi.org/10.1016/J.AAP.2021.105982.

PTV Group. Autonomous Vehicles Base Settings. 2022, pp. 1–4.

PTV Group. PTV VISSIM 11 User Manual. Planung Transport Verkehr AG, Karlsruhe, Germany, 2018, pp. 1–1219.

Rahim, M. A., and H. M. Hassan. "A Deep Learning Based Traffic Crash Severity Prediction Framework." Accident Analysis and Prevention, Vol. 154, 2021, p. 106090.

Rahman, M. S., and M. Abdel-Aty. Longitudinal Safety Evaluation of Connected Vehicles' Platooning on Expressways. Accident Analysis and Prevention, Vol. 117, 2018, pp. 381–391. https://doi.org/10.1016/J.AAP.2017.12.012.

Razmi Rad, S., Farah, H., Taale, H., van Arem, B., and Hoogendoorn, S. P. (2020). Design and operation of dedicated lanes for connected and automated vehicles on motorways: A conceptual framework and research agenda. Transportation Research Part C: Emerging Technologies, 117. https://doi.org/10.1016/j.trc.2020.102664

Rakha, H., Arafeh, M., and Park, S. (2012). Modeling Inclement Weather Impacts on Traffic Stream Behavior. International Journal of Transportation Science and Technology, 1(1), 25–47. https://doi.org/10.1260/2046-0430.1.1.25

Razmi Rad, S., Farah, H., Taale, H., van Arem, B., and Hoogendoorn, S. P. (2021). The impact of a dedicated lane for connected and automated vehicles on the behaviour of drivers of manual vehicles. Transportation Research Part F: Traffic Psychology and Behaviour, 82, 141–153. https://doi.org/10.1016/j.trf.2021.08.010

Regan, M.A., Williamson, A., Grzebieta, R., Charlton, J., Lenne, M., Watson, B., Haworth, N., Rakotonirainy, A., Woolley, J., Anderson, R., Senserrick, T., Young, K., 2013. The Australian 400-car Naturalistic Driving Study: innovation in road safety research and policy. Australas. Road Saf. Res. Polic. Educ. Conf. 2013, Brisbane, Queensland, Aust.

Reiter, U. (1994). Empirical Studies as Basis for Traffic Flow Models. Proceedings of the Second International Symposium on Highway Capacity, 2, 493–502.

Russakovsky, O., J. Deng, H. Su, J. Krause, S. Satheesh, S. Ma, Z. Huang, A. Karpathy, A. Khosla, M. Bernstein, A. C. Berg, and L. Fei-Fei. "ImageNet Large Scale Visual Recognition Challenge." International Journal of Computer Vision, Vol. 115, No. 3, 2015, pp. 211–252.

Saeed, T. U., M. Burris, S. Labi, and K. C. Sinha. An Empirical Discourse on Forecasting the Use of Autonomous Vehicles Using Consumers' Preferences. Technological Forecasting and Social Change, Vol. 158, 2020, p. 120130. https://doi.org/10.1016/j.techfore.2020.120130.

SAE International, 2018. Taxonomy and definitions for terms related to driving automation systems for on-road motor vehicles, Standard No. J3016_201806, Society of Automotive Engineers.

Salvucci, D. D., and A. Liu. "The Time Course of a Lane Change: Driver Control and Eye-Movement Behavior." Transportation Research Part F: Traffic Psychology and Behaviour, Vol. 5, No. 2, 2002, pp. 123–132.

Sen, B., J. D. Smith, and W. G. Najm. "Analysis of Lane Change Crashes." DOT HS 809 571. U.S. Department of Transportation, Washington, D.C., 2003, pp. 1–49.

Sharma, A., E. Vans, D. Shigemizu, K. A. Boroevich, and T. Tsunoda. "DeepInsight: A Methodology to Transform a Non-Image Data to an Image for Convolution Neural Network Architecture." Scientific Reports, Vol. 9, No. 1, 2019, pp. 1–7.

Shirani-bidabadi, N., R. Ma, and M. Anderson. Within-Day Travel Speed Pattern Unsupervised Classification – A Data Driven Case Study of the State of Alabama during the COVID-19 Pandemic. Journal of Traffic and Transportation Engineering (English Edition), Vol. 8, No. 2, 2021, pp. 170–185. https://doi.org/10.1016/J.JTTE.2021.03.002.

Shi, Y., Q. He, and Z. Huang. Capacity Analysis and Cooperative Lane Changing for Connected and Automated Vehicles: Entropy-Based Assessment Method. Transportation Research Record, Vol. 2673, No. 8, 2019, pp. 485–498. https://doi.org/10.1177/0361198119843474.

Shladover, S. E., Nowakowski, C., Lu, X. Y., and Ferlis, R. (2015). Cooperative adaptive cruise control: Definitions and operating concepts. Transportation Research Record, 2489, 145–152. https://doi.org/10.3141/2489-17

Singh, S. Critical Reasons for Crashes Investigated in the National Motor Vehicle Crash Causation Survey. Traffic Safety Facts - Crash Stats, 2015.

Soleimani, S., S. R. Mousa, J. Codjoe, and M. Leitner. "A Comprehensive Railroad-Highway Grade Crossing Consolidation Model: A Machine Learning Approach." Accident Analysis and Prevention, Vol. 128, 2019, pp. 65–77.

Soria I., Elefteriadou L., Kondyli A. Assessment of Car-Following Models by Driver Type and under Different Traffic, Weather Conditions Using Data from an Instrumented Vehicle. Simulation

Modelling Practice and Theory, Vol. 40, 2014, pp. 208–220. https://doi.org/10.1016/j.simpat.2013.10.002.

Stanek, D., R. Milam, E. Huang, and Y. Wang. Measuring Autonomous Vehicle Impacts on Congested Networks Using Simulation. 2018.

Stern, R.E., Cui, S., Delle Monache, M.L., Bhadani, R., Bunting, M., Churchill, M., Hamilton, N., Haulcy, R., Pohlmann, H., Wu, F., Piccoli, B., Seibold, B., Sprinkle, J., Work, D.B., 2018. Dissipation of stop-and-go waves via control of autonomous vehicles: Field experiments. Transp. Res. Part C Emerg. Technol. 89 April 2017, 205–221. doi: 10.1016/j.trc.2018.02.005

Sukennik, P. Micro-Simulation Guide for Automated Vehicles-Final. https://www.h2020-coexist.eu/wp-content/uploads/2020/04/D2.11-Guide-for-the-simulation-of-AVs-with-microscopic-modelling-tool-Final.pdf. Accessed Jun. 19, 2023.

Sukennik, P. Default Behavioural Parameter Sets for Automated Vehicles (AVs). CoExist Project, 2018, pp. 1–12.

Talebpour, A., Mahmassani, H.S., 2016. Influence of connected and autonomous vehicles on traffic flow stability and throughput. Transp. Res. Part C Emerg. Technol. 71, 143–163. doi: 10.1016/j.trc.2016.07.007

Tesla, 2020. Autopilot and Full Self-Driving Capability [WWW Document].

Thiemann, C., M. Treiber, and A. Kesting. "Estimating Acceleration and Lane-Changing Dynamics Based on NGSIM Trajectory Data." Transportation Research Record: Journal of the Transportation Research Board, 2008: 90–101.

Tsugawa, S., Jeschke, S., and Shladovers, S. E. (2016). A review of truck platooning projects for energy savings. IEEE Transactions on Intelligent Vehicles, 1(1), 68–77. https://doi.org/10.1109/TIV.2016.2577499

University at Buffalo, 2016. iCAVE2: instrument for Connected and Autonomous Vehicle Evaluation and Experimentation [WWW Document]. URL https://cse.buffalo.edu/~qiao/Research.htm

Van der Maaten, L., and G. Hinton. "Visualizing Data Using T-SNE." Journal of Machine Learning Research, Vol. 9, 2008, pp. 2579–2605.

Virdi, N., H. Grzybowska, S. T. Waller, and V. Dixit. A Safety Assessment of Mixed Fleets with Connected and Autonomous Vehicles Using the Surrogate Safety Assessment Module. Accident Analysis and Prevention, Vol. 131, 2019, pp. 95–111. https://doi.org/10.1016/J.AAP.2019.06.001.

Wadud, Z., MacKenzie, D., and Leiby, P. (2016). Help or hindrance? The travel, energy and carbon impacts of highly automated vehicles. Transportation Research Part A: Policy and Practice, 86, 1–18. https://doi.org/10.1016/j.tra.2015.12.001

Wang, C., and Stamatiadis, N. (2013). Surrogate safety measure for simulation-based conflict study. Transportation Research Record: Journal of the Transportation Research Board, 2386, 72–80. https://doi.org/10.3141/2386-09

Wang, C., Xie, Y., Huang, H., and Liu, P. (2021). A review of surrogate safety measures and their applications in connected and automated vehicles safety modeling. Accident Analysis and Prevention, 157. https://doi.org/10.1016/j.aap.2021.106157

Wang, M., van Maarseveen, S., Happee, R., Tool, O., and van Arem, B. (2019). Benefits and Risks of Truck Platooning on Freeway Operations Near Entrance Ramp. Transportation Research Record, 2673(8), 588–602. https://doi.org/10.1177/0361198119842821

Working towards a Shared Road Network - CoEXist. https://www.h2020-coexist.eu/. Accessed Jun. 19, 2023.

Wu, C., Cao, J., and Du, Y. (2023). Impacts of advanced driver assistance systems on commercial truck driver behaviour performance using naturalistic data. IET Intelligent Transport Systems, 17(1), 119–128. https://doi.org/10.1049/itr2.12242

Wu, J., E. Radwan, and H. Abou-Senna. Determination If VISSIM and SSAM Could Estimate Pedestrian-Vehicle Conflicts at Signalized Intersections. Journal of Transportation Safety and Security, Vol. 10, No. 6, 2017, pp. 572–585. https://doi.org/10.1080/19439962.2017.1333181.

Xu, D., C. Xue, and H. Zhou. Analysis of Headway and Speed Based on Driver Characteristics and Work Zone Configurations Using Naturalistic Driving Study Data. Transportation Research Record, Vol. 2675, No. 10, 2021, pp. 1196–1210. https://doi.org/10.1177/03611981211015261.

Xuan, Y., and B. Coifman. "Lane Change Maneuver Detection from Probe Vehicle DGPS Data." Proc., IEEE Intelligent Transportation Systems Conference, Toronto, ON, Canada, IEEE, New York, 2006, pp. 624–629.

Xu, T., Z. Zhang, X. Wu, L. Qi, and Y. Han. "Recognition of Lane-Changing Behavior with Machine Learning Methods at Freeway Off-Ramps." Physica A: Statistical Mechanics and its Applications, Vol. 567, 2021, pp. 1–20.

Xu, Z., Zou, X., Oh, T., and Vu, H. L. (2020). Studying freeway merging conflicts using virtual reality technology. Journal of Safety Research, 76, 16–29. https://doi.org/10.1016/j.jsr.2020.11.002

Yang, D., X. Qiu, Y. Liu, C. Wen, L. Zhu, and X. Hong. "Modeling the Discretionary Lane-Changing Decision Behavior Using Random Forest Theory." Presented at 96th Transportation Research Board Annual Meeting, Washington, D.C., 2017.

Yang, G., M. Ahmed, and E. Adomah. An Integrated Microsimulation Approach for Safety Performance Assessment of the Wyoming Connected Vehicle Pilot Deployment Program.

Accident Analysis and Prevention, Vol. 146, No. 105714, 2020. https://doi.org/10.1016/j.aap.2020.105714.

Yang, G., and Ahmed, M. M. (2020). Analysis, modeling and simulation framework for performance evaluation of the Wyoming connected vehicle pilot deployment program. Advances in Transportation Studies, 2(Special Issue), 1–14.

Yang, H., K. Ozbay, O. Ozturk, and K. Xie. Work Zone Safety Analysis and Modeling: A State-of-the-Art Review. Traffic Injury Prevention, Vol. 16, No. 4, 2015, pp. 387–396. https://doi.org/10.1080/15389588.2014.948615.

Yang, H., Z. Wang, and K. Xie. Impact of Connected Vehicles on Mitigating Secondary Crash Risk. International Journal of Transportation Science and Technology, Vol. 6, No. 3, 2017, pp. 196–207. https://doi.org/10.1016/j.ijtst.2017.07.007.

Ye, L., and T. Yamamoto. Impact of Dedicated Lanes for Connected and Autonomous Vehicle on Traffic Flow Throughput. Physica D: Nonlinear Phenomena, Vol. 512, 2018, pp. 588–597. https://doi.org/10.1016/j.physa.2018.08.083.

You, F., R. Zhang, G. Lie, H. Wang, H. Wen, and J. Xu. "Trajectory Planning and Tracking Control for Autonomous Lane Change Maneuver Based on the Cooperative Vehicle Infrastructure System." Expert Systems with Applications, Vol. 42, No. 14, 2015, pp. 5932–5946.

Yu, H., S. Tak, M. Park, and H. Yeo. Impact of Autonomous-Vehicle-Only Lanes in Mixed Traffic Conditions. Transportation Research Record, 2019. https://doi.org/10.1177/0361198119847475.

Zhang, L., Holm, P., and Colyar, J. (2004). Identifying and Assessing Key Weather-Related Parameters and Their Impacts on Traffic Operations Using Simulation. FHWA-HRT-04-131, (September), 80

Zhao, Y., and Sadek, A. W. (2012). Large-scale agent-based traffic micro-simulation: Experiences with model refinement, calibration, validation and application. Procedia Computer Science, 10(2), 815–820. https://doi.org/10.1016/j.procs.2012.06.105

Zheng, Y., and J. H. L. Hansen. "Lane-Change Detection from Steering Signal Using Spectral Segmentation and Learning-Based Classification." IEEE Transactions on Intelligent Vehicles, Vol. 2, No. 1, 2017, pp. 14–24

Zhou, J., Rilett, L., and Jones, E. (2019). Estimating Passenger Car Equivalent using the HCM-6 PCE Methodology on Four-Lane Level Freeway Segments in Western U.S. Transportation Research Record. https://doi.org/10.1177/0361198119851448

Zhu, J., and Tasic, I. (2021). Safety analysis of freeway on-ramp merging with the presence of autonomous vehicles. Accident Analysis and Prevention, 152. https://doi.org/10.1016/j.aap.2020.105966